The Development of Ionophore-Selective Based Optical Chemical Sensors for the Determination of Heavy Metal Ions in Aqueous Environments

A Thesis Presented for the Award of Doctor of Philosophy by

Li Li, MSc. (Hons)

Department of Chemistry Science
National Centre for Sensor Research (NCSR)
Dublin City University

For Research Carried Out Under the Supervision of
Prof. Fiona Regan, School of Chemical Science, DCU

September 2010

DECLARATION

I hereby certify that the material, which I now submit for the assessment on the progress of study leading to the award of PhD., is entirely my own work and has not been taken from the work of others save to the extent that such work has been cited and acknowledged within the text of my own work. No portion of the work contained in this thesis has been submitted in support of an application for another degree or qualification to this or any other institute or university.

Signed: _   Li Li

ID number: 56114338

Date: 27th of September 2010

THESIS ABSTRACT

"The Development of Ionophore-based Selective Optical Sensors for the Determination of Heavy Metal Ions in the Aqueous Environment"

LI LI

The development of optical sensors for *in-situ*, real-time and low-cost monitoring of heavy metal ions is a tremendously and fast growing area of research. This work presents several novel sensing strategies for developing optical chemical sensors that can be used as early warning devices for heavy metal pollution in water.

The optical sensors that are comprised of metal chelating reagent, together with an ion carrier immobilised within polymeric thin films, i.e. hybrid sol-gel thin films, PVC membranes, ORMSOLs, and functionalised cellulose membranes. The developed test strips based on 2-(5-bromo-2-2pyridydylazo)-5-diethylaminophenol (Br-PADAP) immobilised on hybrid nafion/sol-gel membranes are capable of selectively monitoring Ni^{2+} in water samples.

A novel sensing strategy, based on electrostatically immobilisation of water soluble indicators on functionalised cationic cellulose membranes, has provided a real "green" procedure for the fabrication of sensing materials. The promising results have been demonstrated by the optical sensor based on Chromoazo S immobilized on cationic cellulose membranes for the determination of Cu^{2+}.

A novel series of double armed spirocyclic calix[4]arene compounds has been investigated for their binding abilities with heavy metal ions. Compound 2-144 showed a good selectivity of Pb^{2+} over other heavy metal ions. This compound has a potential for the use as selective-ionophore for the development of a Pb^{2+} selective sensing system.

Abbreviation & Symbols

AAS	Atomic absorption spectrometry
EDTA	1,2-diaminoethane-N,N,N'N'-tetraacetic acid
EU	European Union
ISE	Ion Selective Electrode
I	Ionic diameter
LED	Light emitting diode
LOD	Limit of detection
K_f	Complex formation constant
ε	Complex molar absorptivity
nm	nanometer
PAN	1-2-pyridylazo-2-naphtol
PVC	Poly(vinyl chloride)
T_{90}	Time to reach 90 % of the equilibrium signal
WHO	World Health Organization
UV-Vis	Ultra-violet and visible wavelength
THF	Tetrahydrofuran
Me	Methyl
DCM	Dichloromethane
H^+	Proton
HCl	Hydrochloric acid

CAL	Calmgite
Nitroso-PASP	2-Nitroso-(5-N-propyl-N-sulfopropiamino)phenol
BRPADAP	2-(5-bromo-2-pyridylazo)-5-diethylaminophenol
AVN	Acid Alizarin Violet N
CAS	Chrome Azurol S
MES	2-(N-morpholino)ethanesulfonic acid
HEPES	4-(2-hydroxyethyl)piperazine-1-ethanesulfonic acid
TAPS	3{[tris(hydroxymethyl)methyl]amino}propanesulfonic
CAPS	3-(cyclohexylamino)-1-propane sulfonic acid]

Acknowledgements

Firstly, I would like to thank my supervisor Prof. Fiona Regan, for her help, inspiration and encouragement.

Would like to express my gratitude to;

QUESTOR, Queens University, Belfast, UK, for funding of my research.

The members of QUESTOR and Dublin City University for their help during my research. Special thanks to the technicians of School of Chemical Science, DCU:
Brendan, John, Damien, Ambrose, Veronica, Vinny and Mary.

Thanks to Dr. Mary Deasy, Dr. Fintan Kelleher and James Wards in ITT, Dublin, Ireland, Dr Haibo Xie, School of Chemical Science, DCU, for their collaboration work.

To my colleagues in DCU, past and present: Yuliya, Emma, Frank, Keith, Aga, James, Tim, Rachael, Lisa, Imogene, Anton, Audrey, Kris Hart, Dr Qiang Zeng, Dr Fei Chen, Dr Fuqiang Nie, Dr Xiliang Luo, Jie Zhu and Dr Yurong Liu and Dr. Haibo Xie. Thank you for your friendship and support throughout my research. Special thanks for Richard Hoban and Dr Huizhong Wu for your patience and helping me during the last 3 years.

To my family; Mum and Dad! Thank you for your love, support and belief!

Table of Contents

Chapter1

Chapter 2

Appendix I

Appendix II

Appendix III

Appendix IV

Chapter 1

1.1 Heavy Metals in the Environment

1.1.1 The Definition of Heavy Metal Ions

The term of "heavy metals" (HMs) refers to metallic elements or metalloids that have a relative high density and are toxic and poisonous even at low concentration.[1] Commonly, "Heavy metals" is a general collective term, which applies to the metals and metalloids whose atomic density is greater than 4~4.5 g/cm^3.[2] Heavy metals include lead (Pb), cadmium (Cd), zinc (Zn), mercury (Hg), arsenic (As), silver (Ag) chromium (Cr), copper (Cu), iron (Fe), and the platinum group elements.[3]

1.1.2 Occurrence of Heavy Metal Pollution

Heavy metal ions are natural components in the earth's crust and they cannot be destroyed or degraded, so they are ubiquitous in the environments. HMs can be dispersed into the earth's elements: soil, water and air. Mankind's use of metals seriously began to affect the environment since the industrial revolution, especially from the mining operation, electroplating industry, steel industry, machinery and agricultural industry etc. (**Figure 1.1**).[4] There are hundreds of sources of heavy metal pollution in aqueous systems. They can be summarised in four major aspects: burning of heavy metals, heavy metals runoff, dumping of heavy metals and tributary inflow.[5] For example, water pollution by heavy metals is very prominent with mine sites.[6] The potential for contamination is increased when mining exposes metal-bearing ores rather than natural exposure of ore bodies through erosion, and when mined ores are dumped on the earth surfaces in manual dressing processes.[7] Through rivers and streams, the metals are transported as either dissolved species in water or as an integral part of suspended sediments, (dissolved species in water have the greatest potential of causing the most deleterious effects). They may then be stored in river bed sediments or seep into the underground water thereby contaminating water from underground sources, particularly wells; the extent of contamination will depend on the nearness of the well to the mining site. Wells located near mining sites have been reported to contain heavy metals at levels that exceed drinking water criteria.[1, 8]
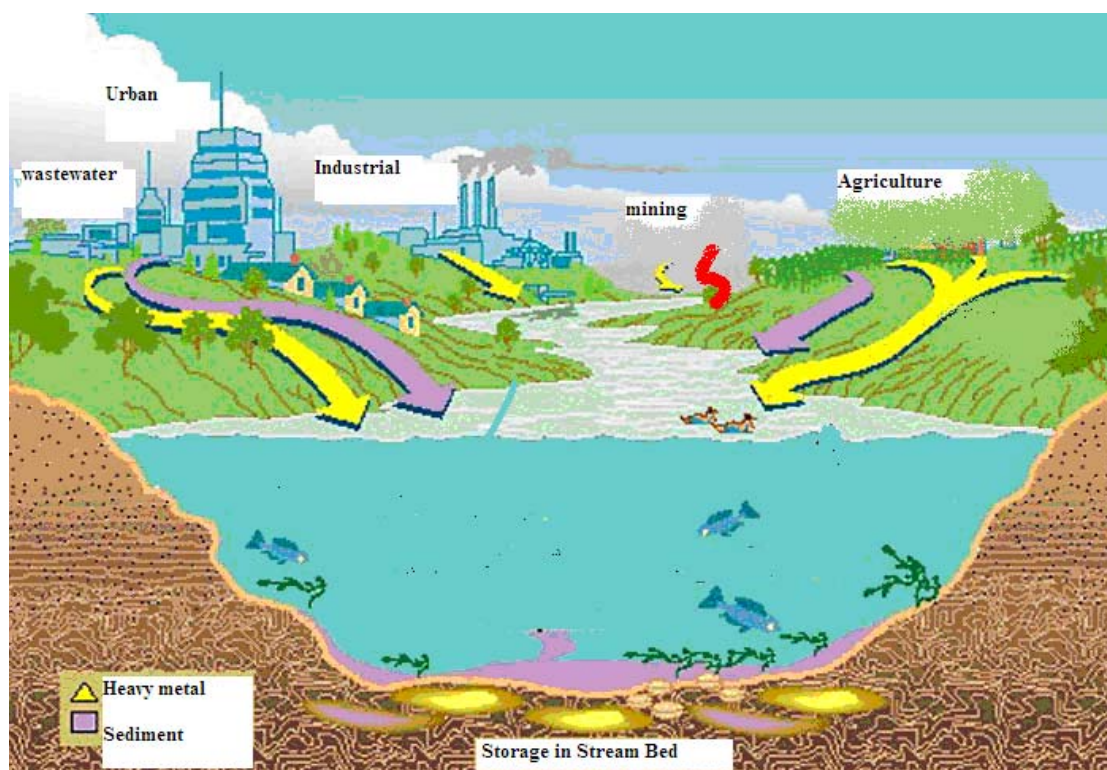
Figure 1.1 Sources of Heavy Metal Pollution for the Aqueous System.[8]

1.1.3 Biochemistry & Bio-toxicity of Heavy Metals

Recently, the term of "heavy metals" has became widely used in biology and environmental studies related to their potential toxicity and ecotoxicity.[8] Human exposure to HMs is through the food chain, air, water chain, industry products and also occupational exposure.[3] The poisoning effects of heavy metals are due to their interference with the normal body biochemistry in the normal metabolic processes. When ingested, in the acid medium of the stomach, toxic metal ions (e.g., Zn^{2+}, Pb^{2+}, Cd^{2+}, As^{2+}, As^{3+}, Hg^{2+} and Ag^{+}) converted to their stable oxidation states and combine with the body's bio-molecules (e.g., proteins and enzymes) to form strong and stable chemical bonds. The hydrogen atoms or the metal groups in the bio-molecules are replaced by the metals and the enzyme is thus inhibited from functioning.[9, 10]

Toxicity of heavy metal ions depends on the type of metal, its biological role and the type of organisms that are exposed to it. Some HMs are essential to maintain the metabolism of the human body at trace concentrations, such as Cu, Fe, Mg, Mn, and Zn.[11] Some are considered to be both very toxic above recommended levels and are relatively accessible, such as As, Cd, Hg, Pb and Sn.[12]   The excess of HMs inhaled by humans in terms of

volatile vapours can cause humans to exhibit the following symptoms: gastrointestinal (GI) disorders, diarrhoea, tremor, ataxia, paralysis, vomiting and convulsion, depression, and pneumonia.[13, 14]

1.1.4 Legislation to Regulate Heavy Metals

On 23 October 2000, the "Directive 2000/60/EC of the European Parliament and of the Council established a framework for the Community action in the field of water policy" or, in short, the EU Water Framework Directive (WFD) was finally adopted. WFD is the most substantial piece of water legislation to date. It requires all inland and coastal waters to reach "good status" by 2015. It will do this by establishing a river basin district structure within which demanding environmental objectives will be set, including ecological targets for surface water. The commission proposal (COM (2006) 397 final) setting environmental quality standards for surface water of 41 dangerous chemical substances includes the 33 priority substances and 8 other pollutants. Metals, such as cadmium, lead, mercury and nickel belong to the priority substances, and cadmium and mercury have been identified as priority hazardous substances.[15] In accordance with toxicity data and scientific studies, the World Health Organization (WHO) as well as the European Water Quality Directive recommends standard and guidelines for heavy metal ions in drinking water, which are summarized in **Table 1.1.**[16]

Table 1.1 Standards and guidelines for heavy metals in drinking water.[17]

Metal	WHO （mg/l）	European Water Quantity Directive[a] （mg/l）
Cd	0.003	0.005
Cu	2	2
Pb	0.01	0.01
Hg	0.001	0.001
Ni	0.02	0.02

[a]Guidelines for drinking water in countries of the European Union are based on these data.

1.2 Conventional Methods for the Determination of HMs

Accurate detection of heavy metal ions is becoming increasingly important to the regulatory agencies, the regulated community and the general public. The development of very sensitive and precise instruments is a big challenge. A variety of analytical methods fulfilling these demands are available. Recommended techniques for the detection of HMs in water samples include inductively coupled plasma mass spectrometry (ICP-MS),[18] hydride-generation (HG) or cold vapour (CV) atomic absorption spectrometry,[19, 20] flame atomic absorption spectrometry (FAAS)[21] or electrothermal atomic absorption spectrometry (ETAAS).[22] These methods are sensitive to heavy metal ions which can provide a wide linear range and low detection limits of heavy metal ions. However, these instruments are large in size and expensive in price and they are suitable for use in the laboratory only. Therefore, the samples have to be collected on site and transported by the labours. During these processes, contamination of samples may occur. The high cost and slow measurement times typically associated with the conventional measurements of regulated heavy metals indicate requirements for novel analytical technologies that are fast, portable and cost effective.

1.3 Chemical Sensors for the Determination of Heavy Metals

In recent years there has been a growing need for constructing chemical sensors for fast, on-time and cost-effective monitoring of environmental samples. The research and development (R&D) in the sensors area has expanded exponentially in terms of financial investment, numbers of paper published, and the number of active researchers worldwide.[23] Compared with the traditional analysis instruments, chemical sensors are portable, simple to use, *in-situ* and miniature in size. These features are ideal for real-time on field measurements, thus the errors caused by the sample transportation and storage can be largely reduced.[24-26]

An appropriate definition of a "chemical sensor" has been described as the "Cambridge definition", whereby a ''chemical sensor'' is that of a miniaturised device/material, that can

deliver real time and on-line information on the presence of specific compounds or ions in complex samples.[27] It normally consists of a chemically selective sensing layer which is capable of chemically or physically responding to the presence of a particular chemical substance in the environment and can be used for the qualitative and quantitative determination of the substance. **Figure 1.2** shows a schematic of a sensor system, illustrating the three main elements: the sample (analyte), transduction platform and signal processing step.

Firstly, there is a region whereas selective chemical reaction takes place. Secondly, there is a transducer where the chemical reaction produces a signal, i.e. colour change or the emission of a fluorescent light and a change in the electrical potential at the surface, etc. Subsequently, the transducer responds to this signal and translates the magnitude of the signal into measure of the amount of the analytes.[28] According to the transducers, the chemical sensors can be divided into electrochemical, optical, mass-sensitive and heat sensitive sensors.[28] For the purpose of the determination of HMs, electrochemical (bio) sensor and optical chemical (bio) sensors are the two most widely used types.[26] It is well recognized that the optical sensor technology has attractive advantages over electrodes, in particular that reference elements are not needed.[29]

```
┌─────────────────────────┐
│         Analyte         │
└─────────────────────────┘
            │
            ▼
┌─────────────────────────┐
│  Platform/ transduction │
└─────────────────────────┘
            │
            ▼
┌─────────────────────────┐
│    Signal processing    │
└─────────────────────────┘
            │
            ▼
┌─────────────────────────┐
│      Signal output      │
└─────────────────────────┘
```
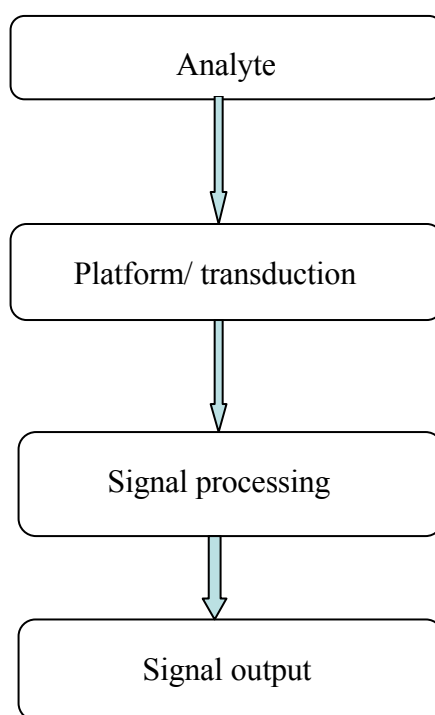
Figure 1.2 Basic schematic of a chemical sensor.

1.4 Optical Sensors for Heavy Metal Ions

1.4.1 Optical Biosensors

An biosensor is an sensor that consists of an immobilised bio-component coupling with transducers and presents a synergistic combination of biotechnology and microelectronics.[30] The use of optical biosensors for the determination of heavy metal ions has been developed based on the recognition phenomena of biological systems. Protein (antibody, enzyme, and metal-binding protein) and whole cell (naturally and genetically engineered microorganism) have all been utilized to yield sensors for heavy metal ions.[31-35] This is because normally heavy metal ions can act as catalysts or inhibitors by chemical reaction with binding groups of protein and microorganisms in the cells.[28, 30, 36, 37] Numerous enzymes including urease,[38] cholinesterase,[39, 40] glucose oxidise [40] protein [41] and etc. have been used for the development of this type of sensors. Jiang and co workers developed an biosensor for the determination of mercury in aqueous samples based on the inhibiting the reaction of urea to urease by addition of Hg^{2+}.[42] Thus the recognition of Hg^{2+} information is transduced via pH or ammonia or carbon dioxide measurements. The biological reaction is illustrated in **Scheme 1.1**. Since Hg^{2+} binds with the thiol and methyl-thiol group of enzyme thus significantly reduce the activity of enzyme.[35] The studies of inhibition by Hg^{2+} was performed using a optical fibre biosensor configuration, where pH changed resulting from the bio-catalytic hydrolysis of urea was monitored at the wavelength of 615 nm spectroscopically, using commercial pH indicator strip before and after the exposure to the HMs solutions. A linear response range between 0.2-200 ng/ mL in water for Hg^{2+} was achieved and the limit of detection was down to 0.2 ng/mL in the samples.[42]

<center>**Urease**</center>
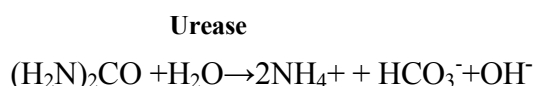
$(H_2N)_2CO + H_2O \rightarrow 2NH_4^+ + HCO_3^- + OH^-$ **Scheme 1.1**

1.4.2 Principles of Optical Chemical Sensors

Optical chemical sensors which produce an irreversible response are referred to as a 'probe' or 'optode'.[24] It normally consists of the following components:[29, 43]

1.   The recognition element, where specific interaction and identification of the analyte take place;

2.   The transducer element that converts the recognition process into a measurable optical signal; the optical properties measured can be absorbance, reflectance, luminescence, light polarization, Raman.

3.   An optical device (process unit) which consists of at least a light source (in its simplest form a LED);

4.   Finally a detector (in its simplest form a photodiode), which detects and converts the change of optical properties, after amplification of the primary signal, into a unit readout.

1.4.3 Advantages of Optical Chemical Sensors

Optical sensors are the youngest members of the sensors family. Chemical optical sensors have many attractive features over other types of sensors. Compared with electrochemical sensors, there is no requirement of a reference electrode therefore the safety, portability and simplicity of the sensors have been increased. Optical chemical sensors are classified conveniently in two categories, the intrinsic ion sensing and reagent-mediated sensors.

1.5 Sensing Schemes of Optical Chemical Sensors

Although the use of a colorimetric detection method is a less advanced approach, it is simple to use in comparison with other spectroscopic methods and it can give a simply visual results for "naked-eye" detection, therefore this technique is still interesting as a sensing technique. Colorimetric sensors,[44] as the name would suggest, are based upon detection of an analyte-induced colour change in the sensor materials.[45-47] Optical chemical sensors based on indicators for heavy-metal ions can provide simple and convenient procedures for on-site analysis and daily monitoring of water quality without using costly instruments. Such sensor will be extremely user friendly in the sense that it can be operated even by less skilled personnel and does not require extensive calibrations and sample preparation. Therefore, nowadays, there is still a large potential market for developed test strips for the determination of heavy metal ions that can be utilized in many applications.

According to the mechanisms, the sensing schemes of optical sensor for the heavy metals can be divided into three types: the intrinsic metal ion sensors, the carrier-based ion sensing, and the indicator-mediated ion sensing. In the following sections, these schemes will be discussed in details.[48]

1.5.1 Intrinsic Ion Sensing

Intrinsic ion sensors rely on the intrinsic optical properties of various heavy metals ionic species since some of them show absorption (ranging from the UV to the near infrared) or luminescence. Solutions of transition metal ions can be coloured (i.e. absorb visible light), because d electrons with the metal atoms can be excited from one electron state to another. For example, cobalt ion can be characterised by a light pink colour in concentrated solution and nickel ion solution is observed as light green. However, such sensors usually are lack of selectivity due to interference of other species absorbing at the same wavelength or sample turbidity. And the molar absorptivities of heavy metal ions are low, typically around $10 \sim 1000 \ l \ mol^{-1} \ cm^{-1}$.[48]

1.5.2 Reagent Mediated Optical sensors

The uses of chemical reagents for the determination of heavy metal ions based on complexation reaction have been widely used for quite a long time. A large number of metal indicators containing various groups for binding exist naturally or be synthesised.[49] A chemical reagent is chosen to react sensitively and specifically to the heavy metal ion and the resultant change in its optical properties (e.g., fluorescence or absorption) is a direct measure of the concentration of heavy metal ions.[48] Dyestuffs have been employed for the analysis of metal ions as these reagents form strong complexes with a large number of metal ions and the complexes can be determined spectrophotometrically. These indicators have been utilized in the titration processes, separation and pre-concentration processes of heavy metal ions for a long time. Edmund et al. have reported detailed information on these indicators for metal ions.[50] They are normally Lewis bases that attached to the metal ions in a complex.[50] These groups are capable of donating a pair of electrons. If a metal forms a complexation, the maximum number of ligands that can be bound to the metal is known as the coordination number. Metal ions can have more than one characteristic coordination number, depending on the valence of the central atom and the coordination lignads.[50] The strongest ligands are those multidentate and form the

particularly stable five-numbered rings.[51] Effective multidentate chelating ligands of this type are those contain oxygen, sulphur and nitrogen which are electron donating atoms.[52] These ligands for HMs are classified into different groups by their functional chemical structure:[53]

1. Ago dyes: R—N=N—R', more than 50% of these ligands are ago dyes;

2. Nitro and nitro so dyes: Compounds containing a $-NO_2$ group or a $-NO$ group are named only by means of the prefixes "nitro-" or "nitro so-", respectively;

3. Polymethine dye is a well known and important class of synthetic colouring materials and has attracted much attention due to their potential functions for specialty and high-technology applications, namely functional dyes. Phthalocyanine dyes are macro-cyclic compounds having an alternating nitrogen atom-carbon atom ring structure. The molecule is able to coordinate hydrogen and metal cations in their centers by coordinating bonds with the four isoindole nitrogen atoms. The central atoms can carry additional ligands;

4. did-and triarylcarbonium dyes and azo-analogues;

5. sulphur dyes: C=S;

6. carbonyl dyes (indigoids, anthrachinones) C=O;

7. Ene: >C<;

8. Azoxy: -N=N-O-;

9. Azoamine: -N=N-NH-.

Desirable properties for the dyes for determination of heavy metal ions can be summarised as follows:

*   Absorb strongly in the visible region

*   Process weak acid nature

*   Absorbance spectrum greatly affected by protonation-depronation

*   Chemical and photochemically stable.

1.5.3 Carrier (Ionophore)-based Metal Ion Sensing

Optical ion sensors based on neutral ionophores benefit from bulk membrane based Ion Selective Electrodes (ISEs) over 30 years.[17, 54, 55] Normally an ionophore-selective optical sensor comprises of highly lipophilic ion-selective neural ion carriers (ionophore) and chromophore or flurophore in a polymeric membrane. Recognition of HMs is

accomplished by neutral ionophores capable of binding the metal ion, while the optical signal is provided by a proton-selective chromophore.[56]

The theory of mechanisms, co-extraction (**Figure 1.3**) and ion-exchange (**Figure 1.4**), has been discussed by the work of Simon and co-workers in their peer reviews.[57-59] The co-extraction scheme is shown in **Figure 1.3**, the metal ions is co-extracted into the bulk along with a proton. Extraction usually is accomplished by exchange catalysts such as lipophilic quaternary ammonium ions. The co-extraction of a proton results in the protonation of a pH dye in the immobilized in the system changing its colorimetric or fluorescence signal for indication of heavy metal ions.[57]
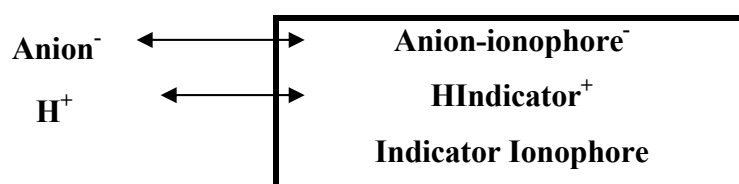
Figure 1.3. Schematic representation of the co-extraction mechanism.

An anion is carried into the membrane by an appropriate ionophore and a proton is co-extracted into the membrane where it protonates the indicator dye. The process is fully reversible.[57]
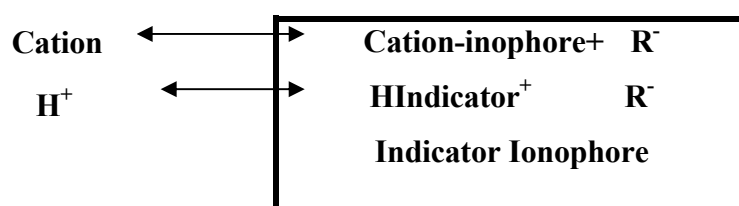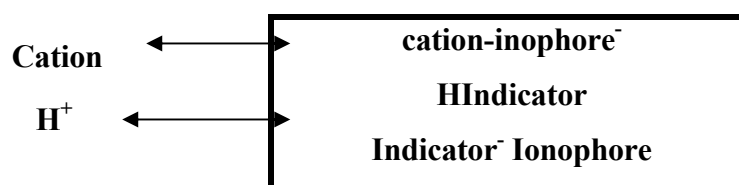
Figure 1.4 Schematic representation of the ion exchange process accruing in optical sensors using neutral ion carriers.[63]

The Ion-exchange processes are illustrated in **Figure 1.4 (A) and (B),** and the analyte is extracted from the aqueous into the lipophilic membrane driven by the host/guest interaction with the neutral ionophore capable of binding with metal ions. Since electro-neutrality must hold for the bulk phase, either a counter ion is extracted into the membrane, or an ion of equal charge is released from it. Frequently, protons are involved within this process and pH indicators were integrated into the membrane as transducers, the pH indicators can be protonated (A) or either uncharged (B). Ion transport into and out of such bulk materials is greatly facilitated by addition of lipophilic anions such as certain tetraphenyl borates [60-63].

A drawback of these sensing schemes is its pH cross-sensitivity, which can be overcome by measuring the pH of the sample simultaneously, but it requires larger efforts in instrumentation. More recently pH independent sensing schemes based on co-extraction of a coloured counter ion have been developed.[64-66] The application of potential sensitive dyes has also been described as a possible sensing mechanism, whereby protons are not involved in the recognition process.[66, 67]

1.6 Characteristics of an Ideal Optical Chemical Sensor

Usually, the quality of an optical sensor device can be evaluated by the following criteria:[29]

1. The sensor should give an optical signal of high signal-to-noise ratio;

2. The signal should strongly change on the exposure to the analyte;

3. The sensor materials should be stable over time on storage;

4. The components used for making the sensor material does not leach or deteriorate on exposure to the analyte;

5. The indicator should be photostable;

6. The sensing materials should adequately adhere to the support;

7. The analytical signal should be referenced to another signal (such as another wavelength);

8. The scheme should be compatible with any of the existing semiconductor optical components (from LEDs and diode lasers to photodiodes);

9. The optical response of the materials should be described (or at least modelled) by a fairly uncomplicated mathematical equation;

10. The materials used should be affordable and come (or can be made) in constant quality;

11. The sensor can be made at adequate cost;

12. The sensor should be fabricated by non-toxic materials.

However, fulfilling all these demands is hardly possible and existing sensors usually suffer limitations, such as insufficient long-term stability, poor selectivity of other species to the target analyte and inadequate limits of detection and the leaching of the sensing materials. Notwithstanding and motivated by this, the field of optical sensing is still of increasing interest, which is reflected by a continuous increase in publications and reviews.

1.7 Challenges in Optical Sensors Research for Heavy Metal

Progress in sensors development increasingly requires a multidisciplinary effort and access to more complex fabrication technologies. The main challenges in optical sensors for the determination of heavy metal ions have been focused on the following area.

1. Improving the recognition mechanism, this is of fundamental importance as it is the basis of the signal that will be obtained from the sensor. Researches are synthesizing new molecular receptors for heavy metal ions, with better selectivity, which respond to target metal ion or undergo a different transduction mechanism (or can provide information via several different transduction mechanisms). Materials under active research include the ion-molecule receptors (based on host-guest chemistry).

2. New materials are being investigated for use as solid matrix in which to immobilise the receptor molecules. Important contributions are being made by polymer technology that have developed new materials with interesting properties, such as non-toxic, ease of preparation, low-cost and multifunctional.

3. New sensor substrates (i.e., materials constituting the body of the sensor, or on which the device is built) are being investigated, arising mainly from a need for new fabrication design.

4. Improvements in signal processing technologies and instrumentation are making important contributions to quality of sensor information.

1.8 Metal Recognition Process Based on Macrocyclic Ligands

1.8.1 Principles

Molecular recognition signifies the process of specific, non-covalent binding of guest species by an organic host molecule. It has the origin in the discovery of macrocyclic compounds, which are capable of selectively binding alkali ions in a field of supramolecular chemistry.[68-71] Supramolecular chemistry is the chemistry of the intermolecular bond, covering the structures and functions of the entities formed by association of two or more chemical species.[72] The molecular recognition process is illustrated in **Figure 1.5.**
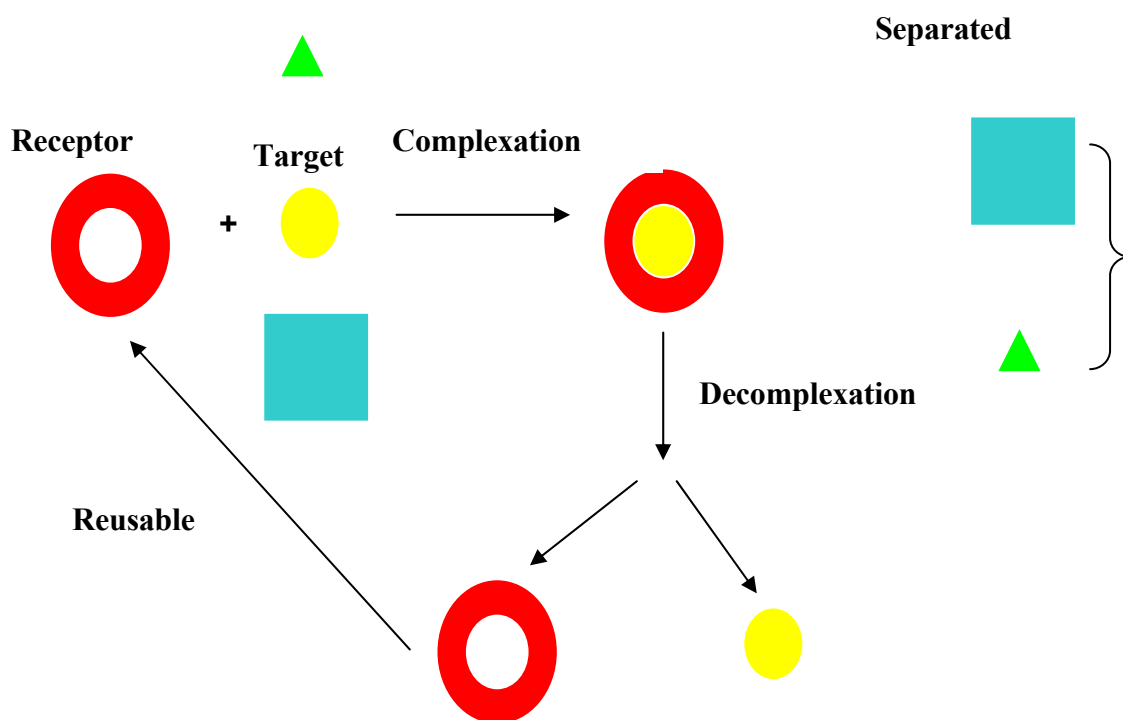
Figure 1.5 An over-simplified view of recognition and separation of calixarenes.

Traditional chemistry focuses on the covalent bonds of molecules, while supramolecular chemistry deals with the weaker non-covalent interactions of chemical systems composed

of a discrete number of assembled molecular subunits.[73] The forces responsible for the spatial organization of these systems include electrostatic or hydrogen bonding, π–π interactions, van der Waals forces, hydrophobic forces etc.[74] The concerted action of specific weak interactions (the *designed* chemistry of the intermolecular forces) prompts the discrete chemical entities to self-assemble into structures with (hopefully) desired properties.[75] The construction of molecular recognition through the coordination of a metal ion with organic ligands has attracted considerable attention and has evolved in an interesting research area of optical sensors. Because of their interesting architectures and properties, a significant number of supramolecules for metal complexes have been synthesized in the last several years.[75-78] However, there have been fewer examples reporting on the role and relative importance of the most prominent intermolecular interactions (*viz*. hydrogen bonds and π–π stacking interactions) on the supramolecular organization of metal complexes[78]

Utilisation of macrocyclic ligands for the determination and separation of metal ions is receiving the ever-increasing attention of researchers. These macrocylic compounds include crown ethers and their derivatives,[70, 79] podants,[80] cyptands,[81-83] cyclophane type macrocycles and calixarene and it derivatives.[81, 84, 85] Ionophores with donor atom containing groups (O, N, S, etc.) immobilized on the macrocyclic platform are of particular interest because the metal-binding properties of such ligands may integrate the selectivity of macrocycles.[84, 86-89] **Figure 1.6** shows a selection of macrocyclic ligands that can be used as ionophores for the determination of heavy metal ions.

Calixarenes are cavity-shaped cyclic oligomers made up of phenol units. Compared with other types of macrocyclic ligands, they are more attractive as ionophore used in sensor technologies because they can be synthesized on a large scale in simple one-pot procedures from inexpensive starting materials.[90]
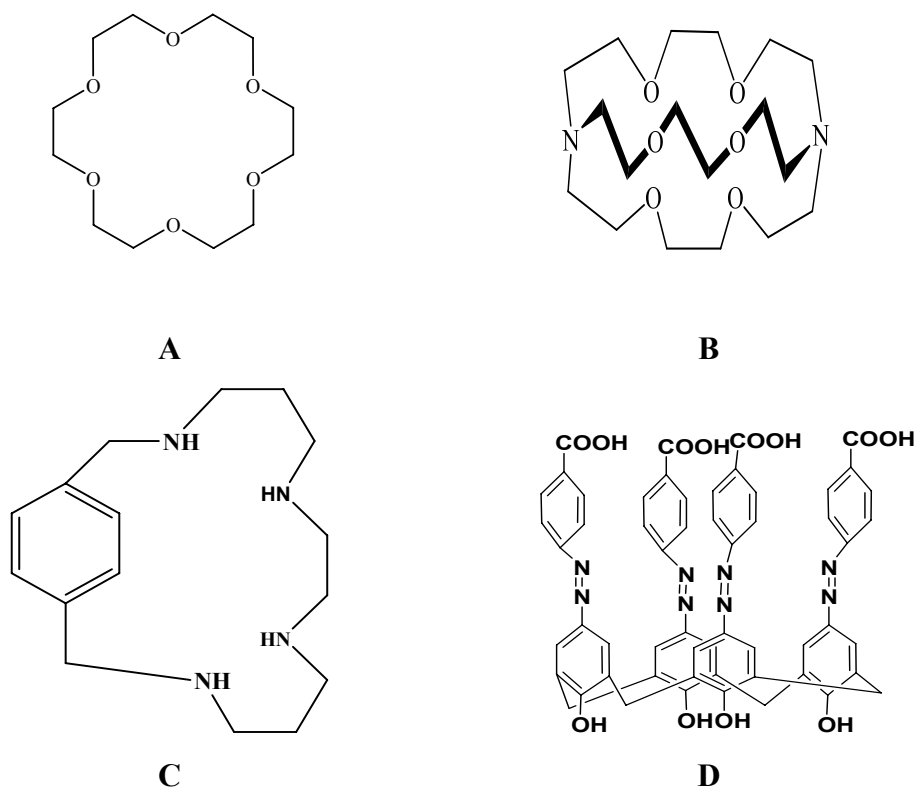
Figure 1.6 Various examples of ionophores for heavy metals utilized in optical sensors or ISEs. (a) a crown ethers based ionophore for Pb^{2+};[70] (b) a cyptant based ionophore for Hg^{2+};[91] (c) Cyclophane microcyclic compounds shows good selectivity to Cu^{2+} and Zn^{2+}, [69] (d) a calixarene based ionophore for Pb^{2+}.[92]

In addition, they are readily accessible for chemical modification on both "lower" and "upper" rims by attachment of a wide range of potential ligating groups,[69] furthermore, calixarenes and its derivatives generally have high melting points, high chemical and thermal stability, low solubility and low toxicity. The variation of their cavity dimensions according to the requirements of different guest is possible.[81]

Dramatic advances in the selective properties of calixarenes have been achieved by altering the ligating groups on the lower rim.[93] McKervey et al. reported that lower rim derivative calixarenes were selective for Ag^{+} and Ca^{2+} ions.[94] The same group then employed calixarenes with a larger number of repeating units for sensor applications, for example, the phosphine oxide hexamer (**Figure 1.7**) displayed remarkable selectivity towards Pb^{2+} and Hg^{2+} ions depending on the pH.[95]
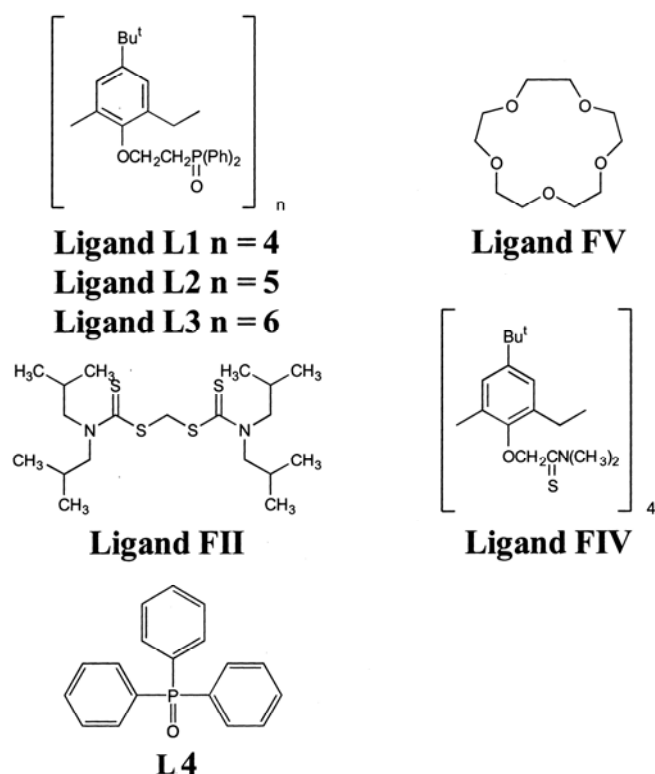
Figure 1.7 General structures of butylcalix[*n*]arene ethyleneoxydiphenylphosphine (*n* = 4, 5, and 6 for ligands L1−L3, respectively).[95]

It has been reported by Pearson that the introduction of soft donor atoms, such as oxygen, nitrogen and sulphur donors in a calixarene framework promotes their complexation with transition and heavy metal ions.[96] This is the principle of hard and soft bases (HSAB). Hence, Ag^+, Cu^{2+}, Cd^{2+}, Hg^{2+} and Pb^{2+} are classified as soft acids, capable of binding favourably to ligands containing sulphur, while the borderline acids such as Ni^{2+}, Cu^{2+}, Co^{2+} and Zn^{2+} prefer binding to nitrogen.[97] **Figure 1.8** shows some examples of calixarene derivatives binding to heavy metal ions. A thiamine moiety containing ligands, **Figure 1.8 (1a) and (1b)** have been used as a Pb^{2+} ionophore.[98] And also it shows a good selectivity to Cd^{2+}, Cu^{2+}, K^+, and Ca^{2+}. Compound 2 containing two thio-amide groups was used for the preparation of Cd-selective film.[99] In the PVC or polysiloxane-based membrane, calixarene 3 shows good selectivity to Cd.[100] The dansyl-groups render a 4a fluorophore which responds to Cd^{2+} with increased emission intensity when the dansyl groups are inside the hydrophobic cavity. The dithioamide groups on the calixarene backbone, represented by

ligands 5a and b were applied for Cu^{2+} selective sensors, although an interference by K^+ occurs.[101] [102]
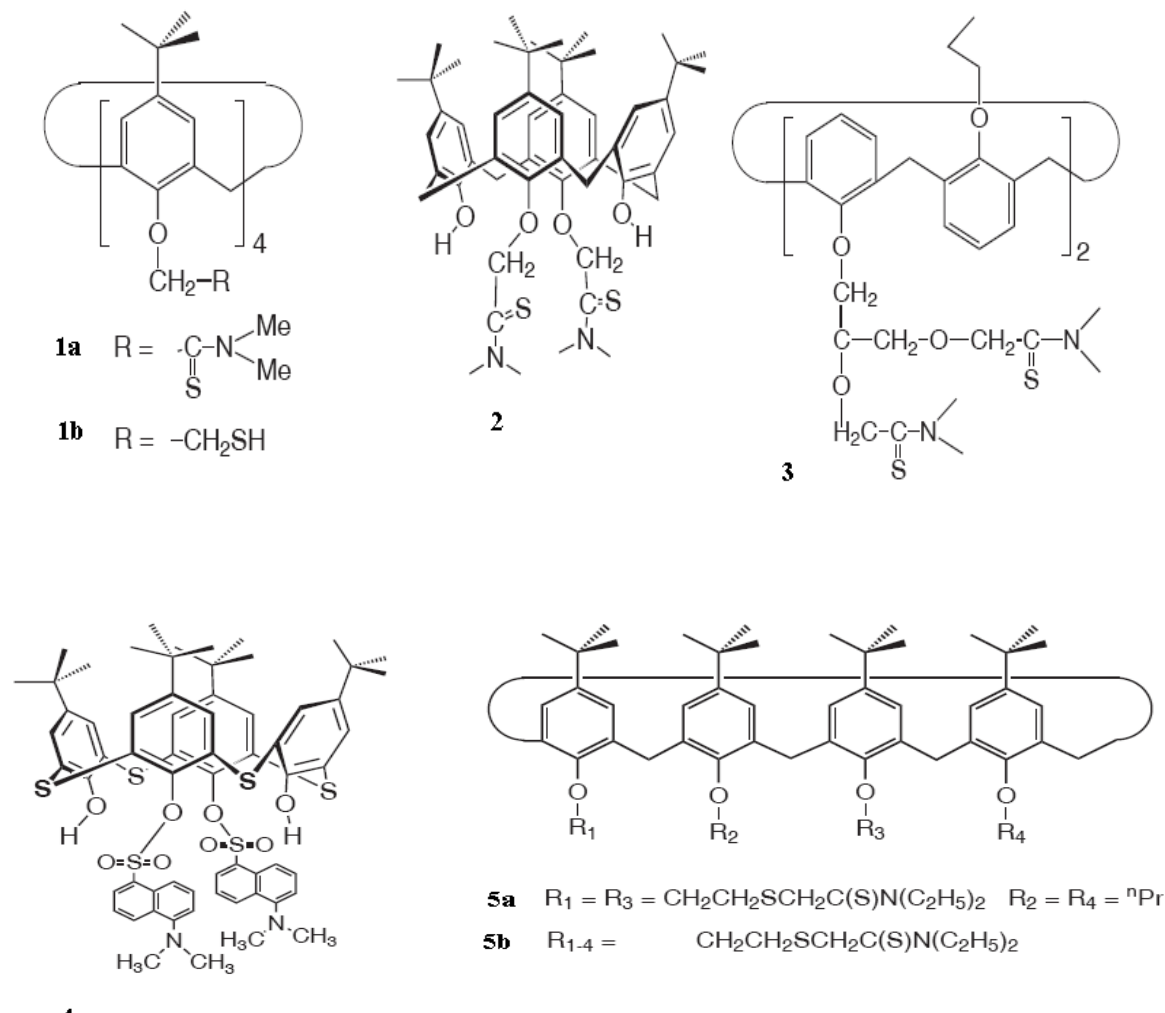
Figure 1.8 Examples of calixarene derived compounds used in HMs recognition.[101]

The calix[4]arenes derivatives modified at the upper rims also show promising binding ability with heavy metal ions.[101] Shim et al. have recently reported the synthesis of a potentiometric sensor based on an upper rim modified calixarene (**Figure1.9**). The group concluded that the circularly arranged azo groups at the upper rim were effective in binding the metal ion. Out of twelve metal ions tested, namely Co^{2+}, Zn^{2+}, Cu^{2+}, Hg^+, Cd^{2+}, Pb^{2+}, Ag^+, Ni^{2+}, La^{3+}, Ca^{2+} and Cr^{3+}, the calixarene was found to be selective for Co^{2+}.[103]
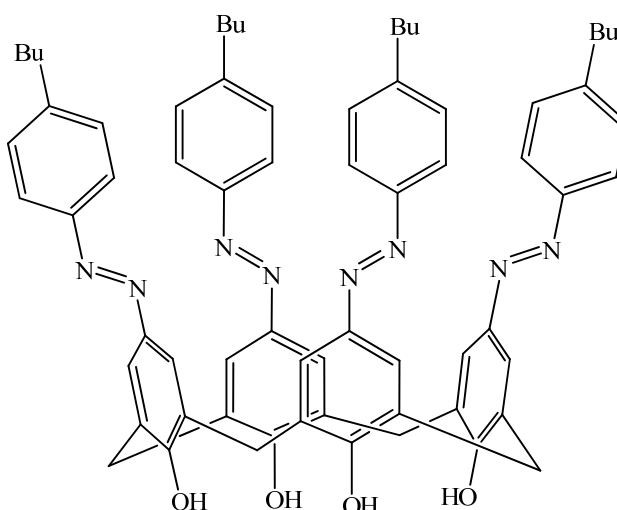
Figure 1.9 *p*-(4-*n*-butyl-phenylazo)calixarene[101-103]

1.8.2 Optical Sensors based on Chromo/Fluoro-ionophores

The field of supramolecular chemistry has brought to light of new binding sites with improved selectivity. Logically, the idea of coupling these ionophores to chromophores or fluorophores emerged some years later, leading to the so-called chrompionophore and fluoroionophore.[104] The chromo-and fluoro-ionophores form a particularly interesting class of probes since they can combine recognition properties with optical transduction, i.e. changing colour or fluorescence.[105] The concept of chromogenic and fluorogenic dyes for neutral and anionic analytes using reversible chemical reactions is shown in **Figure 1.10.**
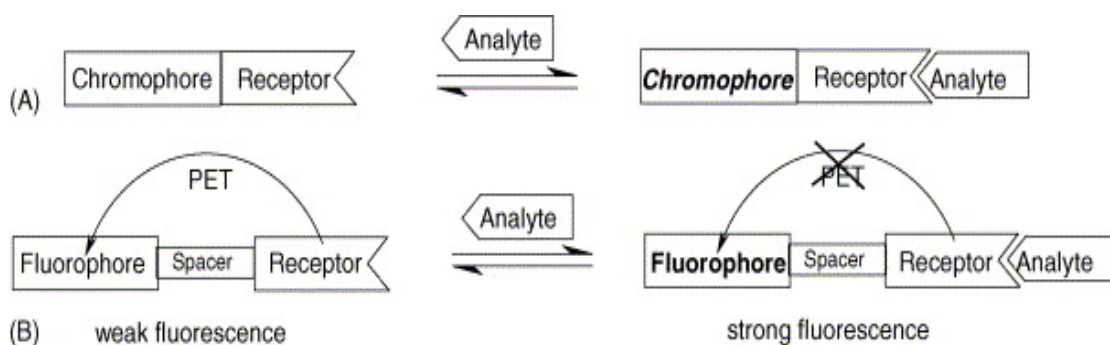
Figure 1.10 Analyte recognition (A) via formation of a covalent bond to the chromophore causing electron delocalisation and colour to change and (B) via formation of a covalent bond with a receptor not directly linked to the chromophore but modulating PET.[75]

Two major optical transduction principles are observed: **Figure 1.10 (A)** a specific functional group of the indicator dye that is an integral part of the chromophore or fluorophore performs a chemical reaction with the analyte molecule. This chemical reaction affects the electron acceptor or donor strength of the functional group and thus changes the electron delocalisation within the dye molecule. As a consequence, the dye shows significant changes in absorbance (and fluorescence) which are usually accompanied by a shift in absorbance maxima. **Figure 1.10 (B)** A functional group that does not affect the electron delocalisation within the dye molecule but quenches luminescence due to photoinduced electron transfer (PET) interacts with the analyte molecule. As a consequence of this interaction, PET from the functional group to the fluorophore is modulated and an increase in luminescence (but no spectral shift) is observed. Silva et al. also suggested that the redox potentials are matched for the electron transfer to happen.[106]

1.9 Development of Immobilization Techniques

To facilitate interaction with the analyte, a probe regent is required to be immobilised in solid matrices, where the reagent can be physically and chemically immobilised. Physical immobilisation is achieved through adsorption, entrapment/encapsulation or ionically (electro-statically) attraction between the probe molecules and the solid matrices.[106] In adsorption, the reagent molecules are held on the surface of the solid matrices by physical forces, such as hydrogen bonding, hydrophobic interactions. In entrapment or encapsulation, the probe molecules are confined in the lattice structure of the sol-gel supports. The electrostatic attraction involves the forces between the ionic groups contained in the probe molecules with the solid supports. The most common approach so far for the immobilisation step is the physical adsorption of the reagent molecules in a polymer matrix.[106] After the entrapment, the polymer is deposited on a device, such as an optical fibre or the surface of a waveguide to create the working sensor.[24] The physical entrapment is simple; however, the physical entrapment of dyes in the polymer produces in-homogeneity in the material and gives stability problems due to the leaching of the indicator probe from the solid matrix, reducing the life time and reproducibility of the sensor.[107]

To improve the stability of these materials, the alternative approach is the covalent attachment of the probes to the supporting materials.[108, 109] Chemical bond involves the formation of the chemical bonding between the probe molecules with the solid supports *via* organically active functional groups, such as NH_2-, -COOH, -SO_3H, etc. The widely used polymeric supports range from the inorganic materials (sol-gels, etc.) to organic polymers (cellulose, nylon, PVC, etc.). Covalent linkage of the dye to a suitable matrix appears to be the most efficient immobilisation method since the resulting membranes reducing leakage of the probe molecules from the solid supports at,[110] while physical immobilisation is attractive because of its simplicity and applicability.[111] For covalent linking of the dye molecules, surface modification of the optical fibre or substrate is required.[112, 113] Although covalent linking results in excellent immobilization, these methods are often more difficult to implement and may lead to loss of dye sensitivity or result in poor absorption and fluorescence.[114]

1.10 Sensing Matrices for Optical Chemical Sensors

The material science as a solid matrix support for probe molecules also plays a major role in the design and fabrication of optical chemical sensors. This is necessary for several reasons. Firstly, the indicator has to be immobilised into an optical wave-guild or optical fibres which are then brought into contact with the analyte solution. Secondly, the probe molecules need a solvent to interact with the analyte. Most commonly, the diffused indicator dissolved in the solid matrices which allowed free diffusion of the analyte to and from the indicators molecules. The probe molecules can be retained in the solid matrices by physically and chemically immobilisation techniques, usually the techniques have their own advantages over to the others.

The solid matrices not only act as solid support, but they can also have an effect on a sensor's performances, such as its selectivity, response time, stability, reusability and the overall production cost.[115] So it is very important to choose a suitable material for metal ion sensing. Hydrophilic polymeric matrices have been widely used to sense metal ions due to their good performance being as a solid matrices for sensor immobilisation.[24]

Among these hydrophilic materials, plasticised PVC membrane, cellulose and its derivates and sol-gel technologies have drawn much attention. Therefore, in the next section, the immobilisation methods and supporting matrices are summarised respectively.

1.10.1 Polymeric Materials

Polymers have been widely used as sensor support materials for a broad range of indicators based optical sensors for heavy metal ions. They are convenient due to their simple process ability to small particles and thin films which can be deposited onto optical fibres, waveguides for sensor fabrication.[24] It is well known that the polymeric properties influence a number of important parameters of a sensor membrane. The selectivity and the dynamic range of an optode membrane are strongly influenced by the partition behaviour of ion and electrically neutral molecules between the organic and the aqueous phase.[115]

The most widely used materials in optical sensors include poly (vinyl) chloride (PVC),[58,63] polymethyl methacrylate (PMMA),[116] polydimethyl siloxanes (PDMS),[117] and cellulose derivatives such as ethyl cellulose.[118] Hydrophobic plasticised PVC membranes were used exclusively as a matrix in the electrochemical sensor and optical sensor for heavy metal ions, since such membranes can be produced at low cost. They also have good mechanical properties, homogeneity, easy preparation and optical transparency.[58] Simon and co-workers have carried out a series investigation of plasticised PVC bulk membrane incorporating a metal ion selective ionophore, a proton selective chromoionophore and lipophilic anionic sites for the measurement of heavy metal ions.[56, 63] This bulk membrane is homogenous and not turbid; most of the time the indicators are dispersed homogenously in the plasticised PVC membrane. Since there is a clear separation existing between the aqueous sample phase and the hydrophobic reagent phase, the electro-neutrality condition has to be strictly considered when establishing models for the response of the sensors. As a result, lipophilic counter-ions (such as tetraphenylborate) are always required in the two major sensing schemes existing for the plasticised PVC based sensors. The plasticizer is a very important component membranes cocktail used in ion sensors are usually based on a matrix containing about 33%（w/w） of PVC and 66 % of plasticizers films with such a high amount of plasticizer have optimum physical properties and ensure relatively high motilies of their constituents.[119] However, it is known that the leaching of plasticizers from the solid matrices may limit the lifetime of the sensors and hamper their applications.[65] So nowadays, the plasticizer-free polymeric support is under interest for the

development of sensors. Bakker and co-workers have reported that copolymerisation of Nile Blue derivatives containing an acrylic side group give rise to multiple reaction products.[64] The limitation of conventional PVC based optical sensors has been overcome by grafting the lipophilic H^{+}-selective indicator Nile Blue to a self-plasticized poly(*n*-butyl acrylate) matrix via an urea or amide linkage between the Nile blue based structure and the polymer. Compared with the conventional PVC based optical sensor membranes using Nile Blue as indicator, these polymerised Nile Blue derivatives have showed agreeable selectivity patterns, reasonably fast response times and reduced dye-leaching.[66]

To increase the stability of indicator dyes in the plasticized PVC membrane, a substantial improvement in selectivity and sensitivity has been observed in the case of the metal-ion indicator pyrocatechol violet (PV) when encapsulated in a PVC membrane. The water soluble indicator was lipophilised in the form of an ion pair with tetraoctylammonium cation (TOA), and there is an electrostatic interaction with the PV indicator, thus greatly reducing the leaching of it from the PVC membrane.[120]

Another interesting polymer that can be applied in sensors is Nafion, due to its hydrophobic and hydrophilic nature, providing very suitable conditions for both trapping the lipophilic ligand and exchanging ionic species; hence, there is no need for incorporation of other membrane ingredients, such as plasticisers and lipophilic additives.[121, 122] Further, Nafion membranes are highly transparent in the UV-Vis-NIR region due to its fluorocarbon chains as backbones; providing good chemical, thermal and mechanical stability, while its sulfonate groups provide ion exchange and swelling capabilities.[123-125] Amini et al. reported an optode for the determination of Ni^{2+} based on 2-(5-bromo-2-pyridylazo)-5-(diethylamino)phenol in Nafion. The developed method was successfully applied to the determination of nickel content in vegetables oil and chocolate samples.[121]

Green chemistry plays a tremendous role in materials chemistry as well as in the area of sensor development. Since there is a drive to develop inexpensive, biodegradable and "green" sensor platform for the detection of pollutants, without leaving toxic materials behind. Cellulose is an abundant 'bio-renewable resource' that has been utilised as a support for sensing agents both in the past and in new applications. Cellulose can be chemically modified and results in celluloses with either hydrophilic functional groups such as carboxyl or amino or lipophilic groups such as long chain fatty acids on their

surface.[118] They also may be rendered with charged functions such as quanternised amino groups with are useful "ion exchangers" for heavy metal ions.[126] However, efficient utilisation of cellulose as a sensing material source has been challenging due to its poor solubility in many organic solvents. Several methods have been used for the dissolution of cellulose.

1 2
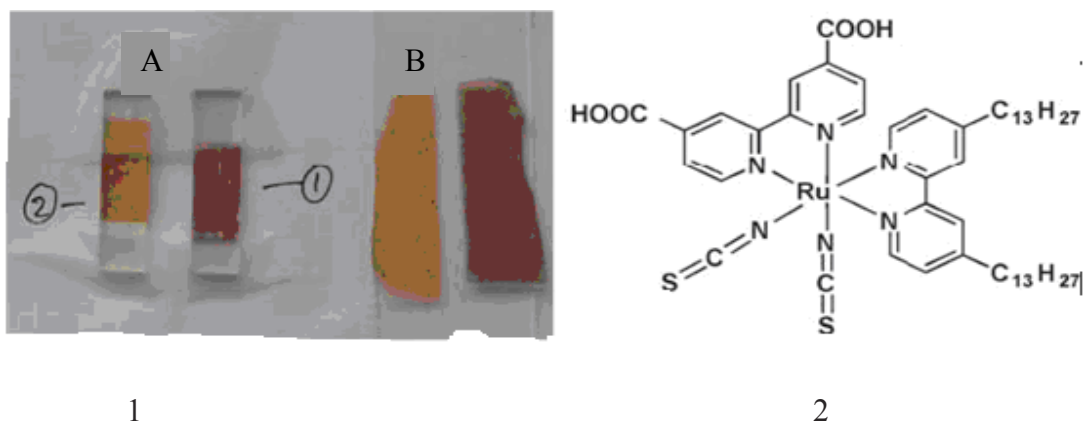
Figure 1.11 An example of ILs modified Cellulose membrane for the detection of Hg^{2+}.[118] (1) The test strips before and after contacting with Hg^{2+}; (2) the structure of the indicator.

Rogers et al. have reported a versatile, inexpensive, simple and biodegradable sensor platform for sensor development based on encapsulating a probe molecule in a cellulose support followed by regeneration from ionic liquid (ILs) solution for the determination of Hg^{2+} in solution.[118] The modified cellulose materials with ILs showed a promising homogeneity with varies types of indicators dyes. For example, **Figure 1.11** shows cis-dithiocyanatobis-2,2'-bipyridine-4,4'-(COOH)$_2$-4,4'-tridecyl-2,2'-bipyridineruthenim *(II)* (N621) indicator immobilized in cellulose regenerated from ILs and it has been used for the detection of Hg^{2+}. **Figure 1.11 (1)** TiO$_2$-based sensors (A) and cellulose-based sensors (B) containing N621. In each set, the sensor on the left was exposed to Hg^{2+} and the one on the right was not. **Figure 1.11 (2)** graph presents the structure of the dye. Such sensors can be tailor-made with relatively little effort and 'sensor kits' are envisioned where the sensing agent and support can be reconstituted and used on-site. And the working linear range is from 5-100 mg/L of Hg^{2+}.

1.10.2 Sol-gel Materials

More recently, sol–gel glasses have gained interest as matrices for chemically sensitive optical materials because of their optical transparency, mechanical stability, chemical inertness, and flexibility in terms of shaping sensor configurations. Hence, sol–gels have been extensively studied with respect to their application to chemical sensing of analytes such as H^+, metal ions, inorganic anions, glucose, oxygen and ammonia. Parallel to the production of organic polymeric materials, new trends in sol-gel technology of materials science, such as in the form of mesoporous materials, sol-gel thin film and sol-gel monolith materials, for chemical sensing are emerging.[37, 127, 128] The advantages of the sol-gel technology are undoubtedly simplicity and versatility. Among these flexibilities, thin films and monoliths are widely used for HMs sensing.[129, 130] There are many properties of sol gels that make them particularly attractive for sensing applications, such as transparency, porosity, and high surface area.[131]
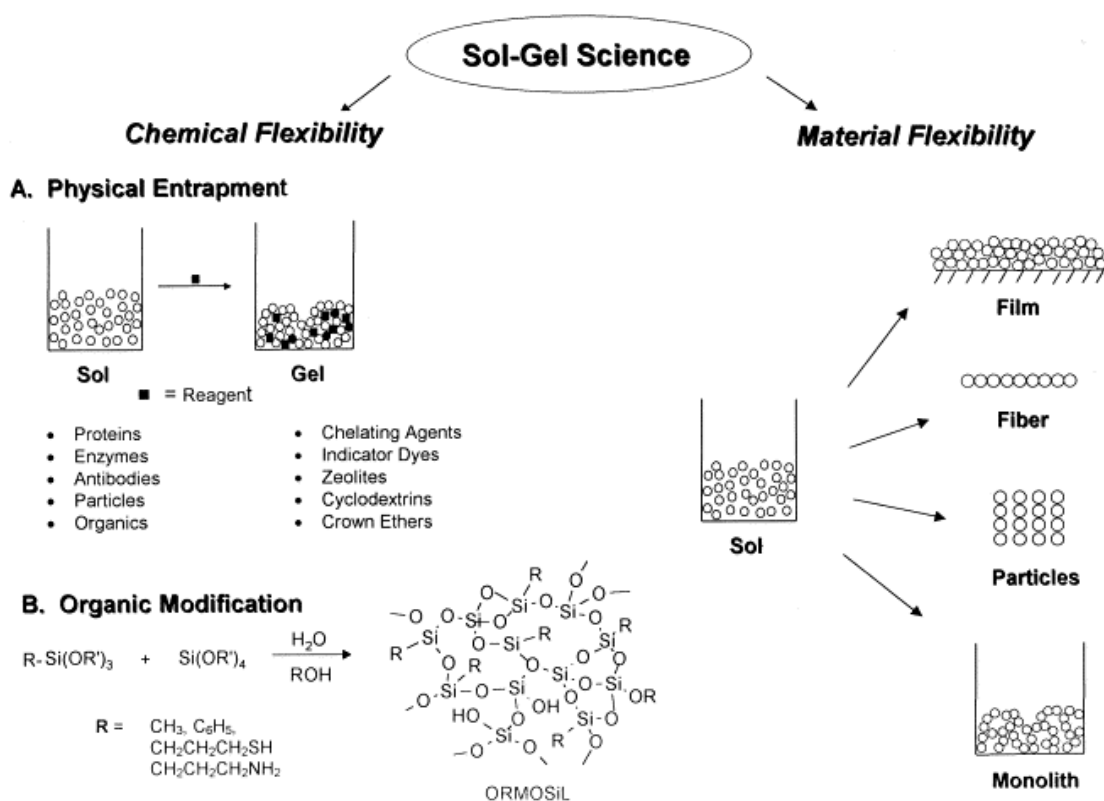
Figure 1.12 The immense flexibility of the sol-gel process.[133]

Sol-gels are compatible with numerous chemical agents, making the incorporation of sensing elements onto sol-gel substrates possibly. Since little or no heating is required during the sol-gel process, thermally sensitive organic molecules have been encapsulated with the gel interiors. This encapsulation is usually accomplished using either doping or a grafting process to give organo-functional sol-gel materials.[132] The reagents immobilised materials can be fabricated into several configurations due to its flexibilities (**Figure 1.12**), such as thin films, coatings of fibbers or waveguides, (nano) particles or monoliths.

The sol-gel process is a simple approach to produce an inorganic polymeric network (silica) through hydrolysis and subsequent poly-condensation of the appropriate metal alkoxide solution to produce a porous material at low temperature.[134] The **Scheme 1.2** presents the sol-gel formation process, the hydrolysis and condensation polymerization processes. The generic precursors are silica alkoxides, such as tetraethyl orthosilicate (TOES) or tetramethyl orthosilicate (TMOS), R is an alkyl group. A range of specific recipes of the production sol gel polymers have been used by different groups in accordance to their requirements. These sol-gel reactions, are profoundly affected by many factors, such as the size of the alkoxode ligand, solution pH, types and concentration of solvents, temperature, and the catalysts.[28, 134]

Hydrolysis

$$\equiv Si-OR \; + \; H_2O \; \rightleftharpoons \; \equiv Si-OH \; + \; ROH$$

Condensation

$$\equiv Si-OR \; + \; HO-Si\equiv \; \rightleftharpoons \; \equiv Si-O-Si\equiv \; + \; ROH$$

$$\equiv Si-OH \; + \; HO-Si\equiv \; \rightleftharpoons \; \equiv Si-O-Si\equiv \; + \; H_2O$$
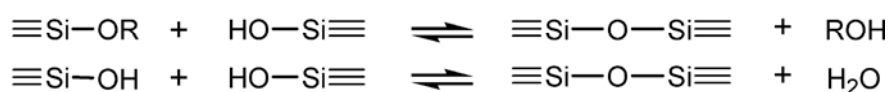
Scheme 1.2 A summary of the basic sol-gel reactions.[134]

Carrington and Xue developed a transparent, pyridine-functionalized sol-gel monolith for Cr (VI) sensing.[135-138] The method is illustrated in **Figure 1.13.** The monoliths were immersed in acidic Cr (VI) containing solutions and the Cr (VI) uptake was monitored using UV-Vis spectroscopy, at concentration of ppm level. The monolith exhibits a yellow colour change characteristic of Cr (VI) uptake and this can be measured by monitoring the absorption change at about the wavelength of 350 nm. Concentrations at the ppb level are

below the limit of detection using this wavelength of 350 nm for measurement. However, by adding a diphenylcarbazide solution to monoliths that have been previously immersed in ppb-level Cr (VI) solutions, a distinct colour change takes place within the gels that can be measured at 540 nm. Concentrations of Cr (VI) at as low as 10 ppb can be detected by this method.[129, 135]
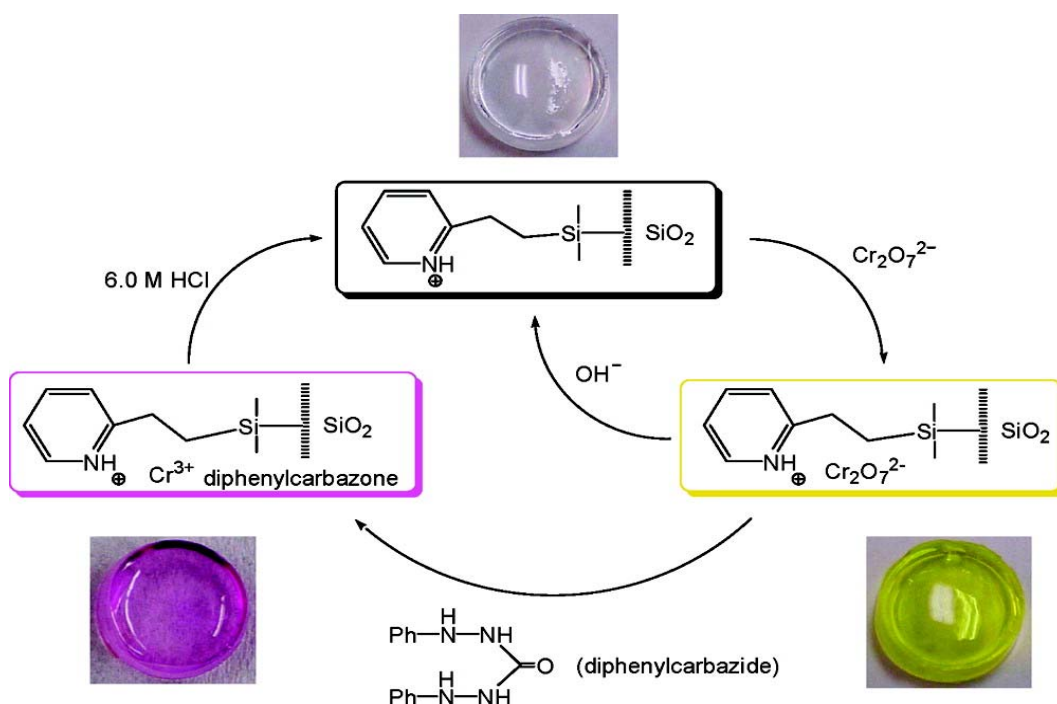
Figure 1.13 A sol-gel monolith optical sensor for Cr IV prepared by Carrington *et al.*[135]

Recently, organically modified silicates (ORMOSILs) can be prepared by organo-silicon precursors (R-Si(OR')$_3$) with TEOS or TMOS, to form an organic-inorganic hybrid film. ORMOSILs have become attractive due to the flexibility and the versatility of the matrix associate with the process of the preparation.[139] It has been reported that the introduction of organic groups into the gel network led to a decrease of the surface area, pore volume and pore size distribution, thus enabled crack-free films, albeit considerably longer response times, compared with the films prepared solely from the inorganic precursors.[131, 140, 141] Therefore, the substituted organic groups of the precursors greatly influence the textual properties of the ORMOSILs. Jerónimo et al. reported a sol gel optical sensor based on co-polymerization of tetraethoxysilane (TEOS) with 3-amynopropyltriethoxysilane (3-APTES) and incorporation 4-(2-pyridylao) resorcinol (PAR) for the determination of

zinc. This sensor featured with high sensitivity and fast response. Collinsons and co workers have reported that the ion-exchange and perm selectivity of ORMOSILs can be greatly affected by the organic functional group of the precursors used during the process.[140] As a result, the parameters, such as organic precursors, pH, basic or acidic catalysts, temperatures, have to be tailored carefully for the preparation of ORMOLs for metal ions sensing.[141]

Since the early steps of the sol-gel process occur in liquid phase, it is possible to add probe molecules at this stage. The reagents can be physically encapsulated (doping) in a nanometer-scale cage-like structure or grafting process to obtain an organofunctional sol-gel.[142] Doping involves the physical entrapment of a reagent inside the substrate, while grafting involves the anchoring of reagent through covalent bonding. Doping techniques are simple and applicable to many organic compounds, but the pore size must be carefully tailored because dopant leaching is often a problem. As an alternative to physical entrapment, the indicator dyes can also be covalently bound to the sol-gel matrix. This procedure normally required the chemical modification of the silicon precursors used. However, doping is actually the most common used method for entrapment of indicators in sol gel membrane, since some authors have suggested that covalent attachment might compromise the sensor performance by slower response time and smaller signal changes.

Thin films have shown morphology suitable for applications in optical sensing devices due to short path length for diffusion, and the versatility of coating on various substrates and commercial supports such as optical fibres. Guo et al. developed an optical membrane for sensing of Hg^{2+} in aqueous solution by doping 5,10,15, 20-tetraphenylporphyrin as fluorescence indicator in an organically modified sol gel membrane. A linear response over the Hg^{2+} concentration range of 5.0 x 10^{-6} to 1.0 x 10^{-4} mol/l with a detection limit of 3.6 x 10^{-6} mol/l is observed.[143]

By varying the sol-gel processing conditions, molecularly imprinted sol-gel materials (MIP) with controlled porosity and surface area have been prepared. Generally speaking, the imprinting process involves three steps: (1) selection of target analytes as templates, (2) incorporation of the template into the sol-gel (or even polymer) networks and (3) removal of the template leaving stable, selective cavities that are recognized as target analytes.[144]

Generally, molecular imprinting technique is another method of molecular recognition, and the process has been illustrated in **Figure 1.14.**
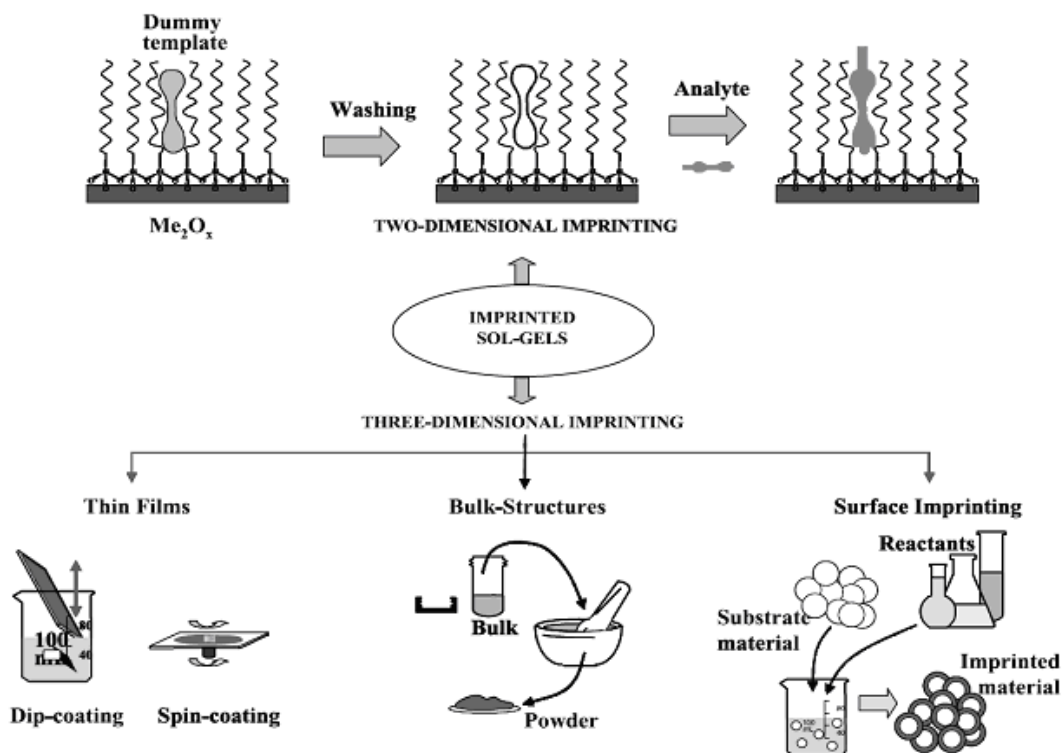
Figure 1.14 Sol-gel molecular imprinting options.[144]

A metal-ion binding affinity may be enhanced by imprinting the coordination environment of the metal ion by incorporation of a complexing ligand, which must be carefully selected as the key step to form a metal complex that survives the sol-gel process and leaves behind a suitable set of binding sites when the metal ion is removed. To form such a complex, ligands must be chosen that exhibit sufficiently large affinities to resist dissociation, otherwise the success of the end materials would be compromised. Dai and co-workers showed that sol-gel glasses prepared with the template $UO_2(NO_3)_2 \cdot H_2O$ exhibit enhanced affinity and selectivity for the uranyl ion relative to that observed for a similarly prepared control blank gel.[145]

The ligand imprinted monoliths for HMs sensing have been demonstrated by Xue and co-works, as an attractive configuration for metal ion application due to their highly porous nature and their longer sensor path length. **Figure 1.15** shows the preparation of a ligand grafted sol-gel monolith for the determination of Cu^{2+} ion. The analyte imprinted sol-gel

membrane can increase the selectivity to target analyte and prevent the leaching of the active reagent in the sensors. The linear detection range is from 200-800 mM.[139]
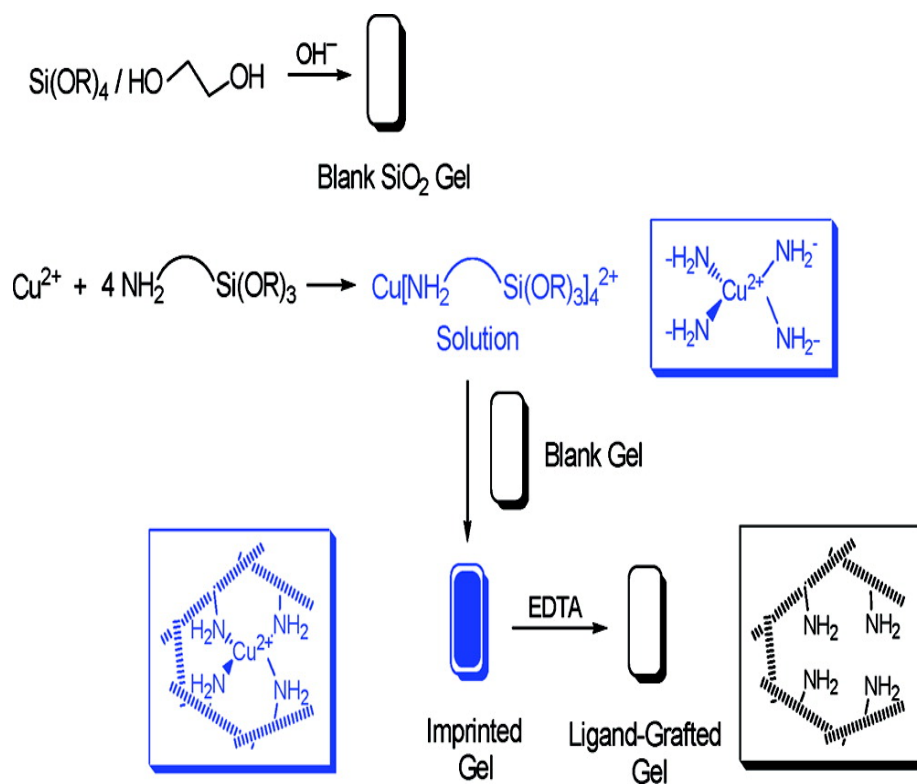
Figure 1.15 Preparation of the blank and amine-grafted sol-gel monolith.[145]

1.11 Mesoporous Materials

In 1992 researchers of Mobil Company discovered MCM (Mobil Composition of Matter)[146] and it is a preventative type of ordered mesoporous materials which display a honeycomb-like structure of uniform mesoporous (3 nm diameter).[147] Standard sol-gel materials have a non ordered, amorphous structure where diffusion of analytes can be limited by the random micro-porosity of the structure. More recently, mesostructured porous materials due to their large open porosity and large surface area, as well as their facile synthesis and robustness, are attractive as a support material for metal ions optical sensing.[148] The open porosity and large surface area can offer enhanced diffusion and accessibility.
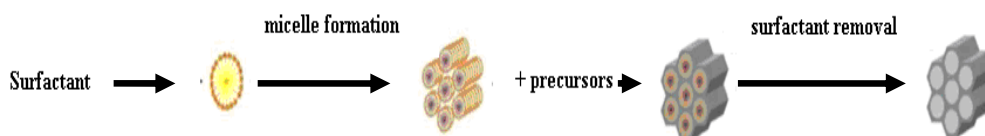
Figure 1.16 Process Of the preparation of MCMs.[148]

Such materials can be prepared by combining sol-gel chemistry with the 'texturisation' imposed by the physical chemistry of the surfactant and are deposited as thin films via surfactant removal approaches, such as the evaporation-induced self-assembly (EISA) approach.[149] The widely used surfactant is cetytrimethylammonium bromide (CTAB).
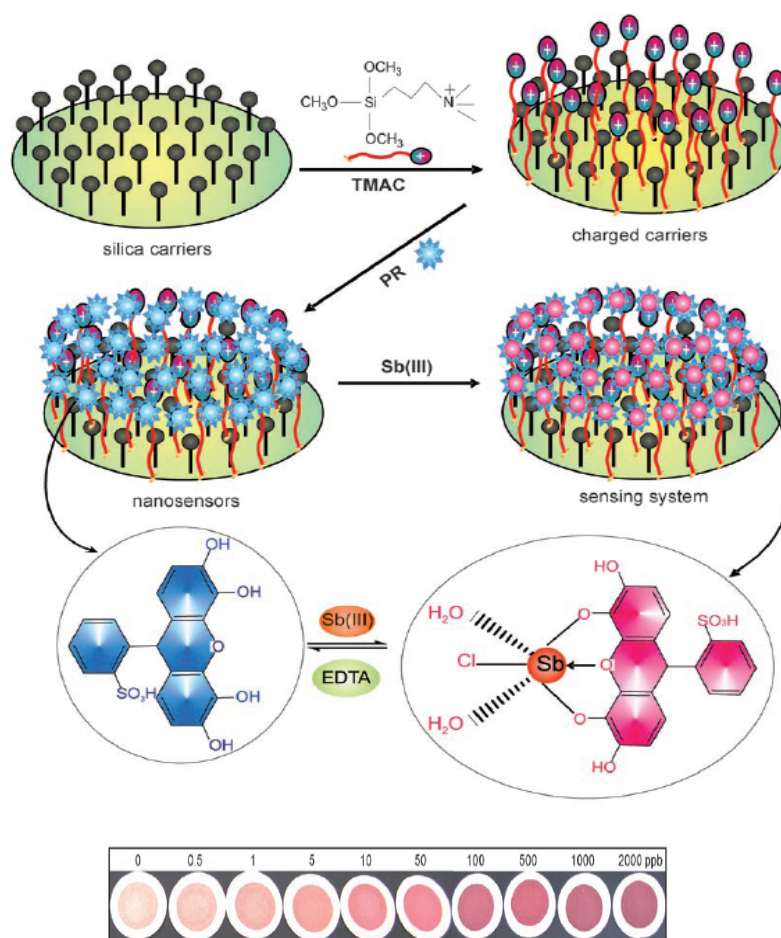
Figure 1.17 The naked-eye detection of various HMs prepared by El-Safty.[150]

These Mesoporous materials with a cubic cage structure were modified with various dyes to provide the potential sensing of Pb^{2+},[101] Sb^{3+},[112] Hg^{2+},[17] and Cd^{3+}.[17] The detection limits was obtained down to ppt level. This system is also called naked-eye nanosensor that was fabricated by the introduction of coupling agents, such as *N*-trimethoxysilylpropyl-*N,N,N*-trimethylammomium chloride (TMAC), on to the surface of hexagonal MCM-41 silica support and the positively charged coupling agent TMAC would trap a negatively charged probe molecule, such as Pyrogallol Red (PR) (**Figure 1.17**). This nano-sensor exhibited a high adsorption capability of the PR indicator and high accessibility to analyte ion transport, leading to possible naked-eye detection of Sb^{3+} ions at concentration as low as 10^{-9} mol/L and at a wide detection range of 0.5 ppb to 3 ppm with a faster response time.[151]

1.12 Aim of the Thesis

The accurate and on-site detection of low concentration of toxic heavy metal ions in aquatic environment is essential because of its lethal effects on the environment and living organisms. Conventional methods require high cost analytical instruments and complicated samples preparations. Nowadays, the development of portable, low cost, simple-to-use and accurate optical chemical sensors for determination of heavy metal ions is a great challenge.

The goal of this thesis is to develop novel optical sensing materials for use in portable, sensitive, selective, low cost and low toxic optical chemical sensors for the determination of toxic heavy metal ions in aqueous samples.

The specific objectives are shown in **Scheme 1.3**:
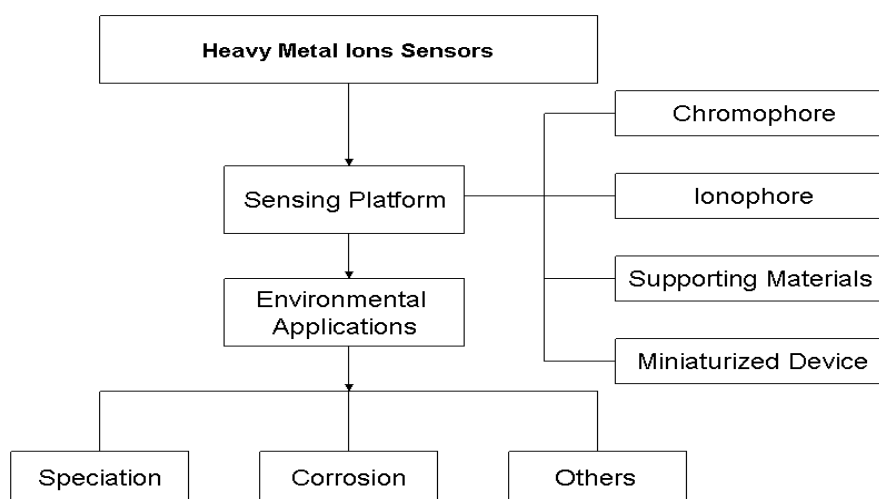
Scheme 1.3 Schematic graph of the objectives of the works.

The objectives of the thesis are: To investigate the potential commercially available organic indicators which can be incorporate with suitable solid support matrices for sensitively and selectively determination of heavy metal ions.

Reference

1. .H. J. Duffus. *Pure Appl. Chem* **2002**, 74(5), 793-807.

2. M. Hutton; Symon, C. *Sci. Total Environ.* **1986**, 57, 129-150.

3. J. G. Ayenimo; Yusuf, A. M.; Adekunle, A. S.; Makinde, O. W. *Bull Environ Contam Toxicol* **2009**.

4. W. O. Frederick. Hazardous and Toxic Substance, Marcel Dekker, INC, New York and Basel, 1978, p23-30.

5. A. Tessier; R.Turner, D. Metal Speciation and bioavailability in aquatic systems, New York: John Wiley, 1995, p102-109.

6. F. J. Cervantes; Pavlostathis, S. G.; Haandel, Advanced biological treatment processes for industrial wastewater: principles and applications, 2006, p89-110.

7. D. McGrath; McCormack, R. J. The significance of heavy metal and organic micropollutants in soils, Wexford: Teagasc, 1999, p65-79.

8. J. O. Duruibe; Ogwuegbu, M. O. C.; Egwurugwu, J. N. *In. J. Phy. Sc*i. **2007**, 2(5), 112-118.

9. W. T. S. lenntech. Heavy Metals.

10. V. Gopal; Parvathy, S.; Balasubramanian, *P. R. Environ Monit. Assess.* **1997**, 48(2), 117-124.

11. S. E. Nielsen; Wium-Andersen, S. Marine Biology 1970, 6(2), 93-97.

12. L. Mercier; Pinnavaia, T. J. Environ. Sci. Technol. 1998, 32(18), 2749-2754.

13. R. Rehwoldt; Lasko, L.; Shaw, C.; Wirhowski, E. *Bull. Environ. Contam. Toxicol.* **1973**, 10(5), 291-294.

14. EU Water Frame Work Directive, Directive 2000/60/EC: European Commission.

15. Guildlines for drinking water quality 3rd ed,. In W. H. Organization (Ed.), Geneva: World Health Organization (2008).

16. E. M. Werner; Ern Pretsch. *Electroanalysis,* **1995**, 7(9), 798-800.

17. E. Curdov; Vavruskov, L.; Suchek, M.; Baldrian, P.; Gabriel, J. *Talanta* **2004**, 62(3), 483-487.

18. K. Itoh; Chikuma, M.; Tanaka, H. *Fresenius' J. Anal. Chem.* **1988**, 330(7), 600-604.

19. M. Chan; Chan, I.; Kong, A.; Osaki, R.; Cheung, R.; Ho, C.; Wong, G.; Tong, P.; Chan, J.; Lam, C. *Pathology* **2009**, 41, 467-472.

20. M. Ghaedi; Niknam, K.; Shokrollahi, A.; Niknam, E.; Rajabi, H. R.; Soylak, M. *J Hazard Mater.* **2008,** 155(1-2), 121-127.

21. R. Q. Aucelio; Curtius, A. J. *J.Anal. Atom.Spec.* **2002**, 17(3), 242-247.

22. D. Diamond. Chemical Sensors. John Wiley & Sons, INC, 1998 p45-60.

23. O. S. Wolfbeis, editor. *Optical Sensors,* Industrial, Springer: Germany, 2004.

24. B. R. Eggins. Chem. Sens.Biosens, John Wiley & Sons, 2002.

25. J. Janata; Bezegh, A. Bibliography of chemical sensors 1985-1987, IE Sensors, Inc, 1988.

26. G. G. Cammann; Guilbault, E. A.; Hal, H. K., R.;; Wolfbeis, O. S. The Cambridge Defination of Chemical Sensors, Cambridge Workshorp in Chemical Sensos and Biosensors, Cambridge University Press: New York: New York, 1996.

27. C. McDonagh; Burke, C. S.; MacCraith, B. D. *Chem. Rev.* **2008,** 108(2), 400-422.

28. O. S. Wolfbeis. *J. Mater. Chem.* **2005,** 15(27-28), 2657-2669.

29. N. Verma; Singh, M. BioMetals 2005, 18(2), 121-129.

30. D. A. Blake; Jones, R. M.; Blake, R. C.; Pavlov, A. R.; Darwish, I. A.; Yu, H. *Biosens. Bioelec.* **2001**, 16(9-12), 799-809.

31. S. F. D'Souza. *Biosens.Bioelec.* **2001**, 16(6), 337-353.

32. I. Bontidean; Ahlqvist, J.; Mulchandani, A.; Chen, W.; Bae, W.; Mehra, R. K.; Mortari, A.; Csöregi, E. *Biosens.Bioelec.* **2003**, 18(5-6), 547-553.

33. S. Lee; Sode, K.; Nakanishi, K.; Marty, J.-L.; Tamiya, E.; Karube, I. *Biosens. Bioelec.* **1992**, 7(4), 273-277.

34. P. Corbisier; van der Lelie, D.; Borremans, B.; Provoost, A.; de Lorenzo, V.; Brown, N. L.; Lloyd, J. R.; Hobman, J. L.; Csöregi, E.; Johansson, G.; Mattiasson, B. *Anal. Chim. Acta* **1999,** 387(3), 235-244.

35. E. M. Bosch; Sanchez, J. R. A.; Rojas, S. F.; Ojada, B. C. *Sensors* **2007**, 7, 797-859.

36. H. C. Tsai; Doong, R. A.; Chiang, H. C.; Chen, K. T. *Anal. Chim. Acta* **2003**, 481(1), 75-84.

37. A. Senillou; Jaffrezic-Renault, N.; Martelet, C.; Cosnier, S. *Talanta* **1999,** 50(1), 219-226.

38. N. F. Starodub; Kanjuk, N. I.; Kukla, A. L.; Shirshov, Y. M. *Anal. Chim. Acta.* **1999**, 385(1-3), 461-466.

39. A. L. Kukla; Kanjuk, N. I.; Starodub, N. F.; Shirshov, Y. M. *Sens. Actuators B: Chem.* **1999**, 57(1-3), 213-218.

40. I. Bontidean; Berggren, C.; Johansson, G.; Csoregi, E.; Mattiasson, B.; Lloyd, J.

R.; Jakeman, K. J.; Brown, N. L. *Anal. Chem.* **1998,** 70(19), 4162-4169.

41. G.-q. Shi; Jiang, G. *Anal. Sci.* **2002,** 18(11), 1215-1219.

42. L. Basabe-Desmonts; Reinhoudt, D. N.; Crego-Calama, M. *Chem. Soc. Rev.* **2007,** 36(6), 993-1017.

43. E. Hirayama; Sugiyama, T.; Hisamoto, H.; Suzuki, K. Anal. Chem. 1999, 72(3), 465-474.

44. R. Sheng; Wang, P.; Gao, Y.; Wu, Y.; Liu, W.; Ma, J.; Li, H.; Wu, S. *Org. Lett.* **2008**, 10(21), 5015-5018.

45. T. Gunnlaugsson; Leonard, J. P.; Murray, N. S. *Org. Lett*. **2004,** 6(10), 1557-1560.

46. R. Martinez; Espinosa, A.; Tarraga, A.; Molina, P. *Org. Lett.* **2005**, 7(26), 5869-5872.

47. I. Oehme; Wolfbeis, O. S. *Microchim. Acta* **1997**, 126(3), 177-192.

48. H. Hisamoto; Tohma, H.; Yamada, T.; Yamauchi, K.-i.; Siswanta, D.; Yoshioka, N.; Suzuki, K. *Anal. Chim. Acta* **1998,** 373(2-3), 271-289.

49. E. Bishop. Indicators 1st ed, Pergamon press: New York, 1972.

50. M. Gerloch; Constable, C. E. Transition Metal Chemistry, The Valence Shell in d-Block Chemistry, VCH, 1994, p103-300.

51. G. R. Pearson. Benchmark Papers in Inorganic Chemistry, John Wiley&Sons, INC, p55-155.

52. Z. Heinrich. Color chemistry : syntheses, properties, and applications of organic dyes and pigments, Zurich : Weinheim : Verlag Helvetica Chimica Acta ; Wiley-VCH, 2003, p34-78.

53. E. W. Morf; Seiler, K.; Lehmann, B.; Behringer, C.; Hartman, K.; Simon, W. *Pure & Appl. Chem* **1989**, 61(9), 1613-1989.

54. E. Pungor. *Microchim. Acta* **1990**, 100(3), 129-130.

55. E. Bakker; Simon, W. *Anal. Chem.* **2002**, 64(17), 1805-1812.

56. E. Bakker. *Anal. Chem.* **2004**, 76(12), 3285-3298.

57. E. Bakker; Pretsch, E. *Anal. Chem.* **2002,** 74(15), 420 A-426 A.

58. W. E. Morf; Wuhrmann, P.; Simon, W. *Anal. Chem.* **2002,** 48(7), 1031-1039.

59. W. E. Morf; Seiler, K.; Rusterholz, B.; Simon, W. *Anal. Chem.* **2002**, 62(7), 738-742.

60. J. Senkyr; Ammann, D.; Meier, P. C.; Morf, W. E.; Pretsch, E.; Simon, W. *Anal. Chem.* **2002**, 51(7), 786-790.

61. W. E. Morf; Kahr, G.; Simon, W. *Anal. Chem.* **2002**, 46(11), 1538-1543.

62. P. C. Hauser; Perisset, P. M. J.; Tan, S. S. S.; Simon, W. *Anal. Chem.* **2002**, 62(18), 1919-1923.

63. Y. Qin; Peper, S.; Radu, A.; Ceresa, A.; Bakker, E. *Anal. Chem.* **2003**, 75(13), 3038-3045.

64. B. Peng; Qin, Y. *Anal. Chem.* **2008,** 80(15), 6137-6141.

65. W. Ngeontae; Xu, C.; Ye, N.; Wygladacz, K.; Aeungmaitrepirom, W.; Tuntulani, T.; Bakker, E. *Anal. Chim. Acta* **2007,** 599(1), 124-133.

66. D. Citterio; Takeda, J.; Kosugi, M.; Hisamoto, H.; Sasaki, S.-i.; Komatsu, H.; Suzuki, K. *Anal. Chem.* **2006**, 79(3), 1237-1242.

67. R. M. Izatt; Christensen, J. J.; Kothari, V. Inorg. Chem. 2002, 3(11), 1565-1567.

68. R. M. Izatt; Pawlak, K.; Bradshaw, J. S.; Bruening, R. L. *Chem. Rev.* **2002**, 95(7), 2529-2586.

69. J. S. Bradshaw; Izatt, R. M. *Acc. Chem. Res.* 1997, 30(8), 338-345.

70. J. L. Oscarson; Liu, B.; Izatt, R. M. *Ind. Eng. Chem. Res.* **2004**, 43(23), 7635-7646.

71. S. H. Gellman. *Chem. Rev.* **1997**, 97(5), 1231-1232.

72. M. H. Keefe; Benkstein, K. D.; Hupp, J. T. *Coord. Chem. Rev.* **2000**, 205(1), 201-228.

73. A. P. de Silva; Gunaratne, H. Q. N.; Gunnlaugsson, T.; Huxley, A. J. M.; McCoy, C. P.; Rademacher, J. T.; Rice, T. E. *Chem. Rev.* **1997**, 97(5), 1515-1566.

74. B. Valeur; Leray, I. *Coord. Chem. Rev.* **2000**, 205(1), 3-40.

75. L. Prodi; Bolletta, F.; Montalti, M.; Zaccheroni, N. *Coord. Chem. Rev.* **2000,** 205(1), 59-83.

76. O. Oter; Ertekin, K.; Kirilmis, C.; Koca, M.; Ahmedzade, M. *Sens. Actuators B: Chem.* **2007**, 122(2), 450-456.

77. S.-Y. Moon; Youn, N. J.; Park, S. M.; Chang, S.-K. *J. Org. Chem.* **2005**, 70(6), 2394-2397.

78. F. Faridbod; Ganjali, R. M.; Dinarvand, R.; Norouzi, P.; Riahi, H. *Sensors* **2008**, 8, 1645-1703.

79. N.Wanichacheva; Siriprumpoonthum, M.; Kamkaew, A.; Grudpan, K. *Tetrahedron. Lett.* **2009**, 50(16), 1783-1786.

80. B. S. Creaven; Donlon, D. F.; McGinley, *J. Coord. Chem. Rev.* **2009**, 253(7-8), 893-962.

81. B. Bag; Bharadwaj, P. K. *J. Luminescence,* **2004**, 110(1-2), 85-94.

82. A. Başoğlu; Parlayan, S.; Ocak, M.; Alp, H.; Kantekin, H.; Özdemir, M.; Ocak, Ü. *J. Fluorescence,* **2009**, 19(4), 655-662.

83. A. T. Yordanov; Whittlesey, B. R.; Roundhill, D. M. *Inorg. Chem.*, **1998**, 37(14), 3526-3531.

84. B. Volker. *Angew. Chem. Int. Ed. in English* **1995**, 34(7), 713-745.

85. A. T. Yordanov; Falana, O. M.; Koch, H. F.; Roundhill, D. M. *Inorg. Chem.* **1997**, 36(27), 6468-6471.

86. H.-Y. Gong; Wang, D.-X.; Zheng, Q.-Y.; Wang, M.-X. *Tetrahedron* **2009,** 65(1), 87-92.

87. K. Belhamel; Ludwig, R.; Benamor, M. *Microchim. Acta* **2005,** 149(1), 145-150.

88. A. Ikeda; Shinkai, S. *Chem. Rev.* **1997**, 97(5), 1713-1734.

89. R. Ludwig; N, D. T. K. *Sensors*, **2002**, 2, 379-416.

90. J. J. Christensen; Izatt, R. M.; Eatough, D. *Inorg. Chem.* **2002**, 4(9), 1278-1280.

91. J. V. D. V. Niels; Ewa, R.; Ln, A. W.; Michal, C.; Jurriaan, H.; Frank, C. J. M. v. V.; David, N. R. *Chem. - A Euro. J.* **2001**, 7(22), 4878-4886.

92. P. Jose; Menon, S. *Bioinorg. Chem. Appl.* **2007**, 2007.

93. S. E. J. Bell; Browne, J. K.; McKee, V.; McKervey, M. A.; Malone, J. F.; O'Lear, M.; Walker, A.; Arnaud-Neu, F.; Boulangeot, O.; Mauprivez, O.; Schwing-Weill. *J. Org. Chem.* **1998**, 63(3), 489-501

94. F. Cadogan; Kane, P.; McKervey, M. A.; Diamond, D. *Anal. Chem.,* **1999**, 71(24), 5544-5550.

95. C. Pedersen. *J. Am. Chem. Soc.* **2002**, 92(2), 391-394.

96. C. J. Pedersen. *J. Am. Chem. Soc.* **2002,** 89(26), 7017-7036.

97. E. Malinowska; Brz.ka, Z.; Kasiura, K.; Egberink, R. J. M.; Reinhoudt, D. N. *Anal. Chim. Acta* **1994**, 298(2), 253-258.

98. P. L. H. M. Cobben; Egberink, R. J. M.; Bomer, J. G.; Bergveld, P.; Verboom, W.; Reinhoudt, D. N. *J. Am. Chem. Soc.* **2002**, 114(26), 10573-10582.

100. R. J. W. Lugtenberg; Egberink, R. J. M.; J., E. F.; Reinhoudt, D. N. *J Chem Soc, Perkin Trans,* 2 **1997**, 1997, 1353-1357

101. X. Zhang; Liu, C.; Wu, W.; Wang, J. Mater. Lett. 2006, 60(17-18), 2086-2089.

102. M. Narita; Higuchi, Y.; Hamada, F.; Kumagai, H. *Tetrahedron. Lett.* **1998**, 39(47), 8687-8690.

103. P. Kumar; Shim, Y.-B. *Talanta* **2009**, 77(3), 1057-1062.

104. H. G. Loehr; Voegtle, F. *Acc.Chem. Res.* **2002,** 18(3), 65-72.

105.   L. Rivera; Izquierdo, D.; Garce, I.; Salinas, I.; Alonso, J.; Puyol, M. *Sens. Actuators B: Chem,* **2009,** 137(2), 420-425.

106.   N. Malcik; Oktar, O.; Ozser, M. E.; Caglar, P.; Bushby, L.; Vaughan, A.; Kuswandi, B.; Narayanaswamy, R. *Sens. Actuators B: Chem.* **1998,** 53(3), 211-221.

107. F. Baldini; Bracci, S.; Cosi, F.; Bechi, P.; Pucciani, F. *Appl. Spec.* **1994**, 48, 549-552.

108. A. A. Ensafi; Katiraei Far, A.; Meghdadi, S. *Sens.Actuators B: Chem* **2008,** 133(1), 84-90.

109. B. S. Rao; Puschett, J. B.; Matyjaszewski, K. J. *Appl. Poly. Sci.* **1991**, 43(5), 925-928.

110. J. Samuel; Strinkovski, A.; Shalom, S.; Lieberman, K.; Ottolenghi, M.; Avnir, D.; Lewis, *A. Mater. Lett.* **1994**, 21(5-6), 431-434.

111. J. E. Lee; Saavedra, S. S. Anal. Chim. Acta 1994, 285(3), 265-269.

112. O. S. Wolfbeis; Rodriguez, N. V.; Werner, T. *Microchim. Acta* **1992,** 108(3), 133-141.

113. J. W. Parker; Laksin, O.; Yu, C.; Lau, M. L.; Klima, S.; Fisher, R.; Scott, I.; Atwater, B. W. *Anal. Chem.* **1993**, 65(17), 2329-2334.

114. B. D. Gupta; Sharma, S. *Opt. Comm.* **1998**, 154(5-6), 282-284.

115. G. Mohr. POLYMERS FOR OPTICAL SENSORS. *In. Opt. Chem. Sens.,* **2006**; pp 297-321.

116. J. Ho Youk. *Polymer* **2003**, 44(18), 5053-5056.

117. J. M. Park; Shon, O. J.; Hong, H.-g.; Kim, J. S.; Kim, Y.; Lim, H. B. *Microchem. J.* **2005**, 80(2), 139-144.

118. J. H. Poplin; Swatloski, R. P.; Holbrey, J. D.; Spear, S. K.; Metlen, A.; Gratzel, M.; Nazeeruddin, M. K.; Rogers, R. D. *Chem. Comm.* **2007**(20), 2025-2027.

119. B. Khezri; Amini, M.; Firooz, A. *Anal. Bioanaly. Chem.* **2008**, 390(7), 1943-1950.

120. I. M. Steinberg; Lobnik, A.; Wolfbeis, O. S. *Sens. Actuators B: Chem.* **2003**, 90(1-3), 230-235.

121. M. K. Amini; Momeni-Isfahani, T.; Khorasani, J. H.; Pourhossein, M. *Talanta* **2004**, 63(3), 713-720.

122. L. d. Coo; Belmonte, C. J. *Talanta* **2002**, 58(6), 1063-1069.

123. J. Ueberfeld; Parthasarathy, N.; Zbinden, H.; Gisin, N.; Buffle, *J. Anal.Chem.* **2001**, 74(3), 664-670.

124. Z. Hu; Seliskar, C. J.; Heineman, W. R. *Anal.Chem.* **1998**, 70(24), 5230-5236.

125. A. N. Khramov; Collinson, M. M. *Anal.Chem.* **2000,** 72(13), 2943-2948.

126.T. Carofiglio; Fregonese, C.; Mohr, G. J.; Rastrelli, F.; Tonellato, U. *Tetrahedron* **2006**, 62(7), 1502-1507.

127.D. Delmarre; Mllet, R.; Bied-Charreton, C.; Pansu, R. B. *J Photochem. Photobio. A: Chem.* **1999,** 124(1-2), 23-28.

128. A. A. Ismail. *J. Colloid   Interface Sci.* **2008,** 317(1), 288-297.

129. C. W. Clavier; Rodman, D. L.; Sinski, J. F.; Allain, L. R.; Im, H.-J.; Yang, Y.; Clark, J. C.; Xue, Z.-L. J. *Mater. Chem.* **2005**, 15(24), 2356-2361.

130. L. Nicole; Boissiere, C.; Grosso, D.; Quach, A.; Sanchez, C. *J. Mater.Chem.* **2005,** 15(35-36), 3598-3627.

131. P. C. A. Jeroimo; Arauo, A. N.; Montenegro, M. C. B. S. M. *Sens. Actuators B: Chem.* **2004**, 103(1-2), 169-177.

132. A. Lukowiak; Strek, W. *J. Sol-Gel Sci.Tech.* **2009**, 50(2), 201-215.

133. M. M. Collinson. *Trends Anal. Chem.* **2002**, 21(1,2002).

134.J. C. Brinker; Scherer, W. G. Sol-gel Science, the Physics and Chemistry of Sol gel Processing, Academic Press, INC. Harcourt Brace Jovanovich, Publishers, 1990.

135. N. A. Carrington; Xue, Z.-L. *Acc. Chem. Res.* **2007**, 40(5), 343-350.

136.H.-J. Im; Yost Terry, L.; Yang, Y.; Bramlett, J. M.; Yu, X.; Fagan Bryan, C.; Allain Leonardo, R.; Chen, T.; Barnes Craig, E.; Dai, S.; Roecker Lee, E.; Sepaniak Michael, J.; Xue, Z.-L. Organofunctional Sol-Gel Materials for Toxic Metal Separation. In. Nuclear Waste Management, American Chemical Society: Washington, DC, 2009; pp 223-237.

137. Nuclear Waste Management, American Chemical Society: Washington, DC, 2006; i-352 p.

138. D. L. Rodman; Pan, H.; Clavier, C. W.; Feng, X.; Xue, Z.-L. *Anal. Chem.* **2005**, 77(10), 3231-3237.

139. H. Xi-Wen; Poe, D. P. *Anal. Chim. Acta* **1981**, 131, 195-203.

140. H. Wei; Collinson, M. M. *Anal. Chim. Acta* **1999**, 397(1-3), 113-121.

141. M. Park; Komarneni, S.; Choi, J. *J. Mater. Sci.* **1998,** 33(15), 3817-3821.

142. B. D. MacCraith; McDonagh, C. M.; O'Keeffe, G.; McEvoy, A. K.; Butler, T.; Sheridan, F. R. *Sens. Actuators B: Chem.* **1995**, 29(1-3), 51-57.

143. L. Guo; Zhang, W.; Xie, Z.; Lin, X.; Chen, G. *Sens. Actuators B: Chem.* **2006**, 119(1), 209-214.

144. M. E. Díaz-García; Laínño, R. B. *Microchim. Acta* **2005**, 149(1), 19-36.

145. S. Dai; Burleigh, M. C.; Ju, Y. H.; Gao, H. J.; Lin, J. S.; Pennycook, S. J.; Barnes, C. E.; Xue, Z. L. *J.Am. Chem. Soc.* **2000**, 122(5), 992-993.

146. P. T. Tanev; Pinnavaia, T. *J. Science* **1995**, 267(5199), 865-867.

147. J. S. Beck; Vartuli, J. C.; Roth, W. J.; Leonowicz, M. E.; Kresge, C. T.; Schmitt, K. D.; Chu, C. T. W.; Olson, D. H.; Sheppard, E. W. *J.Am. Chem. Soc.* **2002**, 114(27), 10834-10843.

148. B. Melde; Johnson, J. B.; Charles, T. P. *Sensors* **2008**, 8, 5202-5228.

149. C. J. Brinker; Yunfeng, L.; Alan, S.; Hongyou, F. *Adv. Mater.* **1999**, 11(7), 579-585.

150. S. A. El-Safty; Prabhakaran, D.; Ismail, A. A.; Matsunaga, H.; Mizukami, F. *Chem. Mater.* **2008,** 20(8), 2644-2654.

151. S. A.. El-Safty; Prabhakaran, D.; Ismail, A..; Matsunaga, H.; Mizukami, F. *Adv. Func. Mater.,* **2007**, 17(18), 3731-3745.

152. C.-C. Huang; Chang, H.-T. *Anal. Chem.* **2006**, 78(24), 8332-8338.

153. J. Kimling; Maier, M.; Okenve, B.; Kotaidis, V.; Ballot, H.; Plech, A. *J. Phy. Chem. B,* **2006**, 110(32), 15700-15707.

Chapter 2

2.1. Introduction

A complex between a synthetic dye and metal ion used as a chemosensing ensemble is given that the complexation of the indicator with heavy metal ion leads to a change in colour or fluorescence. Sensors of this type are commonly referred to probe.[1] UV-Vis spectrometry or fluorescence are normally used to obtain information about the complexation, and thus about the identity and/or quantity of the metal ion. The spectrophotometric method involving the use of the chromophoric chelator of indicators for the assessment of metal ion content sensing heavy metal ions has gained popularity during recent years because it is not only simple but also less costly and labour-intensive than those techniques requiring instrumentations that are more sophisticated. In this research, UV-Vis spectrometry used as the main instrument for the detection is due to its accuracy and simplicity. In this chapter, several indicators were tested in solution chemistry. In the following sections, the principle of UV-Vis spectrometry is briefly introduced and the complexation ability of several ligands (parameters such as pKa, the stoichiometry, formation constants and molar absorptivity) is discussed after having being studied.

2.1.1 Spectroscopic Principles

Spectroscopic methods play an important role in various areas of analytical sensing. These methods rely on the fact that there is an interaction between electromagnetic radiation and matter.[2] In chemical sensors, a wide range of wavelengths covered by optical techniques can be divided into the ultraviolet (200-400 nm), the visible (400-780), the near infrared (780-3000 nm) and the infrared (3-50 μm) regions.[3] When electromagnetic radiations in the optical region interact with matter, dispersion, absorption, diffraction, refraction and inflection of the light can occur.[4]

Absorbance spectrometry is used in conjunction with dry reagent chemistries in the development of optical chemical (biochemical) sensors for the application in the detection of heavy metal ions in aqueous environments.[5] Transition metal complexes often have spectacular colours caused by electronic transitions by the absorption of

light.[6] Most transitions related to the colour of metal complexes are either *d-d* transitions or charge transfer band transitions. In a *d-d* transition, an electron in a *d* orbital of the transition metal is excited by a photon to another d orbital of higher energy. When white light passes through a solution of this ion, some of the energy in the light is used to promote an electron from the lower set of orbital into a space in the upper set. Each wavelength of light has a particular energy associated with it and then the solution of the mixture show the colour of the light it absorbs.[3, 7] A charge transfer band entails promotion of electrons from a metal-based orbital into an empty ligand-based orbital (Metal-to-Ligand Charge Transfer or MLCT).[3] The converse also occurs: excitation of an electron in a ligand-based orbital into an empty metal-based orbital (Ligand to Metal Charge Transfer or LMCT). These phenomena can be observed with the aid of electronic spectroscopy; also known as UV-Vis spectroscopy. Although some modern analytical approaches, such as AAS, ICP-MS, HPLC etc., have been used for the determination of heavy metal ions, none of them rival UV-Vis spectrometry for its simplicity, versatility, speed and cost-effectiveness. In recent years, with the development of miniaturised devices, the application of miniaturised UV-Vis spectrophotometers for environmental monitoring receives has received much attention once again.[4, 8, 9]

2.1.2 Beer-Lambert's Law

The fundamental relationship used in absorption measurements is the Beer-Lambert's Law which is shown in the **Equation (2.1and 2.2)**

$$I_T = I_o \, 10^{-\varepsilon LC}$$
(Eq. 2.1)

Or $A = \lg (I_o / I_T) = \varepsilon LC$
(Eq. 2.2)

Where

I_o = light intensity at wavelength λ;

I_T = light transmitted at wavelength λ;

ε = molecular extinction coefficient at wavelength λ (l mol^{-1} cm^{-1});

L = thickness of cell (cm);

C = concentration of solution contained in cell (cm L^{-1}).

For any wavelength and any given system, the value ε of a specific compound should be constant at all dilutions and all thicknesses of absorbent.

2.1.3 Indicator-Metal Complexation

The metal ion recognition system is based on the interaction/complexation of the various ligands with heavy metals to form highly coloured complexes (chelates). This area is called 'coordination' in modern chemistry.[3] Coordination complexes of transition metal ions with ligands were known since the beginning of chemistry (i.e. the Prussian Blue).[10] The key breakthrough occurred when Alfred Werner was awarded the Noble Prize for chemistry in respect of his work on the recognition of transition metals with ligands.[11] As a result of existing knowledge and expertise with classical spectrophotometric indicators, there is a wide choice in commercially available chromo-reagents for heavy metal ion sensing.[12, 13] Generally speaking, these indicators should include the following basic characteristics:

(1) Stability. The indicator can form a stable HM-Indicator complex either in solution or solid matrix; this could be characterised with the formation constant of the complex and the stoichiometry of the complexes;[14] large value of formation constants indicate stable complexes.

(2) Sensitivity. The indicator can form a strong coloured HM-Indicator complex. The molar absorptivity (ε, from Beer-Lambert's Law in **Equation 2.1**), is the parameter to evaluate how strong the HM-indicator complex absorbing light at the given wavelength is. It is the intrinsic property of the absorbing species;[15]

(3) Two-wavelength indicators are preferable. Their colour changes occur upon binding with HM ions that leads to one band appearing as the other disappears, rather than an intensity change of one single band. These indicators are advantageous over other indicators since they lead themselves to two-wavelength internal referencing methods

where the ratio of intensities of two bands is the analytical information rather than the intensity of a single band; [12]

(4) Rapid and reproducible reaction of complexation with HMs.

(5) Selectivity of the reagent-analyte reaction to metal ions at a specific wavelength.[8]

2.1.4 Metal-Ligand Complex Stoichiometry

The stoichiometric determination of the metal-ligand ratio is the first step in the characterisation of a new complex and provides complementary information in studies to obtain information of the structures. Methods often used are Job's method and mole-ratio method.[16] Job's Method, also called the Method of Continuous Variation, is a simple and effective approach to the determination of chemical reaction stoichiometry. For the following reaction:

$$aA + bB <===> dD \qquad \qquad \textbf{(Eq. 2.3)}$$

Eq. 2.3 can be rewritten in the form of **Eq. 2.4** by dividing all coefficients by "a".

$$A + kB <===> mD \qquad \qquad \textbf{(Eq.2.4)}$$

where k = b/a and m = d/a. Job's method is based on the following fact: if a series of solutions is prepared, each containing the same total number of moles of A and B, but a different ratio, R, of moles B to moles A, the maximum amount of product, D, is obtained in the solution in which R = k (the stoichiometric ratio). To implement Job's Method experimentally, a series of solutions containing a fixed total number of moles of A and B should be prepared, but in which the R is systematically varied from large to small, and measures the amount of product obtained in each solution. One then plots amount of product versus R, and obtains a maximum at the initially-unknown value of k.

That the maximum amount of product should occur at the stoichiometric ratio can be justified mathematically. The mathematical justification is quite simple. Variable "x" is used to represent the moles of A in a particular solution, and assume that the total moles of A and B is to be kept at 1.0 throughout the series of solutions. Then in each solution it will be true that:

$$x = \text{moles of A}$$

$$1-x = \text{moles B}$$

The goal is to show that the maximum amount of product is obtained when R = moles B/moles A = (1-x)/x is equal to k. We approach this by finding the value of x that maximizes product. According to **Eq.2.4**, if x is less than the stoichiometrically correct amount of A, then A is limiting and moles product = mx. A plot of moles product versus x over a series of solutions should be linear, with slope m. Similarly, if x exceeds the stoichiometrically correct amount of A, then B is limiting and moles product = m(1-x)/k. A plot of moles product versus x over a series of solutions should also be linear, with slope = -m/k. The first plot will proceed up to the right as x increases. The second plot will proceed down to the right as x increases. At some point then, the two straight lines will intersect. At the intersection, they have a point in common. The value of x corresponding to this point is obtained by equating the ordinate values and solving for x:

$$Mx = m(1-x)/k$$

Solving gives x = 1/(1+k).

Substituting in the expression for R, (1-x)/x, we find that the two lines intersect when

$$R = (1-x)/x = \{1 - [1/(1+k)]\}/[1/(1+k)] = k.$$

56

Because the amount of product increases as k is approached from either direction, the point of intersection of the lines occurs at the maximum amount of product obtainable. We have therefore shown that maximum product is obtained when R = k. A Job's Method study yields the following data. Plot quantity of product versus moles A to determine the stoichiometry. This methods will be explained in Appendix II and the examples are also demonstrated in Appendix II.

2.1.5 Formation Constants of the Complexes

The formation constant is also called the equilibrium constant. Equilibrium is a dynamic state in which the rate of formation of the products is equal to the rate of formation of the reactants (Also called the Law of Mass Action). A state of chemical equilibrium will remain until the system is altered by some outside factors, such as pH, temperature and the concentration of the reactants, etc. Chelated complexes are more stable than complexes from monodentate lignads. This is because the dissociation of the complex involves the breaking of two or more bonds as apposed to one. Complexes formed between hydrated metal ions and other organic molecules or ions are usually formed by coordination through one or more atoms of oxygen, nitrogen or sulphur. These atoms contain an unshared pair of electrons, which are capable of satisfying the coordination number of the metal. In most cases, the formation and dissociation of the complex proceeds rapidly in a succession of equilibrium reactions. The coordination groups are known as electron donating ligands (L) and electron pair accepting metal ion receptors (M). By the *Brønsted* definition, the ligand is a base, while the metal ion competes with protons in attempting to react with ligands in solvents.[17]

It is expressed by the following **Equation (2.5).**

$$M(H_2O)_n + L = M(H_2O)_{n-1}L + H_2O \qquad \textbf{(Eq.2.5)}$$

Where: M =Metal; L=ligand (mono or polydentate); and n=number of moles.
The formation constant (stability constant) K_f of this stepwise equilibrium is shown in **Equation 2.6:**

$$K_f = \frac{[ML_n]}{[ML_{n-1}][L]}$$
(Eq. 2.6)

The formation constants of indicator-metal complexes can be influenced by the cation size and type of donor atom of the ligands.

2.1.6 Indicators Used for the Sensor Application

Most of the indicators investigated in this chapter are azo dyes. They are the largest group of synthetic colourants.[6, 18] Azo compounds with substituents such as amino groups, hydroxyl groups, or $-SO_3$ groups have been reported as HMs indicators.[19, 20]

2-(5-bromo-2-pyridylazo)-5-diethylaminophenol (Br-PADAP) is a pyridyl-azo. The structure of Br-PADAP is shown in **Figure 2.1 (a).** It contains three possible electron donating sites: the nitrogen atoms of $-N=N-$ bond, the nitrogen atom in pyridine, and the orth-hydroxy oxygen. Br-PADAP can form highly stable complexes with HMs with relatively high molar absorptivity values of up to 1.1×10^5 l mol^{-1} cm^{-1}.[21] Due to its good affinity with heavy metals, it has been proposed as a chelating reagent for the determination of HMs, such as nickel, [21, 22] zinc,[23] mercury,[24] arsenic,[25] lead,[26] and thallium,[27] etc. For example it was used as a preconcentration reagent for the simultaneous determination of Mn^{2+}, Cu^{2+} and Fe^{3+} by adsorptive cathodic stripping voltammetry at a carbon paste electrode.[28] Due to its good compatibility with various solid matrices for optical sensors, it has been used as chromophore immobilised into various solid supports for the fabrication of optical sensors for heavy metal ions.[24, 29, 30] Fouladgar et al. reported an optical sensor for thallium (III) based on Br-PADAP recently. It was found that formation of the complex between thallium (III) and Br-PADAP caused a new peak to appear with a maximum absorbance at 569 nm and the colour of the membrane to change from orange to purple.[31] The solid supports that have been used to immobilise the Br-PADAP include: sol-gel thin films, plasticised PVC membranes, and XRD-4 membrane, etc. It also was reported that Br-PADAP forms complexes with Hg^{2+} and Ni^{2+} usually in ML_2 form.[24]

The second indicator that has been investigated in this work is a sulphonated azo dye, 3-hydroxy-4-[(6-hydroxy-m-tolyl)]-naphthalenesulfonic acid, also called Calmagite

(CAL). The structure of it is shown in **Figure 2.1 (b)**. CAL has been used to pre-concentrate copper ions prior to the determination by ICP-AES and FAAS. It also has three possible electron donating sites, the two nitrogen atoms in the azo group, two -OH groups and a sulfonate group. CAL is a well known indicator for complexometric titration of Ca^{2+}, and a photometric indicator for Al^{3+},[32] Mg^{2+}, [33] and lantanides.[5] The water soluble CAL is characterised with a red colour in acidic solution, blue colour in basic water solution, and reddish-brown colour in solution with pH value above 13. CAL forms strong complexes with a number of HMs and has been employed in colourimetric sensors for heavy metal ions.[34] Ferreira et al. used it for complexation of copper and enrichment of the complex on an XAD-2 column.[34, 35] It has been reported that CAL forms a 1:1 complex with copper ion.[34] Hashemi et al. fabricated a calmagite immobilised agarose membrane optical sensor for selective monitoring of Cu^{2+} and a linear response curve was observed for the membrane sensor in the Cu^{2+} concentration range of 0.4–200 µg l^{-1} with an R^2 value of 0.997. The sensor showed a good durability and short response time with no evidence of reagent leaching. The sensor was successfully applied for the determination of Cu^{2+} in environmental water samples.[34]

Acid Alizarin Violet N (AVN), (also called Acid Chrome K or Mordant Violet 5), is sulphonated azo dye.[36] The structure of it is shown in **Fig. 2.1 (c).** Similar with CAL, it contains a naphthyl group bounding to a phenyl ring through the azo group.[16] The negatively charged sulfonate group is located away from the coordinating sites.[37] AVN is soluble in water and also forms a red solution at pH below 7 solutions. In comparison with CAL, it has no methyl group and it is more slightly hydrophilic. It has been used as a chelating sorbent for copper, zinc, calcium and iron.[20] Swieboda et al. reported that, the complexes of AVN with Ca, Mg and Zn are not stable at high pH values of the solution in comparison with complexes with iron at concentrated acidic solutions when the concentrations of chloric (VII) acid are used.[38] Similarly with CAL, AVN forms a 1:1 or 1:2 complex with heavy metal ions.[39]
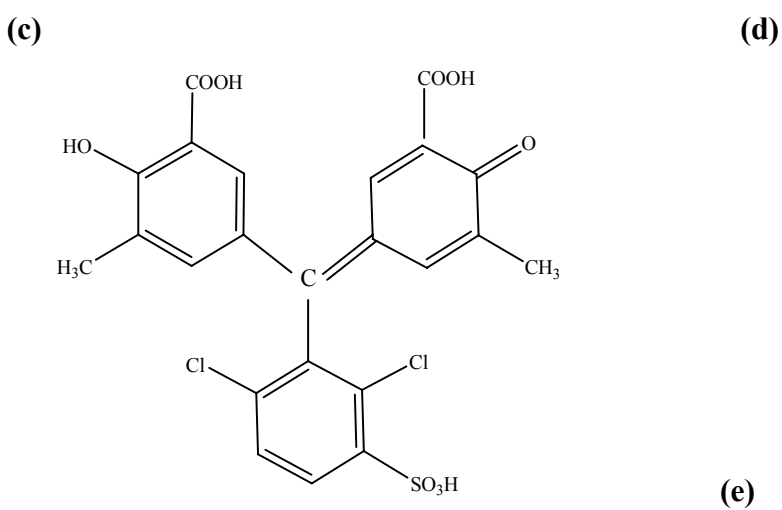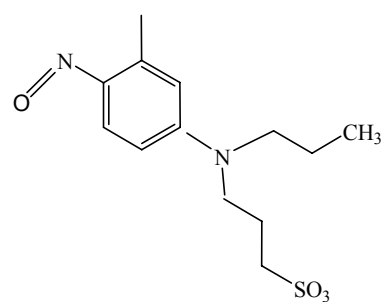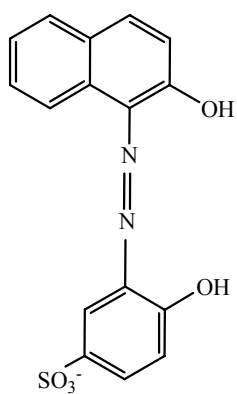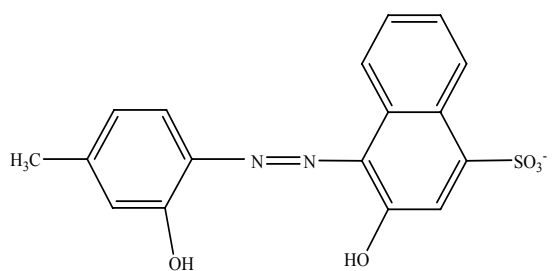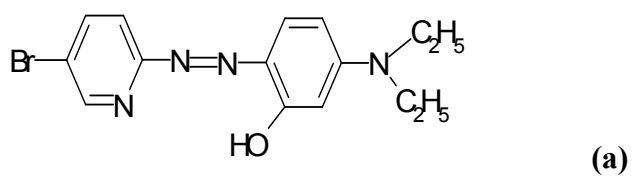
Figure 2.1 Chemical Structures of indicators, (a) Br-PADAP; (b) CAL, (c) AVN, (d) Nitroso-PASP, (e) CAS.

Nitroso-phenol and nitrosonaphthol derivatives were used for the determination of HMs such as iron and nickel in solutions.[40-41] 2-Nitroso-(5-*N*-propyl-*N*-sulfopropiamino) phenol (Nitroso-PAPS) was synthesised by Saito el al.[42] The structure is shown in **Fig.2.1 (d).** It was used for the determination of trace amounts of iron in solution at the wavelength of 720 nm.[40] At this wavelength, Nitroso-PSAP is selective to Fe^{2+} and the stochiometry is 1:1 in solution. Since Nitroso-PSAP is highly soluble in solutions, it is not suitable to be used as an indicator in solid supports and few samples can be found based on the immobilization of Nitroso dyes on to solid supports for the determination of heavy metal ions.[43]

Chrome Azurol S (also called Mordent blue, CAS) is an important member of the hydroxyl-triphenylmethane group of dyes. The structure is shown in **Figure 2.1 (e).** This reagent has pronounced chelating properties due to the presence of donor groups, i.e. –COOH, -OH and =O. It has been extensively employed as a metal indicator for photometric determination of various metals. Sheyanova and co-workers suggested the use of CAS for the determination of vanadium[4+] in steel.[44] It has also been used for photometric determination of Al^{3+}, Fe^{3+}, Cu^{2+} , Zr^{2+} and Cr^{3+}.[45] It was also reported immobilised onto cellulose thin-layers for the determination of HMs. CAS is recognised as a sensitive reagent for the determination of uranyl ion in the nuclear waste water industry.[46] Aguerssif el at. reported a method of simultaneous determination of Fe^{3+} and Al^{3+} by first-derivative spectrophotometry and the partial least-squares (PLS-2) method using CAS as a chelation reagent. It was found that no heating is required for colour formation, and the method is considerably more reproducible and selective.

2.1.7 Aims and Objectives

The aim of this work is to investigate and highlight suitable ligand/metal reactions that show the potential for use in the dye-based metal ion sensors of interest. It involves a detailed solution study on the spectrophotometric behaviour of the chosen ligands over a wide pH range in order to observe their metal binding capability.

The objectives of this work are:

(1) To study the molar absorptivity of these indicators with specific metal ions;

(2) To study the formation constants of the complexation reaction of indicator with HMs;

(3) Optimisation of pH for the determination of metal ions with these indicators;

(4) Study the working range and limit of detection.

Although most of these ligands have already been widely used as complexation reagents for HMs extractions, separations and pre-concentration, they still have a great potential to be used in the optical sensor technology for the determination of heavy metal ions.

2.2 Experimental

2.2.1 Materials

All the reagents are analytical grade unless otherwise stated. Distilled water was used for the preparation of the solutions. Laboratory glassware was kept in 5% nitric acid solution overnight. The glassware was rinsed with distilled water. Calmgite (CAL), 2-Nitroso-(5-N-propyl-N-sulfopropiamino)phenol (Nitroso-PSAP), 2-(5-bromo-2-pyridylazo)-5-diethylaminophenol (Br-PADAP), Acid Alizarin Violet N (AVN), Chrome Azurol S (CAS) were supplied by Sigma Aldrich, Co-Chemicals, Tallaght, Ireland. The effect of pH was tested using the following pH buffers (Sigma-Aldrich, Co-Chemical, Tallaght, Dublin, Ireland): acetate buffer, 2-(N-morpholino)ethanesulfonic acid (MES, >99%), 4-(2-hydroxyethyl)piperazine-1-ethanesulfonic acid, (HEPES, >99.5%). 3{[tris(hydroxymethyl)methyl]amino}propanesulfonic acid (TAPS, >99%) 3-(cyclohexylamino)-1-propane sulfonic acid] (CAPS, >99%). All solutions were prepared using analytical distilled water (18 Ω), purified through a Milli-Q[50] Plus system. The pH values of the solutions were monitored by use of a digital pH-meter calibrated with standard buffers of pH 7.00 and 4.00 at room temperature. Buffer solutions (pH 1-3) were purchased from Sigma-Aldrich, Co-Chemicals, Tallaght, Ireland.

2.2.2 Instruments

A Cary 50 UV-Vis spectrophotometer (Varian, USA) was used for absorbance studies. An ETD digital pH-meter (ETD, Germany) was used for pH adjustment and was calibrated with standard buffer pH 4 and pH 7 solutions.

2.2.3 Preparation of Buffer Solution

The pH buffer solutions were prepared using the following buffer salts to make a concentration of 10 mM. Buffer solutions with pH values of 4, 5, 6, 7 8, 9 and 10, were prepared by acetic acid, MES, HEPES, TAPS and CAPS. The method is illustrated in **Table 2.1.**

Table 2.1 Preparation of buffer solutions.

pH	Buffer Salts	Method
1	HCl solution	hydrochloric acid / potassium chloride
2	HCl Solution	hydrochloric acid / potassium chloride
3	HCl Solution	hydrochloric acid / potassium chloride
4	Acetate Glacial	0.06 g of acetate acid with 0.574 g of NaCl
5	Acetate Glacial	0.06 g of acetate acid with 0.574 g of NaCl
6	MES	0.195 g of MES free acid with 0.561 g of NaCl
7	HEPES	0.238 g HEPES free acid with 0.574 g of NaCl
8	HEPES	0.238 g HEPES free acid with 0.574 g of NaCl
9	TAPS	0.243 g of TAP with 0.54 g NaCl
10	CAPS	0.221 g of CAP free acid with 0.54 g NaCl

2.2.4 Preparation of Metal Ion Solutions

The metal ions salts were prepared from: Copper nitrite $[Cu(NO_3)_2 \cdot 3H_2O]$, cobalt nitrate $[(Co(NO_3)_2 \cdot 6H_2O)$, chromium (III) standard solution (> 99.9%), Ferrous chloride $[FeCl_2 \cdot xH_2O]$, ion nitrate $[Fe(NO_3)_3 \cdot 9H_2O]$, nickel chloride $[(NiCl_2 \cdot 9H_2O)]$, lead nitrate $[Pb(NO_3)_2]$, manganese sulphate $[MnSO_4 \cdot H_2O]$ and zinc nitrate $[Zn(NO_3)_2 \cdot 6H_2O]$, cadmium chloride $(CdCl_2)$, antimony choride $(SbCl_3)$, sodium chloride $(NaCl)$, potassium chloride (KCl).

2.2.5 Preparation of Ligand Solution

The stock ligand solutions were prepared at the concentration of 2×10^{-3} M in DI water by dissolving the calculated amount of CAL, CAS, AVN, Nitroso-PASP. Br-PADAP was dissolved in 100% ethanol.

2.2.6 Procedures

Acid Dissociation Constants

The ligand stock solutions were diluted with the appropriate buffers of pH 1-10 to give a final concentration of 2×10^{-4} M for all of the solutions, with the exceptions of CAS (1×10^{-4} M) and Br-PADAP (2×10^{-5} M). The UV/Vis spectrum of each ligand was recorded at each pH. Absorbance measurements were made at selected wavelengths and graphs of absorbance vs. pH were constructed. The acid dissociation constants were determined by extrapolation from the graph.

Ligand/Metal Complexation

The ligands were investigated for the complexation with the divalent metals Pb, Cu, Co, Ni, Zn, Fe, and trivalent Fe and Sb in the pH range of 4-10. Buffer solutions were prepared as in **Table 2.2**. To make the CAS-Metal complex solution with each pH buffer, 10 mL of CAS stock solution and 1 mL of metal stock solution were transferrred into a 100 mL volumetric flask, and made up to the mark by using different buffer solutions, pH 4-10. The final ratio of CAL: metal ion was of 2×10^{-4} M : 10 mg L^{-1}. The same method was applied to make Nitroso-PASP-Metal complexes and AVN-Metal complexes. For CAS-metal complexes, the final ligand:metal ratio is 1×10^{-4} M :10 mgL^{-1}. For Br-PADAP-Metal complexes, the final lignad : metal ratio is 2×10^{-5} M : 10 mgL^{-1}. The mixed complex solutions were kept standing at room temperature for 30 min before the absorption measurements.

Linear Range, Stoichiometry and Formation Constants

The ligands were tested with the metal of interest over the concentration range 1-100 mgL^{-1}. The linear complexes were then examined to determine their stoichiometry using Job's Method and the mole ratio method. The ligand concentration remained constant, while the metal concentration was varied. Absorbance measurements were recorded at a selected wavelength. Plots of absorbance vs. volume of added ligand, and absorbance vs. mole ratio were constructed and the complex stoichiometry was extrapolated. Using the data obtained with stoichiometry experiments, the K_f values for the complexes were determined as detailed in Appendix II.

2.3 Results and Discussion

This study aimed to characterise a range of ligands, i.e. AVN, CAS, CAL, Br-PADAP and Nitroso-PASP in solution using UV/Vis spectrophotometry and thus determine their stability and sensitivity for metal ion sensing. Preliminary work involved the determination of the acid dissociation constant of each ligand. Although much of this pK_a information is available in the literature, the values measured under certain conditions appropriate for this research are to confirm the literature values. Ligands were subsequently investigated for complexation with a variety of metal ions over a wide pH range. Ligands were compared based on their selectivity towards a particular metal ion and a dynamic range for measurement. The stoichiometry, formation constant and molar absorptivity of each complex was established. Each of these studies will be detailed in this section. This is essential preliminary work required to yield information on suitable reactions for the subsequent design of sensing phases.

2.3.1 The pK_a Study

Most of the indicators for heavy metal ion are Lewis acid-base indicators, compounds that are simply weak acids (or base), exhibit different colours depending on whether they are present in solution as their acidic form (HIn) or as their baisc form (In⁻).[47] An acid dissociation constant, K_a is a quantitative measure of the strength of an acid in solution. It is the equilibrium constant for a chemical reaction known as dissociation in the context of acid-base reactions[48] The equilibrium can be written symbolically as **Equation 2.7**:

HIn　　=　In⁻　　　+　　　H⁺　　　　　　　　　**(Eq. 2.7)**
Colour 1　　　Colour 2
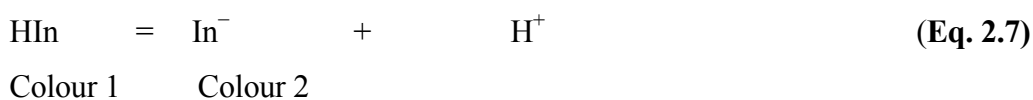
where HIn is a generic acid that dissociates by splitting into In⁻, known as the conjugate base of the acid, and the hydrogen ion or proton, H⁺, which, in the case of aqueous solutions, exists as a solvated hydronium ion. As the pH of a solution containing the indicator changes, the equilibrium shown above will be driven either towards reactants

(HIn) or products (In⁻) causing the solution colour to change depending on the concentration of each form present. For example, in strongly acidic solutions, most of the indicators will be present in the form HIn, causing the solution colour to correspond to that of HIn. In strongly basic solutions, most of the indicators will be present in the In⁻ form, resulting in colour 2 dominating the solution. At intermediate pH values, the solution colour will be a mix of colour 1 and colour 2, depending on the relative amounts of HIn and In⁻ present. Quantitatively, the relationship between the pH and the relative amounts of HIn and In- in solution is described by an acid dissociation constant (K_a) for the indicator, as shown in **Equation 2.8**, where the square-bracketed terms represent the molar concentration of each species in solution (M)

$$K_a = [H^+]\,[In^-]\,/\,[HIn] \qquad\qquad\qquad \textbf{Eq. 2.8}$$

In practice, the pH of a solution is typically measured; therefore, it is useful to perform a few math manipulations to the K_a expression to get the values in terms of experimentally-determined quantities. **Eq.2.8** also can be expressed as **Eq. 2.9** as below:

$$pK_a = pH - \log\left([In^-]/[HIn^-]\right) \qquad\qquad \textbf{Eq. 2.9}$$

Eq. 2.9 suggests that if it is possible to monitor the relative concentrations of HIn and In⁻, it should be possible to determine the K_a for the indicator. Since the acidic (HIn) and basic (In⁻) forms of the indicator have colour, therefore they can be determined by UV-Vis spectrometry. By monitoring the change in absorbance of each form as a function of solution pH, it is possible to extract a value for the K_a of an indicator. When the concentration of In⁻ form is equal to the concentration of HIn. The pK_a is equal to the pH.

Figure 2.2 displays the absorption spectrum of indicator AVN at low pH buffer to high pH buffer solutions (pH 1-10). It was found that the absorption spectrum of AVN in pH

buffer solutions display bands in two main regions. The first region was in the range of 200-350 nm and the second region was above 350 nm. At pH at 1-7, AVN the indicator is in the HIn dominated form, while at pH at 9-10, the indicator is in the In⁻ dominated form and at the intermediate pH (pH 8) the solution contains appreciable concentrations of both HIn and In⁻, and exhibits an absorbance spectrum containing contributions from both forms. As pH changes, the relative concentration of each form will change in accordance with the K_a of the indicator and the resulting absorbance of each form will also change. The band in the first region corresponds to the localised transitions within the phenyl and naphthyl moieties. The bands in the second region were assigned to charge transfer transitions within the molecule.[49] An isobestic point was observed at the wavelength of 540 nm. When AVN is in its acidic form, a band in the visible region at the wavelength around 490 nm was observed, and the AVN solutions were observed with orange colour. With the increase in the basicity of AVN solutions, the maximum absorbance shifted to 560 nm with a colour of purple.
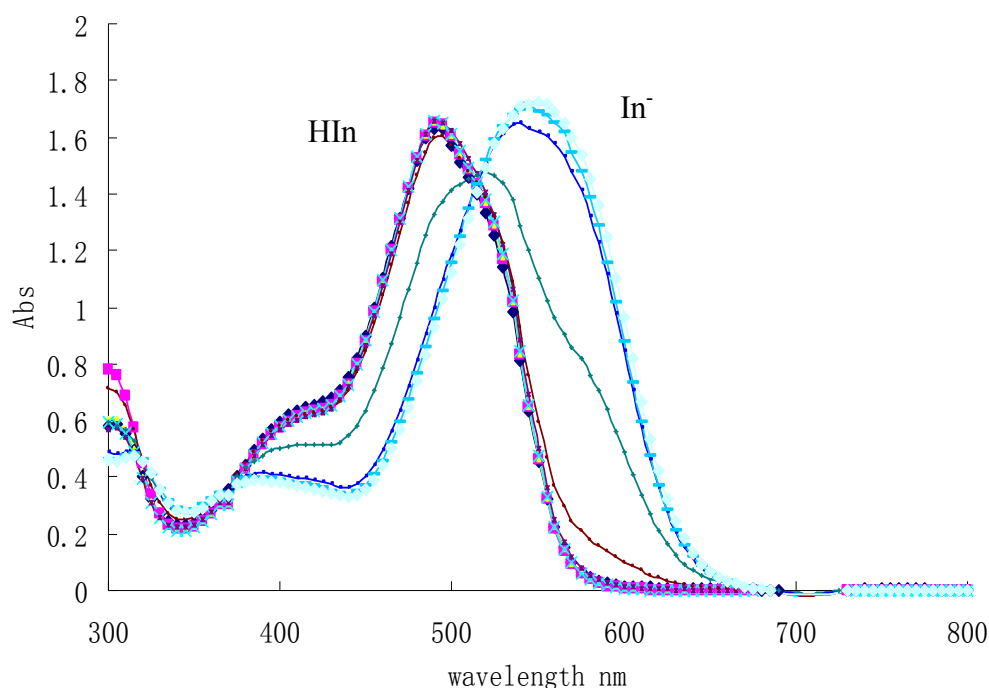
Figure 2.2 UV/Vis absorption spectra of 2×10^{-4} M AVN in buffer solutions in the pH range 1-10. ■ pH 1; ■ pH 2; ■ pH 3; ■ pH 4; ■ pH 5; ■ pH 6; ■ pH 7; ■ pH 8; ■ pH 9; ■ pH 10.

From **Eq. 2.9**, it can be seen that the pKa of indicator will be equal to the pH of the solution when the concentration of HIn and In⁻ in solution are equivalent. Experimentally, this corresponds to the pH where the absorbance of each form is half of its maximum absorbance. At this point, half of the initial number of moles of HIn have been converted to an equivalent number of moles of In⁻.

Consequently, the pK_a of an indicator corresponds to the pH of the solution at the inflection point in a plot of absorbance as a function of pH as shown in **Figure 2.3.** A simple spectrophotometric method for the determination of the pK_a or acid dissociation constant of a ligand is to plot the absorbance at two wavelengths as a function of solution pH. These two wavelengths represent (a) one where HIn, the protonated acidic form of the ligand, absorbs radiation; and (b) another where In⁻, the deprotonated basic form of the ligand absorbs radiation.[50]   However, it is critical that the absorbance at each wavelength corresponds to the absorbance of only HIn at λ =494 nm and only In⁻at λ =560 nm.
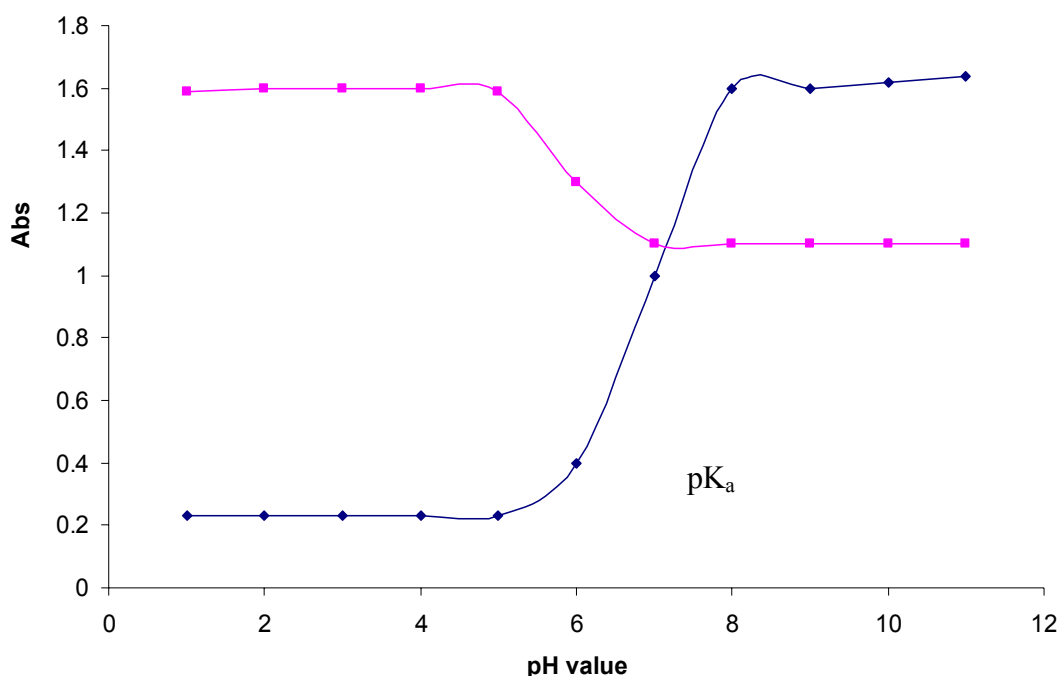
Figure 2.3 Plot of absorbance as a function of pH of 2×10^{-4} M AVN. Measurements made at ■ a wavelength (λ_1 = 494 nm) at which HIn absorbs radiation; ■ a wavelength (λ_2 = 560 nm) at which In⁻ absorbs radiation. pKa = 7.5.

The pKa of AVN was determined by plotting the absorbance vs. pH at selected wavelengths, 494 and 560 nm, respectively. As it can be seen from **Figure 2.3**, at high pH values, AVN is in the In⁻ form and thus the absorbance due to In⁻ is at a maximum; at low pH, AVN is in the HIn form. At pH around 7.5, a shift to the red was observed due to the deprotonation of AVN. Therefore, the pKa of AVN is at pH 7.5.

By using the same method, the pK_a of CAS, CAL,Br-PADAP and Nitroso-PASP have been determined and the values have been summarised in **Table 2.2** below. The UV-Vis absorption spectrum and pH plots are detailed in Appendix I.

Table 2.2 The pKa of AVN, CAS, CAL, Br-PADAP and Nitroso-PSAP.

Ligand	pKa
AVN	7.4
CAS	4.5
CAL	8.2
Br-PADAP	3.0
Nitroso-PASP	8.4

2.3.2 AVN -Metal Complexation Study

The recognition of heavy metal ion gives rise to major colour changes of indicators that are clearly visible to the naked eye, while the quantity of heavy metal ion can be achieved by absorption enhancement. Therefore the simplest method to test the complexation of the metal ion with indicator is to observe the colour change of solution visually. Furthermore, the solution can be scanned using the UV-Vis spectrometry in the visible region (350 nm-780 nm).

Firstly, AVN was used as an example on how the complexation studies of   ligands with transition metal ion were performed. AVN was tested for the complexation with metals ion, e.g. Cr^{3+}, Co^{2+}, Cu^{2+}, Fe^{2+}, Fe^{3+}, Ni^{2+}, Pb^{2+}, Sb^{3+}, and Zn^{2+} in buffers from pH 3-10. The pH is an important factor that can be explained by the acid-base equilibrium.[51, 52] The

H_3O^+ ion is competitive to metal ion at low pH buffer condition, while in the high pH buffer solution, the OH^- will chelate with metal ion. Therefore most of the complexation reactions between heavy metal and indicator complete are in the intermediate pH conditions.[52] AVN was determined to complex with metal ions at pH values below its pKa value, i.e. 7.5, in its protonated form. It is a negatively charged ligand and therefore did not need to become deprotonated to attract cations. Any new bands, wavelength shifts and/or changes in absorbance were noted for potential sensor application. **Figure 2.10** shows the colour changes of the mixture solution of AVN solution and different heavy metal ions. As expected from the original design, in the absence of any metal ion, the AVN remains stable and displays a maximal absorption band at 500 nm, indicating that AVN is at the protonated form, since pK_a of AVN is 7.5. While in the presence of Co^{2+}, AVN displays pink concomitant with a broad absorption of about 620 nm. This result implies that binding of Co^{2+} with AVN forms a complex and the indicator is deprotonated. Similarly, the colours of AVN change to yellow in the presence of Fe^{3+} and Fe^{2+} ion under pH 7 solutions. In contrast, there is no colour changed observed by the addition of other heavy metal ions, such as Ni^{2+}, Cr^{3+}, Zn^{2+}, Sb^{2+} and Cu^{2+}.

a	b	c	d	e	f
g   h   i   j
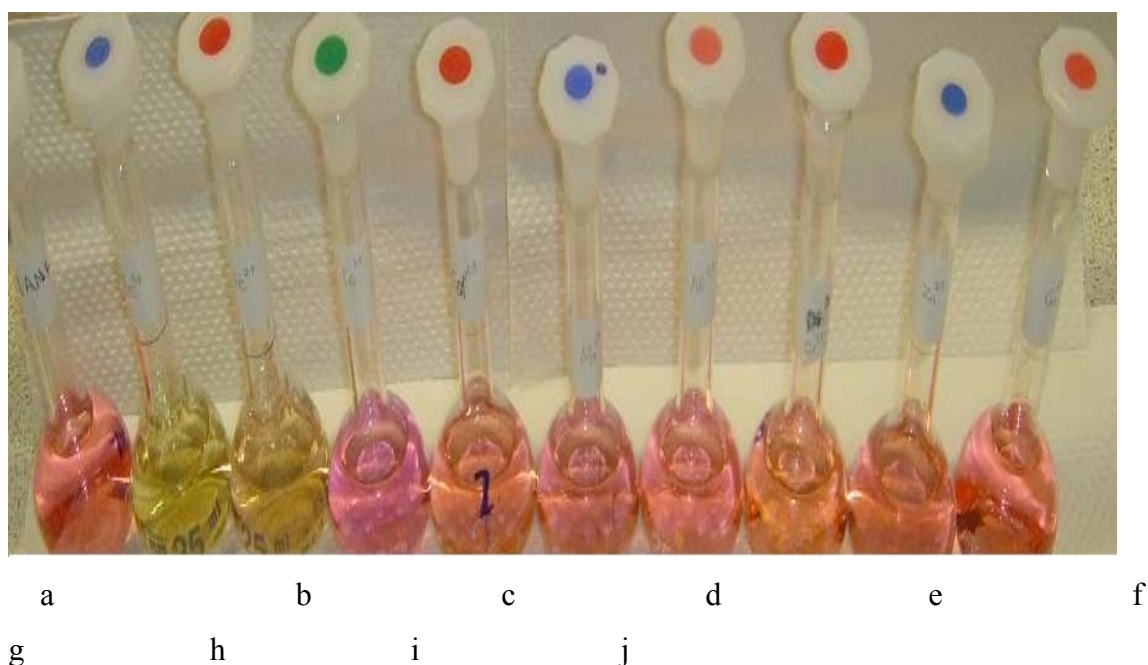
Figure 2.10 a) blank AVN solution b) Fe^{3+} solution; c) Fe^{2+} solution; d) Co^{2+} solution; e) Cd^{2+} solution; f) Sb^{2+} solution; g) Ni^{2+} solution; h) Cr^{3+} solution; i) Zn^{2+} solution; and j) Cu^{2+} solution at pH 7.

Figure 2.11 shows the absorption spectrum of the mixture solution of AVN indicator with the presence of Co^{2+} ion at the pH 7 buffer. It can be seen that the reaction of AVN with Co^{2+} ion at pH 7 solution forms a light pink complex with absorption maxima at 514 nm.
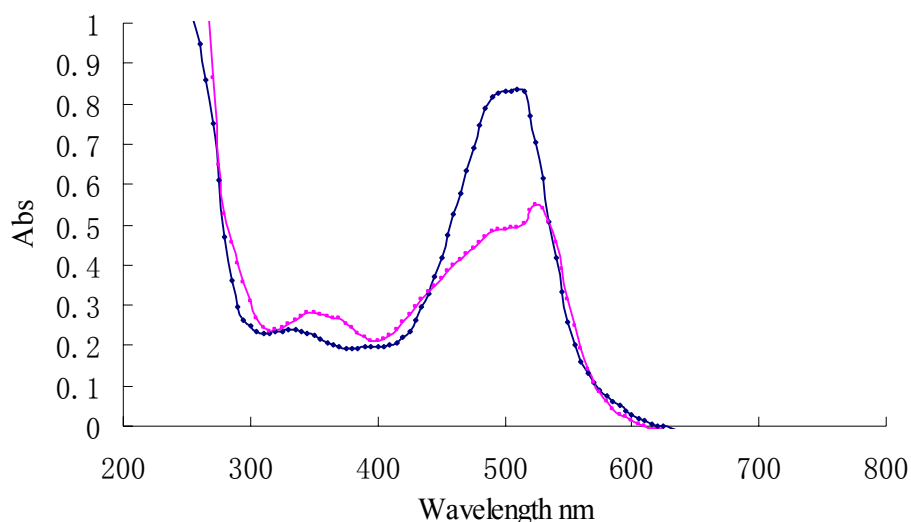
Figure 2.11 The absorption spectra of blank ■AVN ($1x10^{-4}$ M) and ■AVN-Co^{2+} ($1x10^{-4}$ M of AVN/1 mg L^{-1} Co^{2+}) complex at pH **7.**

2.3.3 CAS -Metal Complexation Study

The CAS was tested by the same experimental method as for AVN. The absorption spectrum **(Figure 2.12)** of the mixtures of CAS with metal ion shows that CAS is an unselective indicator and it reacts with many heavy metals, such as Fe^{3+}, Cu^{2+} and Ni^{2+} in pH 9 solutions. In contrast, metal ions such as i.e. Na^{+}, K^{+}, Zn^{2+} Pb^{2+} and Cd^{2+} did not obtain new complexes with CAS at pH 9. **Figure 2.13** shows CAS forming a complex with Fe^{2+} with absorption maxima at 495 nm and also forming a complex with Fe^{3+} with absorption maxima at 580 nm at pH 9. Compared with preliminary studies, it was reported that CAS forms a complex with Fe^{2+} at pH 2, with absorption at 469 nm. Also, at pH 9, CAS forms a complex with Fe^{3+} with absorption maxima at 566 nm.[53] The reaction of CAS with Fe^{3+} is promising from a sensing point of view as it is possible to monitor the Fe^{3+} ion in basic (pH 9) solution and the interference by Fe^{2+} can be estimated.
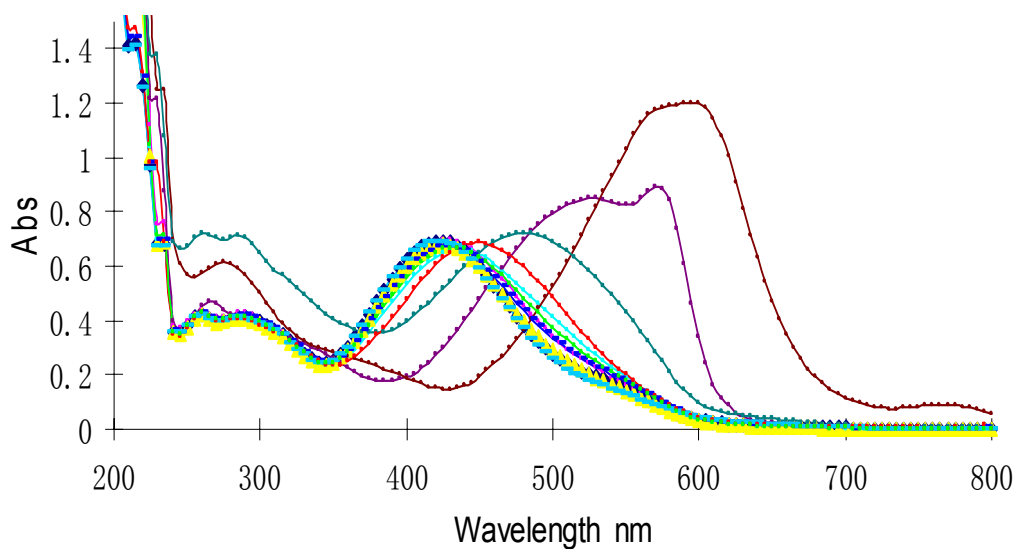
Figure 2.12 CAS with different HMs at pH 9 solution. ■ Blank CAS (1 x 10^{-4}M) ; ■ Pb-CAS complex; ■ Cd-CAS complex; ■ Co-CAS complex; ■ Cu-CAS complex; ■ Fe(III)-CAS complex; ■ Fe(II)-CAS complex; ■ K-CAS complex; ■ Na-CAS complex; ■ Ni-CAS complex; ■ Zn-CAS complex. (Metal: CAS= 10 mgL^{-1} of metal ions/1 x 10^{-4} M).
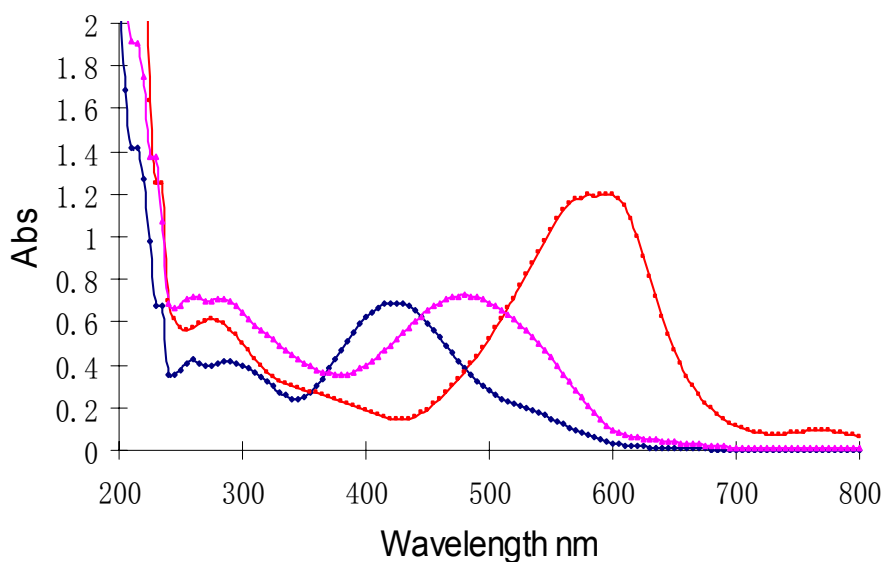
Figure 2.13 UV/Vis absorbance spectrum showing ■ CAS (1 x 10^{-4} M); ■ CAS-Fe^{2+} complex (1 x 10^{-4} M/ 10 mgL^{-1}) at pH 9 solution; ■ CAS-Fe^{3+} complex (1 x 10^{-4} M/ 10 mgL^{-1}) pH 9 solution.

The stoichiometry of ligands with different metal ions was performed by Job's method/molar ratio method as detailed in the Appendix II. The stiochiometry of the complex between Fe^{3+} and CAS is 1:3. So the formation of the complex is Fe $(CAS)_3$. It was also conformed that the stoichiometry of CAS/ Fe^{3+} is 3:1 by Hargis in their study for the measurement of iron in serum.[54] Tabcco et al. also reported that CAS in the presence of surfactant (CTAB) reacts with Fe^{3+}/ Fe^{2+} to give an intensive coloured complex with absorption at 630 nm in suitable conditions. According to their method, the iron in the serum is extracted by the surfactant into the chromogenic phase and reduced to ferrous state by a strong reducer, such as sodium dithionite or ascorbic acid. Then the iron reacted with CAS to produce a coloured complex as stated before. Monohydrate citric acid was used as masking reagents for avoiding the interference from other heavy metal ions.[55] Horiuchi and co-workers have also reported the molar absorptivity of CAS-Fe complex is about 8.5 x10^5 1 · mol^{-1} · cm^{-1}. However, this method used the liquid phase for the measurement. Inspired by this method, CAS can be used for the determination of iron in serum by using solid optical sensors. The possible geometry of Fe$(CAS)_3$ is shown in **Figure 2.14.**
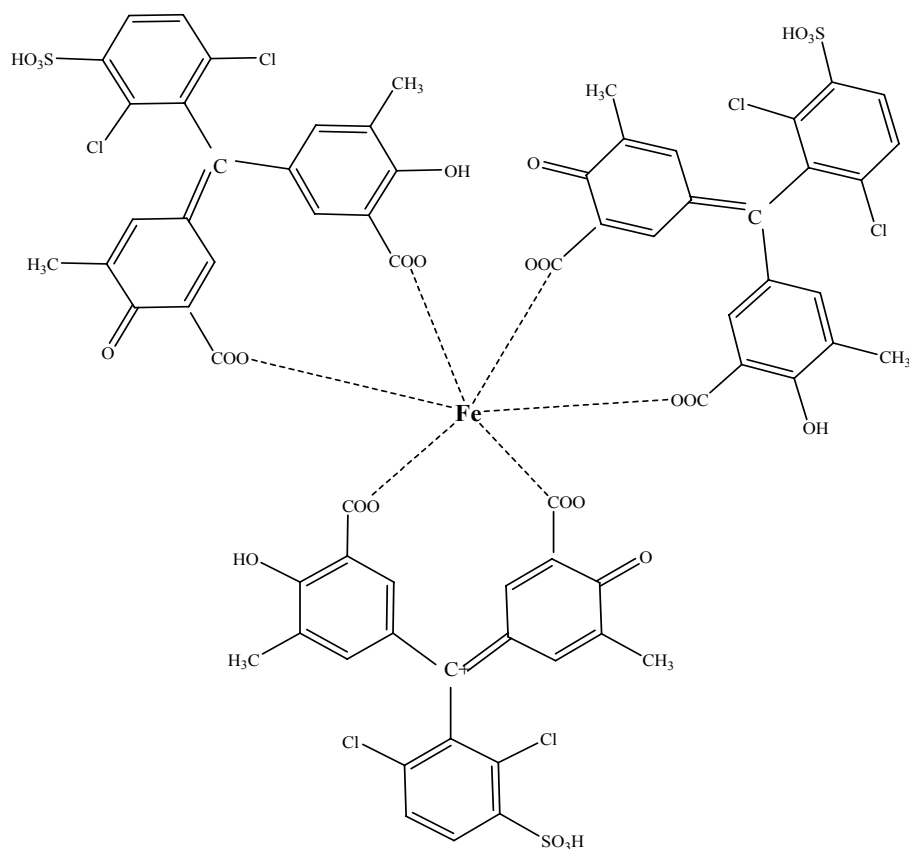
Figure 2.14 The structure of Fe$(CAS)_3$.

CAS was also found to form a complex with Cu^{2+} with absorption maxima at the wavelength of 590 nm at pH 9, and this is shown in **Figure 2.15.** This complex is stable for at least 24 h under room temperature. It has been reported that Cu^{2+} forms a ring-formed dimer complex with CAS under pH 2-4. The stoichiometry of metal to CAS is either 1:1 or 2:1 depending on the pH of the solution. [45, 56] The structures of these complexes are shown in **Figure 2.16**.
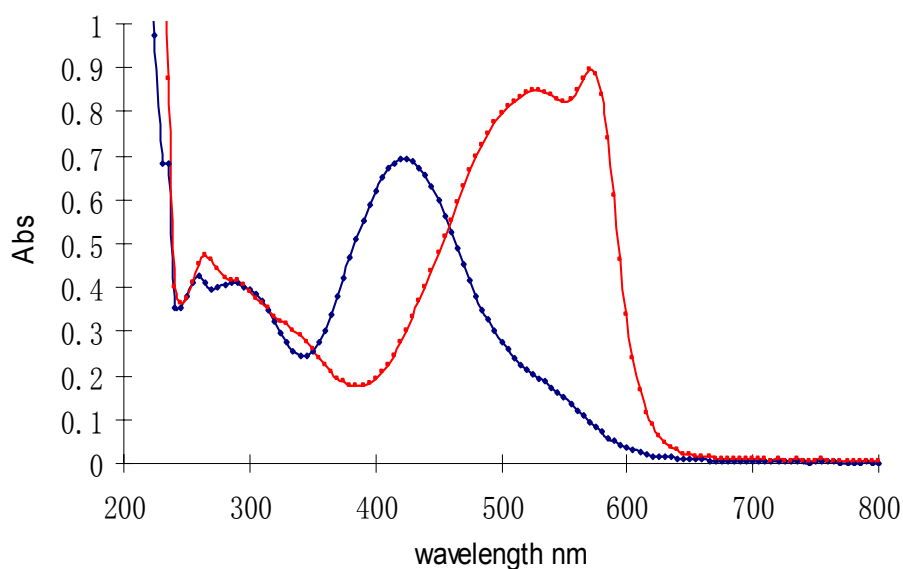
Figure 2.15 UV/Visible absorbance spectrum showing ■ CAS (1 x 10 $^{-4}$ M); ■ CAS- Cu^{2+} complex (1 x 10 $^{-4}$ M/ 10 mgL^{-1}) at pH 9 solution.
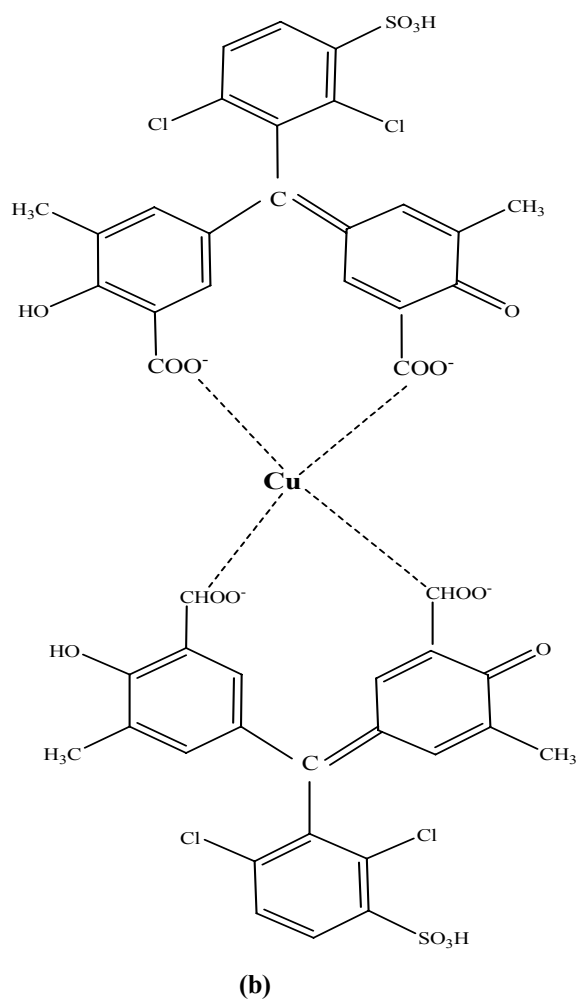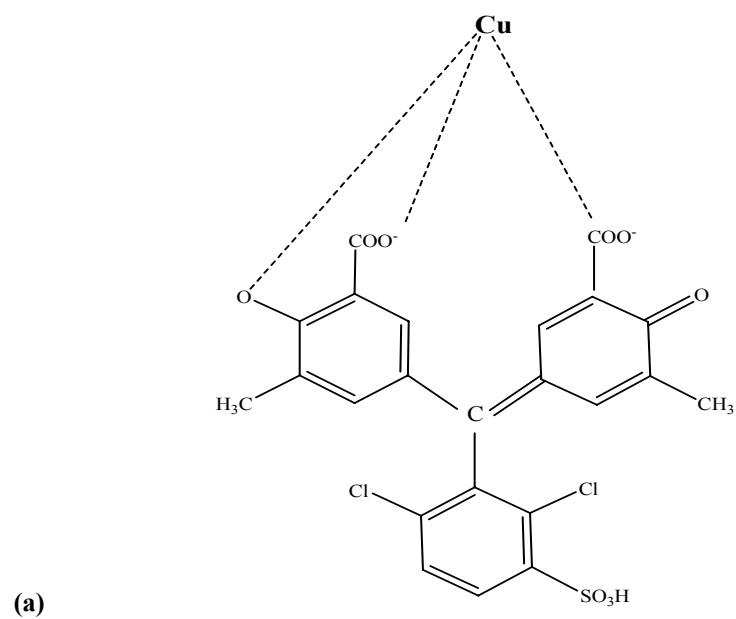
Figure 2.16 Structures of Cu-CAS complex. In the form of (a) 1:1, (b) 1:2 ratio.

There is an example of how the CAS indicator is used for the determination of Cu^{2+} ion. To date there is no method to identify chemical treatments in wood waste that may often be invisible. As a result, the identification and segregation of chemically contaminated materials is not always optimal, thus presenting potential health& safety issues, adding costs to the recycling process and potentially undermining recycled product quality. End users, notably the panel board manufacturing industry, increasingly require verification that chemical contamination is removed. The Waste and Resources Action Programme has developed a practicable method of detecting preservative-treated wood that can be used at wood recycling facilities and other situations. Sawyer and co-workers reported a method to make, store and use CAS for the detection of copper-preservative in wood waste streams for recycling, such as copper-chrome-arsenate (CCA), copper-chrome-boron (CCB), copper-chrome-phosphate (CCP) and also some copper organics. A method prepared by dissolving CAS in liquid solution form and used them for spraying, sponge and brushing has been reported.[57] These liquid forms of CAS are not convenient for portable use in the field and caused wastage of solution during usage. Therefore, there is a need for immobilising the CAS onto suitable solid materials to fabricate a solid optical sensing system. Inspired by this, an optical sensor based on the immobilisation of CAS on to cationic functionalized cellulose membrane has been developed and investigated in Chapter 4. And this reaction will be discussed in details in Chapter 4.

2.3.4 Calmagite-Metal Complexation Study

Calmagite (CAL) was studied as spectrophotometric reagents using the same procedure as above. **Figure 2.17** shows a new band due to the complexation of Cu-CAL obtained in pH 9 solution at the wavelength of 550 nm. Correspondingly, the colour of the solution changed from blue (pure CAL solution) to purple by adding Cu^{2+} ions. This reaction was also confirmed by Mutsuo et al. in aqueous solution and they found that complex copper-CAL obtained a maximum absorption at 550 nm.[58] The stoichiometry of the resulting complexe depends on experimental conditions. Under the current experimental condition, the stoichiometry of Cu-CAL was found to be 1:1 by using Job's plot method as described before and the optimized structure is shown in **Figure 2.18.** The calmagite structure is more or less planar, while in the case of the complex, the structure is somewhat folded to result in the lowest conformational energy. In the optimized complex structure,

calmagite acts as a three-dentate ligand and establishes coordination bonds with Cu^{2+} over its two oxygens and one nitrogen donating group.[58]
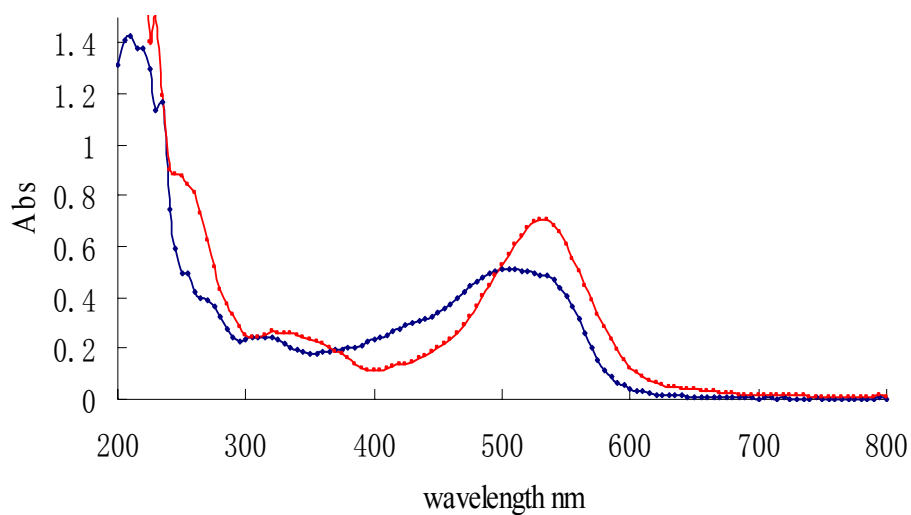
Figure 2.17 UV/Visible absorbance spectra of CAL with Cu^{2+} at pH 9. ■ CAL alone (1 x 10^{-4} M) ■ CAL with Cu^{2+} (1 x 10^{-4} M/ 10 mgL^{-1}).
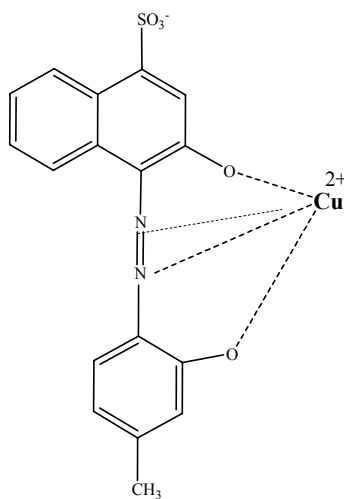
Figure 2.18 Optimized structures of CAL-Cu^{2+} Complex in its 1:1 form.

Based on the relatively high selectivity of calmagite for Cu^{2+} over other heavy metal ions a distinct colour change that was observed for the formation of its complex with Cu^{2+}; the ligand was expected to act as a suitable dye for fabrication of an optical sensor for Cu^{2+} ion.

2.3.5 Nitroso-PASP Complexation Study

Nitroso-PASP is reported as a sensitive and selective spectrophotometric reagent for Fe^{2+}, Pb^{2+}, Cd^{2+} and Cu^{2+} complexes under different conditions.[40] Nariko et al. reported it can be used as a chelation agent for the determination of iron in boiled water and well water, and that the molar absorptivity is 4.3×10^4 l mol^{-1}cm^{-1} at 753 nm. Other divalent heavy metal ion such as Ni^{2+}, Cu^{2+}, Zn^{2+} and Cd^{2+} did not show interference up to 500 μg l^{-1}.[59] The absorption of spectra of the Nitroso-PSAP blank and complexes with metal ions in pH 6 buffer solutions are shown in **Figure 2.19.** Nitroso-PSAP blank presents two peaks: one is at 350 nm and the other smaller one is at 430 nm under pH 6 buffer solutions.
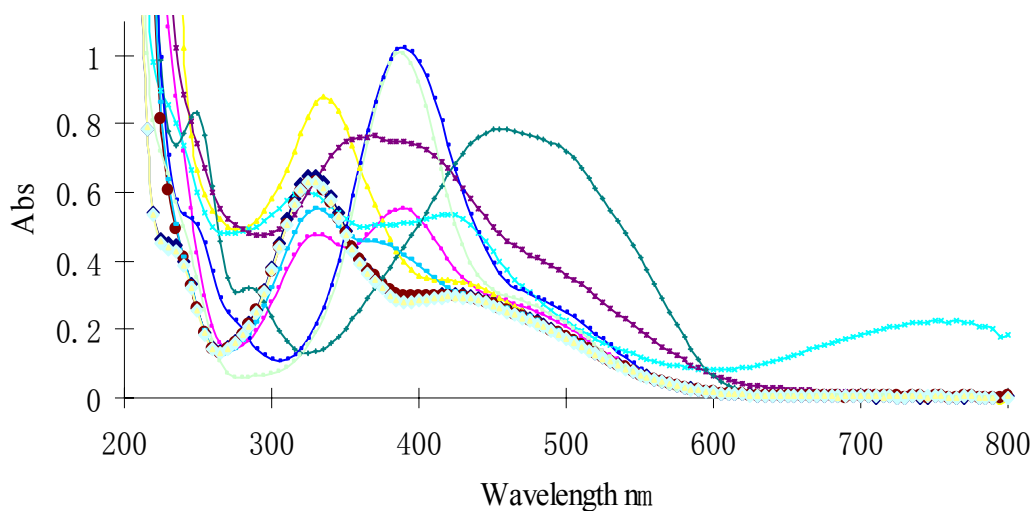
Figure 2.19 UV-Vis spectra of Nitroso-PASP (short for N) with different HMs at pH 6 solution. ■Blank N (2x10^{-4}M) ; ■ Pb-N Complex; ■ Cd-N complex; ■ Co-N complex; ■ Cu-N; ■ Fe(III)-N complex; ■ Fe(II)-N complex; ■ K-N complex; ■ Na-N complex; ■ Ni-N complex; ■ Zn-N complex. (Metal: Nitroso= 10 mgL^{-1} of metal ions/2x10^{-4}M).

Nitroso-PASP is selective for Fe^{2+} and the Nitroso-Fe^{2+} complex produces a distinctive band. **Figure 2.20** shows that Nitroso-PSAP can form complexes with Fe^{2+}, and the absorption maxima of the complex are at 425 and 756 nm.[59] However, it was found that the brown Fe^{3+}–Nitroso-PSAP complex has the absorption maxima at 410 nm and 510 nm at pH 6 buffer. Therefore, the measurements of colour difference in iron (III) and (II) complexes can be used for the determination of these two species simultaneously. The dependence on pH of the complex has also been studied. The peak signals are constant at the pH range of 7-9, the optimum pH range was wide. Above pH 10, the absorbance of Nitroso-PASP-Fe will decrease, since Fe^{2+} will be hydrolysed. The complex of nitroso-iron is stable for at least 12 h. The stoichiometry of nitroso-Fe^{2+} was found to be 3:1.
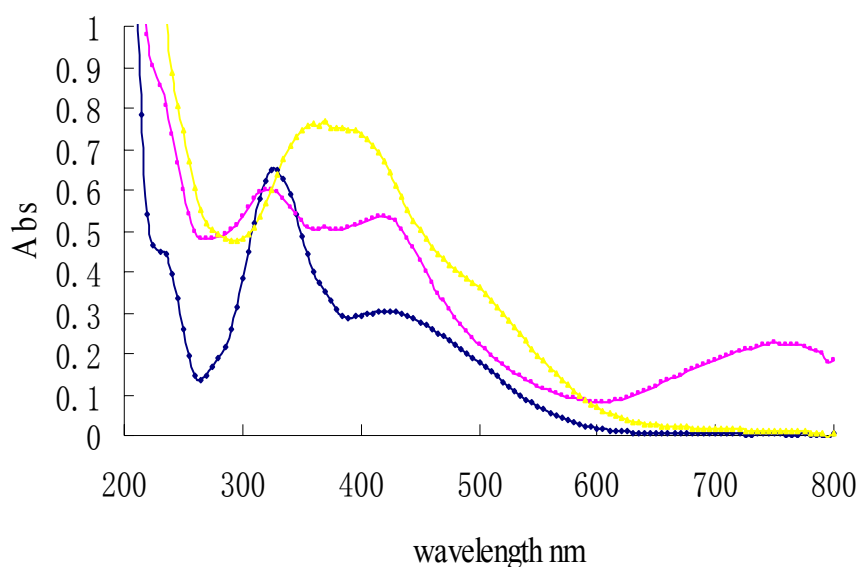
Figure 2.21 UV-Vis spectra of Nitroso-PASP with Fe^{2+} and Fe^{3+}. ◆ Nitroso –PASP blank $(1x10^{-4}M)$ ◆ Nitros-PSAP-Fe^{3+} complex ◆Nitros-PSAP-Fe^{2+} complex. (Nitroso-PASP/ Metal ion=$2x10^{-4}M/10$ mg/L^{-1}) at pH 6 buffer.

Nitroso reacts with cobalt (**Figure 2.22**) and copper (**Figure 2.23**) to form complexes as well. The maximium absorbance of Nitroso-Cu was located at a wavelength of 420 nm.
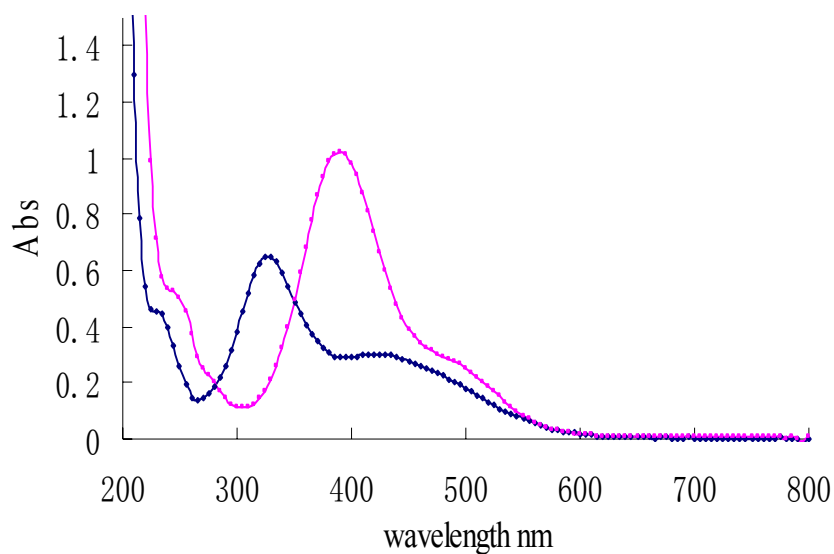
Figure 2.22 UV-Vis spectra of Nitroso-PASP with Cu^{2+}. ◆ Nitroso –PSAP alone (2 x 10^{-4}M) ◆ Nitros-PSAP- Cu^{2+}complex (Nitroso-PSAP/ Metal ion=21x10^{-4} M/10 mg/L^{-1}) at pH 6 buffer.
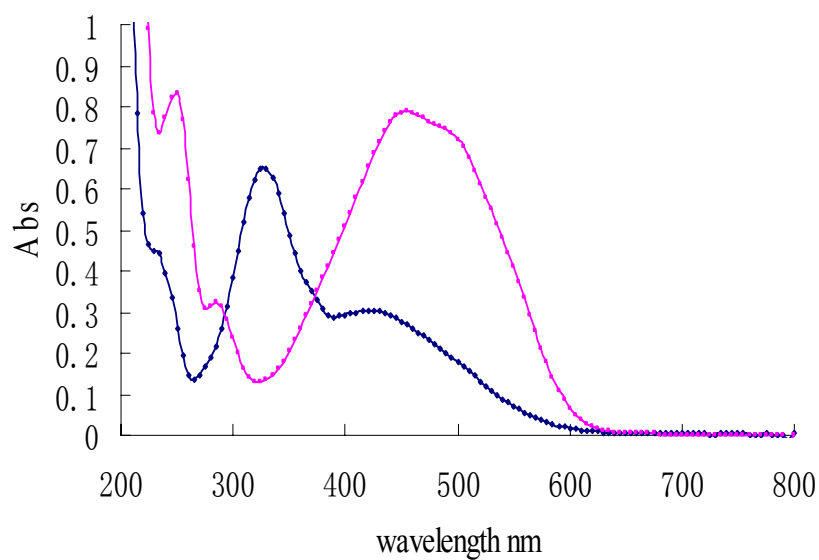
Figure 2.23 UV-Vis spectra of Nitroso-PSAP with Co^{2+}. ◆ Nitroso–PSAP alone (2x10^{-4}M) ◆ Nitroso-PSAP- Co^{2+}complex (Nitroso-PSAP/ Metal ion=2x10^{-4} M/10 mg/L^{-1}) (at pH 6)

2.3.6 Complexation of BrPADAP with Metal Ion

2-(5-Bromo-2-pyridylazo)-5-diethylaminophenol (5-Br-PADAP) forms highly coloured and stable complexes with a number of metals such as with Co^{2+}, Cu^{2+}, Fe^{2+} and Ni^{2+} at different wavelengths.[60, 61] For this reason, it was used as both a colorimetric reagent for spectrophotometric determination and a pre-column or post-column reagent for the simultaneous chromatographic separation and determination of many metal ions.[22, 62-64] The absorption spectrum of Br-PADAP blank and its complexes with metal ions are shown in **Figure 2.24.** The measurement of blank Br-PADAP in ethanol gave an absorbance at around 420 nm. Firstly, a band observed from the reaction of Br-PADAP with Co^{2+}, shows a shoulder band at around the wavelength of 520-620 nm.
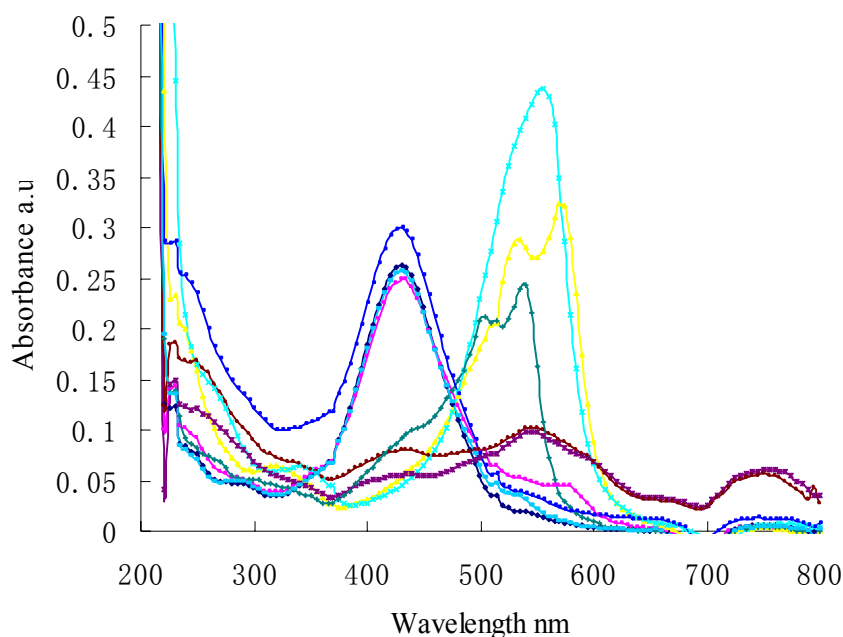
Figure 2.24 UV-Vis spectra of Br-PADAP with different HMs at pH 9. ◆ Blank Br-PADAP (1 x 10^{-5}M) ; ■ Pb-Br-PADAP Complex; ■ Co-BrPADAP complex; ■ Cu-BrPADAP complex; ■ Fe^{2+}-Br PADAP; ■ Fe^{3+}-Br-PADAP complex; ■ K-BrPADAP complex; ■ Ni-BrPADAP complex; ■ Zn-Br-PADAP complex. (Metal: Br-PADAP= 10 mgL^{-1} of metal ions/1 x 10^{-5}M) at pH 9.

New bands of complexes of Cu^{2+}/Br- PADAP and Co^{2+}/Br-PADAP were obtained in the absorption spectrum and they overlapped on the spectrum. The shapes and the intensity of the absorbencies are different. From **Figure 2.24**, it can been seen that there are two sharp peaks in the band for Co^{2+}/Br-PADAP complexes at the wavelength of 570 nm, while the Cu^{2+}/ Br-PADAP complex gave only one broad absorption peak at the wavelength of 540 nm. Sozgen has reported that Co-BrPADAP gave an absorption band at 588 nm in a pH 7 buffer solution.[61] The stoichiometry of Cu-Br-PADAP and Co-PADAP complexes were found to be 1:2 in a pH 9 buffer solution. Their structures are shown in **Figure 2.25**. The ternary structures of the complexes of Co-Br-PADAP and Cu-Br-PADAP have also been reported by Shi et al.[44]
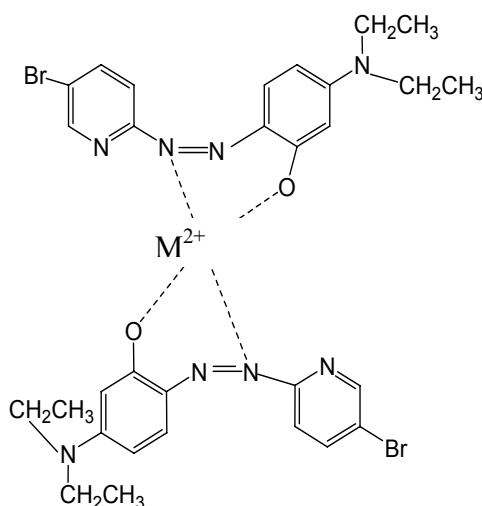
Figure 2.25 Possible coordination formula of $Co2^+$, Cu^{2+} and Ni^{2+} with Br-PADAP molecules.

It was found that the addition of Ni^{2+} to Br-PADAP in pH 9 solutions resulted in a fast change in the colour of the solution from yellow to light pink-red. There was a shoulder band: the first one is at 529 nm and the second one is at 559 nm. Compared with Ni^{2+}/Br-PADAP complexes reported by Sözgen et al. the maximum absorbance was found to be at the wavelength of 555 nm.[61] Wei et al. have reported that the complex of Ni-Br-PADAP gives a shoulder band at the wavelength of 520 nm and 558 nm in pH 6.5 buffer solutions.[30, 65] This is probably due to the difference in the concentrations of the ligands used in the experiments and other experimental condition differences. The

stoichiometry of Ni: Br-PADAP was found to be 1:2 and the structure of Ni-BrPADAP complex is shown in **Figure 2.25**. Amini et al. and Wei et al. reported the same stoichiometry for the complex of Ni-Br-PADAP.[30, 65]   The ternary structure of the complex of Ni-Br-PADAP has also been reported by Shi et   al.[44]   The two absorption bands of Ni-BrPADAP at the wavelength of 529 nm and 559 nm increased by increasing the concentration of Ni^{2+}. However, it can be seen from **Figure 2.24**, the peak at 559 nm is higher than the peak at 529 nm, so in the following study, the peak at wavelength of 559 nm was chosen for further investigation.

2.3.7 The Potential Uses of Indicators as Chromophore in Optical Sensors

According to the preliminary spectrophotometric studies, absorbance of AVN, CAS, Br-PADAP, CAL and Nitroso-PASP with heavy metal ions have been investigated. The promising results and the optimum experimental conditions are summarised in **Table 2.3**. Based on these complexation results, optical sensors based on the immobilisation of indicators onto a suitable solid matrix for the determination of heavy metal ions were investigated and are described in Chapter 3 and Chapter 4.

As can be seen from **Table 2.3**, most of the indicators studied in this chapter are not selective to a specific heavy metal ion. For example, Br-PADAP reacts with Cu^{2+}, Ni^{2+} and Co^{2+}. The complexes of Br-PADAP with these metal ions gave similar absorbance in the spectrum and produces similar colour changes. However, due to their high formation constants, long life time, large molar absortivities, large linear working range and also low-cost of synthesis, they are still widely applied in the development of low-cost and colorimetric optical sensing systems for heavy metal ions. Moreover, the interferences by other metal ions can be estimated by using masking agents. Therefore, the sensors based on these unselective dyes have the potential for multi-metal detection sensors.

Table 2.3 Summary of Promising Ligands Studied and their further Investigation

Promising Ligand/metal Complex	Further Application in Optical Sensors		
	Heavy Metal ions	Optimum pH	Colour change
AVN	Fe^{2+}	6	Pink to Yellow
	Co^{2+}	6	Pink to Red-pink
CAS	Cu^{2+}	7	Yellow to Blue-violet
	Fe^{3+}	9	Yellow to Blue
	Ni^{2+}	9	Yellow to blue
Br-PADAP	Cu^{2+}	9	Orange to pink
	Co^{2+}	9	Orange to pink
	Ni^{2+}	9	Orange to pink
CAL	Cu^{2+}	9	No colour change observed (However New absorbance obtained at 510 nm)
Nitroso-PASP	Fe^{2+}	6	Brown to green (two new bands observed)
	Cu^{2+}	6	Brown to light green
	Co^{2+}	6	Brown to light green

The main focus of this project was to investigate suitable sensing materials and immobilisation techniques for these low-cost commercial available indicators in optical sensing. In the following sections, the complexations of one metal ion with each ligand have been investigated further. The complexes linearity, the formation constants and molar absortivities of each indicator with one metal ion have been studied.

2.3.7 Linear Range Study

The linear range of each complex was studied as explained in the experimental section. Results of interest are outlined in **Table 2.4.** The ligands were complexed with metals in

the concentration range of 0.1-50 mgL^{-1}. The complexes were monitored at their absorbance maxima and at wavelengths around the absorbance maxima in order to determine the wavelength that gave optimum compromise between the dynamic linear range and the regression coefficient (R^2). The linear range of each indicator with ligand is carried out by solution UV-Vis spectrometric method. This is used as an example to illustrate how the linear range was tested.

Figure 2.26 shows the absorption spectrum of the prepared Br-PADAP solution at the presence of different concentration of Ni^{2+} ion under pH 9. **Figure 2.26** confirms that increasing the concentration of Ni^{2+} causes increased absorption of the band of the mixture solution at 559 nm. It is shown that the maximum absorbance of the mixture of Br-PADAP with Ni^{2+} is at 559 nm; therefore this wavelength was used for linear range study.
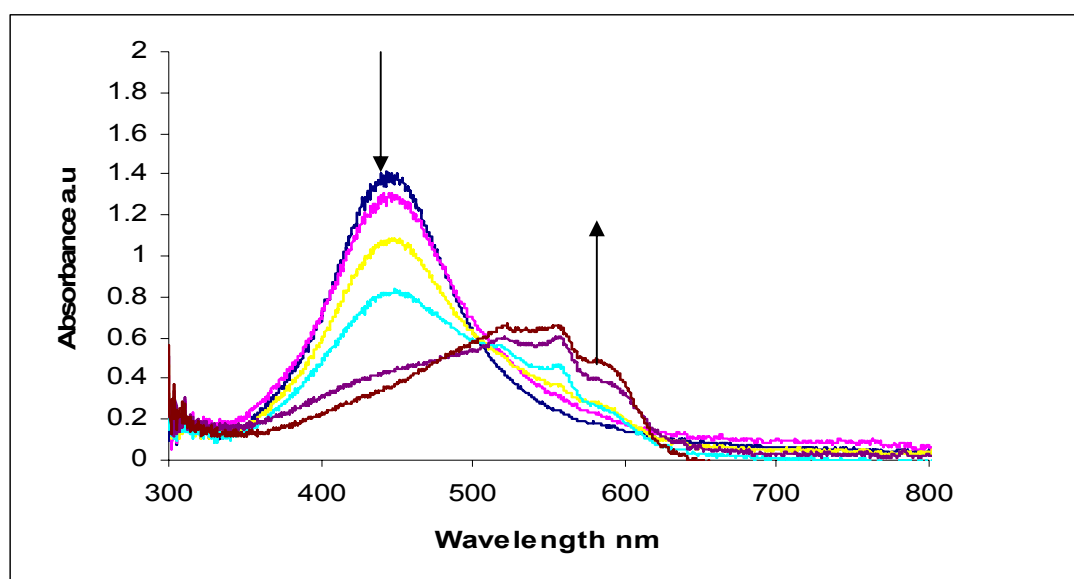
Figure 2.26 Absorption spectra of the Br-PADAP solution with different concentrations of Ni^{2+} at pH 9. The concentration range of Ni^{2+} is from 0-50 ppm. The concentration of Br-PADAP is 2 x 10^{-3} M.

Figure 2.27 shows the working curve of Br-PADAP with Ni^{2+} at pH 9 solution at 559 nm. It was found that the absorbance intensity increases by increasing the addition of Ni^{2+} ion solution upto 20 ppm of Ni^{2+}, there is no absorbance increases by further addition of nickel ion. Under the optimised condition of pH 9, the linear working range of Br-PADAP is

from 0.5 ppm to 20 ppm, with a correlation equation of y = 0.0045x + 0.0058 (R^2 = 0.99, n=3). **Figure 2.28** shows the linear working range of the indicator Br-PADAP for the determination of Ni^{2+} ion.

The lower limit-of-detection (LOD) is the lowest concentration level that can be determined to be statistically different from a blank (95% confidence). In this study, it can be defined as the concentration of analyte required to give a signal equal to the background plus three times the standard deviation of the blank (S).[66] Where S is calculated from **Eq. 2.10,** the experiment were repeated for 3 times, therefore n=3.

$$S = \sqrt{\frac{\sum(X - \bar{X})^2}{n - 1}} \qquad \%RSD = \frac{100 \times s}{\bar{X}} \qquad (\textbf{Eq.2.10})$$

where X is a single measurement and $\bar{X}$ is the mean (average) measurement. The symbol $\sum$ means 'sum of' and 'n' is the number of measurements.[67]

The S of the blank Br-PADAP solution at the concentration of 2 x10^{-3} M is calculated from **Eq. 10** is S= 0.003 and the A_{blank} = 0.005, therefore the lower limit of detection is 1.8 ppm according to the correlation equation of y = 0.0045x + 0.0058 (R^2 = 0.99, n=3). 20 ppm was used as the upper limit of detection, since there is no absorption increases were obtained by further increasing the concentration of 20 ppm of Ni^{2+} ion.
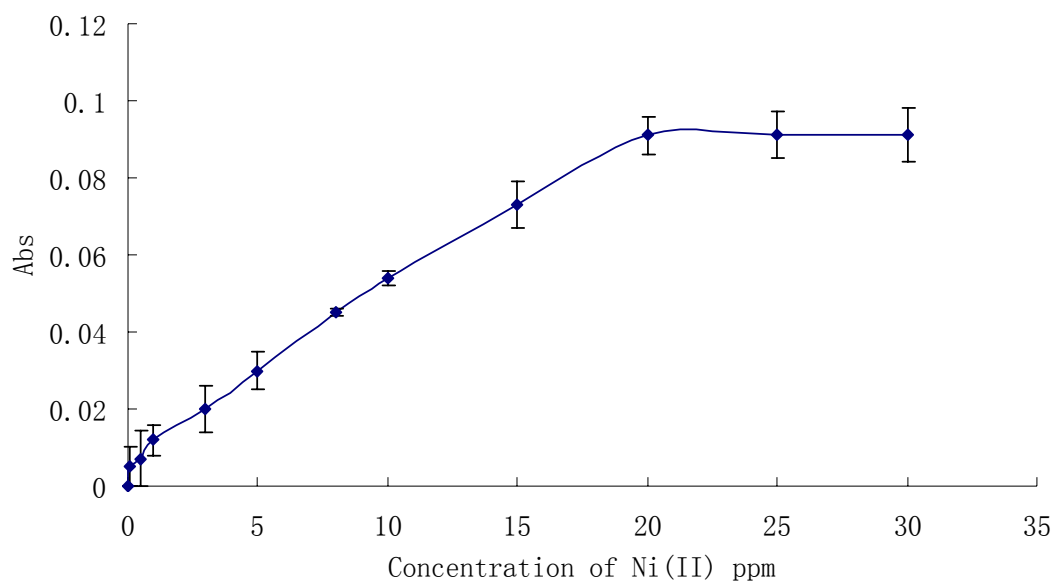
Figure 2.27. The absorption curve of Br-PADAP with Ni^{2+} at pH 9. The curve was recorded at 20 ℃ in pH 9 buffer solution and is represented as the mean of three independed experiments.
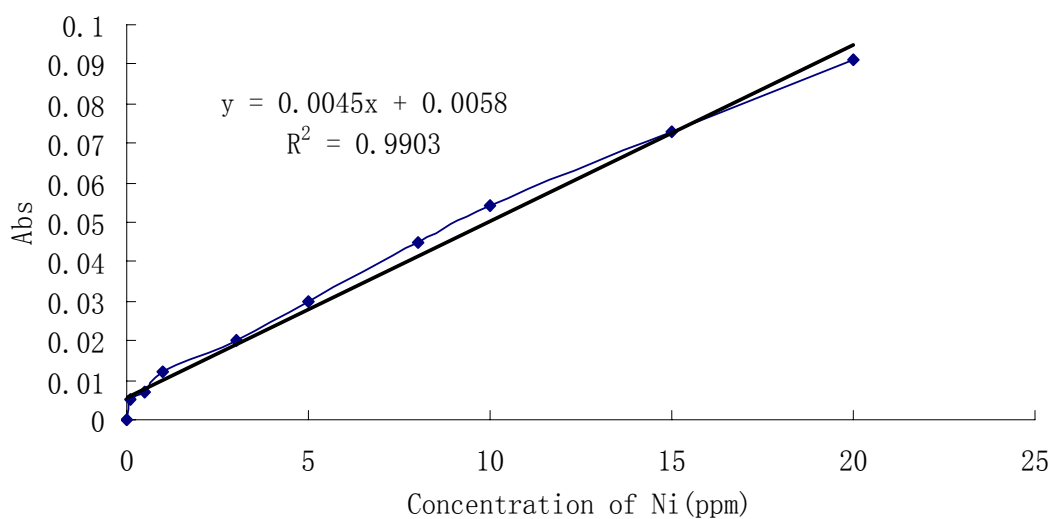
Figure 2.28 Calibration graph for the determination of Ni^{2+} by Br-PADAP at pH 9 (n=3).

The same procedure was used for the study of other ligands with heavy metal ions. A summary of the optimum linear ranges observed for all reactions studies is shown in **Table 2.4**. All the experiments were repeated 3 times and the regression coefficients (R^2) obtained were larger than 0.95.

Table 2.4 Summary of Linearity Studies. (n=3, $R^2 > 0.95$)

Ligand/metal Complex	pH	Measured at Wavelength (nm)	Linear Range ppm
CAS/Cu^{2+}	9	590	0.5-20
Br-PADAP/Ni^{2+}	9	559	1.8-20
CAL/Cu^{2+}	9	510	0.5-10
Nitroso-PASP/Fe^{2+}	6	755	0.4-10

2.3.8 Formation Constants and Molar Absorptivities

The K_f and molar absorptivity values (ε) of each complex that was studied in subsequent chapters are detailed in **Table 2.5**. These values were calculated as shown in the worked example in Appendix II. The complexes formed immediately and were determined to be stable for at least 24 h after they had formed.

It is generally reported that the more points of attachment, the more stable the resulting complex. However, in this case, both monodenate and bidentate lignads were observed to form stable complexes. Each of the complexes displayed a high formation constant, which shows that they are stable and form rapidly. The molar absorptivity values are all in the magnitude of 10^4. From these results, the complexes show potential for sensor design and development.

Table 2.5 Formation constants of metal ion complexes with dyes at room temperature (95% confidence limit, n=3)

| Complex | Conditions | | ε |
	pH	K_f	$mol^{-1}\ cm^{-1}$
AVN/Fe^{2+}	6	1.6×10^6	5.6×10^4
Nitroso/Fe^{2+}	6	4×10^4	1.7×10^4
Br-PADAP/Ni^{2+}	9	1.7×10^8	1.8×10^5
CAS/Cu^{2+}	9	1.59×10^{21}	3×10^4
CAL/Cu^{2+}	9	1.2×10^6	9×10^4

Conclusion

In this chapter, spectrophotometic solution chemistry has been demonstrated as a simple and quick method for the determination of heavy metal ions by using colorimetric indicators. The optical properties of some commercially available indicators and their complexibilities with heavy metal ions have been characterised by using the UV-Vis spectrophotometric method. The binding abilities of these indicators with a variety of heavy metal ions have been investigated. The molar absorptivity, dynamic linear working ranges and the also the formation constants of the indicator-metal complexes have also been studied.

Br-PADAP obtained a relatively high molar absorbtivity and formation constant with many environmentally significant heavy metal ions, i.e. nickel, copper and cobalt respectively. CAS, CAL, AVN and Nitroso-PASP are widely used as water soluble indicators. AVN was found to be a selective indicator for Fe^{2+} which obtained absorption maxima at 655nm. Nitroso-PASP showed an interesting potential for the determination of Fe^{2+} and Fe^{3+} simultaneously. CAL showed a promising result for the determination of copper in solution chemistry, although the new absorption maxima observed by CAL-Cu complex is very close to the original CAL absorption maxima, but it also has the potential as an indicator for the determination of copper in sensor technology. CAS showed promising results on the complexation reactions with Cu^{2+}, Fe^{3+} and Co^{2+} ions in pH 9 buffer solutions. All these results are shown in **Table 2.3.**

Nitroso-PASP, CAS, AVN and CAL are the indicators which contain sulfonated groups. This structure makes them very soluble in water solution which is a drawback in terms of being able to immobilise into a polymertric solid support due to the leaking problem. Therefore, these indicators have not been widely used in the optical sensor area. The purpose of this project is focused on the investigation of suitable solid matrices based on the immobilisation of these indicators for sensing heavy metal ions.

Reference

1.	S. Rochat and K. Severin, *J. Combinatorial Chem.*, **12**, 595-599.

2.	R. Narayanaswamy, in *Encyclopedia of Ocean Sciences*, ed. H. S. John, Academic Press, Oxford, Editon edn., 2001, pp. 6-12.

3.	D.C.Harris, *Quantitative Chemical Analysis*, W.H.Freeman and Co., 2003.

4.	C. P. Bacon, Y. Mattley and R. DeFrece, *Rev. Sci. Instruments*, 2004, **75**, 1-16.

5.	H. G. Brittain, *Anal. Chim. Acta*, 1979, **106**, 401-403.

6.	O. S. Wolfbeis, *Fiber optic chemical sensors and biosensors,*, CRC Press, Boca Raton, 1991.

7.	I. Kuzniarska-Biernacka, A. Bartecki and K. Kurzak, *Polyhedron*, 2003, **22**, 997-1007.

8.	Q. Hu, G. Yang, Y. Zhao and J. Yin, *Anal. Bioanal. Chem.*, 2003, **375**, 831-835.

9.	A. Senillou, N. Jaffrezic-Renault, C. Martelet and S. Cosnier, *Talanta*, 1999, **50**, 219-226.

10.	B.Jens, in *9th International Conference on NDT of Art, Jerusalem Israel,* Editon edn., 2008.

11.	D. H. Busch, *Chem. Rev.*, 1993, **93**, 847-860.

12.	I. Oehme and O. S. Wolfbeis, *Microchim. Acta*, 1997, **126**, 177-192.

13.	I. M. Steinberg, A. Lobnik and O. S. Wolfbeis, *Sens. Actuators B: Chemical*, 2003, **90**, 230-235.

14.	N. Mahendra, P. Gangaiya, S. Sotheeswaran and R. Narayanaswamy, *Sens. Actuators B: Chemical*, 2003, **90**, 118-123.

15.	L. d. Coo and C. J. Belmonte, *Talanta*, 2002, **58**, 1063-1069.

16.	W. C. Vosburgh and G. R. Cooper, *J. Ame. Chem. Soc.*, 1941, **63**, 437-442.

17.	W. R. Thiel, *Chemische Berichte*, 1996, **129**, 575-580.

18.	G. Mohr, M. Wenzel, F. Lehmann and P. Czerney, *Anal. Bioanal. Chem.*, 2002, **374**, 399-402.

19.	T. Werner and O. S. Wolfbeis, *Fresenius' J. Anal. Chem.*, 1993, **346**, 564-568.

20.	G. F.J, *The Sigma-Aldrich handbook of stains, dyes and indicators, 2nd edn.*
, Aldrich Chemical Company, 1990.

21.	R. E. Ferreyra, J. M. Camiña, E. Marchevsky and J. M. Luco, *Fresenius' J. Anal. Chem.*, 2000, **368**, 595-600.

22. S. L. C. Ferreira, A. C. S. Costa and D. S. de Jesus, *Talanta*, 1996, **43**, 1649-1656.

23. J. A. Salonia, R. G. Wuilloud, J. A. Gásquez, R. A. Olsina and L. D. Martinez, *Fresenius' J. Anal. Chem.*, 2000, **367**, 653-657.

24. N. A. Yusof and W. A. R. W. A. Kadir, *Spectrochimica Acta Part A: Molecule. Biomol. Spec.*, 2009, **72**, 32-35.

25. S. F. P. Pereira, S. L. C. Ferreira, G. R. Oliveira, D. C. Palheta and B. C. Barros, *Eclética Química*, 2008, **33**, 23-28.

26. D. Leamy and F. Regan, *Int. J. Environ. Anal. Chem.*, 2003, **83**, 867 - 877.

27. M. Fouladgar and A. A. Ensafi, *Sens. Actuators B: Chemical*, **143**, 590-594.

28. E. M. Ghoneim, *Talanta*, 2010, **82**, 646-652.

29. A. A. Vaughan and R. Narayanaswamy, *Sens. Actuators B: Chemical*, 1998, **51**, 368-376.

30. M. K. Amini, T. Momeni-Isfahani, J. H. Khorasani and M. Pourhossein, *Talanta*, 2004, **63**, 713-720.

31. M. Fouladgar and A. A. Ensafi, *Sens. Actuators B: Chemical*, 2010, **143**, 590-594.

32. C. Woodward and H. Freiser, *Talanta*, 1968, **15**, 321-325.

33. M.H.Abernethy and R.T. Fowler, *Clinical Chemistry*, **28**, 520-522.

34. P. Hashemi, M. M. Abolghasemi, K. Alizadeh and R. A. Zarjani, *Sens. Actuators B: Chemical*, 2008, **129**, 332-338.

35. S. L. C. Ferreira, V. A. Lemos, B. C. Moreira, A. C. S. Costa and R. E. Santelli, *Anal. Chim. Acta*, 2000, **403**, 259-264.

36. R. Kocjan and R. Świeboda, *Sepa. Sci.Technology*, 1999, **34**, 2571 - 2582.

37. O. Abollino, C. Sarzanini, E. Mentasti and A. Liberatori, *Talanta*, 1994, **41**, 1107-1112.

38. D. Pérez-Quintanilla, A. Sánchez, I. d. Hierro, M. Fajardo and I. Sierra, *J. Separation Science*, 2007, **30**, 1556-1567.

39. C. Sarzanini, G. Sacchero, M. Aceto, O. Abollino and E. Mentasti, *J. Chromatography A*, 1993, **640**, 127-134.

40. J. Shida and I. Masuda, *Anal. Sci.*, 1998, **14**, 333-336.

41. X. Shen, W. Huang, C. Yao and S. Ying, *Chemosphere*, 2007, **67**, 1927-1932.

42. H. Wada, T. Murakawa and G. Nakagawa, *Anal. Chim. Acta*, 1987, **200**, 515-521.

43. P. N. Nesterenko and P. Jones, *J. Sepa. Sci.*, 2007, **30**, 1773-1793.

44. L. Shi, Z. Li, Z. Xu, Z. Pan and L. Wang, *J. Chemometrics*, 1991, **5**, 193-199.

45. S. C. Srivastava, S. N. Sinha and A. K. Dey, *Microchim. Acta*, 1964, **52**, 605-608.

46. C. Leong, *Anal. Chem.*, 1973, **45**, 201-203.

47. L. González-Miqueo, D. Elustondo, E. Lasheras, R. Bermejo and J. Santamaría, *Water, Air, & Soil Pollution*, **210**, 335-346.

48. F. I. El-Dossoki, *J. Chem. Eng. Data*, **55**, 2155-2163.

49. A. S. Shalabi, H. A. Dessouki, Y. M. Issa and I. S. Ahmed, *Spectrochim. Acta Part A: Mole. Biomole. Spectro.*, 2002, **58**, 2765-2769.

50. J. C. Strong and D. D. Frey, *J. Chromatography A*, 1997, **769**, 129-143.

51. A. Yari and N. Afshari, *Sens. Actuators B: Chemical*, 2006, **119**, 531-537.

52. M. B. Gholivand, M. Rahimi-Nasrabadi, M. R. Ganjali and M. Salavati-Niasari, *Talanta*, 2007, **73**, 553-560.

53. d. leamy, Limerick Institue of Technology, 2004.

54. L. G. Hargis, J. A. Howell and R. E. Sutton, *Anal. Chem.*, 1996, 68, 169-184.

55. USA Pat., 1987.

56. A. Semb and F. J. Langmyhr, *Anal. Chim. Acta,* 1966, 35, 286-292.

57. G. Sawyer and M. Irle, The Chromazurol S Colour Indicator Technique to Detect Copper Contamination in Wood Waste for Recycling, A Guild for Use, Forest Products Research Centre, 2005.

58. M. Mutsuo and K. Miyamoto, *Bull. Chem. Soc.Jap. Chem. Abs.* , 1969, 71

59. N. Ohno and T. Sakai, ANALYST, 1987.

60. J. Zhou and R. Neeb, *Fresenius' J. Anal. Chem.*, 1990, 338, 905-907.

61. K. Sözgen and E. Tütem, Talanta, 2004, 62, 971-976.

62. J. P. Pancras and B. K. Puri, *Anal. Sci.,* 1999, 15, 575-580.

63. Y. Zhao and C. Fu, Analytica Chimica Acta, 1990, 230, 23-28.

64. H. Lu, X. Yin, S. Mou and J. M. Riviello, *J. Liquid Chromatography & Related Technologies*, 2000, 23, 2033 - 2045.

65. F.S. Wei, P.H. Qu, N. K. Shen and Y. Fang., Talanta, 1981, 28, 189.

66. E. Bakker, P. Buhlmann and E. Pretsch, *Chem. Rev.,* 1997, 97, 3083-3132.

67. S. Lakshmi Narayana, S. Adi Narayana Reddy, Y. Subbarao, H. Inseong and A. Varada Reddy, *Food Chem.,* 121, 1269-1273.

Chapter 3

3.1 Introduction

The toxic effects of heavy metals in the environment have been demonstrated by a great number of studies, and their uncontrolled introduction into the environment has caused serious concern.[1] Among the toxic heavy metals, nickel ion is harmful at certain concentrations. It is toxic to both man and animals at high doses.[2] Chronic Ni poisoning can result in cardiovascular, respiratory and kidney diseases.[2] Nickel compounds are used in the production of Ni-Cd batteries, in electroplating and electroformating procedures. Nickel alloys are used in the production of tools, machinery and jewellery.[3] Human exposure to nickel species occurs primarily via inhalation and ingestion through food, air, and water or dermal contact with nickel-containing jewellery. Nickel is one of the priority pollutants according to the EU WFD.[4] The Maximum Admissible Concentration (MAC) value for nickel in drinking water, which has been set by the European Commission, has been revised from 50 to 20 μgL^{-1}.[2]

There are several conventional techniques that are widely used in analytical control laboratories, such as atomic absorption spectrophotometry (AAS) and inductively coupled plasma mass spectrometry (ICP-MS).[5] They permit selective detection of nickel over other metals with very low detection limits (1 μgL^{-1}). However, the equipment prevents the applications for *in-situ* measurements in real time. Numerous spectrophotometric methods have been developed for the determination of heavy-metal ions.[5] The rapid development of spectrophotometry for the determination of metal ions over the past two decades is mainly due to the introduction of newly developed optical chemical sensors.[6] Extensive research has focused on developing recognition molecules, materials science and device implementation.[7]

Several commercially available spectrophotometric indicators have been used for the determination of Ni^{2+} ions in solution, such as 1-(2-pyridylazo)-2-naphthol (PAN) and Pyrocatechol Violet (PV).[2,8] It has been found that in Chapter 2, 2-(5-bromo-2-pyridylazo)-5-(diethylamino) phenol (Br-PADAP) showed promising results for the determination of Ni^{2+} ions in aqueous media. It is a highly sensitive photometric azo-type reagent and can form very stable and highly coloured complexes with divalent, trivalent state metal ions (molar absorptivities of ca. 10^5 l mol^{-1} cm^{-1}).[3,8] Although Br-PADAP is an unselective indicator for one specific metal ion in solution, the

contamination by other heavy metal ions can be masked using masking agents.[9] Therefore, Br-PADAP has a large potential in developing optical sensors for the determination of nickel ions. In this chapter, the study is focused on implementing this reaction in a one-shot sensor format for the determination of Ni^{2+} ion in aqueous media. Consequently, optical test strips based on the immobilisation of Br-PADAP into solid sensing materials for the determination of heavy metal ions in aqueous samples have been investigated.

3.1.1 Materials Study for the Immobilisation of Br-PADAP

Solid materials can largely affect the overall performance of the optical-test strips. They should have: a good solubility with organic dyes; be chemically inert (in organic or inorganic solutions, *etc*.) and be resistant to different environments (temperatures, pH value of aqueous samples, *etc*.) depending on their various industrial applications.

Solid state membrane and films from Br-PADAP and its analogues have been incorporated with a number of materials for the construction of optical sensors for heavy-metal ions, such as polyvinylchloride (PVC), ethy cellulose, and Nafion membranes[9-11] (**Figure 3.1**).[12]
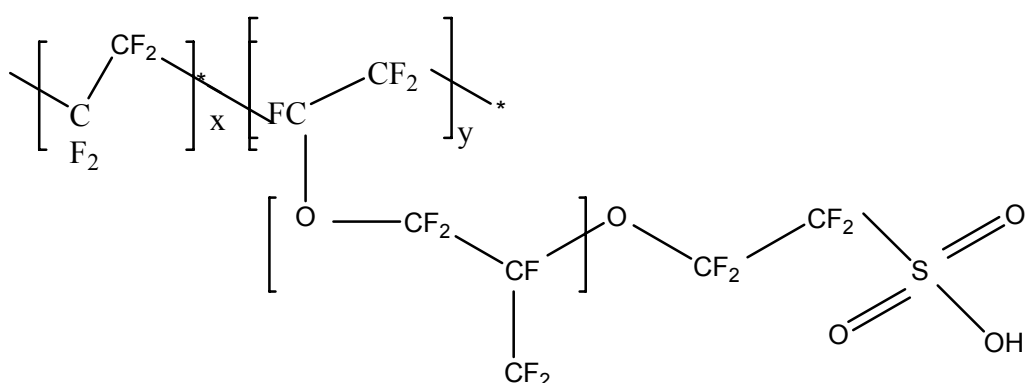
Figure 3.1 Structure of Nafion.

However they suffer from a series of drawbacks:
- They have low stability, especially in organic solvents;
- They are usually not strongly adherent to the glass microscope slide;

- The leaching of dyes from the membranes can reduce the lifetime of optical sensors.

Therefore, the challenge for the development of optical sensors, based on the immobilisation of Br-PADAP, is to investigate more stable polymeric materials.

Sol-gel techniques, based on the hydrolysis and polycondensation of alkoxide precursors, are of intense current interest.[13, 14] There are many advantages to using the sol-gel materials in optical sensor fabrication over organic polymers, for example:

- They are chemically inert, mechanically very resistant and they are optically transparent;[13, 15]
- Their surface area and porosity can be tailored by the chemical composition of the starting materials and by processing conditions;
- They show excellent adhesion to glass and other silica substrates due to the covalent linkage that is formed with the silanol groups of the glass surface;[15]
- They are good hosts for organic dyes.[14] This can reduce the leaching from the sol-gel film into bulk-sample solutions compared with other hydrophilic media.

Inorganically modified sol-gel membranes are cracking during the drying process. Compared with inorganic sol-gel polymers, organically modified silicates (ORMOSILs) have been attracting great interest presently, in the area of chemical sensors.[16] They have been proven to be a better solid matrix to accommodate indicators owing to their better stability, optical transparency, flexibility, permeability and porosity.[17] Recently, ormosils-based optical sensors for metal ions have been extensively studied, since more stable and less cracking ormosils material can be obtained from several types of precursors, such as organotrialkoxysilane or organodialkoxysilane [R–Si(OR′)$_3$ or R$_2$(OR′)$_2$]. Generally, the sol–gel process consists of hydrolysis and condensation reactions.[18] The silicate glasses are typically prepared by mixing alkoxysilanes with a low molecular mass, such as tetramethoxysilane (TMOS) or tetraethoxysilane (TEOS), with water in a mutual solvent like methanol or ethanol.[17, 19] Several types of organosilicon precursors can be hydrolysed and co-condensed with TMOS or TEOS to form an organic–inorganic hybrid.[18, 20, 21] In this regard, ormosils processes are dependent on a large number of processing parameters such as: alkoxide structure; reaction-medium pH; solvent type; water–sol–gel

precursor ratio; aging temperature and pressure; drying temperature and dying time as well.[22] With the substitutes of unreactive and non-hydrolysing alkyl groups for reactive alkoxyl groups in organosilicon precursors, the former ones structurally act as a network modifier that terminates the silicate networks. However, it has been reported that the hydrophobicity of the sol-gel membrane changes by adding the organic precursors. Furthermore, this effects the diffusion of the metal ions into the sol-gel membrane.[23]

Another strategy is to increase the chemical stability of dye molecules within the sensing materials for preparation of organic-inorganic hybrid sol-gel materials.[12] Sol-gel-derived silicate/Nafion composite film as an immobilisation-matrix-probe-molecule for the development of an optical sensor has been introduced. Nafion is a poly(perfluorosulfonic) acid membrane, which is extensively used in: chloroalkali industries, water electrolysis, polymer-electrolyte fuel cells, and Donnan-dialysis-based applications.[23] The special interest in Nafion arises from the fact that its films show very good chemical and thermal stability due to the fluorocarbon backbone and ion-exchange properties caused by sulfonate groups.[24] It has been widely employed for the development of both electrochemical and optical sensors.[25] Electrochemical sensors employing Nafion and based on different principles of operation have been described for the determination of many different species, such as CO, NO, glutamate, hydrazine, uric acid and methyl viologen.[26] It has also been used as a support for the development of optical sensors for ions.[27, 28] Also, an optical biosensor which utilised hybrid Nafion/sol-gel films has also been reported for the determination of phenol. The moderate hydrophobicity and great porosity of this type of film, has been also been reported in terms of facilitating sensing systems.[29]

In this chapter, several types of plasticised PVC membrane materials, inorganic sol-gel thin film, Organically Modified Sol-gels (ORMSOLs) thin films and Nafion/silica composite thin films are prepared by sol-gel techniques as sensing platforms for the immobilisation of Br-PADAP for Ni^{2+} sensing purposes in aqueous solution.

3.1.2 Immobilisation Techniques

Immobilisation of a colorimetric reagent in sensing materials is a critical step in the fabrication of optical sensors and is mainly based on two approaches. They are chemical immobilisation (by covalent bonds) of the dyes onto the functionalized sol-gel materials,

and simple physical immobilisation (physical doping) of dyes into sol-gel matrices.[30] Chemically, bonding of indicators to a sol-gel matrix can greatly stabilize the indicators with the matrix materials and thus reduce the leaching of the dyes from the matrix.[31] However, the direct bonding of dyes to an inorganic sol-gel network is difficult due to the relative inertness of the surface. Therefore, surface modifications are needed, such as adding other organic precursors that contain active groups, such as $-NH_2$, and -SH-. The modification process of covalent immobilisation may alter the structural and optical properties of the sensing reagents leading to loss of sensing properties. Furthermore, the hydrophobicity will be increased by the introduction of organic precursors, thus largely prolonging the response time of the optical sensors.

Physically doping the sol gel solution with the desired compounds is the mostly widely used method for the immobilisation of the organic dyes.[31] The important advantages of physical entrapment are its simplicity, the minimal alteration of spectra and binding properties of the indicators.[31, 32] The technique of doping Br-PADAP in sensor membranes has been successfully used to make sensors for metal-ion determination.[33] In this study, we describe our efforts to extend the use of Br-PADAP immobilised into several sensor materials, such as plasticised PVC membrane, inorganic sol-gel membrane, organically modified sol-gel membrane and the hybrid Nafion/sol-gel membrane in the construction of new, reversible optical chemical sensors for the determination of nickel concentration in bulk systems.

3.1.3 The Aim and Objectives

The work aims to outline the effect of different materials (PVC membrane, inorganic and hybrid sol-gel materials) on the performance of Br-PADAP doped optical sensing films for the determination of Ni^{2+} in aqueous solution.

The sol-gel thin films were prepared via acid-catalysed hydrolysis and condensation of TEOS alone, and with one of the three organosilicon precursors, Me–TriMOS, Bt–TMOS and Ph–TriMOS, in different molar ratios. We are interested in developing materials with a lower pH, but larger absorbance response for Ni^{2+} sensing applications. A lipyphilic azo dye, Br-PADAP was used as the indicator for the prepared-sensing films.

The objectives of this work are:

1. Synthesis of inorganic sol-gel films, ORMOSILs thin films and hybrid Nafion/sol-gel membranes.

2. Preparation of the optical sensors based on the immobilisation of Br-PADAP into plasticised PVC membrane.

3. To fabricate an optical sensing membrane which is based on the immobilisation of Br-PADAP on hybrid Nafion/sol gel membranes for the determination of nickel ions.

4. To optimise the working condition of Nafion/sol-gel thin films for the determination of nickel ions.

3.2 Materials and Methods

3.2.1 Reagents

Reagent-grade plasticiser tributyl phosphate (TBP), poly-vinyl chloride (PVC), activated anion carrier potassium tertrakis chlorophenyl borate (KTClPB), solvent tetrahydrofuran (THF) and 2-(5-Bromo-2-pyridylazo)-5-diethylaminophenol (Br-PADAP) were purchased from Sigma-Aldrich Co Chemical Company, Tallaght, Ireland.

All reagents used in this work were of analytical grade and were obtained from Sigma-Aldrich Co Chemicals, Tallaght, Ireland. Tetramthyl orthosilicate (TEOS) 98% GC, isobutyl-trimethoxysilane (B-TMOS), 97% phenyltrimethoxysilane (Ph-TMOS), 97% trimethoxylsilane (Tri-TMOS), 98% were used as starting materials for the sol-gel films. Nafion$^{\circledR}$117 is a 5 wt. % solution in low aliphatic alcohols and 10% water.

Analytical reagent grade nickel chloride was received from M&B Laboratory Chemicals, Tallaght, Ireland, and it was used without further purification. A stock solution of 1000 mg/ L Ni^{2+} was prepared by dissolving the required amount of $NiCl_2 \cdot 6H_2O$ in deionised water. Other metal-ion stock solutions were prepared at the concentration of 1000 mg/ L with corresponding metal salts: copper nitrite [$Cu (NO_3)_2$] •$3H_2O$ (Sigma-Aldrich, Co Chemicals, Tallaght, Ireland), cobalt nitrate ($Co (NO_3)_2$] •$6H_2O$ (M&B Laboratory Chemicals, Tallaght, Ireland), ferrous chloride [$FeCl_2$ •xH_2O] (Fluka, Tallaght, Ireland), iron nitrate $Fe (NO_3)_3$ •$9H_2O$, lead nitrate ($Pb (NO_3)_2$) (M&B Laboratory Chemicals, Tallaght, Ireland), and zinc nitrate [$Zn (NO_3)_2$] •$6H_2O$)] (Sigma-Aldrich, Tallaght, Ireland). The pH buffer solutions were prepared using the following buffer salts to make the concentration of 10 mM, with an ion strength of 100.

All solutions were prepared using distilled water (18 Ω), purified through a Milli-Q [50] Plus system. Microscope slides (BMS brand, ground edges, 26 mm x 76 mm, 1.0 mm-1.2 mm thick) were purchased from Lennox, Dublin. Glass slides were cut in to 0.9 cm x 2.6 cm pieces and used as solid supports.

Table 3.1 Preparation of buffer solution

pH	Chemicals	Method
4	Glacial Acetate Acid	0.06 g of acetate acid with 0.574 g of NaCl
5	Glacial Acetate Acid	0.06 g of acetate acid with 0.574 g of NaCl
6	MES	0.195 g of MES free acid with 0.561 g of NaCl
7	HEPES	0.238 g HEPES free acid with 0.574 g of NaCl
8	HEPES	0.238 g HEPES free acid with 0.574 g of NaCl
9	TAPS	0.243 g of TAP with 0.54 g NaCl
10	CAPS	0.221 g of CAP free acid with 0.54 g NaCl

3.2.2 Instruments

A Cary 50 UV-Vis spectrophotometer (Varian, USA) was used for recording the visible spectra. The contact angle data were obtained according to the published method[34, 35] The Hitachi S3400 Scanning Electron Microscopy (SEM) was used for the study of membranes surface (Japan). An EDT pH meter (Germany) was used for the pH adjustment of all buffers. A Chemat Spincoater KW 4A was used for the preparation of thin film.

3.2.3 Sol-gel Thin Film Preparation

Sol-gel was deposited on glass slides. The silanol groups on the surface of the glass were activated by concentrated nitric acid overnight; then washed with distilled water and ethanol; and then dried at 100 °C. In this study, 3 types of xerogel thin films were prepared. The first one was prepared with TEOS as precursor; the second one was prepared with ORMOSILs thin films, which comprises of TMOS with 3 different organo-silanzing agents: BTMOS, TrTMOS, and PhTMOS; and the last one is the Nafion entrapped TMOS thin film.

Preparation of the Inorganic Sol-Gel Sensor Films Catalysed by Acid

The preparation of mono-precursor sol gel thin film was adapted from literature,[33] and is illustrated in **Figure 3.2**. The molar composition (Si: Ethanol: H_2O: HCl) of the initial sol was 1:3.14:5:0.046 by molar ratio.

```
┌─────────────────────────────────────────────┐
│ Step 1: 2.2 mL of TEOS, 1 ml of Ethanol, 0.75 mL │
│         of 0.1 M HCl, 1.34 ml of deionised water │
└─────────────────────────────────────────────┘
                      │  Stirred for 10 min and left overnight
                      ▼
┌─────────────────────────────────────────────┐
│ Step 2: Added Br-PADAP until the desired initial │
│ concentration was reached.                     │
└─────────────────────────────────────────────┘
                      │  Sonicated for 20 min
                      ▼
┌─────────────────────────────────────────────┐
│ Step 3: Spin-coated 1 mL of sol-gel cocktail on a │
│ pretreated glass slide at 1650 rpm for 10 s     │
└─────────────────────────────────────────────┘
                      │
                      ▼
┌─────────────────────────────────────────────┐
│ Step 4: Dried the coated sol-gel membranes in a sealed │
│ dark place for 2 h and kept in pH 8 buffer before use. │
└─────────────────────────────────────────────┘
```

Figure 3.2 Preparation of sol-gel materials.

Preparation of Sol-Gel Sensor Films Catalysed by HCl

Three types of multi-component ORMSOLs were prepared through the acid-catalysed method by combining TEOS with PhTMOS, MeTMOS or isobutyl-TMOS. TEOS diluted with ethanol was mixed with PhTMOS, MeTMOS and isobutyl-TMOS at the molar ratio 20 % of organic precursors: TMOS. Water: alkoxyde and acid catalysis ratio (The molar composition (Si: Ethanol: H_2O: HCl) of the initial solution was 1:3.14:5:0.046 by molar ratio). The compositions of the solutions produced are summarised in **Table 3.2.** 2, 5-Br-PADAP was added to the solutions previously dissolved in the ethylenglykol-monoethylether. For each type of film, several increasing concentrations of 2, 5- Br-PADAP were tested in order to study the effect of the immobilised reagent concentration. All the sol-gel solutions were allowed to gel at room temperature and sonicate for 15 min prior to coating. All the films were obtained by spin-coating on glass slides of 3 cm x 2 cm. After coating, all films were dried at room temperature for 2 days.

Table 3.2 The compositions of various organosilanes in the sol gel cocktails.

Precursors	Volume of precursor (mL)	Volume of TMOS (mL)
TMOS with PTMOS	0.5	1.5
TMOS with MTMOS	0.38	1.58
TMOS with Isobutyl-TMOS	0.53	1.58

Step 1: 2.2 mL of TMOS, 1 mL of Ethanol, 0.75 mL of 0.1 M HCl, 1.34 mL of deionised water

Stirred for 10 min and left overnight

Step 2: Added an amount of organic precursor solution

Stirred for 10 min

Step 3: Added Br-PADAP until the desired initial concentration was reached.

Sonicated for 20 min

Step 4: Spin-coated 1 mL of the sol-gel cocktail on a pretreated glass slide at 1650 rpm for 10 s.

Step 5: Dried the coated sol-gel membranes in a sealed dark place for 2 h and kept in pH 8 buffer before use.

Figure 3.3 Preparation of the organically modified sol-gel materials.

Preparation of Nafion entrapped sol gel thin film

The sol gel stock solution was prepared using the same method as described in **Figure 3.2**. The sol gel stock solution was mixed with Nafion solution at different volume ratios (v/v) to form the sol gel silicate/Nafion composite. The procedure is illustrated in **Figure 3.4**.

```
┌────────────────────────────────────────────────┐
│ Step 1: 2.2 mL of TMOS, 1 mLof Ethanol, 0.75 mL of │
│         0.1 M HCl, 1.34 mL of deionized water      │
└────────────────────────────────────────────────┘
                    │  Stirred for 10 min and left overnight
                    ▼
┌────────────────────────────────────────────────┐
│ Step 2: 1 mL of Nafion with 0.01 M of HCl (2:1)    │
│                      solution                       │
└────────────────────────────────────────────────┘
                    │  Stirred for10 min
                    ▼
┌────────────────────────────────────────────────┐
│ Step 3: Add Br-PADAP till the desired initial      │
│                concentration reached.               │
└────────────────────────────────────────────────┘
                    │  Sonicated for 20 min
                    ▼
┌────────────────────────────────────────────────┐
│ Step 4: Spin-coat of 1 mL of sol-gel cocktail on   │
│       pretreated glass slide at 1650 rpm for 10 s.  │
└────────────────────────────────────────────────┘
                    │
                    ▼
┌────────────────────────────────────────────────┐
│ Step 5: Drying the coated sol-gel membranes in a   │
│      sealed dark places for 2 h and kept in pH 8    │
│               buffer before use.                    │
└────────────────────────────────────────────────┘
```

Figure 3.4 Preparation of Nafion/sol-gel materials.

3.2.4 Measurement Procedure

The Br-PADAP immobilised sol-gel thin films were placed into a quartz cuvet (1 cm wide). The thin films were dipped into the test solution and tested with UV-Vis spectroscopy.

3.2.5 Characterisation of the Sensors

The different sensor films were characterised in terms of spectral features, sensing performances and leaching of components. To enable spectroscopic characterization and simultaneously study the effect of pH on the formation of an immobilized 2, 5-Br-PADAP-Ni^{2+} complex, the sensor membranes were immersed in Ni^{2+} solutions of two different concentrations (10.0 and 100 mg L^{-1}) prepared with buffers of pH value ranging from 1 to 10. The corresponding spectra, as well as the blank references of the buffer solution without Ni^{2+} were recorded in the wavelength range between 350 and 700 nm.

Scanning electron microscopy (SEM) was used to examine the surface morphology of the sensors thin films. The light microscope was used to characterise the cracking of the sensors.

The Nafion/Sol gel thin films were characterised with FT-ATR. The extent of leaching of ligands was evaluated by immersing the sol-gel film doped with Br-PADAP repeated at 5 min intervals in 2.0 mL of buffer solution (pH 8). After each interval, the sensor was withdrawn and the absorbance of the solution was measured at a wavelength of 447.0 nm (wavelength of maximum absorbance for 2, 5-Br-PADAP).

3.3 Results and Discussions

3.3.1 Types of Organic -precursors

Types of silicate precursors play an important role on the properties of sol-gel materials. They can influence the textural properties of the sol-gel such as hydrophobicity, surface area, micro-porosity, pore volume and pore-size distribution of the sol-gel thin films.[18] Consequently, these factors can also influence the sensing performance of sensors, such as absorption intensities, the response times, calibration range, the selectivity and also the stability of the dyes within the sol-gel.[14] Therefore, different types of organic precursors have been investigated. Seven types of sol-gel thin films with different precursors have been prepared, i.e. B-TMOS, Ph-TriMOS and MTMOS. The composition of the sensor membranes and the performance of them are shown in **Table 3.3.** It was found that the formation of cracks in inorganically modified sol-gel materials during drying is a problem in the preparation of thin films. For example, thin film 1, which was prepared by TEOS alone, shows the cracking of the materials due to the shrinkage during the condensation of TEOS sol. This has been confirmed by the SEM image of the surface of thin film 1 which is shown in **Figure 3.5.**
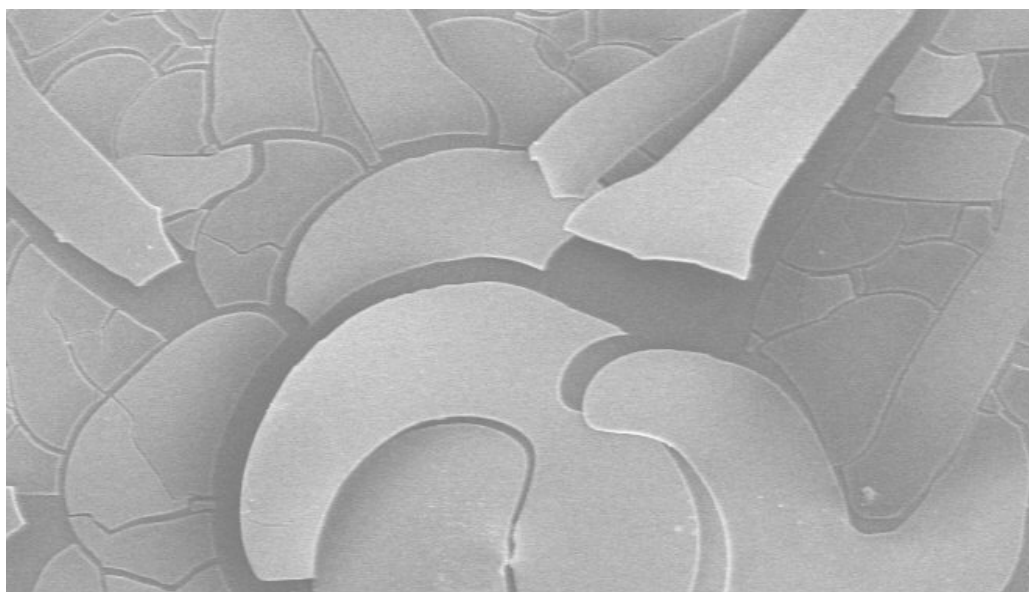

Figure 3.5 SEM of the surfaces of membranes. TOES Thin film 1.

In order to solve the cracking of the sol-gel membranes which were prepared by inorganic precursor TEOS alone, different types of organic precursors were added at different volume ratios. The membranes 2-7 were prepared by the organic modification of the sol-gel method. They obtained transparent and smooth surfaces. Compared with the membrane prepared with inorganic sol-gels, it has been reported that the multi-component sols exhibited higher reaction rates under acid-catalysis conditions than TEOS materials alone. Furthermore, they reduce the number of the free silanol groups on pore walls; thus the shrinkage problem can be solved.[32]   This is the first advantage of OMOSILs over inorganic sol-gel based membrane.

Table 3.3 Sol-gel contains 0, 5, 10, 15 and 20% of organic-precursors (n=3)

Films	Thin Film	Consistency	[a]Response time (h)	Absorption (λ_{max}, nm)	Leaching of dye
1	TEOS	cracking,	72	430	Yes, after 20 hours
2	5% MTMS in TEOS	Transparent, not cracking	90	435	No
3	10% MTMS in TEOS	Transparent, not cracking	95	435	No
4	15% MTMS in TEOS	Transparent, not cracking	124	435	No
5	20% MTMS in TEOS	Transparent, not cracking	168	435	No
6	5% BTMOS in TEOS	Transparent, not cracking	100	435	No
7	5% PhTMOS in TEOS	Transparent, not cracking	102	435	No

[a] Response time: the times required to achieve 95% of the ultimate response, t (95%).

The absorbance spectra of Br-PADAP doped sol gel thin films 2-7 have been tested in pH 8 buffers and Ni^{2+} solution (50 mg/L, prepared with pH 8 buffer solution). The blank sol

gel thin films showed the absorbance maxim at a wavelength of around 430 nm, which was similar with the solution study of Br-PADAP in pH buffer 8 solutions. It was observed that no leaching of the dye occurred when dipping the test strips 2-7 into the pH 8 buffer solution. The leaching of Br-PADAP from the inorganic sol gel thin films was reduced by adding organosilanes. From **Table 3.3,** it is shown that the indicator Br-PADAP started to leach from inorganic sol-gel thin film after 20 h. In contrast, the thin films which were prepared by adding organol silane agents showed no leaching of the dyes. This is probably due to the hydrophobicity of the thin films which have been increased by adding organic silane.[36] It was reported that the hydrophobicity of the thin films can be affected by the types of organol silane.[18] The organic function, *e.g.* $-CH_3$, C_6H_{13} and $-C_6H_5$ increased the solubility of Br-PADAP dye within the thin film, thus reducing the leaching of the dyes from the membrane. This is the second advantage of the ORMOSILs over inorganic sol-gel membranes. The hydrophobicity of these thin films has been tested by contact angle measurements. The results are shown in **Figure 3.6.**
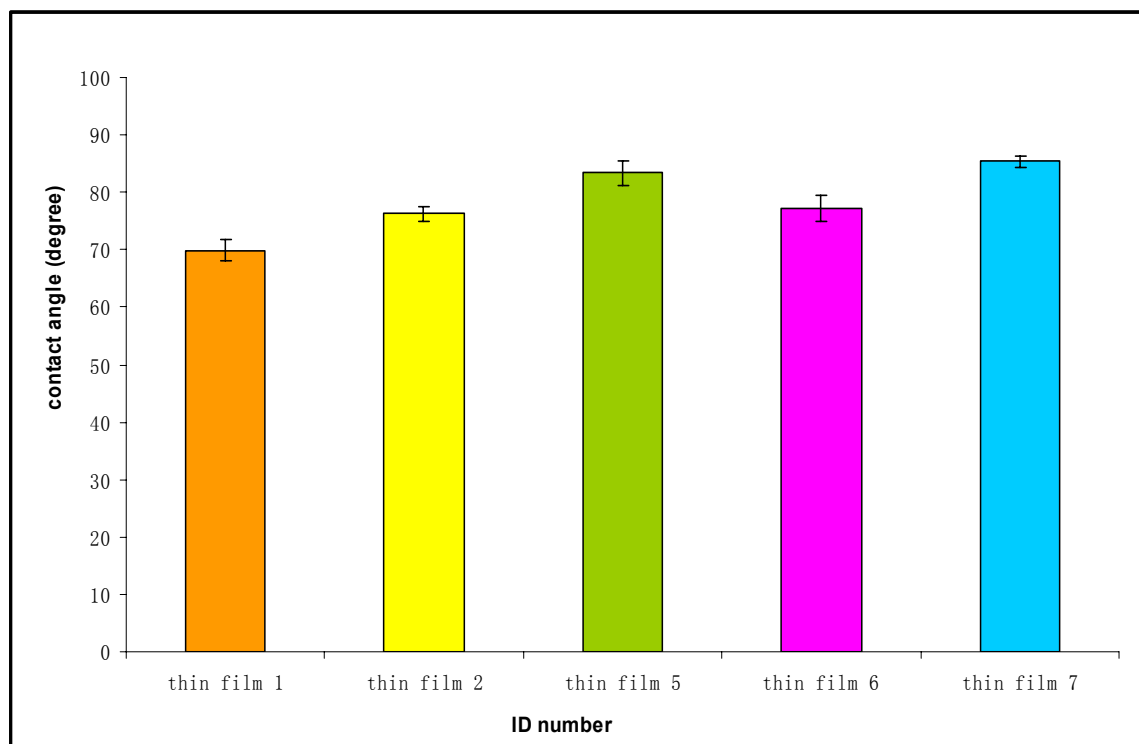

Figure 3.6 Contact angle measurements of thin films prepared by various methods. ■ thin film 1 (TEOS); ■ thin film 2 (5%MTMOS-TEOS), ■ thin film 5 (20 % MTOMS-TEOS), ■ thin film 6 (5%BTMOS-TEOS), ■ thin film 7 (5% PTMOS-TEOS).

It was found that the response times for the Br-PADAP doped thin films for Ni^{2+} (at the concentration of 50 mg/l) were very long, up to several hours. The response times of the Br-PADAP doped sol-gel thin films increased by increasing the amount of the organic silane in the sol-gel thin films. The longest response time was 108 h for the membrane which was prepared with 20% of Me-TMOS with 80 % of TMOS. The hydrophobicity of the sensing film can also be adjusted by changing the organic precursor -TEOS ratio in the starting materials. It was found that leaching of the dye was prevented with increasing the ratio of Me-TMOS to TEOS; the response times of these films have been prolonged. The reason for this slow diffusion rate can be explained by the increased hydrophobicity of the thin film which leads to a slow diffusion rate of hydronium Ni^{2+} from the solution to the indicator dyes which embedded into the sol-gel networks. In these hybrid materials, surface silanol groups are replaced by alkyl groups which have a poor affinity for water—hence rendering the sol-surface hydrophobicity.[36] It was reported that the substitution results in decreased polarity and hydrophilicity of the produced ormosils,[37, 38] which in turn, increases the response of sensing weaker polar substances like oxygen or ammonia.[16, 32]

The ratio of organic silane was tested to study the effect on the ligand leaching and response times to metal ions. It was found that by increasing the ratio of Me-TMOS to TMOS, the number of the $Si-CH_3$ groups in the surface increased. This causes the Si-OH groups to be replaced by $SiCH_3$ groups, thus enhancing the surface hydrophobicity of the thin film. With increasing the content of Me-TMOS, the response sensitivity of the sensing films towards Ni^{2+} ion increased greatly, and the response time decreased. However, under these experimental conditions, when the ratio of Me-TMOS to TMOS reached 20%, the obtained film became sticky and the response time prolonged and the absorption value remained constant. The MeTMOS-TMOS ratio at ~5% was found to be the optimised ratio under these experimental conditions. However, the response time of these organically- modified membranes still exhibited very long response times for the determination of Ni^{2+}. Therefore, the ORMOSILs can reduce the crack of the sol-gel thin film and the leaching of the lipophilic Br-PADAP from the membrane; however, the increased hydrophobicity prolonged the response time of the optical sensor for the determination of Ni^{2+} ions.

3.3.2 Nafion-Entrapped TMOS thin film

In order to reduce the response time of the sol-gel sensing film by increasing its hydrophibicity, the moderate hydrophilic polymer Nafion was mixed with a sol gel membrane. In the following section, sensor membranes for the determination of Ni^{2+}, based on the Br-PADAP immobilised hybrid Nafion/sol gel was investigated in the following sections. Nafion was incorporated in the sol-gel-derived silica and formed optically transparent, smooth materials. The performance of the Nafion/sol-gel thin films is shown in **Figure 3.7.**
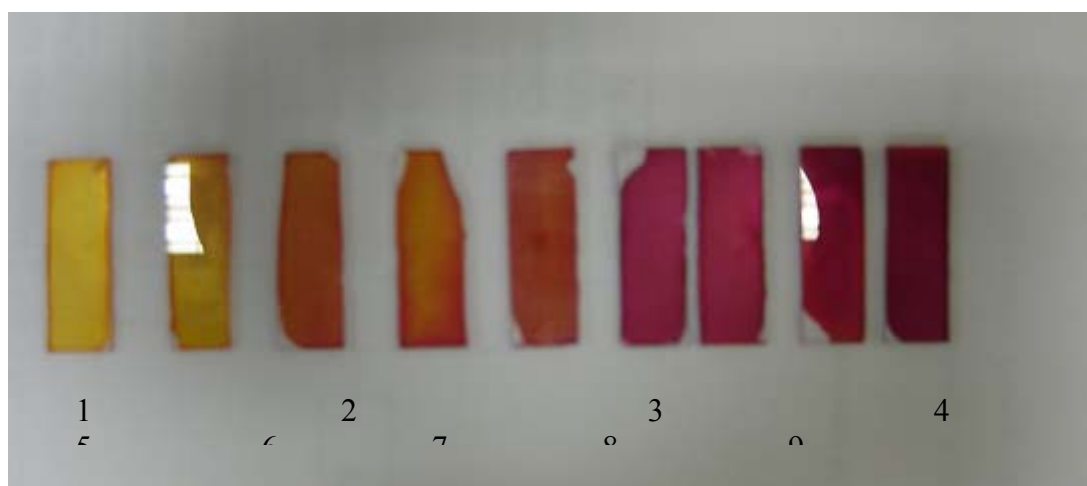
Figure 3.7 Images of nafion-silica composite films after doping into Ni^{2+} solutions. (1) blank nafion/sol-gel membrane; (2) nafion/sol-gel membrane dipped into Ni^{2+} solution with the concentration of 5 ppm; (3) 8 ppm; (4) 15 ppm; (5) 20 ppm; (6) 25 ppm; (7) 30 ppm; (8) 35 ppm; (9) 40 ppm.

Figure 3.7 shows that appearance of the blank Nafion/sol-gel composite films after dipping them into Ni^{2+} solutions with different concentrations. Nafion/sol gel materials were attached to the glass microscope slides firmly and no swelling occurred after immersion for a long period. Furthermore, no cracking of the sol gel occurred. This also has been confirmed by the SEM study of these membranes and the results are shown in **Figure 3.8**. No leaching of the dyes occurred during the process. The hydrophobic fluorocarbon backbone and a hydrophilic cation-exchange site make Nafion with a

moderate hydrophobicity, which can assist in retaining the lipiphylic Br-PADAP in the film and thus reduce leaching of it from the sensing matrices.
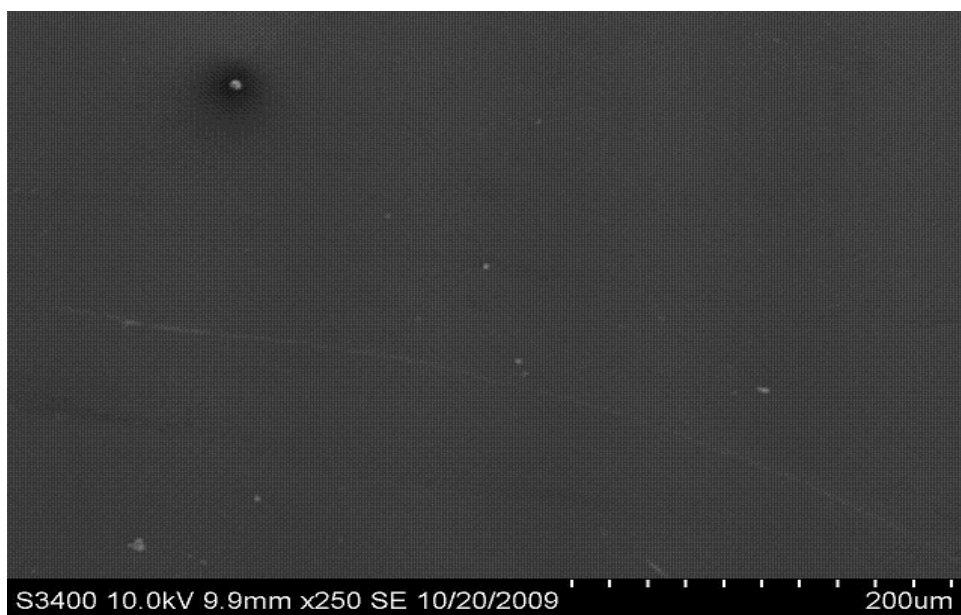
Figure 3.8 SEM of Nafion/sol gel film.

3.3.3 ATR-IR Study of Nafion/sol-gel Membranes

The Nafion polymer is highly dispersed throughout the porous silica network. This can be confirmed by the study of attenuated-total-reflection infrared (ATR-IR) spectroscopy. **Figure 3.9** shows the ATR spectrum of (a) a Nafion-coated membrane, (b) blank sol-gel membrane which contains 50 % (v/v) of Nafion membrane and (c) Nafion-TEOS sol gel membrane. In **Figure 3.9 (a),** a strong band was observed within the 1210-1160 cm^{-1} region, which corresponds to the C-F stretching modes of nafion.[39] The peaks observed at 1054 and 960 cm^{-1} are attributed to the stretching vibrations of SO_3^- and C-O-C moieties, respectively. For sol gel membrane, it can be seen from the spectra in **Figure 3.9 (b),** that bands were observed at 1080 and 800 cm^{-1}. These IR bands correspond to the Si-O-Si stretching vibration of the silica networks, and the broad band near 3450 cm^{-1} corresponds to the structural hydroxyl groups, and the physisorbed water, typical of the silica gels.[39] **Figure 3.9 (c)** is the ATR spectrum of the Nafion/silica composite membrane with a Nafion-Sol gel ratio (v/v) of 1:1, the biggest band at 1100-1000 cm^{-1} is due to the overlap of C-F band and Si-O-Si band and the peak at around 800 cm^{-1} is due to the Si-O-C band of the hybrid nafion/sol-gel membrane.

Figure 3.9 ATR-IR Spectra of Nafion modified sol-gel film. (a) Nafion film; (b) Blank TEOS film; (c) Nafion/TEOS film.

3.3.4 Optimising the Ratio of Nafion to Sol-gel
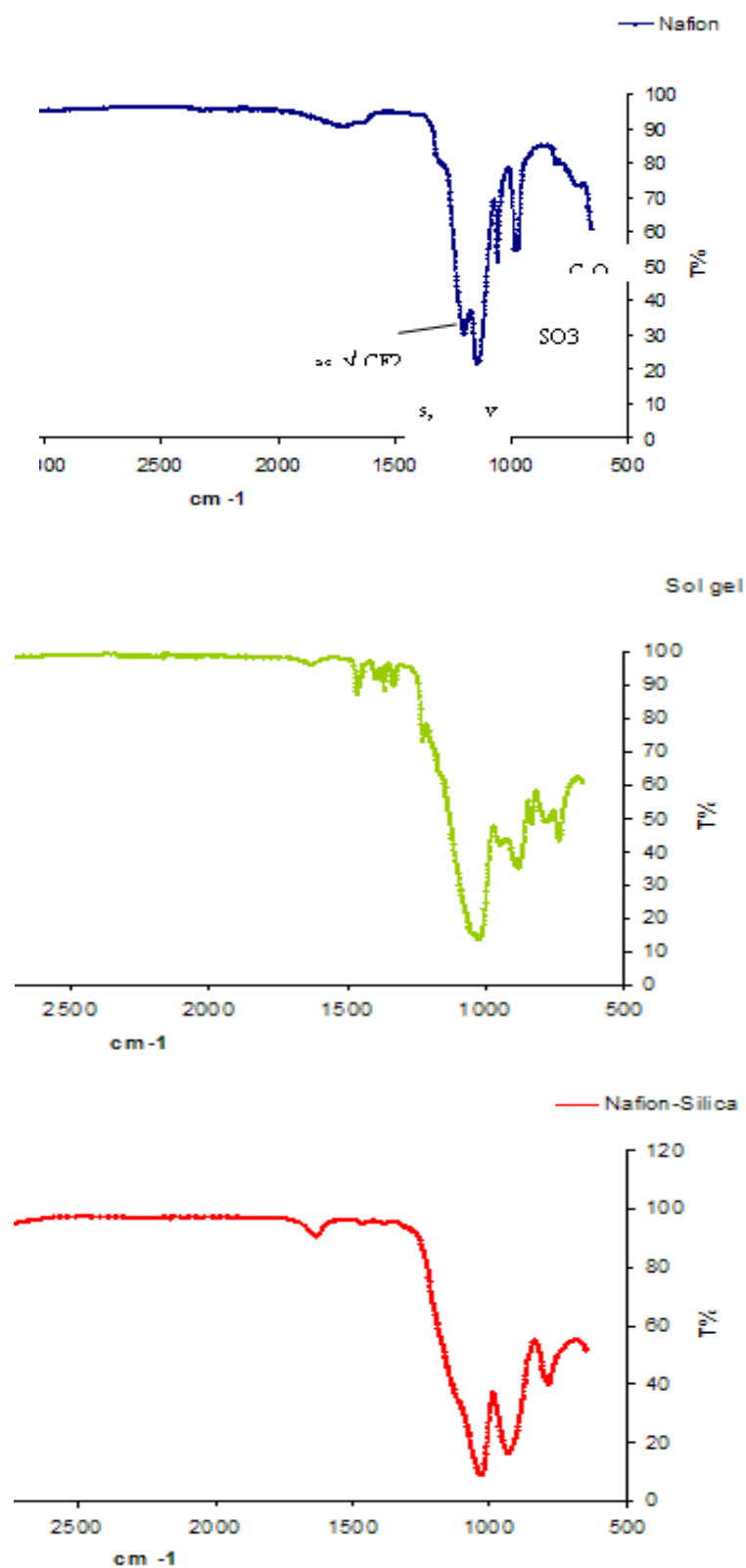
The aim of using Nafion in the materials was to increase the hydrophilicity of the membrane, thus facilitating the transport of metal ions into the membrane to react with Br-PADAP. The response time can be reduced by increasing the hydrophilicity of the sol-gel thin films. The Nafion membrane in the acid form has a terminal $-CF_2CF_2SO_3H$ group, while in the basic form, Nafion is deprotonated and it will exhibit negative charge due to the $-SO_3^-$ group. It is proposed that by changing the amount of Nafion incorporated into the silica sol, the amount of $-SO_3$ sites introduced into the matrix can be varied. Therefore, the Nafion to sol gel ratio is an important factor to affect the performance of the Nafion/sol-gel films. The effects of the Nafion to sol-gel thin film ratio were studied. The sol-gel films were prepared with different Nafion/sol-gel ratio according to **Table 3.4.**

Table 3.4 Nafion/sol-gel Thin Film Composition (Volume ratio).

Thin Film Number	Nafion	Sol-gel
8	Pure Nafion	0
9	3	1
10	2	1
11	1	1
12	1	2
13	1	3
14	1	4
15	1	10

Fig. 3.10 illustrates the effect of various ratios (in **Table 3.4**) of Nafion to sol-gel silicate on the thin film absorption spectra. In this work, the thin film was immersed in 10 mM pH 8 buffer for 2 h prior to evaluation of thin film response with 10 mg/L Ni^{2+} in pH 8 buffer. It can be seen from **Fig. 3.10** that the lowest absorbance response was obtained with the sol- gel thin film 15 (with a composition of 1:10) while the optimum result was obtained from the hybrid Nafion/sol-gel thin film with a volume ratio of 1 to 1 (thin film 11). It is thought that this behaviour is due to the nature of TEOS that could not retain

much of the lipiphilic Br-PADAP reagent in the immobilisation matrix. The hybrid material with ratio of 1:1 shows the optimum sensor response. Further increases in Nafion content decreased the sensor response. This may be attributed to the decrease of porosity of sol–gel silicate film when the content of Nafion increased in the hybrid materials as well as the hydrophobicity of the matrix. Thus, it affects the amount of Br-PADAP trapped in the hybrid Nafion/sol–gel silicate network. Decreasing the porosity of the hybrid material results in lower amount of Br-PADAP trapped in the hybrid film.
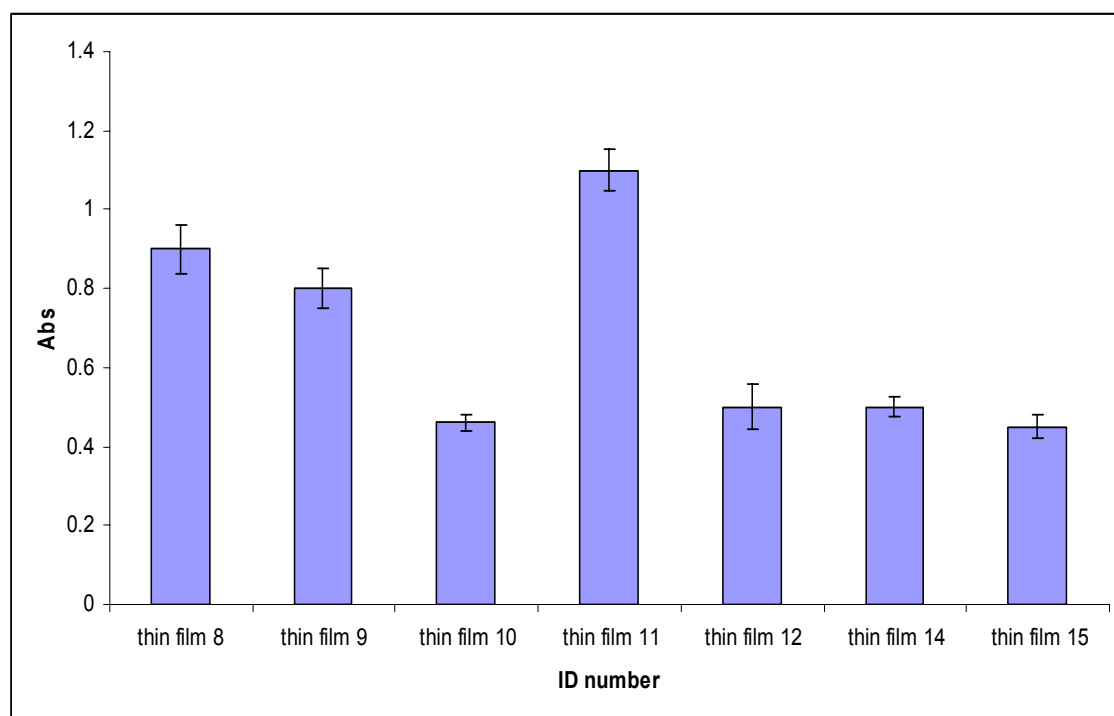
Figure 3.10 The absorbance of Br-PADAP doped thin film before and after contacting with Ni^{2+} at concentration of 10 ppm at pH 8 buffer. (n=3, the error bars = RSD %)

Harmer and co-workers previously showed that the acid groups in Nafion are more accessible in Nafion-silica composite gels, potentially offering greater activity of the materials.[39] Heineman et al. have also shown that the relatively slow diffusion of the cations into Nafion can be improved via the use of Nafion-silica nanocomposites.[40] The positively charged metal ions can be strongly partitioned into the Nafion composite films due to the electrostatic interaction and to some extent, the hydrophobic interaction of Nafion with hydrophobic cations.   In this study, a higher sensitivity and a faster response

time were obtained with the incorporation of Nafion polymer into the Br-PADAP immobilised sol-gel matrix.

3.3.5 Response Time

Generally speaking, response time is the amount of time required for a sensor to respond completely to a change in input. The term of response time in this context is the time required to achieve 95% of the ultimate response. The response time of the optical sensor is also affected by several factors:

i.   The thickness of the membrane, which is controlled by spin speed; the thicker the membrane is and the longer the response time is. The thickness of the membrane also will affect the sensitivity of the sensing membrane. The thicker the sensing membrane, the lower sensitivity of the membrane. On the contrary, the thinner the membrane, the more sensitive the sensor. However, in this study, the thickness of the membranes was controlled at the same level. In this context, the response time of the proposed sensor is defined as the time required for 95% of the total signal change of the Br-PADAP- metal ion complexes.

ii.   The composition of the ligand and other active components in the membrane is due to the diffusion coefficient of the metal ion from the aqueous sample to the binding site in the membrane.

iii.   The concentration of the metal ion in aqueous samples.

Figure 3.11 shows that the response time also depends on the ratio of Nafion/solgel silicate sol in the composite. Thin film 15 which was prepared with Nafion to sol gel ratio at 1-10 (volume ratio) obtained a response time of 90 min. Compared with the thin film which was prepared pure TEOS, the response time of the thin film greatly decreased. From thin film 15 to 11, the response times were deceased from 90 min to 7 min by increasing the amount of Nafion. Further increasing the Nafion content increases the sensor response time and decreases the absorption response. Comparing the pure Nafion membrane with the hybrid Nafion/ silicate membrane (ratio 1/1, v/v) the ion-exchange of pure Nafion membrane is slower under the same conditions, with it taking 10 min. In contrast, the hybrid thin film only took 7 min. This may be due to the hydrophilic cation-exchange site ($-SO_3^-$) in Nafion facilitating the mass transfer of Ni^{2+} into the film to react with Br-PADAP under alkaline conditions. Harmer et al. have also found a faster

uptake rate for 2-propanol into Nafion-silica composite gels relative to the pure polymer.[39]
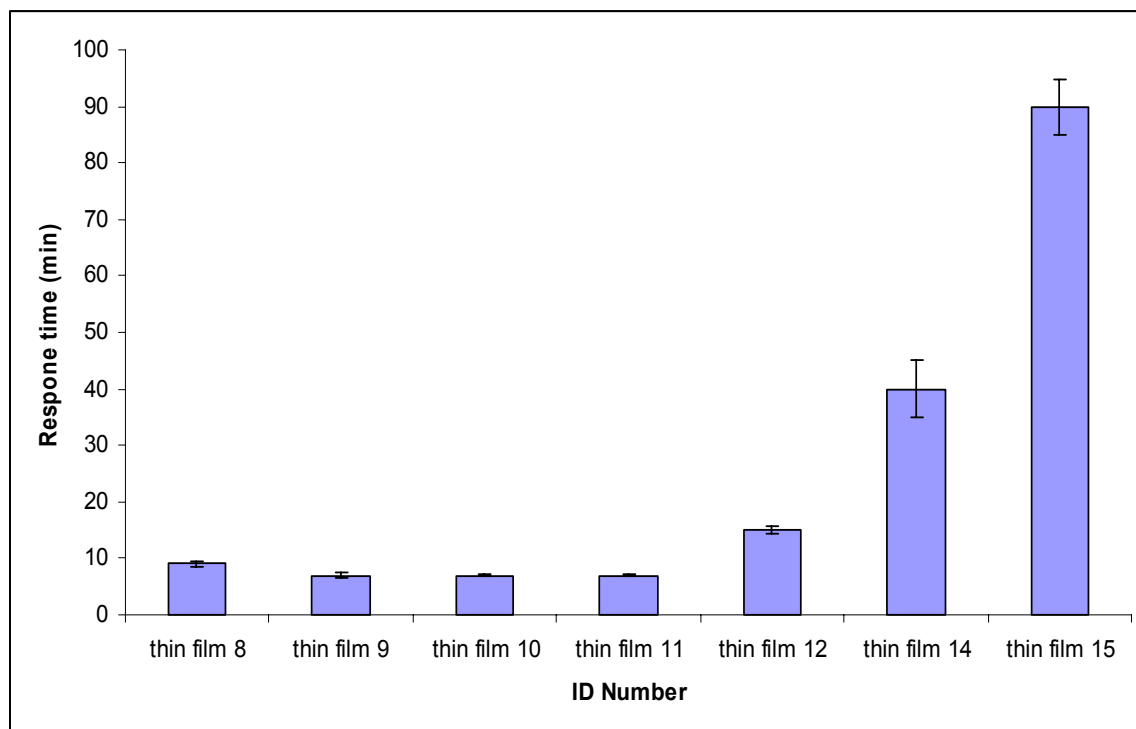
Figure 3.11 Response time of sensing film with different ratio (n=3, error bars = RSD %) in 10 ppm Ni^{2+} solution.

Nafion has been incorporated with SiO_2/ZrO_2 thin films to fabricate an optical sensing film for phenol detection.[41] This hybrid film was shown to enhance the film strength and reduce indicator leaching and also enhance the fast diffusion of ions for phenol sensors.[41] Compared with the thin film without Nafion, the response time of the SiO_2/ZrO_2 thin films dropped from several hours to 50s. However, a large organic polymer content (> 80% of the precursor) will interfere with the transparency of the film and make the thin films easily peeled off from the glass supports.[41] Similar results were obtained by Collinsons et al. They found that the ion-exchange of $Ru(bpy)_3^{2+}$ in a pure Nafion film under the same conditions was much slower compared with that of the hybrid Nafion-sol-gel films.[24, 25] And they claimed that ~2-3 fold increase in the uptake rate of $Ru(bpy)_3^{2+}$ into the composite films can be attributed to greater accessibility of the SO_3^-. Also the response time of the modified xerogel films was considerably shorter than those

of the unmodified xerogel thin film. Compared with the pure sol gel thin film and the organically modified sol-gel thin film, the faster response time of Nafion/Sol-gel composite films can be attributed to the greater accessibility of the SO_3^- sites in the composite materials. The diffusion rate of Ni^{2+} in polymer films depends on the rate of physical diffusion and the rate of complexation reaction of Ni^{2+} with Br-PADAP. The formation constant of Br-PADAP with Ni^{2+} is $\sim 10^5$. Since the complexation rate for the Br-PADAP with Ni^{2+} is large, the complexation rate can proceed rapidly enough to affect the overall rate of the diffusion. Nafion-silica composite films prepared with lower content of Nafion will have a lower density of SO_3^- sites in the film. Therefore, in the subsequent experiment, the Nafion-TEOS ratio at 1:1 was chosen to prepare the composite films.

3.3.6 Contact Angle Measurement

The hydrophobicity of each film might be the factor affecting the difference in the response times of the films.
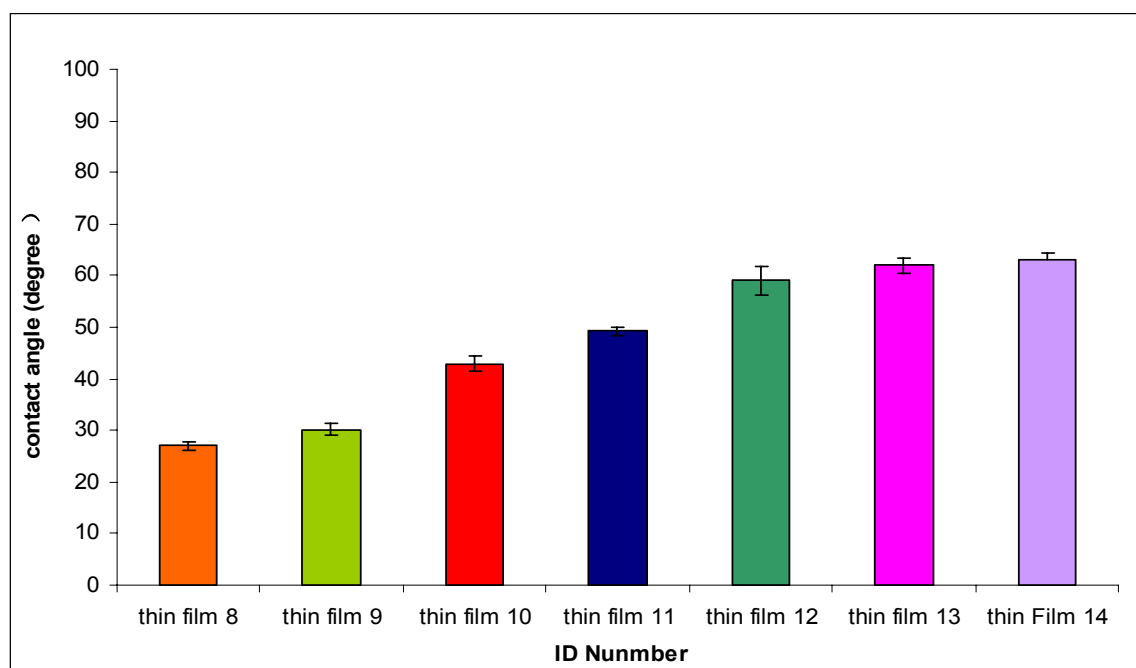

Figure 3.12 The contact angle measurement of thin films. ■ Nafion; ■ Nafion-TEOS at ration of 3:1 (v/v); ■ Nafion-TEOS at ration of 2:1 (v/v); ■ Nafion film-TEOS at ratio of 1:1, ■ Nafion film-TEOS at ratio of 1:2; (v/v), ■ Nafion-TEOS at ratio of 1: 3 ■ Nafion-TEOS at ratio of 1: 4.

To ascertain if this is the case, the contact angles of each film at different composites were measured. **Figure 3.6 (section 3.3.1.1)** shows how the contact angle of the thin films which was prepared by using pure TEOS was 78 degrees. This film is quite hydrophilic.

It was found from **Figure 3.12** that the hydrophobicity of the sol-gel membrane did not greatly change by adding Nafion solution. When mixing Nafion into the TEOS, the hydrophobicity was slightly decreased with the increase in the content of Nafion. When the Nafion to TEOS ratio was 1:3, the contact angle slightly decreased to 76 degrees. When the ratio changes to 1:1, the contact angle of the films was about 73 degrees. The pure Nafion membrane is slightly more hydrophobic than the Nafion/sol-gel composite film. Nafion films are known to contain microscopic domains or phases composed mainly of the hydrophobic-fluorocarbon skeleton. It is believed that these domains allow for a greater occurrence of hydrophobic interaction with hydrophobic cations. There is also ample evidence that suggests the remarkable affinity of Nafion for hydrophobic cations. For instance, Nafion-based chemically modified electrodes were found to preferentially incorporate hydrophobic cations over hydrophilic and less hydrophobic cations.[40]

3.3.7 Optical Response as a Function of Pre-concentration Time

During the Ni^{2+} ion sensing studies, the effects of experimental sensing factors such as, condition time, pH, temperature, sample volume and the response time of the thin film were studied to optimise batch equilibration conditions for a quick detection. It was found that the Nafion/Sol-gel thin films prolonged the response time greatly without the conditioning process and thus reduced the response intensity of the sensor. From **Figure 3.13,** it was shown that the sensor thin films must be conditioned for 2 min, prior to obtaining a stable response. This is an important step to retain a steady response of a sensor. Goswami et al. reported that absorption of water onto Nafion surfaces causes the surfaces to switch from being hydrophilic. Liquid water draws $-SO_3$ group to the surface of Nafion. This structure produces a large contact-angle hysteresis for water with Nafion. The results indicate that the liquid drops can change the surface compositions of Nafion. Fresh membranes showed very weak responses to Ni^{2+} ions. In this experiment, acetate buffer at pH 6.5 was used for the preparation of the metal-ion solution. It was found that, the response time of the sensor and sensitivity can be affected by the conditioning time. It should be mentioned that although the sol gel matrices are often treated as chemically

inert, interactions between the matrix and the analyte or the dopant molecules (electrostatic, hydrogen bonding or hydrophobic interactions) exist.
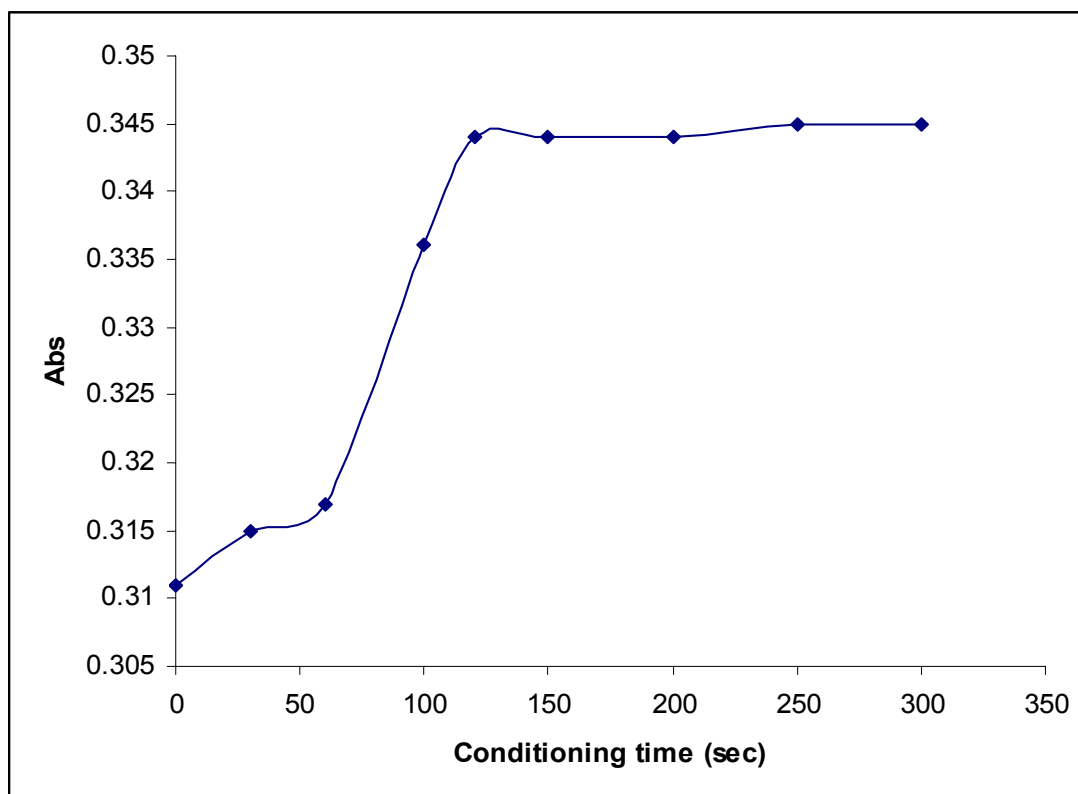
Figure 3.13 The effects of conditioning times on the sensor's absorbance. The Nafion/sol-gel thin film contained 7.5 mg/ml^{-1} of Br-PADAP. The concentration of Ni^{2+} ion is 2.5 mg/l. (n=3, error bar =% RSD).

The study of these interactions is very important because they are found to affect the diffusion properties or change the surface properties; for example, in aqueous solutions, intrinsic properties of the surface-silanol groups can be exploited as the optical transducer in a pH sensing system. From the experience of preparation of a sol gel film, when the thin film under the sol-gel-domain condition (ratio of Nafion/Sol gel is less than 1), after spin coating, the thin film obtained, is a pink colour corresponding to an absorbance at 400 nm. In contrast, under the Nafion-domain condition, the thin film has a yellow colour corresponding to an absorbance at 400 nm. Therefore, it is very important to immerse the thin film into pH 6.5 buffer solution for 2-3 min.

3.3.8 Nafion/sol gel Thin Film Nickel Sensing Procedure

The efficiency of the Ni^{2+} ion sensor was influenced by the pH conditions of the measurement. Since Br-PADAP can be deprotonated or protonated at different pH. The absorbance spectra of Ni^{2+}-Br-PADAP, which was obtained at λ=560 was carefully monitored over a wide range of pH solutions. It was found from **Figure 3.14** that the sensor is optimised at pH 5-8. The pH values >8 were not suitable because hydrolysis of Ni^{2+} may occur, which results in lowering its interaction with the ligand. This finding is in agreement with the work reported by Amini and co workers. They found that, pH 6.5 is the optimum pH for the determination of Ni^{2+}, by using the optical sensors which are based on the immobilisation of Br-PADAP into Nafion.[42]

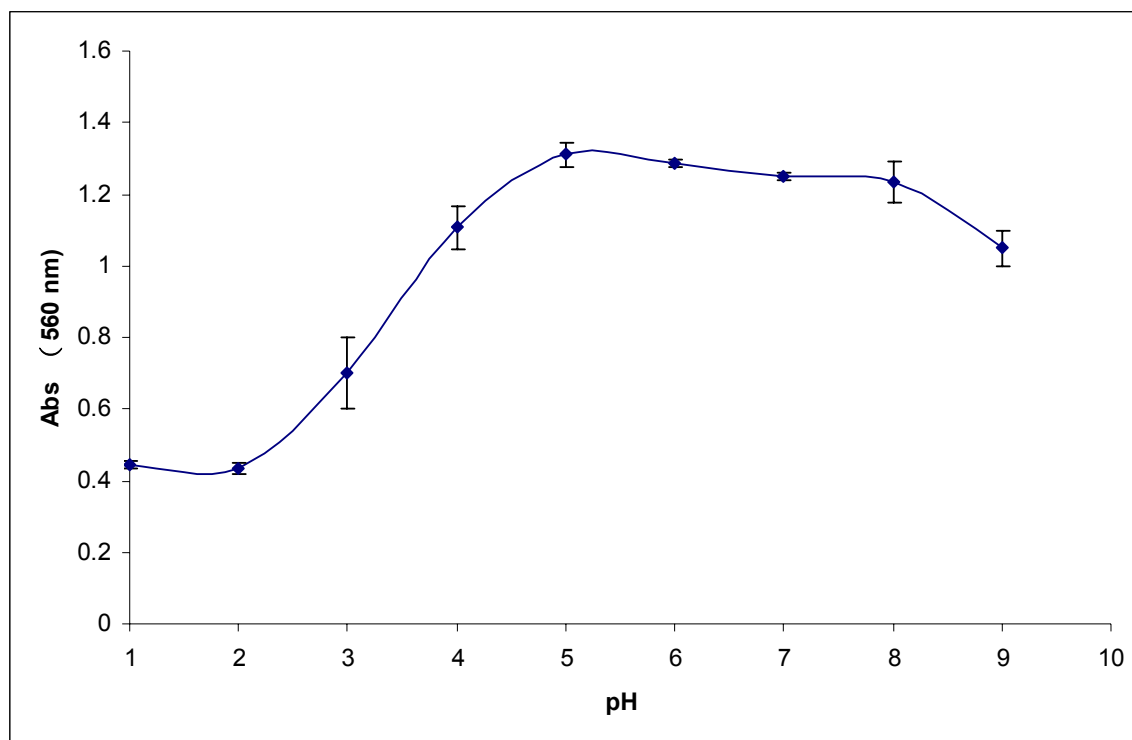**Figure 3.14** pH study of sensor materials. The Nafion/sol-gel thin film contained 7.5 mg/mL^{-1} of Br-PADAP and the concentration of Ni^{2+} was 10 ppm.

3.3.9 The Concentration of Br-PADAP in sensor Membranes

The concentration of Br-PADAP used to prepare the sensor membrane is an important parameter, since it determines the signal intensity, sensitivity, dynamic working range and the detection limit of the sensor. The influence of the ligand concentration was studied by preparing membranes containing 0.6–18 mg Br-PADAP in 2 mL of Nafion/sol gel solution as described above (the concentration ranged from $0.33 - 9$ mg mL^{-1}). The sensors were used for the determination of reaction with Ni^{2+} by the procedure described. The results of this study, which are shown in **Table 3.4**, indicate that the sensitivity increases by increasing the ligand concentration. Generally, a high sensitivity, wide dynamic range and low detection limit were obtained for a coating-solution containing 7.5 mg mL^{-1} of Br-PADAP in Nafion/sol gel solution. Lower amounts of the ligand provided membranes with lower sensitivity, while higher concentrations resulted in membranes with lower transparency, probably due to phase separation inside the membrane. It is noted that from **Table 3.4,** the leaching of indicators occurred when the concentration of immobilised Br-PADAP was higher than 7.5 mg mL^{-1}.

Table 3.4 The sensing performance of sol-gel thin film doped with different concentration of Br-PADAP for Ni^{2+} determination.

ID	Concentration (mg/mL)	LOD (mg/L)	Working range of Ni^{2+} (mg/L)	Leaching (after 1 h)
16	0.33	0.03	0.05-2	No leaching
17	2.5	0.04	0.05-2.5	No leaching
18	3	0.05	0.1-2.5	No leaching
19	5.5	0.078	0.1-4	No leaching
20	7.5	0.05	0.1-15	No leaching
21	12	0.6	1-10	Slightly leaching

Several quantification measurements (n=3) were carried out using wide-range concentrations (0.33-9.0 mg mL^{-1}) of the standard solutions of Ni^{2+} ions at the specific sensing conditions and in the absence of both cation and anion interferences. It was found

that in **Figure 3.15,** 7.5 mg mL^{-1} was the optimised concentration of ligand necessary for the films. The absorbance reached the maximum when 7.5 mg ml^{-1} of Br-PADAP was incorporated with the sol gel membrane. No further increase in absorbance was found by increasing the amount of Br-PADAP.
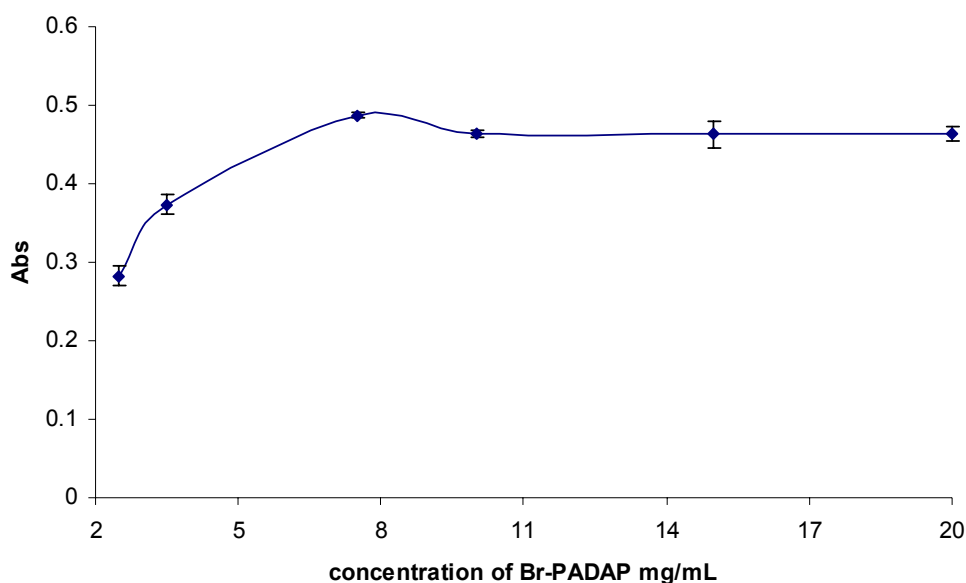
Figure 3.15 The concentration study of Br-PADAP immobilized in nafion/sol-gel membranes. (n=3 and error bars shown based on % RSD of these 3 different measurements)**.** The concentration of Ni^{2+} is 3 mg/L.

3.3.10 Calibration Curve of the Sensing Membranes

A key factor in the development of an optical sensing system for quantitative measurements is the ability to yield a response over a dynamic range suited to the application. The calibration graph was obtained by measuring Ni^{2+} solution at different concentrations.
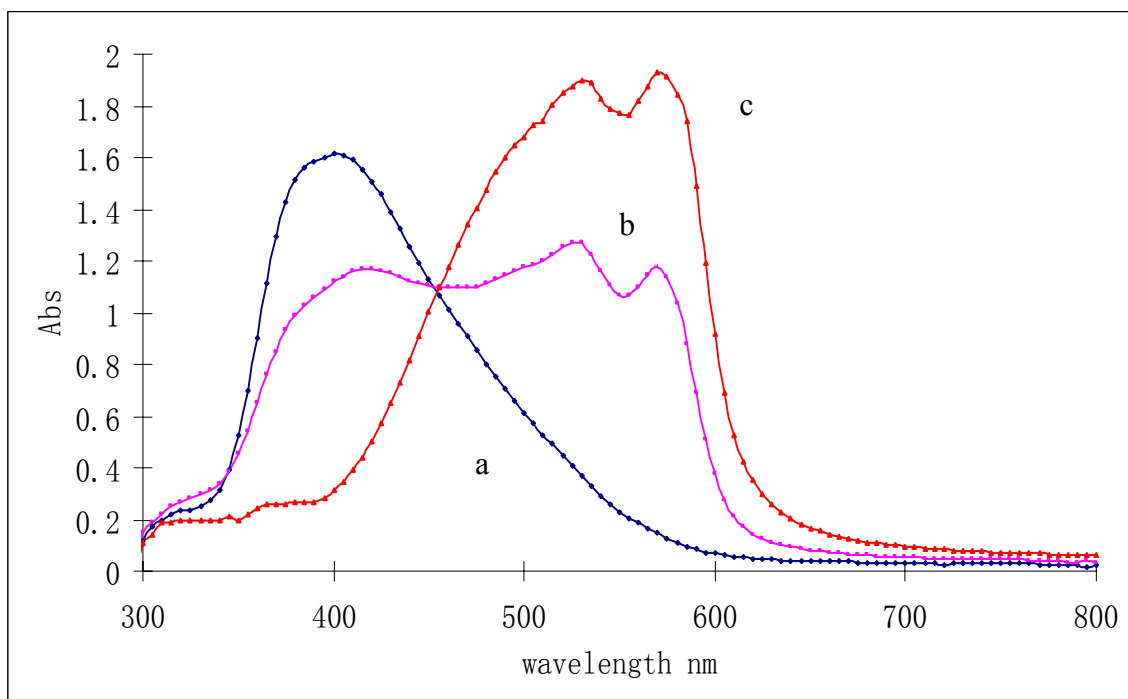
Figure 3.16 Absorption spectra of (a) a solution contains 0 mg/L of Ni^{2+}; (b) a solution contains 10 mg/L of Ni^{2+} at pH 8 buffer; (c) a solution contains 15 ppm of Ni^{2+} ion at pH 8 buffer.

The UV-Spectra of the sensor strip with the addition of Ni^{2+} is shown in **Figure 3.16**. The spectra variation of Br-PADAP sensor in pH 8 buffer solutions was observed upon the gradual addition of Ni^{2+}. As a function of the concentration of Ni^{2+}, a new absorption band appeared at around 530-590 nm leading to an obvious colour change from yellow to dark pink. The working range is from 0.1 to 17 mg/L, which is shown in **Figure 3.17 a,** and the dynamic linear range is from 0.1 to 15 mg/L, shown in **Figure 3.17 b.**

The limit-of-detection (LOD) is the lowest concentration level that can be determined to be statistically different from a blank (95% confidence). In this study, it can be defined as the concentration of analyte required to give a signal equal to the background (blank) plus three times the standard deviation of the blank. So, before any calibration or sample measurement is performed, the blank is evaluated, namely calculating the instrument response with no analyte. The LOD is then determined by **Equation 3.1**:

$$y_{LOD} = y_{blank} + 3\sigma_{blank}$$ **Eq. 3.1**

In the above equation σ is the standard deviation of blanks, and it is 0.078 mg/L of the test strip for Ni^{2+} ion. Therefore, the lower working range is 0.1 mg/L. The upper limit of linearity can be graphically established as the amount of concentration at which the deviation exceeds the specific 5% value of the linear plot. Therefore, a regression coefficient of 0.997 was obtained for the dynamic linear range of 0.1-15 mg/L of Ni^{2+} at pH 8. A new sensing membrane was used for each calibration point. For each measurement, the sensing membrane was placed in contact with a Ni^{2+} solution buffered to pH 8 for 2 min. The linearity could possibly be improved if a regenerated sensing phase was used as opposed to a new sensing membrane for each calibration point. The use of different films added an extra degree of variability to the measurement.
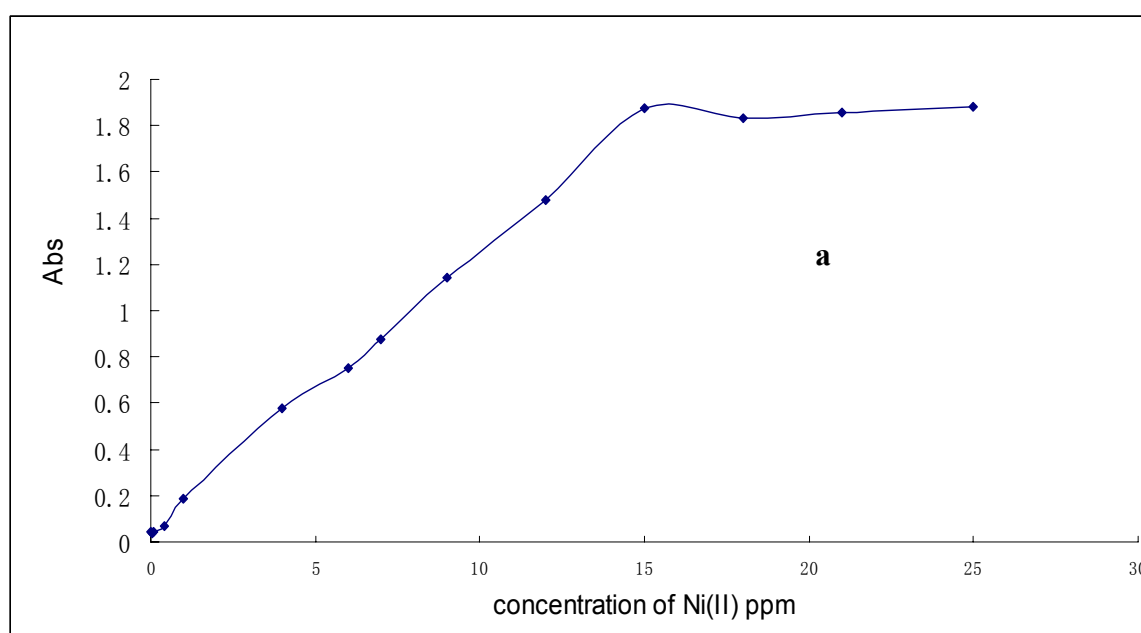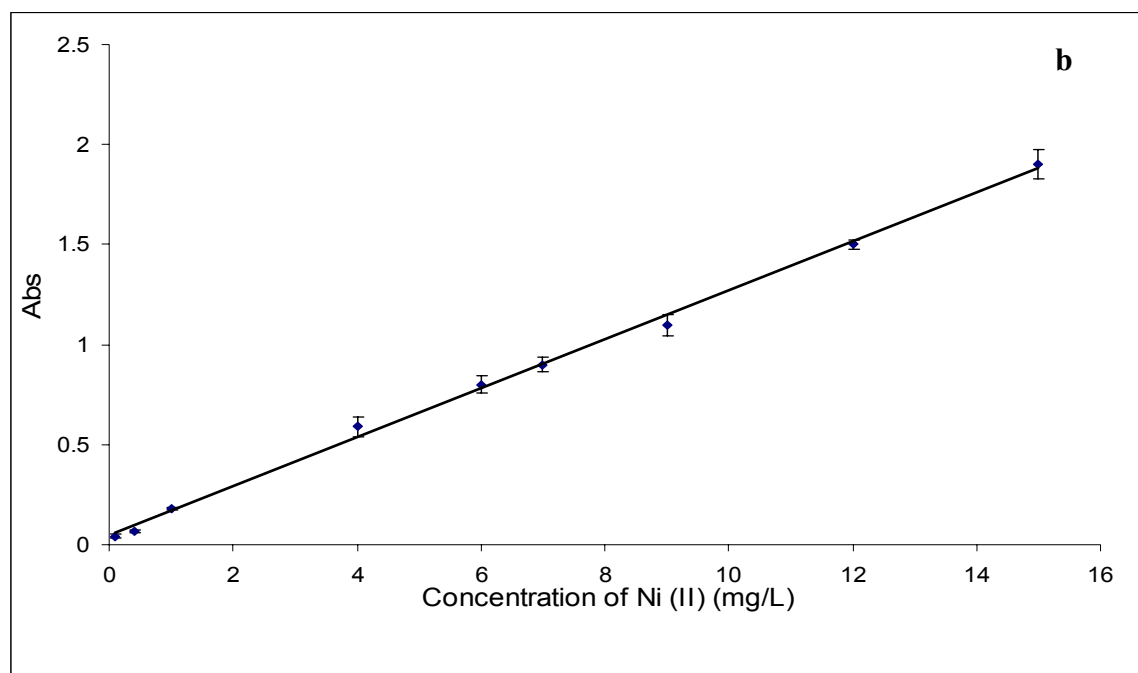
Figure 3.17 The linear range for sensing membrane reacted with 0.1-15 mg/mL Ni^{2+} at pH 8 when a new sensing membrane was used for each calibration point. y = 0.1225x + 0.0445, R^2 = 0.9978. The Nafion/sol-gel thin film contained 7.5 mg/mL^{-1} of Br-PADAP. n=3 and error bars were based on % RSD of these 3 different measurements

3.3.11 The Reusability of Nafion/sol-gel Thin Film

The reusability of a sensing response is a desirable characteristic in the design of a sensing membrane. Various solutions were investigated to regenerate the sensing phase after it complexing with Ni^{2+} in buffered solution. These regenerating agents included HCl, EDTA and buffers with different pH values. Promising results were observed with 1 M HCl solution. The reusability of the Nafion/Sol-gel strips was revealed after multiple regeneration/reuse cycles.
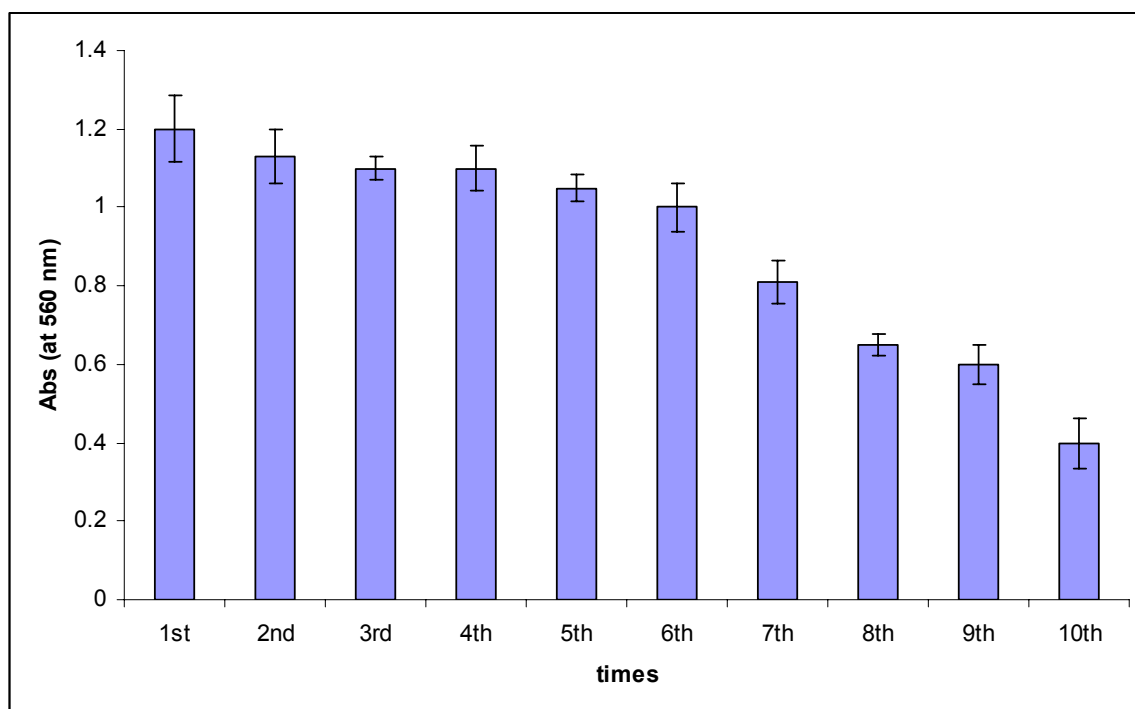
Figure 3.18 The reusability of Nafion/sol gel film and nafion film tested in 10 mg/L Ni^{2+} solution at the same condition. The same sensor membrane was treated with 1 M HCl of solution. (n =3 and error bars shown based on % RSD).

The thin film, which was prepared with Nafion as the single component, and immobilised with 7.5 mg/ml of Br-PADAP, has been tested under the same conditions. In such a treatment procedure, 1 M HCl was used as a regeneration agent to remove Ni^{2+} ions after a complete detection process. The test strip was tested for 10 times as a cycle. After each time, the used test strip was dipped into 1M HCl for 1 min, conditioned in a pH buffer for 2 min and washed with fresh DI water. The UV-Vis spectrum of Br-PADAP immobilised thin film was measured at λ= 560 nm. The results are shown in **Figure 3.18**. It reveals that for the first 6 runs, little changes (less than 2.5%), in terms of the absorbance intensity of the test strip after each run. However, from the 7th run, the signal was decreased significantly. This decrease was due to leaching of the indicator reduced by using Nafion/sol gel materials. This has also been confirmed by other researchers; they used acidic solutions to regenerate sensing phases based on Br-PADAP.

3.3.12 Interference Studies

In the design of sensors for environmental determinations, the interference due to other species in the sample poses a challenge to the analysts. Depending on the proposed end-use of the sensor, interference from other species can cause problems for measurement. However, in industrial wastewater streams, where only certain metal ions are known to be present, this may not pose a concern. Br-PADAP is an unselective ligand which can bind with several heavy metal ions. An important issue related to chemical sensor feasibility is the selectivity factor in which high range of linearity is required for the practical determination of Ni^{2+} ions over multi-component analytes using Br-PADAP under specific sensing procedures. The selectivity of metal ions can be affected by the diffusion kinetics of the metal ions into the films and also the binding affinity of metal ions with ligand Br-PADAP. Several commonly existing metal ions were tested. The selectivity of the method was determined by adding different amounts of potential interfering ions, such as Cu^{2+}, $Co^{2+},$ and Pb^{2+} ions to solutions containing 10 mg/L Ni^{2+} in pH 8 buffer solutions. **Figure 3.19** displays the changes in the UV-Vis absorption spectra of Ni-Br-PADAP doped sensor membrane 10 min after adding various heavy ions at different concentrations (The concentration ratio of interference ion to Ni^{2+} ranges from 0 to 200). In this series, it was found that the presence of Cu^{2+} and Co^{2+} led to an absorbance decrease of Ni-BrPADAP in the sensor membrane by various degrees immediately at the C_{Cu}^{2+}/C_{Ni}^{2+} and C_{Co}^{2+}/C_{Ni}^{2+} ratio is of 1:1, whereas, the absorbance of Br-PADAP doped sol/gel membrane starts to change at the concentration ratio of 2, 10, and 100 for Cd^{2+}, Al^{3+} and Pb^{2+}. After adding 50 folds of Zn^{2+}, Fe^{2+} and Fe^{3+}, the absorption of sensing membrane starts to change greatly. Contrary to heavy metal ions, it was found from **Figure 3.20**, that the alkaline metal ions and some anions have no effects on the response of the sensor towards Ni^{2+}, even at a high concentration ratio.

Figure 3.19 The interfering effect of heavy metal ions on the absorption of BrPADAP-coated sol-gel membranes towards Ni^{2+} ions at pH 8 buffer condition. The concentration ratio of interference ion to Ni^{2+} ranges from 0 to 200, C_{Ni}^{2+} = mg/l. ■ Al^{3+}, ■ Cu^{2+}, ■ Co^{2+}, ■Zn^{2+}, ■Pb^{2+}, ■Fe^{2+}, ■Fe^{3+}, ■Cd^{2+}.
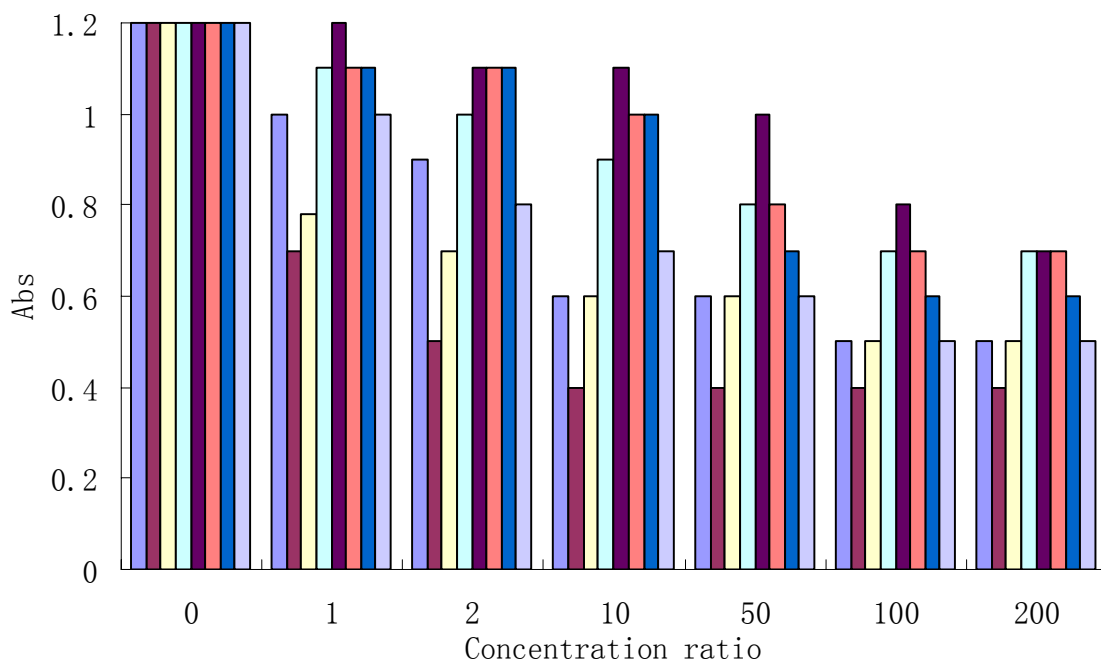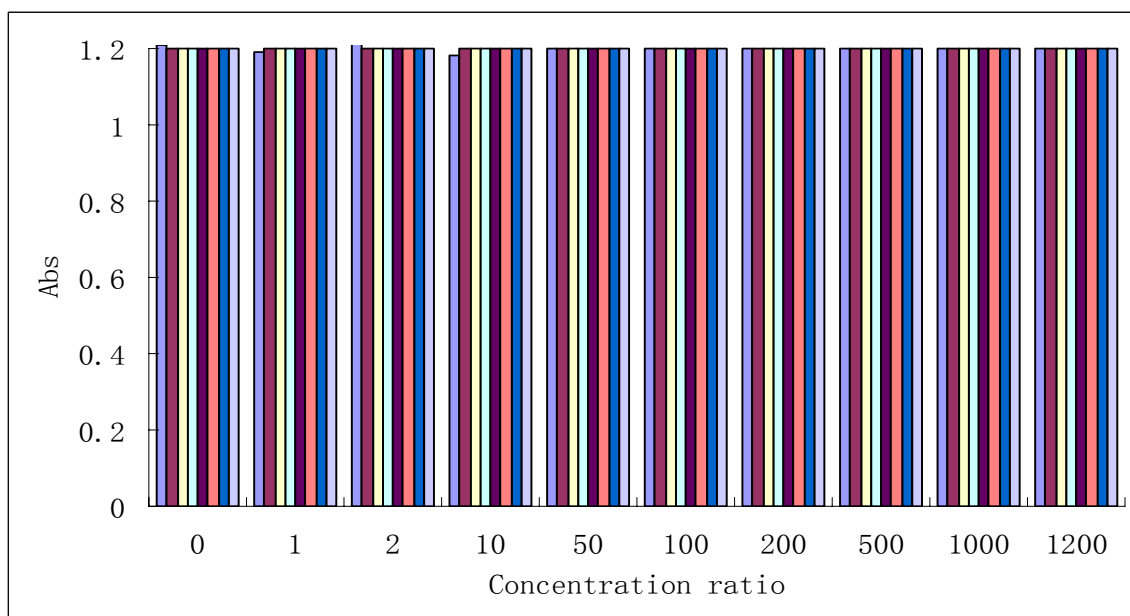

Figure 3.20 The interfering effect of other ions on the absorption of BrPADAP-coated sol-gel membranes towards Ni^{2+} ions at pH 8 buffer condition. The concentration ratio of interference ion to Ni^{2+} ranges from 0 to 200, C_{Ni}^{2+} =10 ppm. ■ Na^+ ■ Li^+, ■ Mg^{2+}, ■Ca^{2+}, ■Cl^-, ■Citrate, ■ Ammonia, ■EDTA.

Table 3.5 summarised the tolerance ratio for several cations and anions. The tolerance limit was taken as the concentration of the interference ion causing an error of not more than 10% in the determination of Ni^{2+}, where the initial absorption was obtained in the replicate measurement of 10 mg/L of Ni^{2+}. The tolerance (T) can be defined by the following **Equation 3.1:**

$$T = \frac{Abs_1(\text{without Interf. Ions})}{Abs_2(\text{with Interf. Ions})} \qquad \textbf{Eq. 3.1}$$

Where Abs_1 is the absorbance measured at the Ni^{2+} solution without any interference ions, while Abs_2 is the value measured with one specific interference ion.

Table 3.5 Effect of different interferences on the determination of Ni^{2+}.

Foreign Ions	Tolerance	Foreign Ions	Tolerance
Al^{3+}	10	Na^+	1000
Cu^{2+}	1	Li^+	1000
Co^{2+}	1	Mg^{2+}	1000
Zn^{2+}	50	Ca^{2+}	1000
Pb^{2+}	100	Cl^-	1000
Fe^{3+}	50	Citrate	1000
Fe^{2+}	50	Ammonia	1000
Cd^{2+}	2	EDTA	1000

Generally, negative interference was observed for anions whereas cations showed positive interference. From **Table 3.5**, it can be seen that alkali and alkaline metal have no interference with Ni^{2+} selectivity; this was demonstrated in the solution study in Chapter 2 already. Anions such as F^-, Cl^-, NO_3^- produced no interference. This was thought to be because Nafion is a cation-exchange membrane, which prevents the interference of anions. There are several ways that could be used to eliminate or minimise the interference ions,

such as using precipitation methods and using mask agents such as thiosulfate for Pb^{2+}, Zn^{2+} and Cu^{2+} and Co^{2+}.

3.3.13 (Photo) Stability Study

For investigation of long term stability, the leaching behaviour of Nafion modified and unmodified xerogel films was examined by immersing the films in pH 8 buffer solution (the buffer solution was changed every day with fresh material), and storing a sample of them in a normal room, while storing another sample in a dark box for a period of 7 days. Samples were monitored for changes in absorbance on a daily basis. The films stored in the dark room and in bright room showed good stability at the room temperature. The spectra were measured on a daily basis for 7 days.

3.3.14 Application

This method was validated with an atomic absorption spectrophotometer (AAS). The spiked samples were prepared by adding 5 mg/L of Ni^{2+} into river water obtained from Lee River, Cork, Ireland. Three sample replicates were quantified by using the calibration curve obtained from the developed test strips and by using the standard AAS method. **Table 3.6** shows the results of the comparative study of the developed sensors and AAS. The results show that the mean from both methods are not significantly different, thus indicating that the method developed is in good agreement with the established method. The pH of the river is about 6.

Table 3.6 Detection if Ni^{2+} in an environmental sample (n=3).

Samples	AAS (mg/l)	Sensor Method （mg/l）	Spiked samples
Sample 1	5.3±0.5	Absent	5.2±0.36

3.3.15 Optical Sensors Based on the Immobilisation of Br-PADAP into PVC

The optical sensors based on the physical immobilisation of Br-PADAP into plasticised PVC membrane for the determination of Ni^{2+} ion in aqueous solution were investigated in our preliminary work. The lipophilic indicator Br-PADAP can be incorporated with

plasticised PVC membrane homogenously. The preparation process is very simple and straightforward.[10] The transparent film was observed as orange before contacting with Ni^{2+} and it changed to pink in the addition of the Ni^{2+}. However, this material showed serious leaching of the dyes from the PVC membrane by the comparison with Nafion/sol-gel thin films. Furthermore, PVC membranes did not attach to the glass slops firmly; they were easy to peel-off. Therefore, we carried on our work into the investigation of sol-gel membranes.

Conclusion

An optical sensor based on the immobilisation of Br-PADAP in hybrid Nafion/sol-gel silicate film for the determination of Ni^{2+} was successfully developed. The performance of the sensor based on several sensing materials, i.e. inorganic sol-gel, ORMOSILs thin films, Nafion/Sol-gel hybrid sol-gel thin film and plasticised PVC membranes, were evaluated. It was found that the Nafion/sol-gel membrane can not only overcome the brittleness of the pure sol-gel-derived silicate film but also increase the reusability and reduce the leaching of the indicators from the sol-gel network. In addition, the hybrid Nafion/sol-gel film can be easily prepared in comparison to other composites based on ORMOSILs films. Since Nafion has negative charge, therefore, it could facilitate the diffusion of positively charged metal ions into the membrane to react with Br-PADAP that are entrapped in the hybrid Nafion/sol-gel film network. Furthermore, it also reduces the interferences from the negatively charged ions.

Due to the increased hydrophobicity and pore size of the hybrid Nafion/sol-gel thin films, the proposed sensor exhibited a relatively fast response time (7 min). The sensing film generated was sensitive to low concentrations of Ni^{2+} in real environmental samples. Quantitative determination of Ni^{2+} was practical in the range of 0.5-15 mg/L. The behaviour of the indicator in Nafion-modified-sol-gel thin film was compared with unmodified sol-gel thin films. It was shown that the co-entrapment of the Nafion with dopant molecules within the xerogel matrix could be modified with the cage properties. Also, the analytical performance of the dopant can be modified by the entrapped Nafion in the sol gel films. Consequently, the shrinking and cracking problems of the xerogel thin films were solved. The optical sensing films can be regenerated by using 1M HCl solution and the membrane can be reused 10 times. The fabrication of the sensing films was cheap and easy to prepare and portable. The preparation of plasticised PVC membrane was simple and straightforward, and it showed good homogeneity with Br-PADAP. However, the leaching of Br-PADAP occurred after the membrane came in contact with Ni^{2+} ions due to the weak interaction of Br-PADAP with PVC membrane. This membrane also showed weaker adhesion with the glass supports compared with sol-gel membranes.

References

1.   M. Puyol, I. Salinas, I. Garces, F. Villuendas, A. Llobera, C. Dominguez and J. Alonso, *Anal. Chem*, 2002, **74**, 3354-3361.

2.   Mohammad R. Ganjali, M. Hosseini, M. Salavati-Niasari, T. Poursaberi, M. Shamsipur, M. Javanbakht and Omid R. Hashemi, *Electroanalysis*, 2002, **14**, 526-531.

3.   H. Watarai, M. Gotoh and N. Gotoh, *Bull. Chem.   Soc. Jan.*, 1997, **70**, 957-964.

4.   European Commission, Editon edn., 2000.

5.   N. Ertas, E. U. Akkaya and O. Yavuz Ataman, *Talanta*, 2000, **51**, 693-699.

6.   I. Oehme and O. S. Wolfbeis, *Microchim. Acta*, 1997, **126**, 177-192.

7.   L. Basabe-Desmonts, D. N. Reinhoudt and M. Crego-Calama, *Chem. Inform*, 2007, **38**.

8.   R. E. Ferreyra, J. M. Camiña, E. Marchevsky and J. M. Luco, *F. J. Anal. Chem.*, 2000, **368**, 595-600.

9.   S. Sadeghi and S. Doosti, *Sens. Actuators B: Chemical*, 2008, **135**, 139-144.

10.   M. Shamsipur, J. Tashkhourian and H. Sharghi, *Anal. Bioanal. Chem.*, 2005, **382**, 1159-1162.

11.   B. Peng and Y. Qin, *Anal. Chem.*, 2008, **80**, 6137-6141.

12.   J. Abdullah, M. Ahmad, L. Y. Heng, N. Karuppiah and H. Sidek, *Talanta*, 2006, **70**, 527-532.

13.   C. W. Clavier, D. L. Rodman, J. F. Sinski, L. R. Allain, H.-J. Im, Y. Yang, J. C. Clark and Z.-L. Xue, *J.   Mater.   Chem.*, 2005, **15**, 2356-2361.

14.   L. L. Hench and J. K. West, *Chem. Rev.*, 1990, **90**, 33-72.

15.   D. L. Rodman, H. Pan, C. W. Clavier, X. Feng and Z.-L. Xue, *Anal. Chem.*, 2005, **77**, 3231-3237.

16.   X. Chen, L. Lin, P. Li, Y. Dai and X. Wang, *Anal. Chim. Acta*, 2004, **506**, 9-15.

17.   C. J. Brinker, *J.   Non-Crystalline Solids*, 1988, **100**, 31-50.

18.   M. M. Collinson, *Microchim. Acta*, 1998, **129**, 149-165.

19.   D. Avnir, *Acc. Chem. Res.*, 1995, **28**, 328-334.

20.   U. Schubert, N. Huesing and A. Lorenz, *Chem. Mater.*, 1995, **7**, 2010-2027.

21.   R. C. Chambers, Y. Haruvy and M. A. Fox, *Chem. Mater.,*   1994, **6**, 1351-1357.

22.   P. F. James, *J.   Non-Crystalline Solids*, 1988, **100**, 93-114.

23. L. C. Klein, Y. Daiko, M. Aparicio and F. Damay, *Polymer*, 2005, **46**, 4504-4509.

24. M. M. Collinson, B. Novak, S. A. Martin and J. S. Taussig, *Anal. Chem.*, 2000, **72**, 2914-2918.

25. A. N. Khramov and M. M. Collinson, *Anal. Chem.*, 2000, **72**, 2943-2948.

26. B. Barroso-Fernandez, M. Theresa Lee-Alvarez, C. J. Seliskar and W. R. Heineman, *Anal. Chim. Acta.*, 1998, **370**, 221-230.

27. F. V. Bright, G. E. Poirier and G. M. Hieftje, *Talanta*, 1988, **35**, 113-118.

28. Y. P. Patil, T. A. P. Seery, M. T. Shaw and R. S. Parnas, *Industrial Engin Chem. Res.*, 2005, **44**, 6141-6147.

29. J. Abdullah, M. Ahmad, L. Heng, N. Karuppiah and H. Sidek, *Anal. Bioanal. Chem.*, 2006, **386**, 1285-1292.

30. N. A. Carrington, G. H. Thomas, D. L. Rodman, D. B. Beach and Z.-L. Xue, *Anal. Chim. Acta.*, 2007, **581**, 232-240.

31. Y. Guo, A. R. Guadalupe, O. Resto, L. F. Fonseca and S. Z. Weisz, *Chem. Mater.*, 1998, **11**, 135-140.

32. B. Craith, C. Donagh, A. McEvoy, T. Butler, G. O'Keeffe and V. Murphy, *J. Sol-Gel Sci.Tech.*, 1997, **8**, 1053-1061.

33. N. A. Yusof and W. A. R. W. A. Kadir, *Spectrochim. Acta Part A: Mole Biomole. Spec.*, 2009, **72**, 32-35.

34. D. Y. Kwok, R. Lin, M. Mui and A. W. Neumann, *Colloids Sur. A: Physicochem. Eng. Aspects*, 1996, **116**, 63-77.

35. D. Li and A. W. Neumann, *J. Colloid Inter. Sci.*, 1992, **148**, 190-200.

36. A. Lobnik and O. S. Wolfbeis, *Sens. Actuators B: Chemical*, 1998, **51**, 203-207.

37. H. H. Huang, B. Orler and G. L. Wilkes, *Macromole*, 1987, **20**, 1322-1330.

38. B. Wang and G. L. Wilkes, *J. Polymer Sci. Part A: Polymer Chem.*, 1991, **29**, 905-909.

39. M. A. Harmer, W. E. Farneth and Q. Sun, *J. Am. Chem, Soc.*, 1996, **118**, 7708-7715.

40. A. F. Slaterbeck, T. H. Ridgway, C. J. Seliskar and W. R. Heineman, *Anal. Chem.*, 1999, **71**, 1196-1203.

41. N. A. Carrington and Z.-L. Xue, *Acc. Chem. Res.*, 2007, **40**, 343-350.

42. M. K. Amini, T. Momeni-Isfahani, J. H. Khorasani and M. Pourhossein, *Talanta*, 2004, **63**, 713-720.

Chapter 4

4.1 Introduction

4.1.1 The Uses of Water-Soluble Indicators for Optical Sensors

In the recent decades, there is an increase in the development of optical sensors based on the immobilisation of probe molecules for sensing heavy metal ions. Most of the probe molecules are either commercially available (also called conventional indicators) neutral ionophores or biological-recognition molecules.[1] The water-soluble indicators play an important role in the development of optical sensors for the determination of heavy metal ions. There is a large group of well known water soluble fluorometric and spectrophotometric indicators which can be used for visually indicating and quantitative determination of heavy metal ions.[2] These types of indicators normally contains one or more hydrophilic groups ($-SO_3H$, $-COOH$ etc.) in their structures and make them very soluble in water.[3] These indicators have good binding abilities with heavy metal ions associated with a high optical signal. They also display high molar absorptivities at the visible-range wavelengths and they can also form strong-coloured and stable complexes with metal ions. The molar absorption coefficients are normally larger than 10 000 l mol^{-1} cm^{-1}. These dyes have long stability and a long life time once stored in a dry place. Furthermore, they are commercially available and easy to synthesis from inexpensive starting materials. For example, CAS based sensor has been used for the determination of Cu^{2+} by absorption spectroscopy.[4] The molar absorptivity of Cu-CAS complex is 3 x 10^4 and the formation constant is 1.59 x10^{21}. The solution of CAS changed its colour from yellow to strong blue after adding Cu^{2+} in pH 7 solution.[5]

The immobilisation of these water soluble indicators into suitable solid supports is a key challenge for their application in optical sensors for the determination of heavy metal ions in aqueous environment. Two types of polymeric support have been used in this area. One of them is based on the non-transparent polymers such as cellulose papers[6-8] and silica monolith.[9,10] And the other is based on the transparent support such as sol-gel glass,[11] plasticised PVC membrane,[12-14] and triacetylcellulose.[15,16] A common weakness of all these membranes is the leaching of the water soluble indicators into aqueous solution after contact with aqueous solution.

In this work, a novel method by using raw cellulose materials to fabricate the optical sensors membranes based on the immobilisation of water soluble indicators has been described. An optical sensor based on the immobilisation of water soluble indicator CAS onto solid sensing matrices for the determination of Cu^{2+} ion has been demonstrated as an example. This study shows the potential of combining the cellulose materials and water soluble indicators for chemical sensing.

**4.1.2 Immobilisation of Water Soluble Indicators onto Solid Matrices**

The immobilisation of the indicator dyes into solid matrices is a crucial step in the preparation of optical chemical sensors. The water soluble indicators can be physically or chemically immobilised on the solid supports. The immobilisation method based on the physical doping of dyes into solid matrices is simple and widely used. In 1995, Plaschke et al. developed a very sensitive and selective fluorimetric method for the detection of Hg^{2+} ions in aqueous solution by doping tetra(*p*-sulfonatophenyl)porphyrin (TPPS) in sol-gel thin films.[17] Alkaline catalysis of the chelation and physical encapsulation of TPPS resulted in sensitive layers for Hg^{2+}. The response time is 15 min and the limit of detection is 1.4 µg/L. However, the main shortcoming is the limited life-time of the optical sensor caused by leakage of the water soluble dye TPPS into the aqueous solution after contact with heavy metal ions.[17] In order to enhance the stability of the sensor which is terminated by leaching of the dyes from the membrane, in 1996, Reichert and co-worker developed an optical sensor for the detection of Hg^{2+} based on the immobilisation of monofunctionalised porphyrin derivative 5-(4′-aminophenyl)-10,15-20-tris(4′-sulfonatophenyl) porphyrin (ATPPS) covalently bound to poly(2-hydroxyethylmethacrylate) (PolyHEMA).[18] The sensor was prepared by layering PolyHEMA coupled prophyrin as a thin film onto a poly(methycrylate) (PMMA) substrate.[18] This method has greatly reduced the leaching of the water soluble dyes from the solid matrices. Compared with Plaschke's method, the response time of this method has been reduced to 10 min, however, the limit of detection for Hg^{2+} increased to 63 µg/L. In 2000 and 2001, Wang and co-workers[19] and Yu and co-workers[20] dissolved 5,10,15,20-tetraphenylporphyrin and 5-*p*-[[4-(10′,15′,20′-triphenyl-5′-porphinato)phenyloxyl]-1-butyloxyl]-phenyl-10,15,20-tri phenyl-porphine into a plasticised poly(vinyl chloride) (PVC) membrane with a relative satisfactory result. The response times dropped to 4 min, but the sensor still suffered the leaching of the dye from the membranes. In 2008, Ensafi et al. reported that dyes can be

linked to cellulose acelate films by using thiourea and a selective optical sensor based on covalent immobilisation of water soluble dye 4-hydroxy salophen by using thiourea plus polyvinyl alcohol as a bridge to cellulose acetate film has been synthesised for determination of Hg^{2+} in solution.[21] This greatly reduced the leaching of indicators from the solid matrices into aqueous solution. However, the preparation processes are complicated and more than 3 reaction steps were needed. Therefore, it has been concluded that the physical immobilisation of water soluble dyes into the membrane gives a fast response to the target analytes and a lower limit of detection; however, the shortcoming is the leakage of the dye from the solid materials. On the other hand, by using the chemical bonding method, the leakage of the indicators can be reduced and the lifetime can be increased but the sensor normally requires a longer response time and the limited of detection is increased as well. Also the chemical modification of the sensing materials normally required complicated chemical preparations.

Wolfbeis and coworkers reported an alternative method of immobilisation of a water soluble indicator by lipophilisation of the indicator dyes by chemical modifications through synthesis of a lipophilic derivative of the dye.[22] In 2003, Steinberg reported the water soluble dye, Pyrocatechol Violet, can be lipophilised in the form of an ion pair with tetraoctylammonium cation and subsequently the whole ion pair was immobilised in a plasticised PVC membrane for the determination of copper ions. It was found that this type of immobilisation can significantly reduce the leaching of Pyrocatechol Violet dyes from the membrane.[14, 23] Consequently in 2005, the water soluble metal ion indicator, Alizarin Red S, was lipophilised in the form of an ion pair with tetraoctylammonium bromide, and subsequently immobilised on a triacetyl cellulose membrane for its potential use in uranium selective optode membrane.[24] The membrane responds to uranium ions, giving a colour change from yellow to violet in acetate buffer pH 5. This optode has a linear range of $(1.70 - 18.7) \times 10^{-5}$ M of UO_2^{2+} ions with a limit of detection of 5×10^{-6} M. The response time of the optode was within 6 min. The sensor can readily be regenerated with hydrochloric acid solution (0.01 M). The optode is fully reversible. In 2008, a test strip was developed for the spectrophotometric determination of trace amounts of uranyl ions, UO_2^{2+}, based on immobilisation of water soluble Chromazurol S/cetyl *N,N,N*-trimethyl ammonium bromide ion pair on a triacetyl cellulose membrane.[25]

Although the approach based on the lipolised water soluble dyes with tetraoctylammonium forms the ion pair cation, this Indicator/cation ion pair can greatly reduce the leaching of the indicator from the membranes. However, the indicator/ion pair was physically immobilized onto the membranes; therefore the leakage of the whole indicator/ion pair system can occur.

In order to improve the interaction of positively charged ion pair with solid matrices, Balaji et al. have reported a solid optical sensor for the rapid detection of low concentration of Hg^{2+} in aqueous solution.[26] It is based on the monolayer functionalisation of mesoporous silica with TPPS, anchored by *N*-trimethoxysilypropyl-*N,N,N*-trimethylammonium chloride (TMAC). This sensor obtained a low limit of detection of 1.75×10^{-8} mol/ml. It is also exhibits good chemical and mechanical stability and did not show any degradation of TPPS for a period of eight months. **Figure 4.1** shows the schematic graph of the reaction. The positively charged N centre of TMAC allows the electronic attachment of the $-SO_3^{2-}$ group of TPPS. The TPPS will also allow the entry of Hg^{2+} through its porphyrine centres consequently.
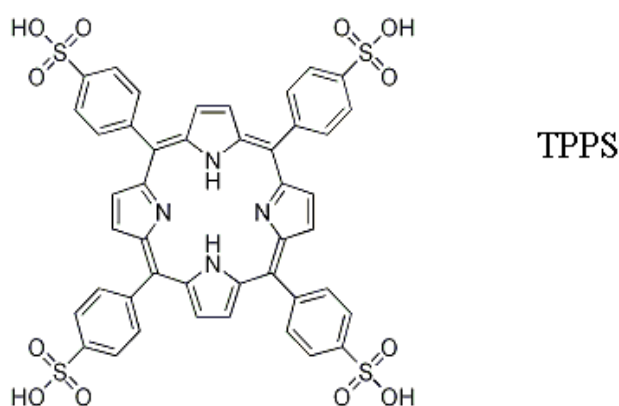

Host   **Complex**
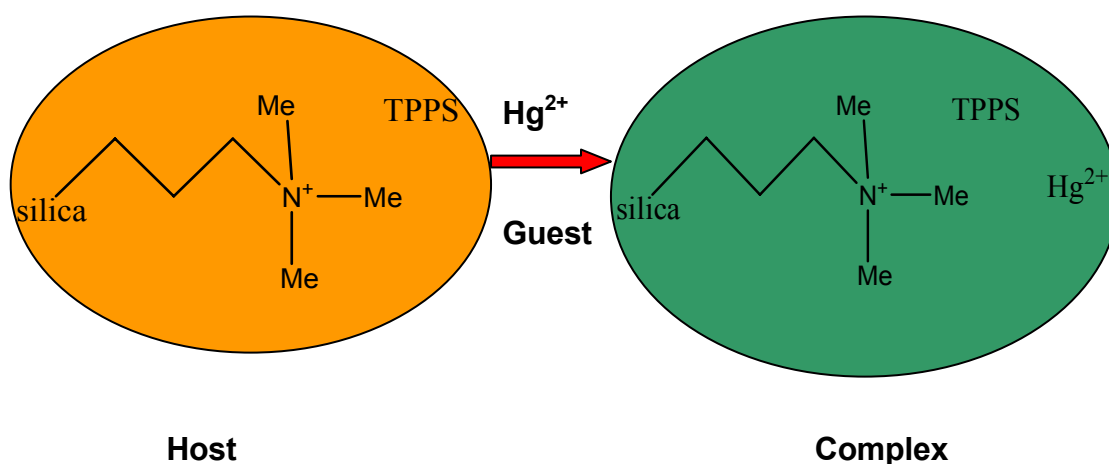
TPPS

Figure 4.1 Synthesis of MFMS and its reaction with TPPS. Adapted from literature.[26]

4.1.3 Cellulose Materials in Sensing Applications.

Cellulose is the most abundant renewable biopolymer in the world which has attracted much attention as sensing materials because of its outstanding properties.[27, 28] It is inexpensive, biodegradable, renewable, exhibits very good mechanical properties and is also water-absorbing.[28] Cellulose is a prime candidate for a sensor support due to its hydrophilic nature and its ability to resist chemical attack and degradation and it has been used as reagent support in chemical test methods of analysis.[29, 30] Since cellulose is composed of β-(1→4)-linked d-glucopyranosyl units with three hydroxyl groups, which can form complex inter- and intra-molecular hydrogen bonds, which results in its high crystalline structure and low solubility in common organic solvents.[31-33]

The known mechanisms of reagent immobilisation on cellulose paper can be classified into two types and discussed as before, the physical immobilization (physical adsorption) and chemical immobilization (covalent bonding).[5-7] Amelin et al. have successfully immobilized CAS onto natural cellulose papers for the determination of metal ions. The preparation method is simple and low cost although the retention of CAS onto cellulose films is low and only 10-20 % of the dye can be fixed into the cellulose membrane.[8] The main disadvantage of this cellulose material is the short life time and the non-transparency. The physical immobilisation based on weak absorption of CAS onto cellulose membrane caused the leakage of the dye and, hence, the indicators are washed out upon contact with analytes solution. Since this dyed cellulose paper is not transparent, the performance of the

test strip only can be detected visually without using a more accurate spectrometer. Recently, Rogers and coworkers developed a new approach to sensor development based on encapsulating 1-(2-pyridyazo)-2-naphthol (PAN) in a cellulose support followed by regeneration from ionic liquid (ILs) solutions. The test strip, through the codissolution of cellulose and PAN in 1-butyl-3-methylimidazolium chloride followed by regeneration with water, forms a strip which exhibits a proportionate (1:1) response to Hg^{2+} in aqueous solution.[34] The test strip is transparent and the dyes can be homogeneously encapsulated into the cellulose membranes. They claimed that the test strip could be reused 5 times; however, leaching of the dyes did occur for each time of use. The leaching was observed visually in the acetic acid solution.[34]

The optical sensors for the determination of heavy metal ions based on water soluble reagents immobilised on cellulose paper due to covalent have been reported.[6] Epoxy[35] or aldehyde-cellulose paper was used for the chemical immobilization of formazans and hydrazones bearing different complexing groups. This paper was used for the determination of Fe^{2+}, Fe^{3+}, Cu^{2+}, Hg^{2+}, Zn^{2+}, Cd^{2+}, Co^{2+}, Pb^{2+} and other ions.[36] Compared with physical adsorption, the covalent bonding of reagents into cellulose are more stable and can be reused after the decomposition of the complex formed with water or acids. However, the application of these systems is restricted because of the complicated multi-step synthesis of reagents required; thus both increasing the cost and modifying the performance of the sensor.

Therefore the research for simple and environmentally friendly methods for preparation of transparent and functionalised cellulose materials binding with water soluble dyes for the optical sensing purpose has drawn much attention.[37-40] Traditionally, production of regenerated cellulose fibres and films was largely based on viscose technology, which requires the use of harmful CS_2 and produces H_2S.[41] More recently, Zhang and co-workers found that NaOH/urea and NaOH/thiourea aqueous solutions can dissolve cellulose directly and quickly. Both solvent systems are inexpensive and less toxic, and good cellulose fibres can be prepared using this simple technology.[42] However, spinning solutions containing high concentrations of cellulose in these two solvents are unstable, which is a disadvantage in industrial applications. Moreover, the dissolution mechanism for cellulose in these ternary solvent systems is not clear. Recently, a NaOH/thiourea/urea aqueous solution that can dissolve cellulose quickly has been identified. The most

important finding is that the new solvent is more powerful in dissolving cellulose, and can be used to prepare more stable spinning solutions containing higher concentrations of cellulose than NaOH/urea (or NaOH/thiourea) aqueous solution systems.[40] In 2008, Song et al. reported a method to synthesise the transparent homogenous quaternised cellulose solution by reacting cellulose with 3-chloro-2-hydroxypropyltrimethylammonium chloride (CHPTAC) in NaOH/Urea aqueous solutions.[43] This quanternised cellulose deterivatives prepared could be considered as promising nonviral gene carriers. **Figure 4.2** illustrates the homogeneous quaternisation of cellulose dissolved in NaOH/Urea aqueous solution by using CHPTAC as etherifying agent.
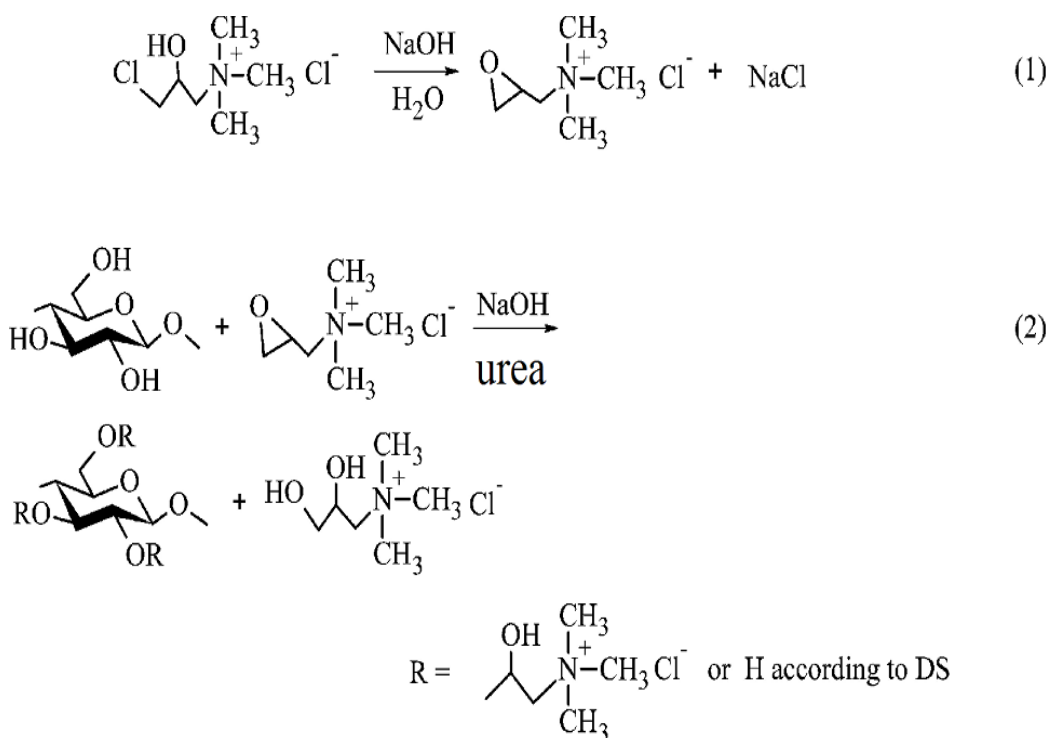

Figure 4.2 Derivatisation of cellulose with cationic functionalities.

4.1.4 The Immobilisation of CAS into Cationic Cellulose Membrane

Inspired by the method of preparation of functionalised cationic cellulose reported by Song et al.[43] and the immobilisation of water soluble indicators onto cationic sol-gel

matrix reported by Balaji et al.[26], this work describes the development of a quatuamminium cationic NaOH/Urea modified cellulose sensing membranes that can electro-statically bind with a group of indicator dyes that contains sulfonic groups for the determination of heavy metal ions.

In this work, we hypothesized an inexpensive, simple and "green" route for the manufacture of cellulose-based materials that can be electrostatically interacted with water soluble sensing molecules and that could be developed as sensing materials. We present here a proof of this concept with a class of sensors based on water soluble CAS electrostatically binded in a cationic cellulose matrix for the determination of Cu^{2+} ion in aqueous media. These cellulose-based sensors have several advantageous features, including low cost, high flexibility, a huge diversity of physical forms that can be realised and easy preparation and handling. Additionally important, they can be environmentally benign if the probe is chosen wisely and the sensor is disposed of properly. Here we demonstrated that the water soluble indicator CAS can be electrostactically anchored with the positively charged CHPTAC of the functionalised cellulose membrane. And this functionalised cellulose membrane can be used for the detection of Cu^{2+} ion in aqueous solution. The structure of the proposed membrane is illustrated in **Figure 4.3.**
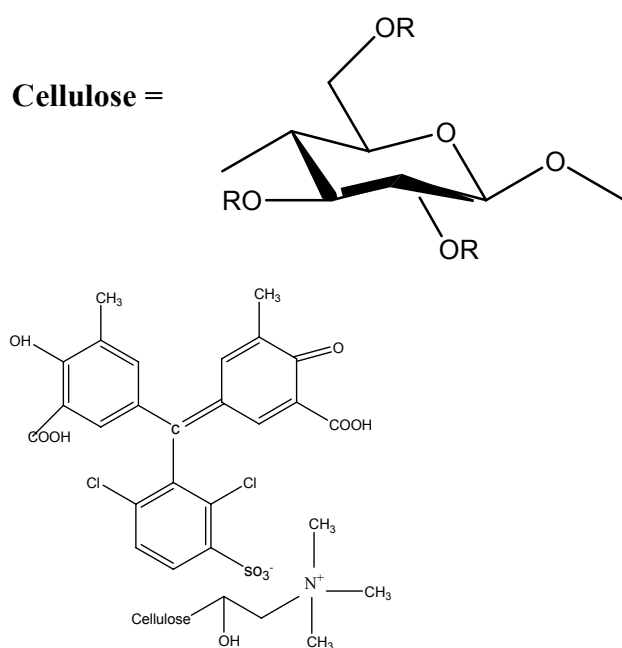
Figure 4.3 Structure of the CAS indicator anchored cationic cellulose membrane.

4.1.5 Aim and Objectives

This aim of this work is to develop optical sensors based on the incorporation of water soluble indicators into quaternised cellulose matrices using the electrostatic immobilisation approaches for the determination of heavy metal ions.

The objectives of this work are:

1.   To synthesis the cationic functionalised cellulose materials,

2.   To immobilise the water soluble indicators, i.e. CAL, CAS, Nitroso-PASP and AVN into these materials and to test the performance of these sensing membranes,

3.   To develop an optical sensor film based on the immobilisation of CAS onto cationic cellulose membrane for the determination of copper ions.

4.2 Materials and Method

4.2.1 Materials

NaOH, Urea and Ethanol were analytical grade and were purchased from Sigma-Aldrich, Co-Chemicals Company, Tallaght, Ireland. Pure cellulose samples were microcrystalline cellulose obtained from Sigma-Aldrich, Co-Chemicals Company, Tallaght, Ireland (Particle size 40 μm) and were used as etherifying reagents without further purification. 3-chloro-2-hydroxypropyltrimethylammonium chloride (CHPTAC) was purchased from Sigma-Aldrich, Co Chemicals, Tallaght, Ireland. All tested metal indicators, i.e. CAL, CAS, Nitroso-PASP, and AVN were purchased from Sigma-Aldrich, Co-Chemicals Company, Tallaght, Ireland and were used without purification. The preparation of buffers (pH 1-10) solutions used in this work has been previously detailed in Chapter 2.

4.2.2 Preparation of Indicator Solutions

The indicators were made by dissolving a desired amount of CAL, CAS, Nitroso-PASP, and ANV into DI water to make the final concentration of 2×10^{-4} M.

4.2.3 Instrument

Absorption spectra in the range of 200-800 nm were recorded with a UV-Visible Cary 50 spectrophotometer (Varian, USA), with a matched 1 cm quartz cells. An ETD Rex 3400 pH meter with a glass electrode was used to measure pH in the solution. The morphology of the modified cellulose was studied by Hatachi SEM 3400, Japan. The samples for SEM measurement were sputter coated with gold for 1 min by using sputter-coater. ATR was used for the infrared spectra determination. The contact angle was measured by using drop shape method according to the literature method.[44]

4.2.4 Preparation of the Quaternised Cellulose Solution

147

The procedure is illustrated in **Figure 4.4.** Cellulose solution was prepared according to the previous method with slight changes.[42] 50 mL of NaOH, Urea and distilled water aqueous solution (weight percentage was 7:12:81) were mixed in a 250 mL beaker.

A   B

C   D
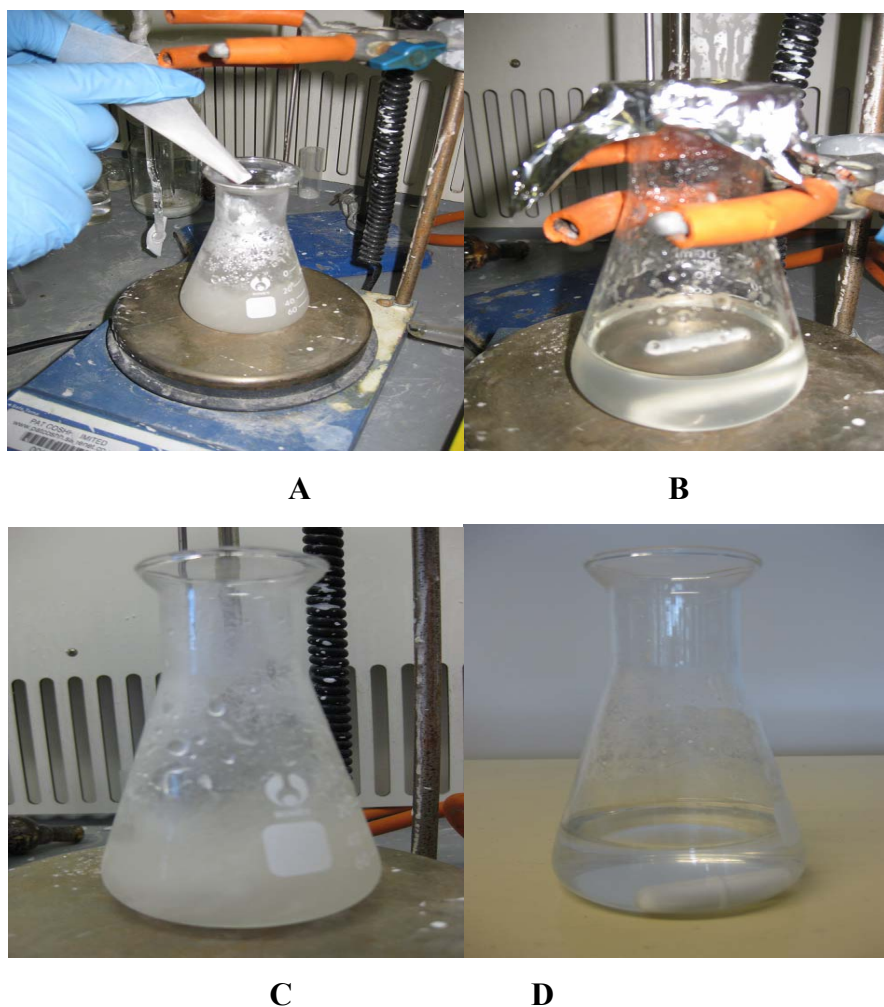
Figure 4.4 Preparation of modified cellulose membranes. (a) added materials in a 250 mL volumetric flask with frozen solvent; (b) stirred the mixture; (c) kept the mixture in the freezer at - 4°C; (d) the cellulose dissolved and the solution became clear.

The mixture solution was stored at -4°C in a refrigerator for 12 h. A 2 g quantity of cellulose was dissolved immediately into this ice-cold solution and stirred vigorously at ambient room temperature (~ 20 °C) for 1 h to obtain a clear solution. The cellulose solution was subjected to centrifugation at 8000 rpm for 20 min at 10 °C to exclude the slightly remaining undissolved cellulose before using any further. In a typical procedure,

specified amount of CHPTAC as shown in **Table 4.1** was added and then stirred for another 8 h until the solution became clear. Then the solution was degassed by centrifugation at a spin speed of 10,000 rpm for 10 min. The quaternised cellulose solution was kept at room temperature and ready for use.

Table 4.1 The amount of CHPTAC used for the preparation of Cellulose membrane QC1-7.

Number	Amount of CHPTAC (g)
QC-1	0
QC-2	0.2
QC-3	0.4
QC-4	0.8
QC-5	1.2
QC-6	1.6
QC-7	2

Note: The volume of cellulose used for each of the film was fixed to 2g.

4.2.5 Sensor Preparation

The quaternised cellulose solution was poured at a quantity of 1 mL in a thick line from the vial onto a clean microscope glass slide (1.5 cm x 4 cm) and was cast into a thin film using coating rod. The solution was pulled by hand across the slide in one direction with the coating rod using even pressure, yielding films of even thickness. Then cationic cellulose solution poured on the glass was immersed into ethanol solution for 10 min at room temperature. A white gel-like membrane was obtained. The cellulose solution was immersed into the ethanol solution for 1 h is to remove the organic salts such as Urea. The resulting film was washed with copious amounts of deionised water for 2 h in order to remove the inorganic salts, such as NaOH. After removing the inorganic salts by washing with deionised water, the cationic cellulose membrane became opaque after drying. The process is illustrated in **Figure 4.5.** In this section, indicator CAS was used as example to demonstrate the electrostatic immobilization process. As it has been shown in chapter 2, CAS is a photometric reagent for various metal ions.

The functionalised cellulose membrane was fabricated with a CAS indicator solution by immersing it into CAS solution at pH 7 and the membrane was kept into the solution for 10 min. During this process, the negatively charged sulfonate group in CAS bounded with the positive charged cellulose surface by electrostatic binding. The dyed membrane was immersed in DI water for at least 12 h each time; twice to make sure that the unbounded CAS dyes washed out in each washing cycle and there was no free CAS ligand left into the cellulose membrane. The dyed membranes were stored in DI water before use. It was noted that, during the first washing cycle, a lot of indicators were washed out. The colour of the washing water became clearer each time due to the reduction of free CAS left in the dyed cellulose membrane. Finally, the membranes were placed into the fresh DI water and no dye-leaching was noticed during 7 days observation. The resulting films were immersed into prepared dye solutions for 1 hour. Before use, the dye-doped cellulose film was washed with distilled water and kept in deionised water for 24 h before use.
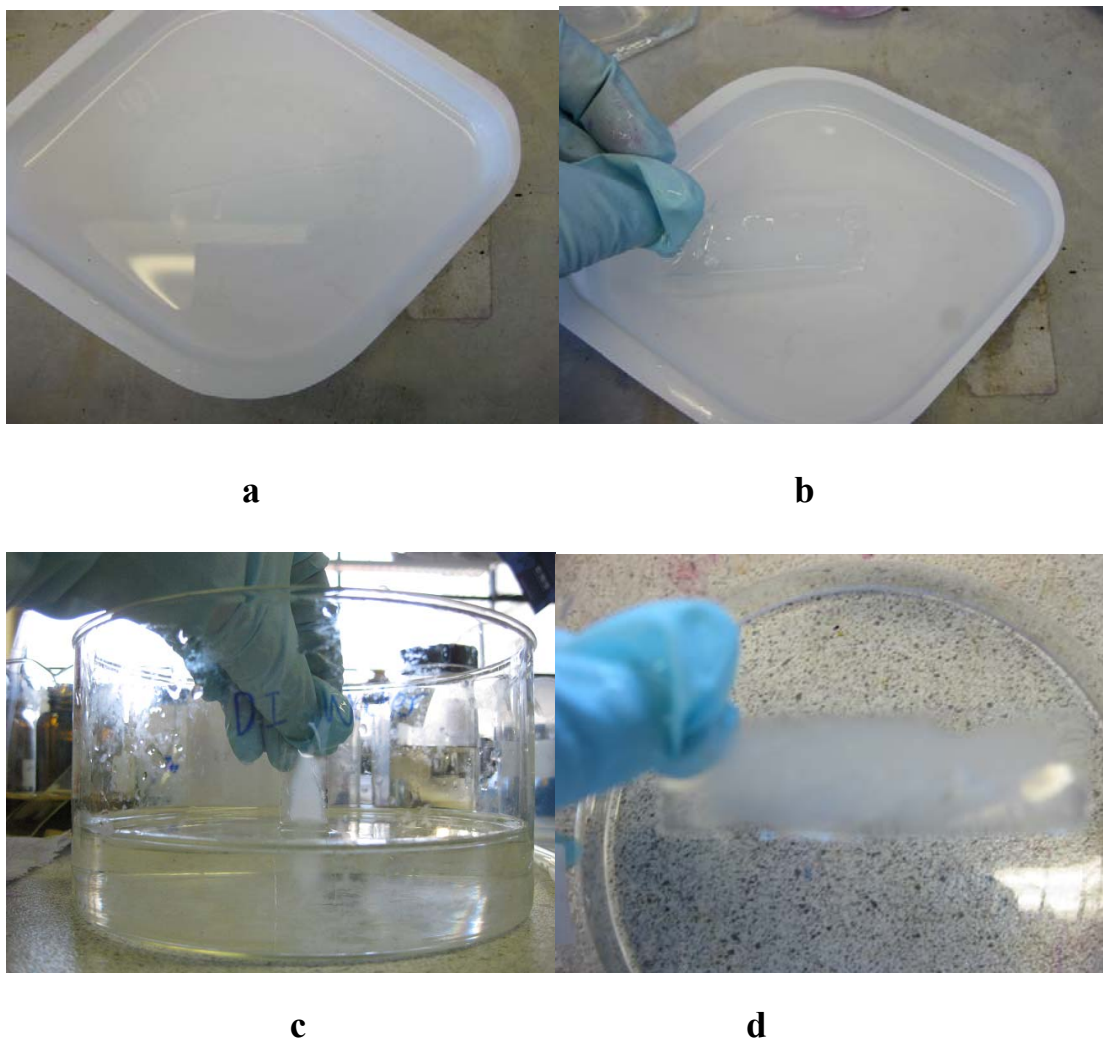
Figure 4.5 (a) 1 mL of the cellulose solution was spread on a glass slide and washed in 100 % ethanol solution; (b) The membrane was stored in DI water for 2 h; (c) and washed the membrane with DI water for 2 h;(d) washed again with DI water.

4.2.6 Characterisation of the Cationic Cellulose

The blank cationic cellulose membrane without dying was dried at room temperature for 24 h until it became dry and clear. The membrane was carefully peeled off the glass support and cut into small pieces. Attenuated Total Reflection (ATR, Agilent, Germany) was used for the Infrared spectra measurement.

The morphology was observed on a scanning electron microscopy (SEM 3400, Hitachi, Japan) with 20 kV as the accelerating voltage. The dried cellulose membrane was used. The samples were sputtered with gold, followed by observation and photography. The optical

absorption of the film was measured with a Cary 50 Spectrophotometer at wavelength from 200 nm to 800 nm.

4.2.7 Cu^{2+} Solution Preparation

A stock solution of 1000 mg/mL Cu^{2+} from $Cu(NO_3)_2 \cdot 6H_2O$ was prepared by dissolving an appropriate amount of metal salt in 0.01 HNO_3. Standards of lower concentration were prepared by diluting from this 1000 mg /L stock solution with the pH buffer solution.

4.2.8 Preparation of pH Buffers

The effect of pH was tested using the following pH buffers (same as in Chapter 2): Acetate buffer, 2-(N-morpholino)ethanesulfonic acid (MES, >99%), 4-(2-hydroxyethyl)piperazine-1-ethanesulfonic acid (HEPES, >99.5%). The pH buffers solutions were prepared using the buffer salts to make the concentration of 10 mM. To study the pH effects on sensor performance, buffered solutions of 50 mgL^{-1} aqueous Cu^{2+} were prepared at pH values of 1-10.

4.2.9 Testing CAS Sensors

The CAS/ quaternised cellulose (QC) membranes (except for a blank) were exposed to buffered Cu^{2+} solutions at different pH solutions for 5 min and they were removed. Their UV-Vis absorbance spectra recorded for reacted films. Spectra were collected by mounting the films on microscope glass slides after the baseline absorbance of the microscope slide was substrated. The wet films adhered easily to the glass slides.

A series of Cu^{2+} solutions of different concentrations were prepared and tested by dilution from the 1000 mgL^{-1} stock solution with pH 7 buffer. CAS/QC films were allowed to soak in the solution for 5 min, after their UV-Vis absorbance spectra were measured as described above. Complex formation was achieved within 1-5 min, depending on the concentration of the ion solutions. For higher concentrations of Cu^{2+}, a visual colour change was observed almost immediately. At lower concentrations of Cu^{2+}, a visual colour change could be observed after approximately 3 min contact time.

4.3 Results and Discussion

4.3.1 "Green" Process of Preparation

The heterogeneous quaternisation of cellulose dissolved in NaOH/Urea aqueous solution by using CHPTAC as etherifying agent. It was found that cellulose dissolves rapidly in 7 wt% NaOH/12 wt% urea aqueous system pre-cooled to -4°C to obtain transparent cellulose solution. Under the alkaline conditions, epoxide is produced in situ from CHPTAC, and then quaternised cellulose is formed through reaction between the cellulose sodium alkoxide and the epoxide or CHPTAC. This procedure is very rapid (less than 10 min). It has been reported that the temperature needs to be cooled under -12°C,[43] however, in the current method, - 4°C is enough for dissolving the cellulose completely. The formation of regenerated cellulose films is a physical process, mainly related to the diffusion between non-solvents of the gel sheet, followed by drying. In this system, NaOH and urea are nontoxic and inexpensive. The byproducts could be easily separated and recycled to be reutilised. The main byproducts are inorganic sodium salt and urea, which can be separated easily by washing with 100% ethanol solution and DI water. The membranes were kept in 100% ethanol solution for 1 h to wash out urea from the membrane. In this step, the liquor membrane becomes gel-like when dipped into the ethanol solution. The membrane is kept in a large amount of DI water for 2 h to wash out the sodium salt and this is repeated twice to make sure that the sodium salt is cleaned. Afterwards, the membrane was kept in DI water. It is noted that during the process, there is no evaporation of any chemical agents and the reaction temperature occurred at room temperature.

4.3.2 Optimisation of the Membrane Composition

The performance of the quarternised cellulose (coded as QCs) membrane was critically dependent on the solubility of cellulose in aqueous solution; therefore the solubility of the cellulose was investigated.[42] The degree of etherification of a certain cellulose fibre is characterised by the so-called "degree of substitution" (DS). The solubility of the cellulose is affected by the degree of substitution of the cellulose. Because raw cellulose materials are not soluble in water solution and each glucose (as cellulose monomer) contains three free –OH groups, this degree ranges from DS = 0 (all –OH groups are free) to DS = 3 (all

groups are etherifies). CHPTAC is a water soluble cation ion. The solubility of the cationic functionalised cellulose can be affected by the substitution of the –OH group by CHPTAC.

The quaternised cellulose membrane can be prepared in either heterogeneous or homogeneous form depending on the mole ratio of anhydrous-glucose unit (AGU) to the CHPTAC. Therefore the amount of CHPTAC needed for the preparation of heterogeneous cellulose membrane must be carefully optimised firstly. According to **Table 4.2**, 7 quaternised cellulose derivatives were prepared by changing the mole ratio of anhydrous-glucose unit (AGU) to the CHPTAC. All of these cellulose membranes were prepared with the same procedure as described previously; the working condition such as temperature, amount of solvent used and reaction times remained the same, except the amount of CHPTAC added into the cellulose solution was varied. The molar ratio of AGU: CHPTAC is increased, from 0 to 1. The reaction conditions and the performance of the QC membrane for quaternisation of cellulose are summarized in **Table 4.2**

Table 4.2 Conditions of the heterogeneous quaternisation of cellulose with CHPTAC in NaOH/Urea aqueous solution

Number	Molar Ratio[a]	Time (h)	Performance
QC-1	0	8	Heterogeneous
QC-2	1:0.1	8	Heterogeneous
QC-3	1:0.2	8	Heterogeneous
QC-4	1:0.4	8	Heterogeneous
QC-5	1:0.6	8	Heterogeneous
QC-6	1:0.8	8	Heterogeneous
QC-7	1:1	8	Heterogeneous

[a] The molar ratio of AGU to CHPTAC

During the process of quaternisation, the solution (QC1-7) kept its transparent nature and remained completely homogenous as the reaction proceeded. The transparent QC 1-7 solutions turned into heterogeneous membranes after immersing into ethanol solution for 10 min. After washing with DI water, the heterogeneous QC membranes became transparent films. Therefore, the heterogeneous QC membranes can be prepared by

keeping the molar ratio of AGU to CHPTAC within 0 to 1:1. Song et al. have synthesised homogeneous quaternisation of cellulose membranes in NaOH/Urea aqueous solutions by reacting with of CHPTAC.[43] They have found that the QC membranes are soluble in water with the molar ratio of AGU to CHPTAC of cellulose from 3-12. The reaction time varied from 4 to 16 h.[43]

4.3.3 The Effect of the Molar Ratio of AUG to CHPTAC

As it was described in **Figure 4.3,** CAS reacted with CHPTAC at the 1:1 molar ratio. Therefore the amount of CAS can be immobilised into quaternised cellulose membrane can be also affected by the molar ratio of AUG to CHPTAC. Therefore, a range of CHPTAC-Cellulose ratio has been studied. The QC membranes 1-7 **(Table 4.2)** were cut into the same size and stored on 7 cleaned weight boats. 1 mL of 2 x 10^{-4} M CAS was added to each of the weight boats and this is shown in **Figure 4.6 (a)**.

It was observed that 1mL of CAS solution was enough to cover the QC membranes. The membranes were dyed into the CAS solution for 10 min and then washed with fresh DI water to wash out the free CAS that physically absorbed to the surface of the membranes. Then the dyed QC membranes were stored with fresh DI water. It can be seen that from **Figure 4.6 (b)** that the colour of QC membranes 1-7 was reduced. For QC membranes 1-3, the yellow colour of the dyed membranes reduced greatly, on the contrary, the colour of dyed QC membranes 4-7 changed slightly by comparing the **Figure 4.6 (a)** with **Figure 4.6 (b).** After the second wash cycle, it was found in **Figure 4.6 (c),** the QC membranes 1 and 2 became transparent. QC 3-7 remained the same colour compared with **Figure 4.6 (b).** This result showed when the molar ratio of AUG to CHPTAC is smaller than 1:0.1, the cellulose membrane cannot be etherified and therefore the immobilisation of CAS into the membranes was not stable.
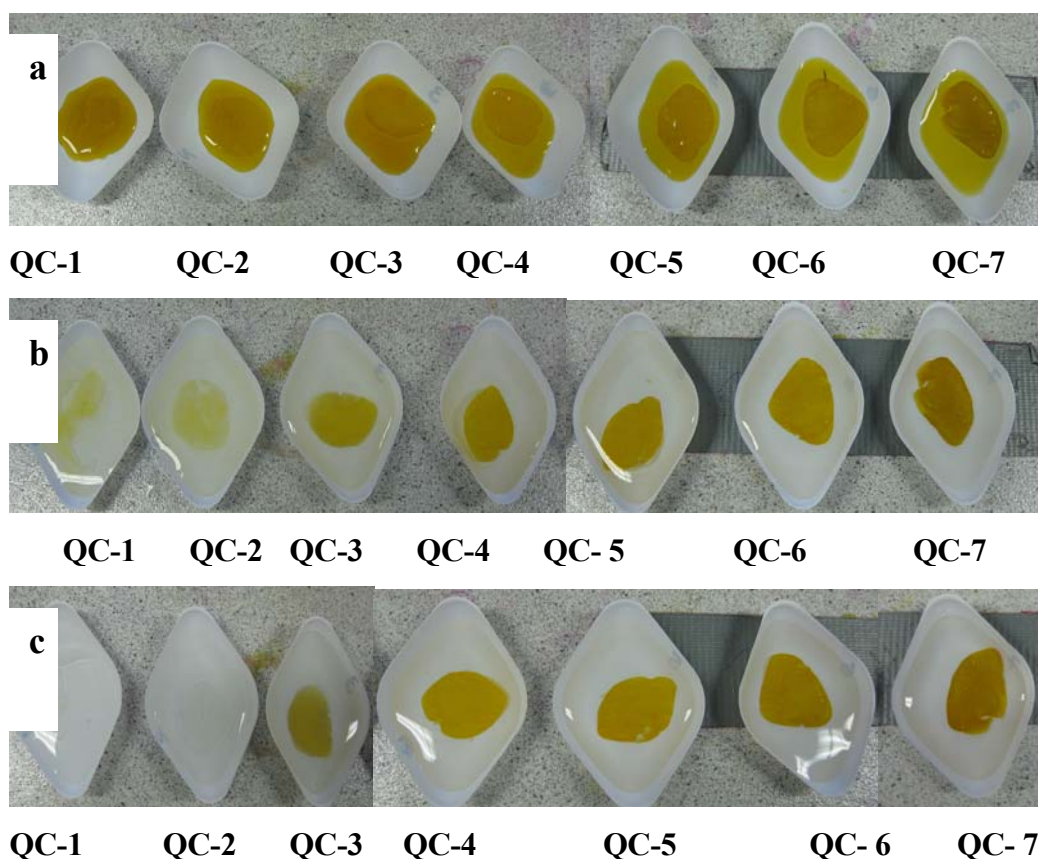
Figure 4.6 Photos of the dyed cationic cellulose membranes with the indicator CAS (2 x 10^{-4} M). (a) The cellulose membranes were dyed in CAS solutions; (b) photos taken after the first wash cycle; (c) photos taken after the second wash cycle.

The CAS was physically doped into the cellulose membrane and can be washed out easily. This has been confirmed by Amlin et al.[5, 8] They claimed that, the CAS indicator can be immobilised into unmodified cellulose fibre through the weak hydrogen bound.[8] Because an increase in the pH of the impregnating solution of the reagents leads to a small decrease in the retention, which is due to the dissociation of the reagents and the disappearance of hydrogen bonds (e.g., the retention for CAS decreases by 10% upon increasing the pH from 1.0 to 5.0), therefore, it can be explained that hydrogen bonds in the adsorption role of CAS on unmodified cellulose is not strong enough to retain the interaction firmly. The absorbance (at the wavelength of 430 nm) of the dyed cellulose membrane 1-7 with CAS (2 x 10^{-4} M) is shown in **Figure 4.7**.
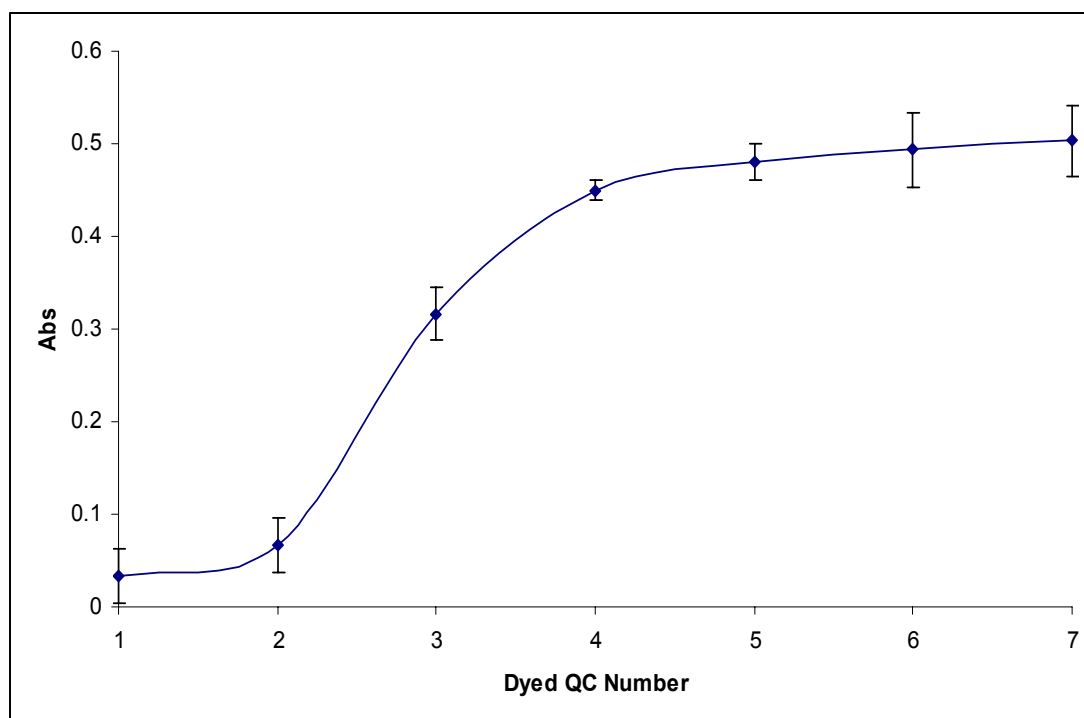
Figure 4.7 Absorbance spectra of dyed QC membrane 1-7.

For the QC membranes 3-7, with the molar ratio of AGU to CHPTAC from 1:0.2 to 1:1, the cellulose membranes can be esterified but at different degrees. It was shown in **Figure 4.7,** the absorbance increased with the increases of molar ratio of CHPTAC to AGU. The absorbance of QC 1 and 2 were very low. The absorbance greatly increased from QC 3 and increased slightly from QC 4. There was not much increase for QC 5-6 membranes which were prepared with larger amount of CHTPAC. This is due to the fact that the cellulose obtained the optimum quaternised degree at the molar ratio of AGU to CHPTAC at 1:0.4. Therefore, QC 4 was used for further investigation. The dyed-cellulose membrane which was kept in DI water for 7 days showed that there was no leaching of CAS from the cellulose membrane. Therefore, we successfully immobilised the water soluble photometric reagent CAS onto the cationic functionalised cellulose membranes.

Rather than CAS, a variety of water soluble indicator dyes was briefly studied using similar procedures. Retention of the water soluble indicators that have been investigated in Chapter 2, immobilised on QC membranes is shown in **Table 4.3.** All of these indicators were embedded into cationic functionalised cellulose membranes and produced coloured transparent thin films.

Table 4.3 Retention of indicator dyes onto the QC membrane

Indicator Dyes	Results	Remarks
AVN	Stable	Pinky-red colour at pH 7 solution
CAL	Stable	Blue colour at pH 7 solution
CAS	Stable	Yellow colour pH 7 solution
Niroso-PSAP	Stable	Dark green colour at pH 7 solution

As a conclusion, we have demonstrated that the functionalised cationic cellulose membranes can entrap negatively charged water soluble indicators. These membranes are highly transparent and have a large potential for sensing applications. In the next chapter, one of the water soluble indicators that have been studied in Chapter 2 in terms of its solution chemistry is described in terms of its sensing material and immobilisation method. CAS was chosen as the indicator and the target is Cu^{2+}.

4.3.4 Characterisation of the QC Membrane

4.3.4.1 FT-IR Spectra of the Cellulose and QC film

In order to confirm the cellulose membrane has been quaternised by CHPTAC, the raw cellulose materials and the QC 4 film have been characterised with FT-IR. The ATR spectra of unmodified cellulose and modified cationic cellulose (QC 4) are shown in **Figure 4.8.**
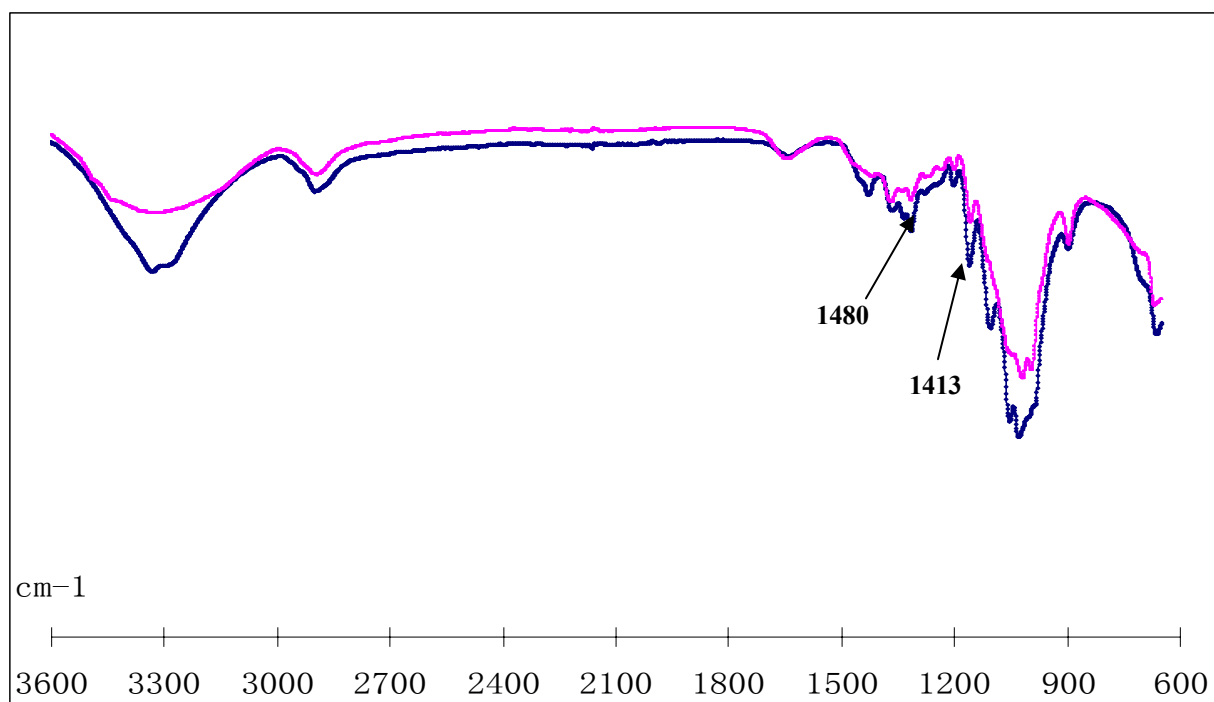
Figure 4.8 ATR Spectra of the cellulose and the quanternied cellulose sample QC 4.

■ Native cellulose; ■ QC-4.

The unmodified cellulose membrane showed a broad band at 3600 cm^{-1}, assigned to stretching vibration modes of O-H groups. The bands at 2900, 1375, and 1062 cm^{-1} were assigned to stretching vibration of –CH$_2$– groups. The peak near 1637 cm^{-1} was attributable to the bending and/or stretching of quaternary ammonium group; the peak at 2916 cm^{-1} was a stretching vibration band from the C-H bond; the peak at 1386 cm^{-1} is from the C-H of -CH$_3$ stretching vibration band, and the antisymmetric absorption peak of C-O-C was in 1050 cm^{-1}. The most significant difference between the unmodified cellulose with the cationic cellulose is the band at 1480 cm^{-1}, which has been reported to correspond to methyl groups of ammonium groups of CHPTAC.[45] Furthermore, the band at 1410 cm^{-1} was assigned to the C-N stretching vibration.[46, 47] Therefore, the IR spectra have given evidence of the introduction of the quaternary ammonium salt group on the cellulose backbone.

4.3.4.2 SEM Study of the Membranes

The retention of the water soluble indicator into the QC membrane also benefits from the porous structure of modified QC membranes. The microscopic investigation of the surface

of raw cellulose material and the modified cellulose material with CAS has been carried out. **Figure 4.9** shows the SEM images of cellulose powder and modified cellulose which was treated with NaOH/Urea and CHPTAC solutions.
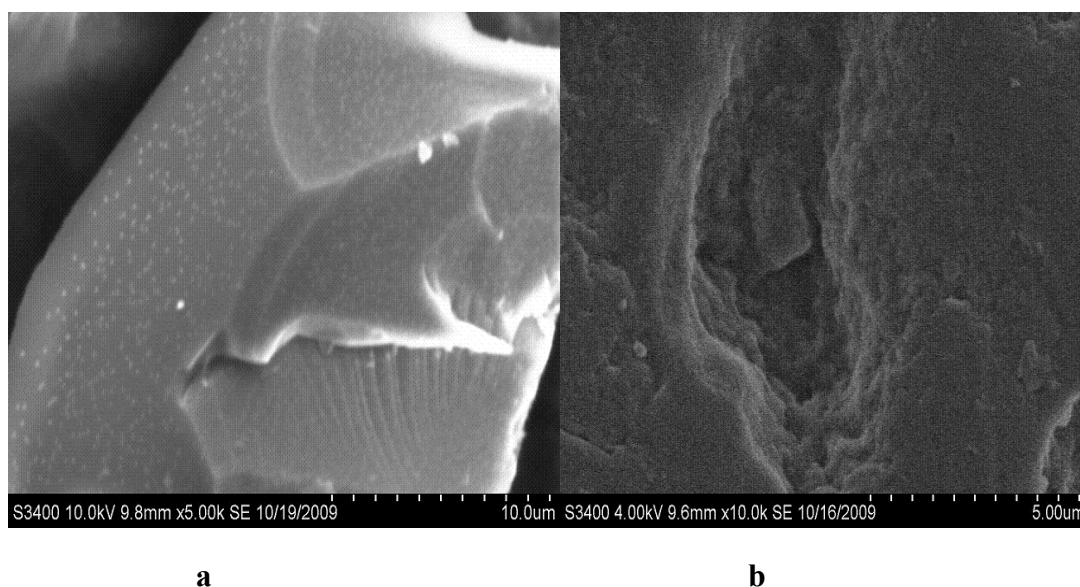

<div align="center">a   b</div>

Figure 4.9 SEM of dried treated cellulose membranes. (a) untreated cellulose powder; (b) QC membrane 4.

It is apparent from **Figure 4.9 a,** that the surface structure of the unmodified cellulose material is quite uniform; this has also been reported by Egorov et al.[39] In contrast, to **Figure 4.9 b,** the modified cationic QC 4 membrane exhibited a porous and rugged structure. It is believed that this porous structure can provide sufficient space for the entrapment of CAS and thus reduce the leaching of the indicators from the membrane. The CAS molecules were immobilised in the porous 3D networks of the QC membrane through electrostatic interaction between cationic cellulose membrane and CAS. Compared with the untreated cellulose, the treated cellulose membrane shows slight swelling, but little breakage of the structure. It also can be seen from image **Figure 4.9 (b)**, that the hydride cellulose membrane displayed some microporous structure, which was different from the pure cellulose filter papers **Figure 4.9 (a)**. The morphology implied large surface areas of this material and preferable blending of the polymers.

4.3.5 Absorbance spectra of CAS/QC films for the Determination of Copper Ions

CAS was used previously in immobilised form for preconcentration purposes. For example, Ameline et al. immobilised CAS on different thin-layer matrices, such as paper, cloth, and silk and artificial cellulose fibers and nylon. They studied the reaction of these dyes thin-layer matrices with metal ions, such as Al^{3+}, Zn^{2+}, and Fe^{3+}.[8] As discussed in Chapter 2, CAS is a photometric reagent for various metal ions, especially sensitive to Cu^{2+}. The selectivity to Cu^{2+} can be achieved or improved by appropriate separation pretreatment or with the combining of masking agents.[48] The treated cellulose membranes are polymer-like on the surface. It was white in colour when it was wet. The dried membrane became opaque and it was very clear and bendable. This indicated that the urea had been washed out completely. Its blending properties have also been reported by Zhang and co workers.[33] Therefore, it noted that the dried QC membranes can be used as a sensing test strip without any extra solid support (i.e. glass slides) like the sensors developed previously based on sol-gel or PVC materials as solid matrices.
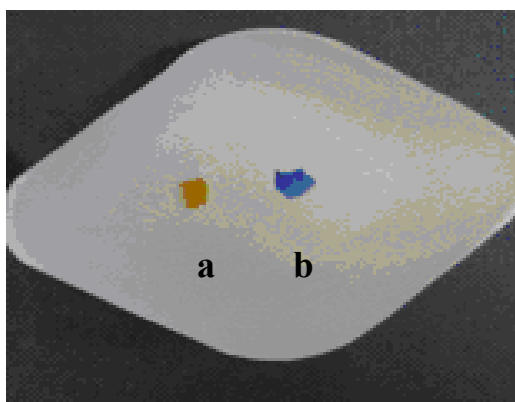
Figure 4.10 The dyed QC membrane 4 immobilised with CAS. (a) Unreacted CAS/QC-4 membrane. (b) The CAS/QC-4 membrane reacted with Cu^{2+} at pH 8 (10 mg/L).

Figure 4.10 shows the picture of the unreacted CAS/QC (4) membrane **(a)** and the fully reacted CAS/QC-4 films with Cu^{2+} **(b)**. The blank CAS/QC-4 membrane obtained a yellow colour. After contacting with Cu^{2+} ion (10 mg/L), the colour of the membrane changed to blue.

The absorption spectrum of the CAS immobilised QC membrane showed a maximum at the wavelength of 430 nm in pH 8 buffer solutions. By the addition of Cu^{2+} ions, a decrease in absorbance is observed at this wavelength and a new band at the wavelength of 620 nm is formed. **Figure 4.11** depicts the spectra of CAS after addition of different concentrations of Cu^{2+}. By decreasing the absorbance maximum at 430 nm, a peak at 620 nm is continuously increased that corresponds to the formation of a Cu^{2+}-CAS complex. There is an isosbestic point observed at 470 nm.
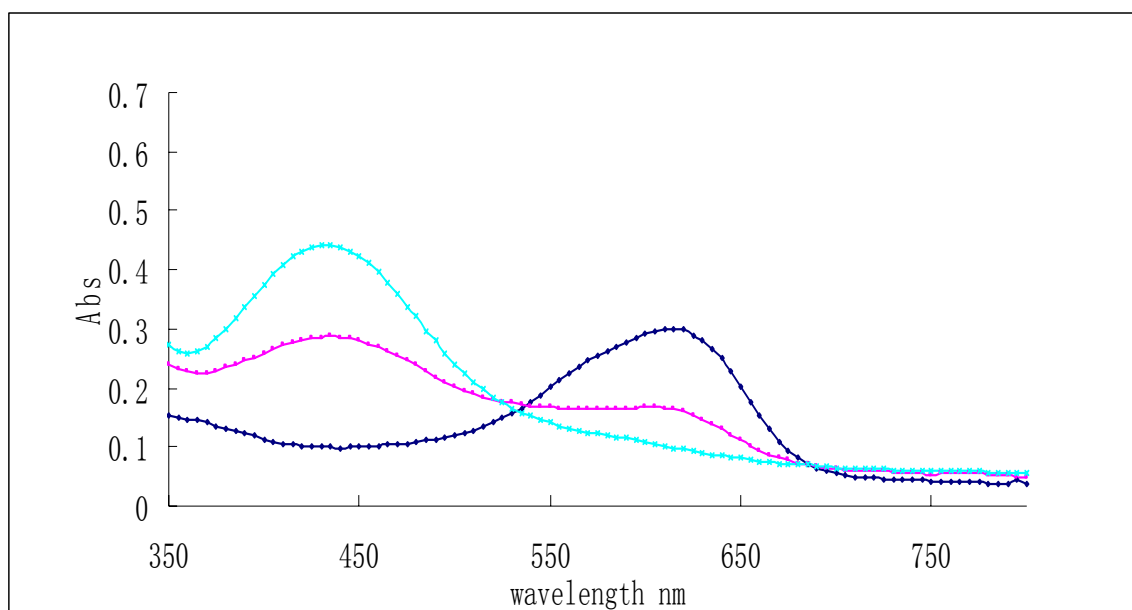
Figure 4.11 Absorption Spectra of CAS/QC membrane in the presence of Cu^{2+}.
■ 0 mg/L, ■ 15 mg/L; and ■ 50 mg/L in pH 8 buffer solution.

Compared with the study of CAS and the complexation study of CAS with Cu^{2+} in solution study, the optical properties of the CAS immobilised into QC membrane have changed. From **Table 4.4**, it was found that the absorbance maximum of CAS showed a red shift from 410 nm in solution to 430 nm in the QC membrane. There is a significant bathochromic shift of about 20 nm observed for the CAS/QC-4 membrane compared with the absorbance spectra of the CAS-unbounded indicator in pH 9 buffer solutions. The absorption of pure CAS at pH 9 buffer solution is shown in Chapter 2, **Figure 2.9**, and the absorbance was at about 410 nm. This is probably due to a more flat structure of the immobilised CAS that may cause an easier electron resonance.

162

Table 4.4 Absorption maxima of the CAS and CAS-Cu^{2+} complexes in pH 9 buffer solution and immobilized on QC-4 membranes at pH 8 buffer.

Reagents	Solution (nm)	QC-4 (nm)
CAS	410	430
CAS-Cu^{2+}	530, 600	620

Similarly to the case of CAS indicator in solution and in CAS/QC membrane, the absorption spectra of CAS-Cu and on CAS-QC-Cu complexes in pH buffer 9 solutions are different as well. This is shown in **Table 4.4**; it is shown that the CAS-Cu complexes obtained absorbance maxima with a shoulder band at the wavelength of 530 nm and 600 nm in solution. Compared with the absorption spectra of the CAS/QC-4-Cu complexes in pH 9 solution, there is a bathochromic shift observed and a broad band obtained at 620 nm.

The blue-violet colour of the CAS/QC-Cu complexes indicated that the CAS-Cu complexes in the ternary complex formation.[4] It has been reported that in weakly acid to neutral solution, the CAS-Cu complexes are blue-violet.[49] Therefore, absorbance of the complexes of CAS/QC-Cu at 620 was chosen for further studies. This agrees well with literature data on the pH profile for Cu^{2+} determination by using CAS with quaternary ammonium surfactant salt in solution.[4]

4.3.6 Effect of pH

The pH is an important factor that not only can affect the loading of CAS dye onto the QC membrane but also can affect the performance of the CAS dye loaded QC membrane. In order to obtain an appropriate dye loading on the QC membrane, the effect of pH of the reaction solution on the maximum absorbance of the membrane was studied at 430 nm. It was found that a maximum immobilisation of CAS is achieved in a pH range of 7-9 as demonstrated in **Figure 4.12.** When the pH is smaller than 7, the CAS loaded QC membrane is not stable; in our work, the CAS leached out from the membrane quickly when it was washed with DI water. When the pH is larger than 10, the –OH group in the solution is competitive with the CAS loaded onto the QC membrane.
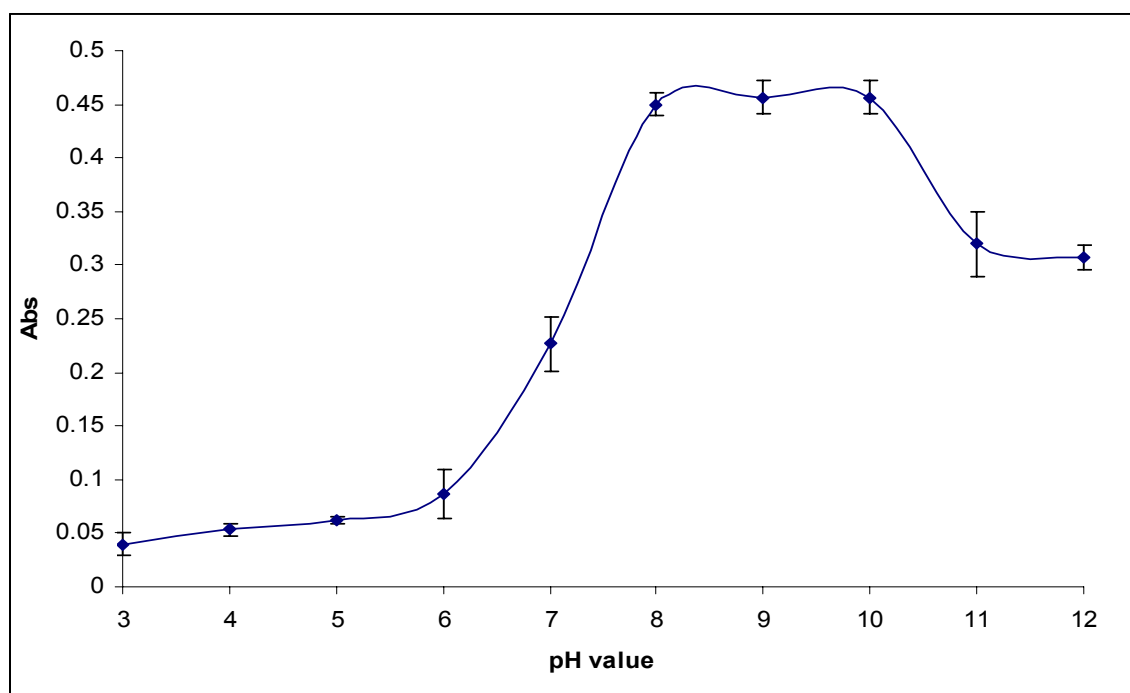
Figure 4.12 Effect of pH of the reaction solution on the immobilisation of CAS on QC membrane. Experimental Conditions: CAS concentration, 2×10^{-4} M; absorbance measured at wavelength 430 nm.

The leaching of the dye from the QC membrane at low acidic solution (pH range from 3-6) was observed. Therefore, the absorbance of the CAS/QC membrane at 430 nm is very low. During the pH ranges of 7-9, the leaching of CAS was reduced. Leaching of dyes occurred again when the pH increased to 11 and 12.

In the study of the pH effect on the performance of CAS loaded QC membrane with Cu^{2+} in solution, the response to copper ion is highly pH dependent because the signal is related to the ratio of the activities of copper ion and the protons.[4] The pH dependence of the sensors was determined by contacting the sensor strips with Cu^{2+} at different pH values. The effects of pH on the complexation of Cu^{2+} with CAS/QC-4 membrane are shown in **Figure 4.13.** It was found that in weak acidic buffer solution (pH < 7); the absorbance value response to 40 mg/L of Cu^{2+} was very low. At pH 7-9 buffer solution, membranes were highly sensitive to Cu^{2+}. Interestingly, when the pH is > 9, the absorbance decreases again dramatically, this accompanies the leaching of CAS from the QC membranes. This is because the electrostatic interaction of CAS with the cationic membrane can be destroyed

164

under the basic condition. Therefore, the pH 8 buffer solution was used for the preparation of metal ions solutions.
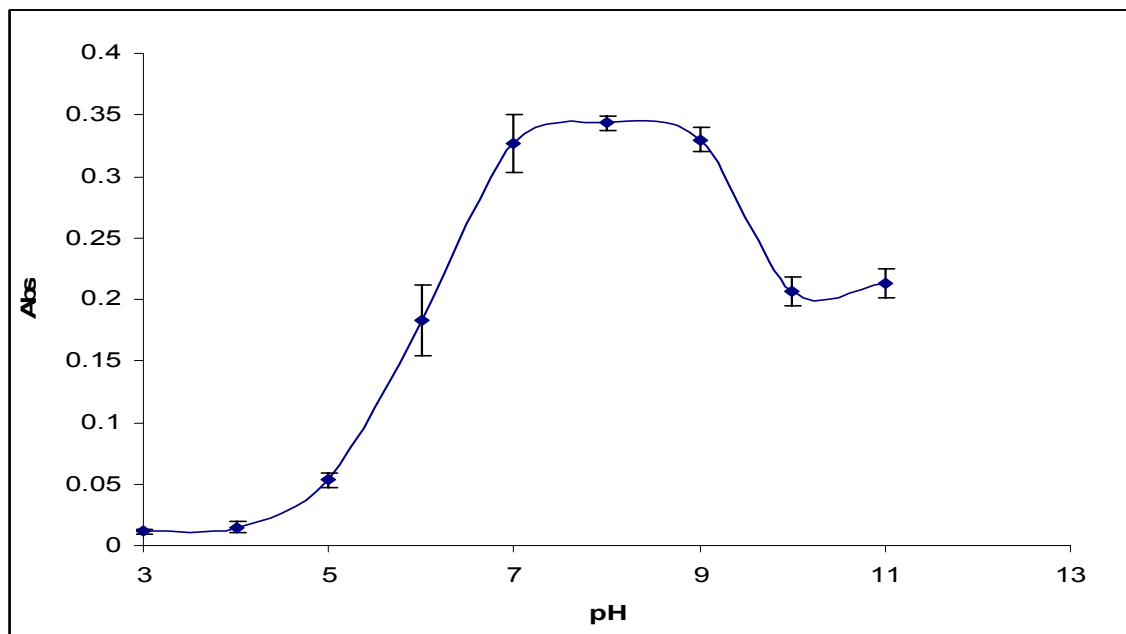
Figure 4.13 Effects of pH on binding of dyes with cellulose membranes. The absorbance was measured at 620 nm in the Cu^{2+} ions solution with a concentration of 40 mg/L.

An aqueous solution of CAS is yellow and its colour changes with pH as a result of proton dissociation, as described by the following **Table 4.5**:

Table 4.5 The Forms and Colours of CAS in different pH solution.

Forms	H_4L	H_3L^-	H_2L^{2-}	HL^{3-}
pK	$pK_1=1$	$pK_2=2.3$	$pK_3=4.9$	$pK_4=11.5$
Colour	Orange	red	yellow	blue

Under pH 8 solution, the CAS-QC-4 membrane exhibits a red-yellow colour, therefore, CAS should be in its HL^{3-} and H_2L^{2-} combination form.[7] On the exposure to Cu^{2+} ions pH 9 buffer solution, the membrane changes the colour from yellow, λmax = 430 nm, to violet-blue colour, λmax =620 nm, i.e. the concentration of the yellow form of indicator $[HL-QC]^{3-}$ decreases while the concentration of the blue complexes $[CuHL-QC]^-$ increases.

165

The extraction of Cu^{2+} ions into the membrane phase is coupled with the release of protons from the membrane into the solution, as described by **Eq. 4.1**

$$Cu^{2+} （aq） + [HL-QC]^{3-} (org) \rightarrow [CuHL-QC]^{-} (org) + 2H^{+} \qquad \textbf{(Eq. 4.1)}$$
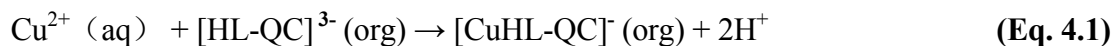
4.3.7 Calibration Curve

The dynamic linear range (DLR) can be defined as a detector's response increasing proportionally with increased quantity of detected material. The lowest concentration of the linear dynamic range is the minimum detectable concentration or the detector sensitivity. The largest concentration is that where the response factor (r) falls outside the range specified. The working range of the sensor has been tested with Cu^{2+} solutions over a wide range of 0-60 ppm. The sensor strips were immersed into different Cu^{2+} solutions with concentration intervals at 10 ppm and the absorption spectrum were collected. The working range plot is shown in **Figure 4.14 (a).** As it is shown in **Figure 4.11 (a)**, the absorption spectrum at Cu^{2+} concentration at 0, 10 and 50 ppm are selected and discussed. When the concentration of Cu^{2+} reached 50 ppm, the absorption at wavelength 620 nm reaches the maximum point; there is no further increase of the absorbance intensity by increasing the concentration of Cu^{2+}, such as 55 ppm and 60 ppm.
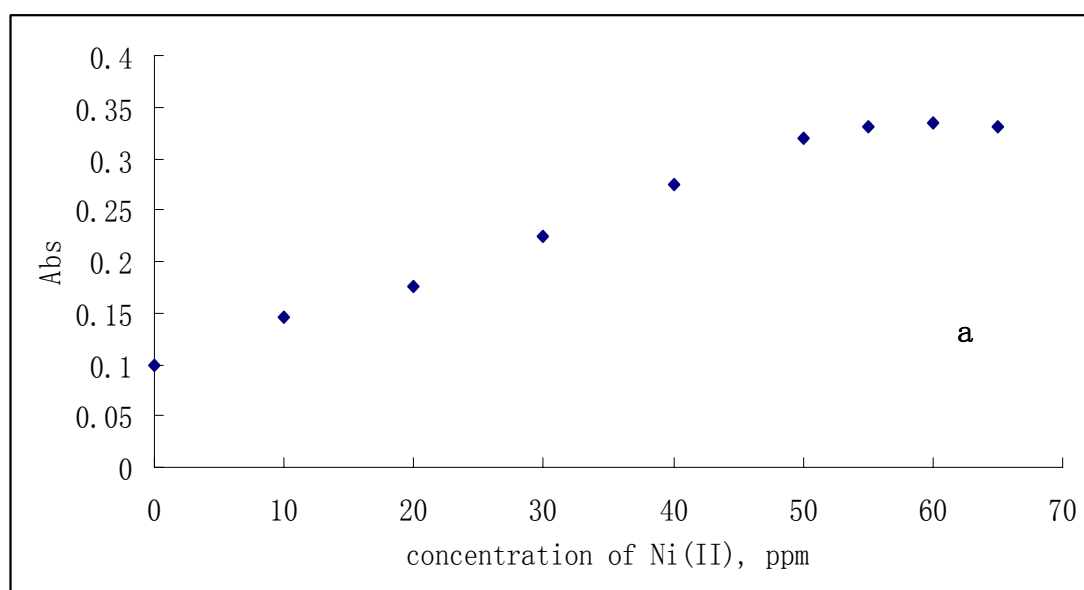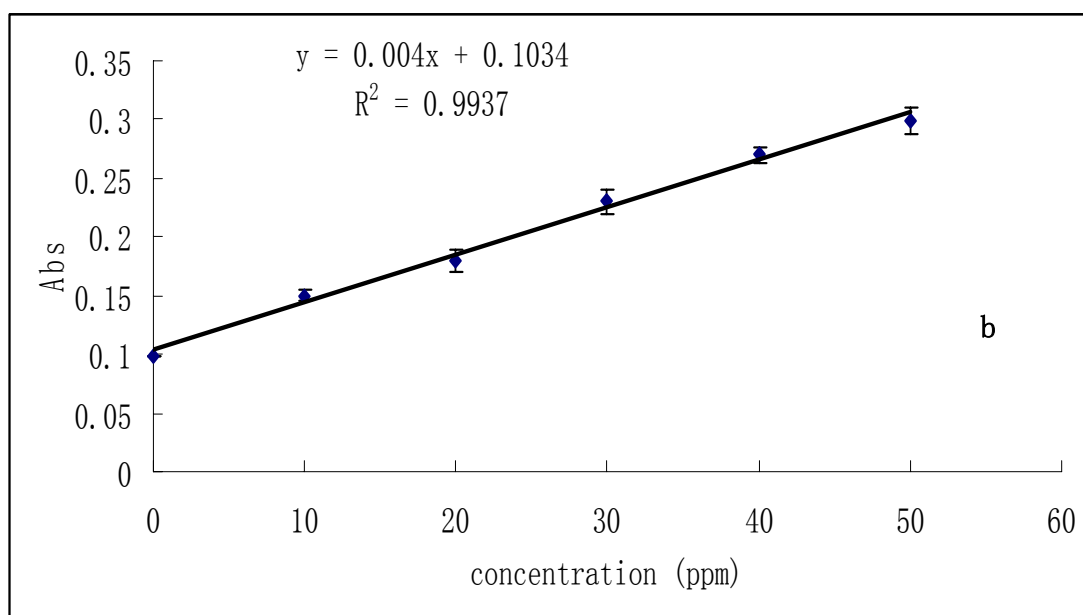
Figure 4.15 Working range (a) and linear working range (b) of CAS/QC-membranes over Cu^{2+} solutions. Calibration curve for the CAS/QC-4 membranes reacted with 0-50 ppm Cu^{2+} at pH 8 when a new membrane was used for each calibration point. n=3, error bars shown based on %RSD of 3 measurements.   y=0.004x +0.1034

The working range of the sensor is plotted by using the absorption value of the sensor strips at wavelength 620 nm vs the concentration of Cu^{2+} (range from 0-65 ppm). There is a linear range obtained from 6.6-50 ppm from the working range plot. The CAS/QC membranes obtained can be used for quantitative determination of copper ions. The response of the sensing phase to Cu^{2+} was calibrated in order to ensure the sensing membrane had a linear dynamic range that permitted the determination of expected copper concentrations in the environmental samples. The CAS/QC membranes were dipped in solutions containing different concentrations of Cu^{2+} ions at pH 8. The calibration curve is shown in **Figure 4.14 (b)**.

The non-zero intercept is due to the blank i.e. no-dye QC membrane in the reference cell with the exposed dyed QC membrane in the sample cell. The linear dynamic range was determined to range from 6.6-50 mg/L

The response time is within 5 min even for the solutions with low concentration of copper ions. **Figure 4.14** shows a good calibration graph, since the error bar is small. The

167

preparation of the membrane is simple and low cost, and the reproducibility is very good (as can be seen from **Figure 4.14 (b)**), therefore, for each measurement, a new sensing membrane was used. In analytical chemistry, the lower limit of detection (LOD) is the lowest quality of a substance that can be distinguished from the absence of that substance (a blank value) within a stated confidence limit (95%). By using the same statistical method as illustrated in **Equation 3.1**, the lower detection limit is 6.6 ppm（$\sigma=0.01$）and the upper limit linear point is 50 ppm (within 95% confidence).

4.3.8 Response Time

As it has been discussed in Chapter 3, the response time can be affected by many factors like the film thickness, the concentration of the Cu^{2+} solution etc. In this study, the thickness of the membrane remained the same. It was found from the experience that the metal ion diffuses quicker into the sensing membrane from the higher concentrated metal ions solution than from the lower concentration of metal ions solution. **Figure 4.15** shows the response time of the sensing membranes in different concentrations of Cu^{2+} (ranges from 10-50ppm). It was found that the sensing membrane reached the maximum absorbance in 50 ppm solution in ~1 min, while it reached the maximum absorbance in 10 ppm solution in ~5 min. In order to make sure the sensing membrane can be saturated in any concentration, the 10 ppm solution was used to measure the response time. According to the definition of response time, the response time is 5 min for achieving the full saturation of the membrane in different concentrations of Cu^{2+}.
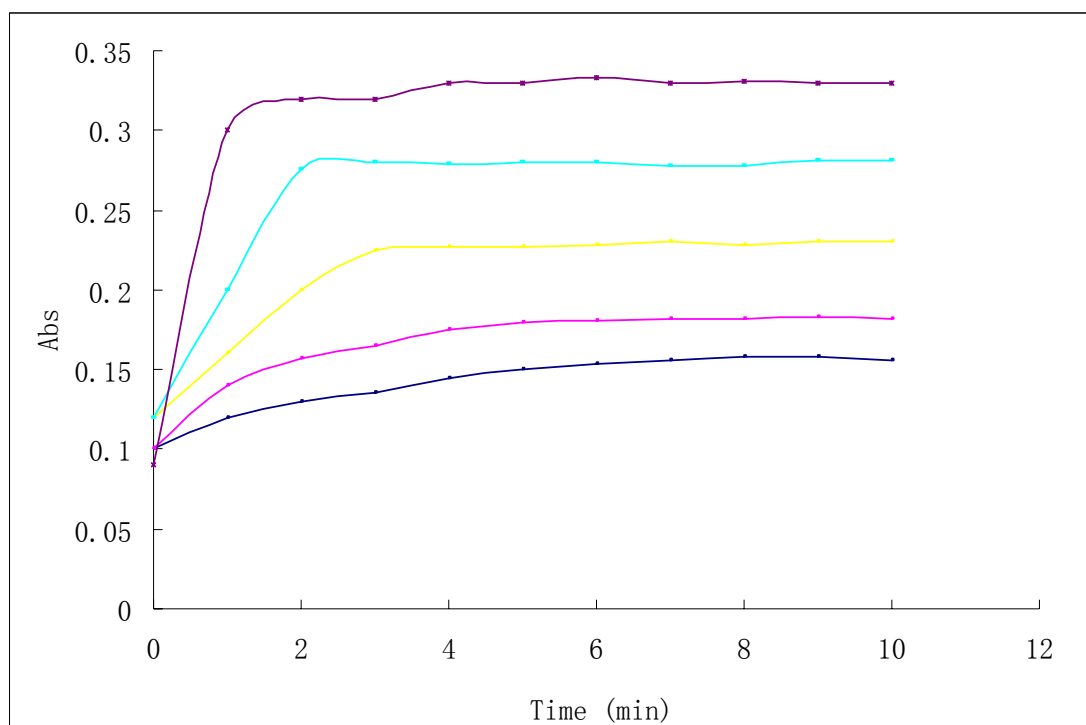
Figure 4.15 Plots of time-dependence absorption of the sensing membrane over 10 min in the presence of different concentration of Cu^{2+} solution. The concentration of Cu^{2+}: — 10 ppm; — 20 ppm; — 30 ppm; — 40 ppm; — 50 ppm.

Conclusions

In this work, cationic derivatives of cellulose were heterogeneously synthesised and applied to immobilise a series of water-soluble indicators. To the author's best knowledge, this is the first time that water-soluble ligands have been immobilised onto cellulose membrane with electrostatic binding. Through this interaction, the water-soluble indicator CAS, Nitroso-PASP, CAL and AVN are embedded onto cationic cellulose and the leaching of these indicators from the membrane has been overcome. This technique has provided a new way to immobilise water soluble chelators onto cellulose, which can be applied to metal ion sensing, separation and pre-concentration processes. Since cellulose is a biodegradable, nontoxic and abundant raw material, therefore, the starting materials are environmentally friendly. The fabrication of the cationic cellulose used a "green" synthesis approach by using NaOH/urea as solvent and the byproducts can be recycled.

The CAS/QC membrane was used as a test strip for the determination of copper ions in aqueous solution. The working conditions have been optimised. No response at the working wavelength was observed from other potential heavy metal interferences. The membrane responds to copper by changing colour irreversibly from yellow to violet-blue (λmax = 620 nm). The test strips are sensitive to Cu^{2+} in the 6.6-50 ppm range for an exposure time of 5 min. The membranes are also sensitive to pH. The determination of Cu^{2+} must be performed in buffer solution, ideally at pH 8. The developed CAS/QC membranes are transparent and bendable; thus the membranes are suitable for use with commercially available miniaturised optical devices.

Copper is one of the important heavy metal ions that must be monitored in many aqueous environments. The raw materials used in the preparation of this sensor strip are low cost, renewable and simple to prepare. Therefore this one-shot sensing strip has a large potential market for on-line portable environmental monitoring, e.g. for organic and inorganic pollutants in aqueous environments.

Reference

1. A. A. Ensafi and M. Fouladgar, *Sens. Actuators B: Chem.,* 2006, **113**, 88-93.

2. T. Mayr, D. Wencel and T. Werner, *Fresenius' J. Anal. Chem*, 2001, **371**, 44-48.

3. I. Oehme and O. S. Wolfbeis, *Microchim. Acta*, 1997, **126**, 177-192.

4. H. Xi-Wen and D. P. Poe, *Anal. Chim. Acta*, 1981, **131**, 195-203.

5. V. Amelin and A. Tret'yakov, *J. Anal. Chem.*, 2006, **61**, 396-401.

6. V. G. Amelin and I. S. Kolodkin, *J. Anal. Chem.*, 2001, **56**, 182-187.

7. V. Amelin and O. Gan'kova, *J. Anal. Chem.*, 2007, **62**, 285-290.

8. V. G. Amelin and O. B. Chernova, *J. Anal. Chem.*, 2008, **63**, 799-804.

9. N. A. Carrington and Z.-L. Xue, *Acc. Chem. Res.*, 2007, **40**, 343-350.

10. José V. Ros-Lis, R. Casasús, M. Comes, C. Coll, M. D. Marcos, R. Martínez-Máñez, F. Sancenón, J. Soto, P. Amorós, Jamal E. Haskouri, N. Garró and K. Rurack, *Chem. Eur. J.* 2008, **14**, 8267-8278.

11. L. R. Allain, K. Sorasaenee and Z. Xue, *Anal. Chem.*, 1997, **69**, 3076-3080.

12. I. Oehme, S. Prattes, O. S. Wolfbeis and G. J. Mohr, *Talanta*, 1998, **47**, 595-604.

13. M. Shamsipur, J. Tashkhourian and H. Sharghi, *Anal. Bioanal. Chem.*, 2005, **382**, 1159-1162.

14. I. M. Steinberg, A. Lobnik and O. S. Wolfbeis, *Sens. Actuators B: Chem.*, 2003, **90**, 230-235.

15. A. Flamini and A. Panusa, *Sens. Actuators B: Chem.*, 1997, **42**, 39-46.

16. Y. Kalyan, A. K. Pandey, P. R. Bhagat, R. Acharya, V. Natarajan, G. R. K. Naidu and A. V. R. Reddy, *J. Haz. Mater.*, 2009, **166**, 377-382.

17. M. Plaschke, R. Czolk and H. J. Ache, *Anal. Chim. Acta*, 1995, **304**, 107-113.

18. D. Radloff, C. Matern, M. Plaschke, D. Simon, J. Reichert and H. J. Ache, *Sens. Actuators B: Chem.*, 1996, **35**, 207-211.

19. W. H. Chan, R. H. Yang and K. M. Wang, *Anal. Chim. Acta*, 2001, **444**, 261-269.

20. X.B. Zhang, C.H. Guo, Z.Z. Li, G. L. Shen and R. Q. Yu, *Anal. Chem*, 2000, **74** 821–825.

21. A. A. Ensafi and M. Fouladgar, *Sens. J. IEEE*, 2008, **8**, 347-353.

22. I. Oehme, B. Prokes, I. Murkovic, T. Werner, I. Klimant and O. S. Wolfbeis, *Fresenius' J. Anal. Chem.*, 1994, **350**, 563-567.

23. K. Macek and L. Moravek, *Nature*, 1956, **178**, 102-103.

24.   A. Safavi and M. Bagheri, *Anal. Chim. Acta*, 2005, **530**, 55-60.

25.   S. Sadeghi and S. Doosti, *Dyes   Pigments*, 2009, **80**, 125-129.

26.   T. Balaji, M. Sasidharan and H. Matsunaga, *The Analyst*, 2005, **130**, 1162-1167.

27.   C. Chang, J. Peng, L. Zhang and D.-W. Pang, *J. Mater. Chem.*, 2009, **19**, 7771-7776.

28.   J. Liesiene, *Cellulose*, 2010, **17**, 167-172.

29.   Y. Lu, W. Shi, L. Jiang, J. Qin and B. Lin, *Electrophoresis*, 2009, **30**, 1497-1500.

30.   X. Li, J. Tian and W. Shen, *Cellulose*.

31.   N. M. L. Hansen and D. Plackett, *Biomacromolecules*, 2008, **9**, 1493-1505.

32.   R. Rodriguez, C. Alvarez-Lorenzo and A. Concheiro, *Biomacromolecules*, 2001, **2**, 886-893.

33.   Q. Yang, A. Lue, H. Qi, Y. Sun, X. Zhang and L. Zhang, *Macromole. Biosci.*, 2009, **9**, 849-856.

34.   J. H. Poplin, R. P. Swatloski, J. D. Holbrey, S. K. Spear, A. Metlen, M. Gratzel, M. K. Nazeeruddin and R. D. Rogers, *Chem. Commun.*, 2007, 2025-2027.

35.   G. Larin, V. Ostrovskaya, G. Zvereva, D. Man'shev, A. Tsygankov and V. Minin, *Russian J. Coord. Chem.*, 2006, **32**, 33-38.

36.   V. M. Ostrovskaya, *Fresenius' J. Anal. Chem.*, 1998, **361**, 303-305.

37.   J. A. Hestekin, L. G. Bachas and D. Bhattacharyya, *Ind. Eng. Chem. Res.*, 2001, **40**, 2668-2678.

38.   I. S. Chronakis and P. Alexandridis, *Macromolecules*, 2001, **34**, 5005-5018.

39.   V. Egorov, S. Smirnova, A. Formanovsky, I. Pletnev and Y. Zolotov, *Anal. Bioanal. Chem.*, 2007, **387**, 2263-2269.

40.   H. Qi, C. Chang and L. Zhang, *Green Chemistry*, 2009, **11**, 177-184.

41.   S. Zhu, Y. Wu, Q. Chen, Z. Yu, C. Wang, S. Jin, Y. Ding and G. Wu, *Green Chemistry*, 2006, **8**, 325-327.

42.   J. Cai and L. Zhang, *Macromole. Biosci.*, 2005, **5**, 539-548.

43.   Y. Song, Y. Sun, X. Zhang, J. Zhou and L. Zhang, *Biomacromole.*, 2008, **9**, 2259-2264.

44.   D. Li and A. W. Neumann, *J. Colloid Interface Sci.*, 1992, **148**, 190-200.

45.   E. Loubaki, M. Ourevitch and S. Sicsic, *Eur. Polymer J.l*, 1991, **27**, 311-317.

46.   M. Ka, ccaron, uráková, A. Ebringerová, J. Hirsch and Z. Hromádková, *J. Sci. Food. Agri.*, 1994, **66**, 423-427.

47.   S. Pal, D. Mal and R. P. Singh, *Carbohydrate Polymers*, 2005, **59**, 417-423.

48. K.L. Cheng, K. Ueno and T. Imamura, *Handbook of Organic Analytical Reagents*, CRC Press, Boca Raton, 1982.

49. M. Malát, *Anal. Chim. Acta.*, 1961, **25**, 289-291.

Chapter 5

5.1 Introduction

In the previous chapters, the highly sensitive sensing membranes for heavy metal ions based on commercially available indicators incorporated with different solid supports have been described. They have obtained high sensitivities over heavy metal ions and provided wide linear ranges towards heavy metal ions in aqueous solutions. However these indicator-based optical sensors lack selectivity towards only one specific metal ion. Masking agents are normally required in the sensing process.

Therefore, the challenge is to find the probe molecules which can allow selectivity for detecting particular target ions. Optode membranes containing separate ionophores and proton-exchanging dyes are commonly used for optical sensing of heavy metal ions.[1] The working scheme of this sensing mechanism is described in chapter 1. These systems were pioneered by Charlton and co-workers[2] and further developed in the group of Simon[3, 4] The extraction of metal ions into the membrane by an ionophore leads to the deprotonation of a lipophilised pH indicator resulting in a change in absorption or fluorescence.[1, 5] Metal ion recognition *via* artificial receptors is one of the challenging areas of current research in terms of the field of non-covalent chemistry due to its wide application in chemical, biological and environmental assays. Because of simple instrumentation, high sensitivity and easier synthesis, many efficient chromogenic/fluorescent sensors for transition-metal ions have been developed during the last two decades. In the last 30 years, numerous ionophores for different metal ions have been reported.[6-9] Investigations on metal ionic recognition by calixarenes and their derivatives as synthetic receptors have attracted increasing attention in recent years because of their potential to serve as molecular devices and functional materials.[10-12] One system of current interest is the use of chromogenic calix[4]arene derivatives as selective optical sensing materials for heavy metal ions.[13]

In this work, a new generation of double-armed spirocyclic calix[4]arene compounds have been designed and synthesized. They have been investigated as ionophores which are capable of selectively binding with target heavy metal ions both in liquid phase and on plasticised PVC membranes.

5.1.1 Metal Ions Recognition Process Based upon Calixarenes Derivatives

Gutsche first published the one-pot synthesis of calix[4]arene-based macrocycles.[14] Since then calixarenes and their derivatives, which appeared after the crown ethers and cyclodextrins, have been used as the third generation of outstanding supramolecules for metal ion recognition.[7, 8, 15] They are described as "molecular baskets" with a defined upper and lower rim and a central annulus (**Figure 5.1**) which enable them to possess high selectivity and form inclusion complexes with many specific metal ions.[14]
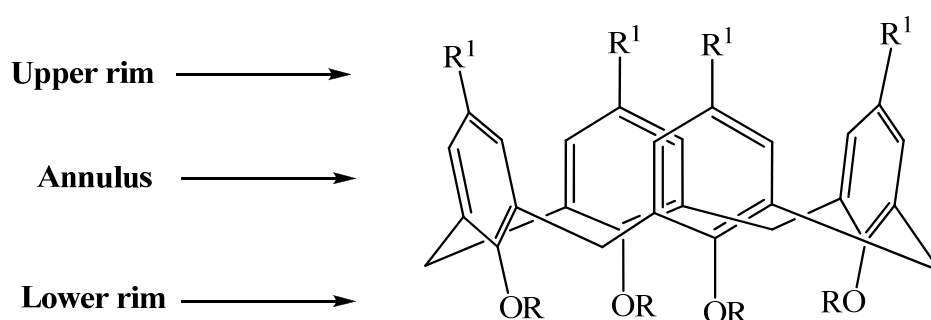

Figure 5.1 Calix[4]arene with three distinct regions.

It has been reported that three factors are influential for the recognition of calix[4]arene with the target ions, i.e. the cavity sizes, the nature of the substituent groups and the conformations of the calix[4]arene derivatives.[16-18]

Parent calixarenes often display poor solubility properties, poor binding and transport abilities with metal ions in neutral media.[14] Recently, chemical sensors are normally based on probe molecules with suitable substituents for binding; thus the guest molecules can be detected and measured. Therefore, research in the area of calixarenes for metal ion recognition has been focused on their derivatisation by the modification of calixarenes.[19, 20] The calixarene framework has two distinct sites where derivatisation can occur, namely the *lower rim* phenolic oxygens and the *upper rim para*-position. Diamond and McKervey have investigated the chromogenic response for lithium by calix[4]arene tetraesters bearing nitrophenol residues and showed the concentration dependence of the selective chromoionophore for Li^+.[21, 22] Rouis et al. reported a di- and tri-β-cétoimine calix[4]arene-based receptor designed for the optical detection of Cu^{2+} and Eu^{3+} metal ions

in solution.[20] Bitter et a*l*. studied the complex forming behavior and selectivity of a calix[4]arene derivative with alkali and alkali earth ions.[23] Lu et al. reported a lead ion-selective ionophore based on a calixarene carboxypenyl azo derivative.[24]

Since Diamond reported calixarenes as the ionophore for ions, i.e. Na^+-ISE, a number of calixarenes derivatives containing pendant ether, amide, ketonic, ester and crown ether groups have been incorporated as neutral ionophores for the recognition of metal ions for alkali and akaline earth metal ions.[1, 21,25] There is limited literature reported in terms of calixarene derivatives used for soft heavy metal ions such as silver, copper, lead etc.[26] The soft heavy metal ions Ag^+, Pb^{2+}, Tl^+ and Hg^{2+} display great affinity for soft coordination centres, i.e. nitrogen, sulphur, selenium and phosphine atoms.[27] It is expected that calixarene derivatives with functional groups containing these soft coordination centres improve the selectivity towards soft metal ions against alkali metal ions significantly. Taking this into consideration, in recent years, a number of calixarene derivatives containing S, Se, N, P, such as thioether, thiaamyloxy, arythiaalkoxy, pyridyl, benzothiazoyl groups have been synthesised and tested as ionophores for heavy metal ions in sensors.[28-30]

Parent calix[4]arene compounds have four rigid confirmations, that are shown in **Figure 5.2 (a, b, c and d)**. However, these host systems tend to respond to total guest molecules rather than a single molecule. This is due to the flexibility of the host molecules. Therefore, it is very important to constrain the calix[4]arene compounds with the suitable cavity size and confirmations by using suitable pendant substituents. It has been reported that the modification of the lower rim has the added effect of locking the calixarene into one conformation.[31, 32]

177

Cone

Partial Cone

1,3-alternate

1,2-alternate
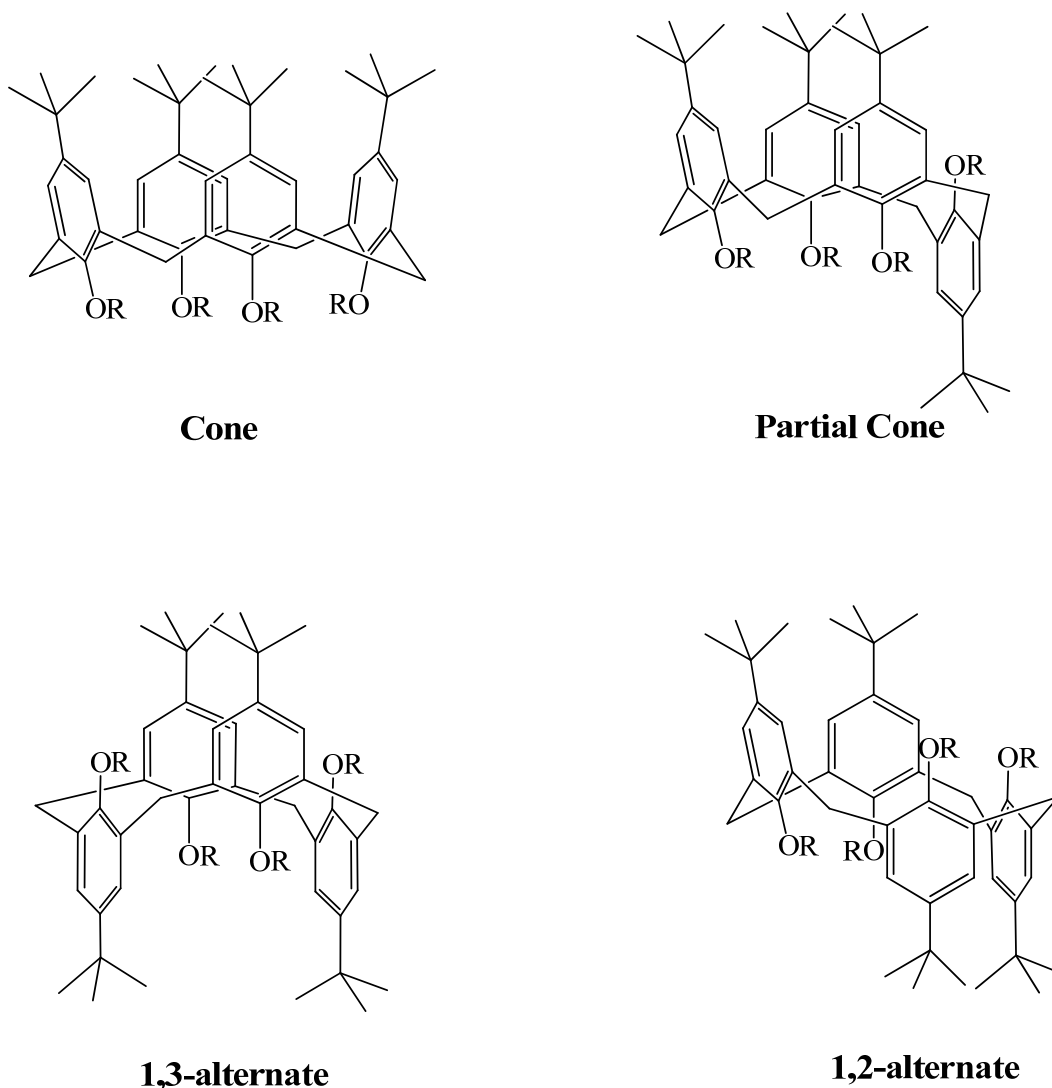
Figure 5.2 Conformational isomers of *p-tert*-butyl-calix[4]arene.

5.1.2 Spirocyclic Calix[4]arene Compounds

A nitrogen-containing ligand is one of the popular soft coordination centres containing substituents that have been widely incorporated with calixarene derivatives.[28] However, these N-containing ligands have many different possible conformations for complexing to the target metal ions or neutral molecules.[33, 34] By constraining the ligating groups in a ring system or within a larger macromolecular structure, the conformational freedom should be reduced and then the ligating groups should then bind more selectively to the guest molecule.[35] The presence of the ring forces the molecule to adapt a particular conformation, which, in turn forces the nitrogen to point in a fixed direction. Directionality is very

important in selective complexation of the target ions/neutral molecules in chemical sensors; it also improves performance.[34, 35]

Taking this advantage into consideration, in recent years the spirocyclane has been used as the substituent for the modification of calixarenes.[30, 36] The name "spirocyclane" was introduced by Baeyer in 1900 to describe hydrocarbons of a bi-cyclic nature.[37] Spirocyclic systems are composed of two or more ring structures fused together by a "spiro" atom—frequently a quaternary carbon **(Figure 5.3).**
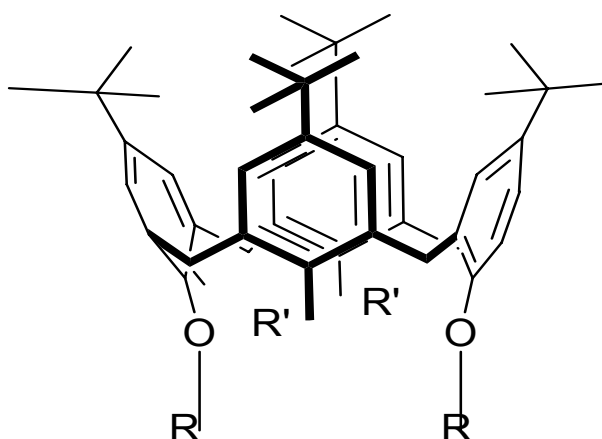

Figure 5.3 General structure of a Spirocycle

Spirocycles have been used to constrain the conformation of flexible molecules, in particular peptides, leading to an improvement in their chemical and biological properties.[32] This highly-organised and rigid unit represents an important structural feature in many natural products and biologically active compounds.[38] For example, L-Proline exhibits a remarkable constraint of configuration when incorporated into a calix[4]arene compound Proline spirocyclic systems are therefore extremely conformationally immobile. This feature was initially utilised by Ward et al. when they incorporated a spirocycle into a hexapeptide, which acts as an agonist of neurokin (NK) receptors. NK is found in the central nervous system and is classified into three groups; NK-1, NK-2 and NK-3. The human NK-1 receptor has been identified as a target in drug development for the potential treatments of several diseases, including migraine, Parkinson's disease and asthma.[38]
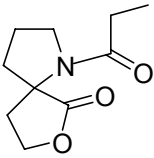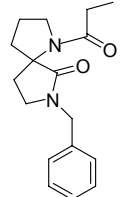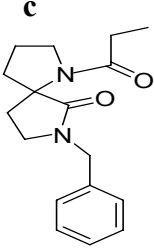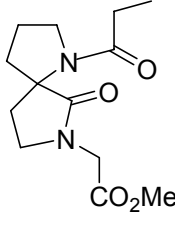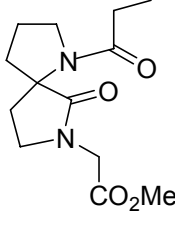
In this research, the host system was based on saturated spiro bicyclic N-containing heterocycles**.** The incorporation of an asymmetric (chiral) centre in the molecule leads to the possibility of stereoisomers. The stereochemistry was scrambled at the chiral centre (i.e. a racemic mixture of enantiomers was used) for the generation of the target spiro bicyclic compound, since it is not known which diastereoisomer would give the optimal product with the ligating groups best oriented for binding to a particular metal ion. It was proposed

to separate the enantiomers at the final stage, leading then to the generation of two new spirocycles that could be investigated for preferential binding to one enantiomer of a neutral guest. The inclusion of a chromaphoric moiety at lower rim renders a potentially large number of novel spiro calixarene based host compounds which may find applications as optical sensors. The structures of the newly synthesized calix[4]arene compounds are shown in **Table 5.1.** The synthesis of the spirocyclic calix[4]arene compounds was carried out by researchers in ITT (contact Dr. Mary Deasy at the address detailed in the experimental section for information).

Table 5.1 Proposed structure of spirocyclic calix[4]arenes derivatives.

	Calixarene compounds	Function group R, R'	
2-144	a	R'	OH
3-201		R'	OMe
2-145	b	R'	OH

3-204	R	R'	OMe
3-176	R **c**	R'	OH
3-203	R	R'	OMe
3-175	R **d**	R'	OH
3-202	R	R'	OMe

In the first step, a Picrate-acid-extraction method was used for the investigation of the binding properties of these newly synthesised spirocylic calix[4]arene derivatives. It is a useful method for studying the binding ability of macrocyclic molecules with metal ions. Furthermore, complexation was determined by UV-Vis spectrometry by noting the changes in the λ_{max} of the compounds after addition of the metal salts. The results were compared to those obtained with other closely related spirocyclic calix[4]arene derivatives, and discussed in terms of substituent, cavity size and conformational effects of the macrocycles. Finally, an attempt was made to disperse the promising spirocyclic calix[4]arene into plasticised PVC membrane for determination of heavy metal ions.

5.1.3 Aims and Objectives

In order to improve the selectivity of the optical sensors for specific heavy metal ion determination, a series of ionophores based on double armed spirocyclic calix[4]arene compounds were designed and investigated. These compounds are based on amide and ester ligating groups on the lower rim. This work describes the complexation studies of metal ions with the newly synthesised spirocyclic calix[4]arene compounds by using Pederson's picrate-metal-extraction method. A general view of the binding properties of these compounds to a variety of metal ions, indicating which metal ion can bind to the corresponding spirocyclic calix[4]arene compounds is discussed.

The aim of this chapter is to find out the binding properties of the newly synthesised double-armed calix[4]arene compounds with heavy metal ions. Successful complexation could lead to the development of "smart materials" for molecular recognition and potential use in the sensor technology, especially the optical sensor for toxic heavy metal ions in the environmental solutions and also clinical applications in the future.

The objectives of this work are:

1. To investigate the binding properties of the novel double-armed calixarenes with heavy metal ions by using Pederson's extraction method;

2. Immobilise the promising spirocyclic calix[4]arene into plasticised PVC membrane for the determination of heavy metal ions.

5.2 Materials and Methods

5.2.1 Materials

Picrite Acid, ethanol HPLC grade and Dichloromethane (DCM) were purchased from Sigma-Aldrich, Co Chemicals, Tallaght, Dublin, Ireland, and used as received on analytical grade. The L-proline derived spirocycles and spirocyclic calix[4]arenes were synthesised by Dr. James Ward, Dr. Mary Deasy, and Dr. Fintan Kelleher from the Department of Science, Institute of Technology, Tallaght, Dublin. The synthesis procedures of these compounds were illustrated and detailed.[38] All other reagents used were analytical reagent grade unless otherwise stated.

Aqueous solutions were prepared from double-distilled water. Heavy metal ion stock solutions (0.01 M) were prepared by dissolving appropriate amounts of metal salts in 2% w/v HNO_3 or HCl solutions to prevent hydrolysis. The buffer solutions (pH: 1.0 – 11.0) were prepared as stated in chapter 2.3.3. A Model KW-4A spin coater (Germany) was used for the preparation of the PVC membranes.

Reagent-grade plasticiser tributyl phosphate (TBP), Poly-vinyl chloride (PVC), ion carrier potassium tertrakis chlorophenyl borate (KTClPB) and solvent tetrahydrofuran (THF) were purchased from Sigma-Aldrich Co chemical company Tallaght, Ireland.

5.2.2 Instruments

A Cary 50 UV-Vis spectrophotometer with a 1.0 cm quartz cell was used for absorbance studies. An EDT RE 357Tx digital pH-meter was used for pH adjustment. Stuart® reciprocating Shaker (SSL2) was used for extraction process. A Model KW-4A spin coater (Germany) was used for the preparation of the PVC membranes.

5.2.3 Procedures

2.5×10^{-3} M of each ligand was prepared in DCM. 2.5×10^{-3} M solutions of the nitrite salts of lithium, sodium, potassium, iron, cobalt, nickel, copper, lead and zinc were also prepared in DI water. An initial scan of each ligand was performed in the range of 780 - 200 nm by transferring 1 mL of ligand solution into a 10 mL volumetric flask and made up to the mark

using ethanol. The same parameters were then used after 1 mL equivalent of the metal salt solution were added to the solution of the ligand and made up to 10 mL using ethanol. The solutions were sonicated for 10 min and allowed to stand for 1 h before testing. The same solutions were tested again 24 h later with no differences in any spectra being observed. The compelxation of metal ions with ligands can be determined by one of two types of shifts. Hypsochromic shift results in a lower λ_{max}. Since the blue colour in the visible spectrum has a lower wavelength than other colours, this type of shift is often termed as a "blue shift". Bathochromic shift results in the change of spectral band position in absorption (the $\lambda_{max)}$ appearing at a longer wavelength and is often referred to as a "red shift".

5.2.4 Preparation of metal picrates

Pedersen's method involves the preparation of a dilute solution of the receptor or ionophores in a chlorinated solvent.[27] The solution was shaken with an aqueous metal picrate solution. The percentage extraction of the metal ion was measured, by UV-Vis, as a function of picrate ion (transported as the counter-ion) concentration in the organic phase. It must be independently established so that no extraction occurred in the absence of the receptor and that the receptor was insoluble in water. **Figure 5.4** shows a schematic diagram of the two phases, before and after extraction.
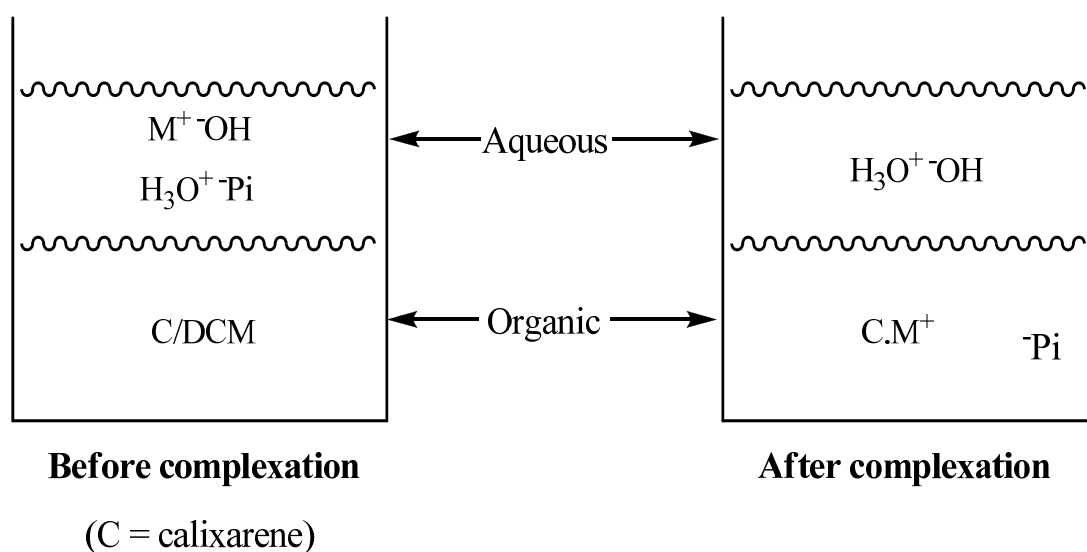

Before complexation   **After complexation**

(C = calixarene)

Figure 5.4 Schematic diagram of Pedersen's picrate extraction method.

Picrate-extraction experiments were performed following Pedersen's procedure.[27] All inorganic compounds were reagent grade, and all solvents and available organic materials were commercial products and were used without purification. The extraction experiments were processed by the following steps:

i.   Preparation of the picric acid stock solution. A 2.5×10^{-3} M solution of picric acid was prepared by dissolving 57.2 mg of picric acid in 1L of DI water.

ii.   The metal stocks were prepared at a concentration of 2.5×10^{-3} M.

iii. Preparation of the calix[4]arene compounds solutions: Appropriate amounts (calculation is shown in Appendix III) of the calix[4]arene compounds were dissolved in DCM solvent and made up to 100 mL. The final concentration of calix[4]arene compounds was 2.5×10^{-3} M ($C_{calix.}$).

iv.   Preparation of the metal-picrate solutions at the concentration of 2.5×10^{-4} M: (C_{p-m}). These metal-picrate solutions were prepared by the stepwise addition of 10 ml of 2.5×10^{-3} M metal ions stock solution to 10 mL of 2.5×10^{-3} M picric acid solution. The mixture was made up to 100 mL with DI water and shaken at $25\,^{\circ}$C for 1 h.

v.   The Pedersen's extraction procedure: Mixed 10 mL of metal-picrate solution ($C_{p-m} = 2.5 \times 10^{-4}$ M) and 10 mL of calix[4]arene ligand solution ($C_{calix.} = 2.5 \times 10^{-3}$ M) in plastic tubes, a few drops of 0.01 M KOH/HCl solution were added in order to obtain the desired pH at equilibrium. The mixtures were shaken vigorously in a mechanical water bath for 3 h and left standing for an additional hour. The water bath temperature was kept at $25\,^{\circ}$C.

vi.   The concentration of the picrate metal ions remaining in the aqueous phase was then determined spectrophotometrically at 355 nm.

vii. Blank experiments showed that no picrate-metal extraction occurred in the absence of calix[4]arene.

5.2.5 Extraction Ability Measurement

Picrate-extraction studies were carried out and the % extraction values of various metal ions were calculated using the following **Eq. 5.1**:

$$\% E = 100 \times \frac{(A_1 - A)}{A_o} \qquad \textbf{(Eq.5.1)}$$

Where $(A)_o$ is the absorbance of the initial metal-picrate solution at a concentration of 2.5 x 10^{-4} M, (A) is the absorbance of the picrate salt in the aqueous layer after extraction and $(A)_1$ is the absorbance yielded from the blank experiments which were run under the same condition but without putting any ligand into the metal-picrate solution. The calibration curves for each of the metal-picrates were drawn according to data collected from standard solutions of metal-picrates. The coefficient of determination (R^2 value) for each calibration curve was > 99 % and these records were used to calculate the percentage extraction of metal-picrates into the organic layer.

5.2.6 Preparation of sensing membranes

The general procedure for the preparation of the polymetric membrane was as adapted from the literature.[26, 39] Mixtures for the preparation of sensing membranes were made from a batch containing ionophore (2-144 compound), chromoionophore (Nile Blue) and lipophilic salt potassium tetrakis(*p*-chlorophenyl) borate (KTpClPB) in 1:1:1 molar ratio (2.2 x 10^{-3} mmol each), next to 64 mg of plasticizer (TBP) and 35 mg of PVC was added to complete the 100 wt %, all dissolved in 1mL of freshly distilled THF (3 mL). The membranes were cast by placing 0.2 mL of the cocktail on 0.7 cm x 50 mm square glass sheet using spin-coater and dried slowly in a dryer with a saturated THF atmosphere at room temperature. The membranes were produced on a glass substrate using a spin-coating technique. In this way, a membrane of approximately 0.1 mm thickness was coated on the plate,[40] and it was allowed to stand in ambient air before use. The compositions of the membranes 1-5 are illustrated in **Table 5.2**.

Table 5.2 Composition of the prepared plasticised PVC membranes 1-5.

Membrane ID	Chromophore (Nile Blue)	Ionophore (ligand 2-144)	Lipophilic Salt (KTpClPB)
1	0.8	2.2	6.1
2	1.6	4.1	6.2
3	2.4	4.3	6.1
4	3	4.1	6.5
5	3.6	4.0	6.2

Note: the unit for all the compositions for the preparation of membrane is mg.

5.3 Results and Discussion

The synthesis of the spirocyclic calix[4]arene compounds was carried out by researchers in ITT (contact Dr. Mary Deasy at the address detailed in the experimental section for information). These compounds are in an attempt to increase the selectivity of the calix[4]arene compound and expand its application for the development of sensors for heavy metal ions. Eight of the synthesised spirocyclic calix[4]arene compounds (**Table 5.1**) were investigated for their metal-binding capability. These compounds were tested against the divalent transition heavy metal ions picrates and alkaline metal ion picrates. Any selective reactions (good binding ability between spirocyclic ligand and metal ion) those are found by Pedersen's extraction experiments could therefore have the potential to be applied to the development of sensors for metal ions and also they would have a large potential for separation techniques. The spirocyclic calix[4]arene compounds are divided into four types. The first type which includes 2-144 and 3-201 that derives from calixarenes by the replacement of the H atoms from two phenolic –OH by groups (a); the second type which includes 2-145 and 3-204 that derives from calixarenes by replacement of the H atoms from two phenonic –OH by groups (b); the third type which includes 3-176 and 3-203 that derives from calixarenes by replacement of the H atoms from two phenonic –OH by groups (c); and the last one includes 3-175 and 3-202 that derives from calixarenes by replacement of the H atoms from two phenonic –OH by groups (d). The difference between the two compounds in each type is the remaining two phenolic groups R' (-OH) are either replaced by -OCH$_3$- (OMe) or remain as -OH.

The metal-picrate extraction experiments were performed by using a host solution of calix[4]arene derivatives or the spirocyclic groups in dichloromethane (DCM) and picrate solution in deionised water according to the procedure described by Pedersen.[27,41] The absorption of the extracted picrate was measured from the aqueous layer at 355 nm and compared with the blank (with no calix[4]arene compound in DCM) of appropriate picrate. 1 h for shaking and 2 h for separation of the two phases was used as the required extraction time to yield equilibrium.[41] The calculation method is explained elsewhere for Pedersen's method as shown in **Equation 5.1** in **section 5.2.5** above. These extraction experiments were carried out under alkaline conditions by the addition of several drops of 0.01 M KOH solution. It was reported that a calixarene, carrying dimethylthioamide groups on its lower rim, binds a hydroxonium H$_3$O$^+$ ion in an equimolecular ratio and makes a

very stable complex.[42] The H_3O^+ ion is a competitor for metal ions during the extraction experiment. Therefore, it is very important to keep the extraction process under the alkaline condition.

5.3.1 Binding Ability and Selectivity with Different Metal-ions

The binding properties (expressed as a percentage of cation extracted, E%) of the spirocyclic attaching groups (a-d) and the spirocyclic calix[4]arene compounds towards alkali, alkaline earth, transition, and heavy metal ions were tested. The results are shown in **Table 5.2-5.5** in **Appendix III** and they can be summarised as follows:

i.   The spirocyclic calixarenes 3-201, 3-204, 3-202 and 3-203 showed good affinities with heavy metal ions, e.g. Pb^{2+}, Cd^{2+}, Zn^{2+}, Cu^{2+}, Ni^{2+} and Co^{2+}. For example, ligand 3-202 obtained a good binding ability towards Pb^{2+}, the E% value was 86.5% and 3-201 obtained the lowest E% value at 64% among these four ligands. Ligand 3-204 obtained the highest E% value towards Zn^{2+} at 90%, while the other three ligands, 3-201, 3-202 and 3-203 obtained E% values at 50%, 66% and 42%, respectively. 3-204 obtained a good binding ability with Cd^{2+} with the E% around 88%, while the E% values of other ligands were much lower. On the other hand, the spirocyclic calixarenes 3-201, 3-204, 3-203 and 3-203 showed low extraction efficiency towards alkaline earth and alkali metal ions.

ii. The spirocycle groups (a-d) obtained low binding ability with almost all metal ions. However, the spirocycle groups b and c showed good binding abilities towards Fe^{3+} ion with an E% values at 56% and 58%.

iii. The spirocyclic calixarene ligands 2-144, 3-175, 2-145 and 3-176 showed selective bindings with Pb^{2+} and Fe^{3+} ions. From the E% data in **Table 5.5 (2)**, it was observed that the spirocyclic calixarene compound 3-176 is a good extractant for Pb^{2+} and Fe^{3+} with the E% values being 75% and 82% respectively. However, spirocyclic calixarene compounds 2-144, 2-145, 3-175 and 3-176 showed lower extraction efficiency towards alkaline earth, alkali metal ions, and most of the heavy metal ions compared with Pb^{2+} and Fe^{3+}.

The difference in sensitivity and selectivity for metal ions between the extractant compounds with phenolic –OH groups (e.g. 2-144, 2-144, 3-175, 2-145 and 3-176) and the compounds with phenolic –OCH$_3$ groups (e.g. 3-201, 3-204, 3-202 and 3-203) could be affected by the spirocyclic attachments groups, the attaching phenolic -OH and -OCH$_3$ groups and also may be due to their resultant confirmation structures. In the following sections, these factors will be disused in detail. It should be stated here that the following discussion is based on the results obtained from the extraction experiments only and it would be greatly assisted by further experimental measurements, e.g. NMR, XRD, LC-MS, or molecular modelling information about the whereabouts of the metal ion with respect to the ligating groups in the complexes, and the form of the ligand (cone, patial cone, altermate) and the impact of ion-binding on these conformations (readily accessible via NMR). Further experimental measurements will be performed in future work.

5.3.2 Effect of the Spirocyclic Groups

There are two possible ion-binding sites of the calixarene ligands for metal ions: the cavity of the calixarene backbones; or the attaching groups on the parent calixarene compounds. In order to determine the binding site of these calixarene derivatives, the extraction studies of the spirocyclic groups were performed. Interestingly, the proline-derived spirolactom groups obtained a very low extraction percentage for metal ion picrates from the aqueous phase, especially for heavy metal ions. It was found that all the spirocyclic calix[4]arenes obtained binding affinities towards the metal ions tested in this work. For example, comparing the spirocyclic group (a) with compounds 2-144, it was found from **Figure 5.6** that the extraction % of spirocycle (a) for metal ions ranged from 1 % to 18 %, whereas, the extraction % of compound 2-144 for metal ions ranged from 5 % to 56.8 %. The difference in extraction % was large for Fe^{3+} and Pb^{2+}. The same trend was found with the comparison of spirocycles (b-d) with their corresponding spirocyclic calix[4]arene compounds in **Table 5.3-5.5.**
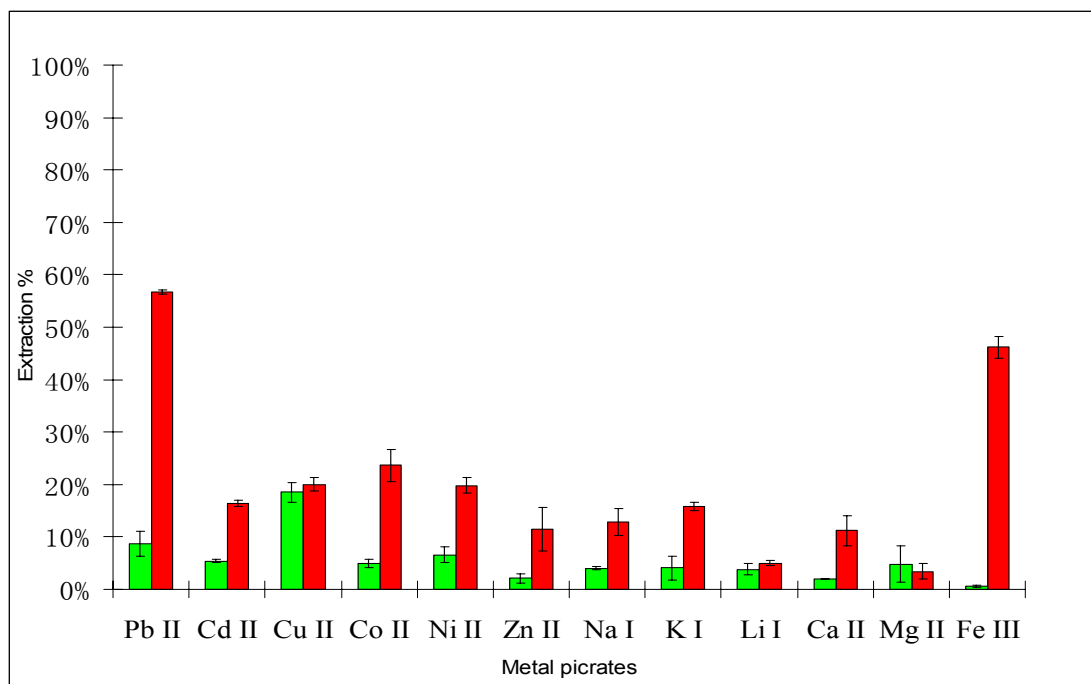
Figure 5.6 Bar profiles of E% of metal ions picrates with spicrocyclic calix[4]arene ligand and spirocyclic group a. ■ spirocyclic a; ■ spirocyclic calix[4]arene 2-144. (Error bars were calculated from the standard deviation, n=3).

For Pb^{2+}, the E % of spirocyclic (a) is 8.7 %, compared to 56.7 % and 65.8 % of compounds 2-144 and 3-201 respectively. This is shown in **Figure 5.7**. These results suggest that the spirocylic groups (a-d) have very weak binding affinities with those metal ions which were tested in this experiment. Therefore, the increase of the extraction efficiency for Pb^{2+} of the spirocyclic compounds 2-144, 2-145, 2-175, 3-176, 3-201, 3-204, 3-203 and 3-302 is probably not affected by the molecular reaction of the spirocyclic groups with Pb^{2+} ion. This inference could be assisted by further experimental measurements, e.g. NMR, XRD, LC-MS, or molecular modelling information.
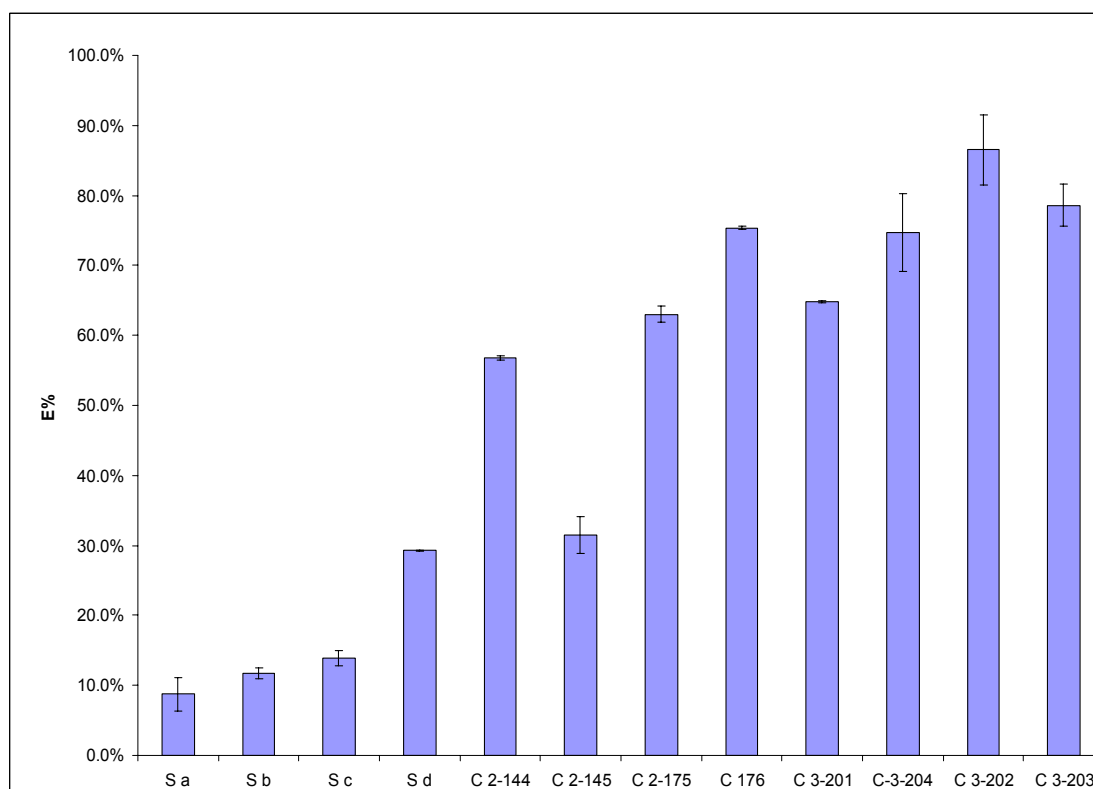
Figure 5.7 Extraction values of spirocyclic groups (a-d) spirocyclic calix[4]arenes against Pb^{2+} picrate. (Error bars were calculated from the standard deviation, n=3)

5.3.3 Effect of the Phenolic –OH and –OMe groups

Interestingly, it was found that the phenolic attaching groups, such as –OH and –OMe groups also play an important role on the extraction efficiency for metal ions. **Figure 5.8** summarises the difference of E% values of these spirocylic compounds for heavy metal ions. Comparing with compound 2-144 and 3-201—although both of them have the same spirocyclic group attached—the E% however, of 3-201 is higher than compound 2-144. For example, the E% of 2-144 for Pb^{2+} is 56.8 %, but it is 64.8 % of compound 3-201. A similar trend is observed for 2-145 and 3-204, 3-176 and 3-203, and also 3-175 and 3-202 for heavy metal ions. It was found that, the spirocyclic calix[4]arene compounds with two –CH$_3$ groups attached to the phenolic oxygen atoms, i.e., 3-201, 3-204, 3-203 and 3-202, are observed with low selectivity but higher sensitivity for heavy metal ions. It is shown in **Figure 5.8,** that compound 3-201 obtained a better selectivity for Pb^{2+}, Cd^{2+}, Cu^{2+}, Ni^{2+} and Zn^{2+} than its phenolic hydroxyl analogues.
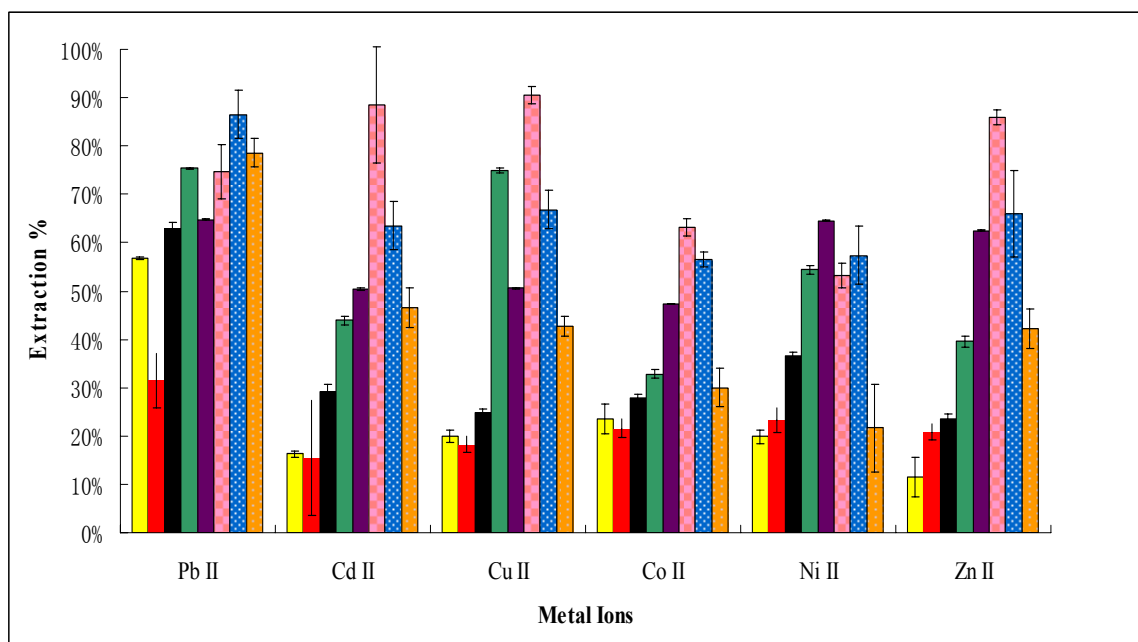
Figure 5.8 Bar profile of E% of spirocyclic calixa[4]renes compounds with heavy metal ions. ■ spirocyclic calix[4]arene 2-144; ■ spirocyclic calix[4]arene 2-145; ■ spirocyclic calix[4]arene 3-175; ■ spirocyclic calix[4]arene 3-176; ■ spirocyclic calix[4]arene 3-201; ■ spirocyclic calix[4]arene 3-204; ■ spirocyclic calix[4]arene 3-202; ■ spirocyclic calix[4]arene 3-203. (Error bars were calculated from the standard deviation, n=3).

These results indicate that the –OH substituent group at the lower rim of the calix[4]arene's backbone can affect the selectivity and sensitivity of the binding ability of spirocycle calix[4]arene compounds with heavy metal ions.[34] It also has been reported by Luding et al. that chelating groups increase the flexibility of the ligand and may reduce the overall selectivity.[25] The conformation of the compounds could also be influenced by the presence of an –OH group on the lower rim and possibly hydrogen bonding between ligand sites. The replacement of the -H from phenolic –OH by –CH$_3$ groups increase the flexibilities of these compounds, thus reducing their selectivity to heavy metal ions.[32] However, in the future work, NMR studies and molecular modelling studies are needed to confirm the hypothesis based on these results.

5.3.4 Effect of Spirocyclic Groups on the Selectivity of Calixarenes for Metal Ions

The selectivity of these extractants for metal ions is one of the important factors for improving performance of the ion recognition system. There are three main factors that may affect the extraction selectivity of these macromolecules, e.g. the cavity size, the conformation and the attaching groups on the parent calixarene compounds.[10, 43] In **Figure 5.9**, comparing compound 2-144 with compound 2-145, 3-175 and 3-176, it was found that the response sensitivity of these compounds for the extraction of Pb^{2+} ions from an aqueous solution decreases in the following order: 3-176 > 3-175 > 2-144 > 2-145, which may be ascribed to the introduction of the different functional spirocyclic side arms to the lower rims of the calix[4]arene platforms. Spirocyclic calix[4]arene 3-176 shows the highest extraction percentage at 74.6 %, while ligand 2-145 shows the lowest at 31.5 %.
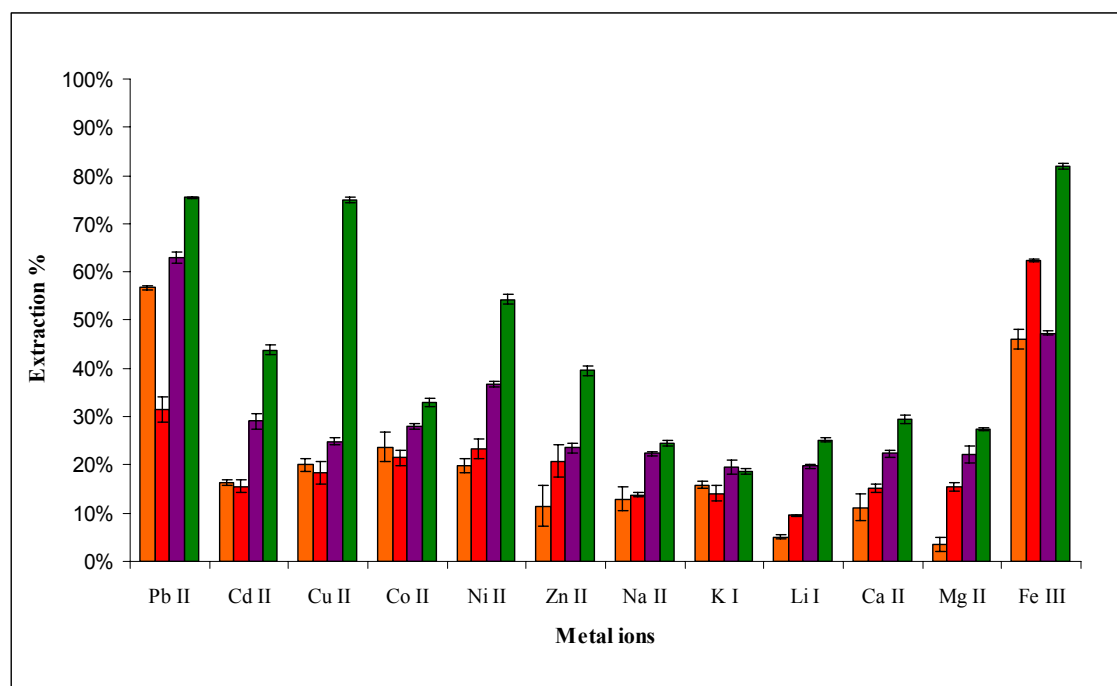

Figure 5.9 Bar profile of E% of spirocyclic calixa[4]renes with metal ions. ■ compound 2-144; ■ compound 2-145; ■ compound 3-175; ■Compound 3-176. (Error bars were calculated from the standard deviation, n=3).

The reason that compound 3-176 shows the most responsive behaviour may be due to the existence of two phenolic rings of side arms possessing electron-donating character, which

increases the electron density of spirodiamine and provides the optional surrounding "best-fit" recognition of the complexing Pb^{2+}. On the other hand, 2-145 with a spirolactone-possessing low electron density provides the lowest response sensitivity towards Pb^{2+}. The medium complexation efficiencies of compounds 2-144 and 3-175 endowing the relatively weaker electron donating preference and larger flexibility lead their medium complexation upon Pb^{2+}. In this case, the existence of two side-arms with electron donating characteristic groups in the ionophores has the optimal surrounding of its complex formation with Pb^{2+}.

For the selectivity of these compounds, it was found (**Figure 5.9**), that the selectivity of these compounds for heavy metal ions is higher than alkali metal and alkaline earth metal ions. This result is due to the introduction of pendant moieties which contain soft-base coordination centers such as N atoms which are in favour of adjusting the cavity size and conformation of the macrocyclic compounds.[24] Furthermore, there is a synergistic effect between the cavity and the donor sites of the ligand and thus the selective complexation with soft-acid metal ions, such as Pb^{2+}, Cd^{2+}, Hg^{2+}, etc. is easily achieved with significant avoidance of the interference from other metal ions.[35]

It was found (as shown in **Figure 5. 10**), that compound 2-144 possesses remarkable extraction selectivity for Pb^{2+} and Fe^{3+} over a wide variety of heavy metal ions. For instance, the E% value of 2-144 for Pb^{2+} ion is 57%, which is nearly 2 times higher than other heavy metal ions, such as Ni^{2+}, Cd^{2+}, Cu^{2+} etc. It could be because of the phenol attached with 3-176 and the carboxymethoxy group attached with 3-175 having extra donor atoms with heavy metal ions. It reduces the selectivity. These spirocylic groups (b, c and d) also increase the flexibility of compounds 2-145, 3-176 and 3-175, thus reduce the selectivity. On the contrary, the spirocyclic group (a) can constrain the conformation of compound 2-144 and increase its selectivity to Pb^{2+}. The ionic radius (Å) for Pb^{2+} is 1.18,[35] therefore the cavity size of 2-144 might be the 'best-fit' for this size. Again all these inferences need to be confirmed by further work in terms of molecular modelling and NMR studies.
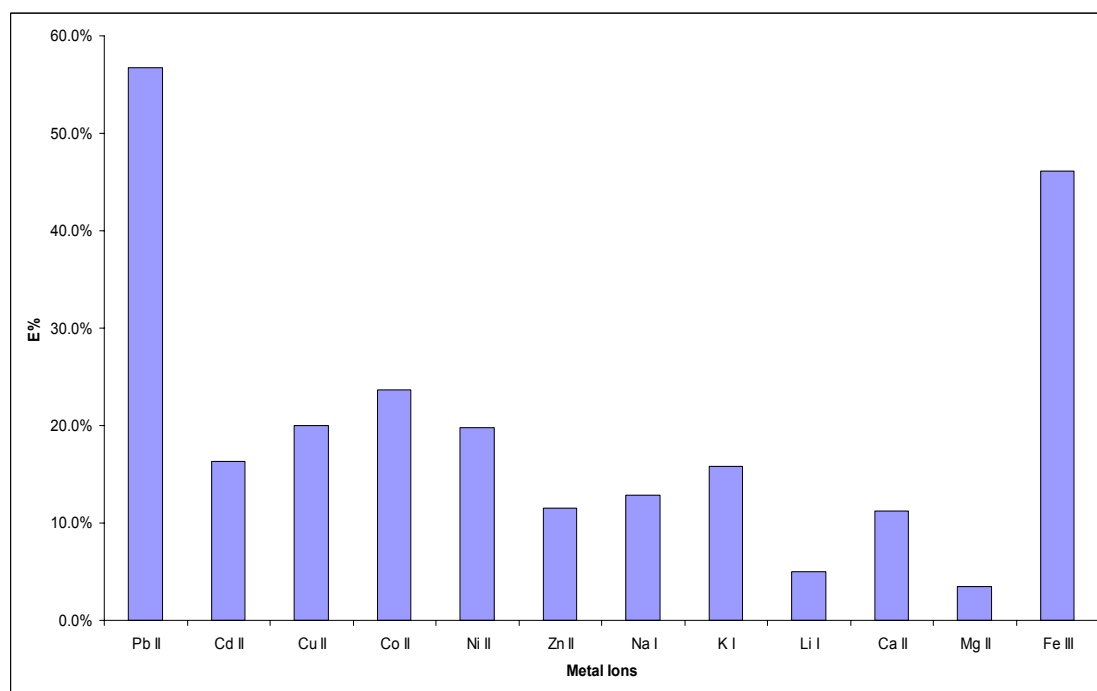
Figure 5.10 Bar profile of E% of 2-144 to metal ions, (n=3).

F. Kelleher et al. reported the complexation of spirodiamine with zinc chloride ions based on crystal-structure study using the Lewis Acid-Base principle.[44,45] The complexation binding of spirolactone with metal ions depends on its stereo-or diastereochemistry. They also recently demonstrated that the S, R-diastereisomer of L-proline derived "purity" spicrolactame can bind with zinc dichloride in ethanol solution, whereas, the "impurity" the R,R-diastereoisomer of L-proline derived spirolactame does not. Since the spirocyclic ligands 2-144 obtained a good selectivity with Pb^{2+} heavy metal ions. We suggest that this is probably due to the S, R-diastereoisomer as the main product of the tested compounds in solution DCM. Since it was not possible to obtain the crystal structure for X-ray study of the L-proline derived spirolactones in DCM, in this chapter, the crystallographic study cannot be discussed.

As a summary, we have succeeded in determining the non-integer host-guest compound of 2-144, 2-145, 2-175, 2-176, 3-201 and 3-202, 3-203 and 3-204 with several metal ions based on Pederson's technique and molar ratio techniques. Further investigations, e.g., X-ray structure of the complexes, molecular simulation, etc., are needed in order to progress.

5.3.5 The Potential Use of the Spirocyclic Calixarene Compounds

Metal-ion recognition and sensing via artificial receptors are of great importance not only in the clinical field but also in chemical,[46, 47] biological and environmental science.[46,48] Calixarenes are synthetic macrocyclic compounds and have been extensively used as hosts or building blocks for the accurate arrangement of binding sites in space, which cooperatively display high selectivity for a wide range of metal ions in selective transport, potentiometric, optical and chromoionophoric systems.[49-51] According to the results obtained from current extraction studies, several spirocyclic ligands have shown their potential uses in terms of metal ion recognition in a variety of fields, such as optical/potential-metric chemical sensors, separations techniques and waste treatment (such as heavy metal accumulations) etc.

5.3.5.1 Investigation of Spirocyclic Calix[4]arene Inclusion in Plasticised PVC

Chemosensors for metal ions have both receptor and reporter contributions that act in a complementary manner. In order for selectivity to be achieved the receptor must have specific binding properties and the reporter must effectively communicate with the receptor. One strategy to achieve this complementary goal is to design a receptor–reporter combination within a molecule, in which each binding site cooperatively plays its role accordingly.

From the results, it was found that the spirocyclic compound 2-144 shows a good selectivity for Pb^{2+} ion in solution. Therefore, the next stage of the investigation involved the attempt to incorporate spirocyclic calix[4]arene 2-144 into the plasticised PVC membranes. The plasticised PVC membrane is widely used as solid matrix for the immobilisation of calix[4]arene and its derivatives for application in sensors.[1, 5] In this approach, the sensing membrane based on the immobilisation of a selective ionophore 2-144 and a proton selective chromophore Nile-blue into plasticised PVC membrane for detecting of Pb^{2+} in aqueous solution is used. The Pb^{2+} was prepared at different concentrations (1 mg/l -25 mg/l) with a pH buffer solution range from pH 3-7. Nile-blue is a lipophilic H^+ selective chromo(fluoro)phores and is widely used in ISE-based pH

sensors and bulk optodes; they are also commonly dissolved in a plasticised matrix such as PVC for sensing metal ions.[52-54]

The usual evaluation of the bulk optode response is based on the assumption that the chromophore in acid solution is quantitatively protonated based on the transportation of cationic metal ion carried by an ion-selective ionophore.[21] This working principle has been successfully applied to many spirocylic calixarenes for the determination of heavy metal ions.[55,56] As described elsewhere,[56] the spirocyclic calix[a]arene was immobilised into plasticised PVC homogenously, according to experimental section **5.2.6**. Five different transparent blue polymeric films with different compositions according to **Table 5.2** were obtained. The blue colour was due to the colour of the lipophilic indicator Nile-blue. The films were submerged in Pb^{2+} ions solution at concentrations from 10-50 mg/L at pH 3-7 for 10 min. Next, the membranes were tested by UV-Vis absorption measurement. Compared with the blank sensing membrane (which was not submerged in Pb^{2+} solution), any absorption band due to the protonation of Nile-blue indicator (also caused by the complexation of metal with spirocyclic calixarene compound) was recorded. However, in our current study, there was no response produced by the sensing membrane for Pb^{2+}. The metal ion was not extracted into the PVC membrane from the aqueous solution. This is maybe due to the low lipophilicity of the spirocyclic calix[4]arene 2-144 in the PVC membrane.

For further investigation of these spirocyclic calix[4]arene compounds as metal-recognition receptors, potentiometric measurement can be applied in future work.

5.3.5.2 Other Uses

These spirocylic calix[4]arene compounds showed their potential application in separation/extraction technologies based on the attachment of ion-sensitive chelating molecules. There is an urgent need, for economic and environmental reasons, to develop new recognition ligands that can be used in solid phase extraction to remove heavy metal ions from water, while at the same time not affecting "favourable" elements in the water.[57] The spirocyclic calixarenes 3-201, 3-204, 3-202 and 3-203 showed promising extraction ability with heavy metal ions, e.g. Pb^{2+}, Cd^{2+}, Zn^{2+}, Cu^{2+}, Ni^{2+} and Co^{2+}. Although the selectivity of the spirocyclic calixarenes are not preferable for the development of

selective chemical sensors for one particular metal ion, their outstanding sensitivity and extraction efficiency provide a potential application in other areas. For example, they are good extractants for the separation of heavy metal ions from other ions and this could be use in the pre-treatment of waste water pollutions, such as for industrial waste water. These calixarenes could be applied to the development of separation columns for HPLC, LC-MS and GC-MS etc. The use of these spirocyclic compounds in these areas could be performed in future work.

Conclusion

In this work, eight double-armed spirocyclic calix[4]arene compounds have been designed, synthesised and tested as chelating agents for metal ions. Their binding abilities have been investigated with metal ions by using Pedersen's extraction method. Extraction study with metal picrates from an aqueous solution into DCM solution showed that all of these spirocyclic calix[4]arene compounds obtained strong binding affinity with heavy metal ions over alkali metal ions and alkaline earth metal ions.

Furthermore, compound 2-144 showed a sharp selectivity to Pb^{2+} and Fe^{3+} in the presence of other alkaline earth metal ions, alkali metal ion and other heavy metal ions. This could be due to the fixed cavity size and constrained conformation of compound 2-144 which are suitable for Pb^{2+} and Fe^{3+}. The flexibility of the structure of the calix[4]arene backbone has been reduced by the introduction of the spirocyclic attaching group (a).

Future work for this research will focus on detailed structural and conformational studies on these spirocyclic compounds and their complexes with metal ions by using NMR studies and molecular modelling studies.

The optical sensor based on the immobilisation of 2-144 as selective ionophore and Nile blue as chromophore into plasticised PVC has been investigated for the determination of Pb^{2+}. However, the results reported in this work indicated that the spirocyclic calix[4]arene 2-144 cannot be adequately incorporated into the PVC membranes. Future work should be carried out using different support materials, such as hybrid sol-gel materials and/or cellulose materials. The spirocyclic calixarene ligands, such as 3-202, 3-204 and 3-203 also displayed promising extraction efficiency towards heavy metal ions. Therefore, they have a potential in the use of separation- chelating- groups in separation technologies.

References

1.   P. Buhlmann, E. Pretsch and E. Bakker, *Chem. Rev.*, 1998, **98**, 1593-1688.

2.   S. Charlton, R. Fleming and A. Zipp, *Clin. Chem*, 1982, **28**, 1857-1861.

3.   W. E. Morf, K. Seiler, B. Lehmann, C. Behringer, K. Hartmann and W. Simon, *Pure Appl. Chem.* , 1989   **61**, 1613-1618.

4.   W. E. Morf, K. Seiler, B. Rusterholz and W. Simon, *Anal. Chem.*, 1990, **62**, 738-742.

5.   E. Bakker, P. Buhlmann and E. Pretsch, *Chem. Rev.*, 1997, **97**, 3083-3132.

6.   A. P. de Silva, H. Q. N. Gunaratne, T. Gunnlaugsson, A. J. M. Huxley, C. P. McCoy, J. T. Rademacher and T. E. Rice, *Chem. Rev.*, 1997, **97**, 1515-1566.

7.   D. Diamond and M. A. McKervey, *Chem. Soc. Rev.,*1996, **25**, 15 - 24,.

8.   C. D. Gutsche, *Acc. Chem. Res.*, 1983, **16**, 161-170.

9.   A. Cadogan, Z. Gao, A. Lewenstam, A. Ivaska and D. Diamond, *Anal. Chem.*, 1992, **64**, 2496-2501.

10.   R. J. Forster, A. Cadogan, M. Telting Diaz, D. Diamond, S. J. Harris and M. A. McKervey, *Sens. Actuators B: Chem.*, 1991, **4**, 325-331.

11.   B. T. T. Lan, Oacute, K. Th, *Anal. Sci.*, 1998, **14**, 191-197.

12.   A. K. Hassan, A. V. Nabok, A. K. Ray, F. Davis and C. J. M. Stirling, *Thin Solid Films*, 1998, **327-329**, 686-689.

13.   L. Aogán, E. Kathrin, M. Gillian, W. Rachel, K. Paddy, N. Kieran, S. Wolfgang and D. Dermot, *Electroanalysis*, 2002, **14**, 1397-1404.

14.   C. D. Gutsche, B. Dhawan, K. H. No and R. Muthukrishnan, *J. Am. Chem. Soc.*, 1981, **103**, 3782-3792.

15.   S. Shinkai, *Tetrahedron*, 1993, **49**, 8933-8968.

16.   R. J. M. E. Niels J. van der Veen, Johan F. J. Engbersen, Frank J. C. M. van Veggel and David N. Reinhoudt, *Chem. Commun.*, 1999, **1999**, 681 - 682.

17.   A. Casnati, A. Pochini, R. Ungaro, C. Bocchi, F. Ugozzoli, R. J. M. Egberink, H. Struijk, R. Lugtenberg, F. D. Jong and D. N. Reinhoudt, *Chem. Eur. J.*, 1996, **2**, 436-445.

18.   R. Ungaro, A. Casnati, F. Ugozzoli, A. Pochini, J.-F. Dozol, C. Hill and H. Rouquette, *Angew. Chem. Inter. Ed. Engl.*, 1994, **33**, 1506-1509.

19. Y. M. Shirshov, S. A. Zynio, E. P. Matsas, G. V. Beketov, A. V. Prokhorovich, E. F. Venger, L. N. Markovskiy, V. I. Kalchenko, A. V. Soloviov and R. Merker, *Supramole. Sci.*, **4**, 491-494.

20. A. Rouis, R. Mlika, C. Dridi, J. Davenas, H. Ben Ouada, H. Halouani, I. Bonnamour and N. Jaffrezic, *Mater. Sci. Eng.: C*, 2006, **26**, 247-252.

21. Mary McCarrick, B. Wu, S. J. Harris, D. Diamond, G. Barrett and M. A. McKervey, *J. Chem. Soc., Chem. Commun.*, 1992, **1992**, 1287 - 1289.

22. D. Diamond, *J. Incl. Phenom. Mac. Chem.*, 1994, **19**, 149-166.

23. I. Bitter, A. Grün, L. Toke, G. Tóth, B. Balázs, I. Mohammed-Ziegler, A. Grofcsik and M. Kubinyi, *Tetrahedron*, 1997, **53**, 16867-16876.

24. J. Lu, R. Chen and X. He, *J. Electroanal. Chem.*, 2002, **528**, 33-38.

25. R. Ludwig, *Fresenius' J. Anal. Chem.*, 2000, **367**, 103-128.

26. L. Chen, J. Zhang, W. Zhao, X. He and Y. Liu, *J. Electroanal. Chem.*, 2006, **589**, 106-111.

27. J.J. Pedersen, *J. Fed. Proc. Fed. Am. Soc. Exp. Biol.*, 1968, **27**, 1305.

28. L. Chen, H. Ju, X. Zeng, X. He and Z. Zhang, *Anal. Chim. Acta*, 2001, **437**, 191-197.

29. L. Chen, X. Zeng, X. He, Zhengzhi and Zhang, *Fresenius' J. Anal. Chem.*, 2000, **367**, 535-538.

30. X. Zeng, H. Sun, L. Chen, X. Leng, F. Xu, Q. Li, X. He, W. Zhang and Z.-Z. Zhang, *Org. Biomol. Chem.*, 2003, **1**, 1073-1079.

31. J. N. Babu, V. Bhalla, M. Kumar, R. K. Mahajan and R. K. Puri, *Tetrahedron Lett.*, 2008, **49**, 2772-2775.

32. P. M. Marcos, J. R. Ascenso, M. A. P. Segurado, R. J. Bernardino and P. J. Cragg, *Tetrahedron*, 2009, **65**, 496-503.

33. L. Zhang, J. Fan and X. Peng, *Spectrochimica Acta Part A: Mole. Biomole. Spectroscopy*, 2009, **73**, 398-402.

34. P. M. Marcos, S. Felix, J. R. Ascenso, M. A. P. Segurado, J. L. C. Pereira, P. Khazaeli-Parsa, V. Hubscher-Bruder and F. Arnaud-Neu, *New J. Chem.*, 2004, **28**, 748-755.

35. P. M. Marcos, J. R. Ascenso and P. J. cragg, *Supramole.   Chem.*, 2007, **19**, 199 - 206.

36. C. Wu, W.-J. Zhang, X. Zeng, L. Mu, S.-F. Xue, Z. Tao and T. Yamato, *J. Incl. Phenom. Mac. Chem*, **66**, 125-131.

37.   M. Vartanyan, O. Eliseev, K. Skov and R. Karakhanov, *Chem. Heterocyclic Compounds*, 1997, **33**, 625-646.

38.   J. Ward, Institute of Technology, Tallaght, 2009.

39.   S. Capel-Cuevas, I. de Orbe-Payá, F. Santoyo-González and L. F. Capitán-Vallvey, *Talanta*, 2009, **78**, 1484-1488.

40.   M. Hosseini, M. R. Ganjali, B. Veismohammadi, F. Faridbod, P. Norouzi and S. D. Abkenar, *Sens. Actuators B: Chem.*, **147**, 23-30.

41.   C. Pedersen, *J. Am. Chem. Soc.*, 1970, **92**, 391-394.

42.   J. KŘÍŽ, J. Dybal, E. MakrlÍk and P. VaŇura, *Supramole. Chem.*, 2008, **20**, 387 - 395.

43.   H. Deligoz and E. Erdem, *Solvent Extraction Ion Exchange*, 1997, **15**, 811 - 817.

44.   F. Kelleher, S. Kelly, J. Watts and V. McKee, *Tetrahedron*, **66**, 3525-3536.

45.   F. Kelleher, S. Kelly and V. McKee, *Tetrahedron*, 2007, **63**, 9235-9242.

46.   I. Qureshi, M. A. Qazi and S. Memon, *Sens. Actuators B: Chem.*, 2009, **141**, 45-49.

47.   M. A. Qazi, I. Qureshi and S. Memon, *J. Molecular Structure*, **975**, 69-77.

48.   H. Chen, Y.-S. Gal, S.-H. Kim, H.-J. Choi, M.-C. Oh, J. Lee and K. Koh, *Sens. Actuators B: Chem.*, 2008, **133**, 577-581.

49.   L. Pu, *Chem. Rev.*, 2004, **104**, 1687-1716.

50.   G. W. Gokel, W. M. Leevy and M. E. Weber, *Chem. Rev.*, 2004, **104**, 2723-2750.

51.   A. Castillo, J. L. Martez, P. R. Martez-Alanis and I. Castillo, *Inorg. Chim. Acta*, **363**, 1204-1211.

52.   X. Chen, F. Wang and Z. Chen, *Analytica Chimica Acta*, 2008, **623**, 213-220.

53.   W. Ngeontae, C. Xu, N. Ye, K. Wygladacz, W. Aeungmaitrepirom, T. Tuntulani and E. Bakker, *Anal. Chim. Acta*, 2007, **599**, 124-133.

54.   A. Safavi, A. Rostamzadeh and S. Maesum, *Talanta*, 2006, **68**, 1469-1473.

55.   E. Bakker, M. Lerchi, T. Rosatzin, B. Rusterholz and W. Simon, *Anal. Chim. Acta.*, 1993, **278**, 211-225.

56.   V. V. Cosofret, T. M. Nahir, E. Lindner and R. P. Buck, *J. Electroanal. Chem.*, 1992, **327**, 137-146.

57.   I. Urban, N. M. Ratcliffe, J. R. Duffield, G. R. Elder and D. Patton, *Chem. Commun.*, **46**, 4583-4585.

Chapter 6

6.1 Overall Conclusions

Over the last two decades, the development and applications of optical chemical sensors has been pursued with great interest by many researchers. Furthermore, there is tremendous growth and potential in employing such devices in the determination of pollutants in the environment. Compared with conventional laboratory-based instruments, optical sensing systems provide a portable, efficient, accurate and low-cost method for the monitoring of metal species in aquatic systems. In this work optical sensors based on the immobilisation of a commercially available indicators as chromophores and (or) a heavy metal ion selective ionophore into a suitable solid matrix have been developed for the determination of heavy metal ion in aqueous environments. Two novel optical sensors based on the immobilisation of colorant reagents (Br-PADAP and CAS) into sol-gel material and cellulose materials have been investigated for the determination of Ni^{2+} and Cu^{2+}. This mechanism is based on the colour changes of the sensor membrane due to the complexation of ligands with heavy metal ions. This method has been widely used for the development of one-shot cost effective optical sensors or ISE sensors for ions. This type of sensor is: cost effective; easy to prepare; and can be used as a 'naked-eye' optical sensor which can produce a signal due to the colour changes occurring in the sensor membrane. Therefore, there is a large potential in the market for the development this kind of sensor for on-site detection of particular heavy metal ions.

In Chapter 2 and Chapter 3, suitable materials for the immobilisation of indicators have been investigated. Materials science plays an important role in the development of optical sensors for their various applications. A hybrid nafion/sol-gel composite film was prepared and optimised as solid matrices for the immobilisation of a lipophilic indicator Br-PADAP for the determination of Ni^{2+} ion. Studies show that nafion/sol-gel composite films have many advantages over plasticised PVC membranes, such as: better chemical and physical mechanical stability; ease of fabrication; the midrate hydrophobicity for facilitating the diffusion of metal ions and the adsorption of indicators at the same time. A case study of using nafion/Sol-gel film as solid support has been demonstrated in Chapter 3.

The immobilisation of water soluble indicators into suitable solid materials for the determination of heavy metal ions is a big challenge in the domain of sensing. A functionalised cationic cellulose material has been prepared by an environmentally friendly

process. It was incorporated with water soluble indicators through electrostatic binding and thus reduced the leaching of indicators from the material. An optical sensor based on the immobilisation of CAS with cationic cellulose has been investigated for the determination of Cu^{2+}. This method demonstrated an environmentally friendly method by using bio-renewable and biodegradable material for sensor application. This is of interest for the sensor industry and would benefit the sensor market in the future.

The selectivity is always an important factor for sensor technology. Although the two sensors discussed in Chapter 2 and Chapter 3 displayed good performance towards heavy metal ions, they are lacking in selectivity; therefore, the mask reagents (to avoid interference from other heavy metals) are normally needed. The use of selective molecular recognition ionophores for analytes can increase the accuracy and simplicity of optical sensors to achieve the real *on-site* and portable application. Therefore, the heavy metal ions recognition properties of a novel series of spirocyclic calix[4]arene compounds have been investigated. The first study was performed by solvent extraction of heavy metal ions from water into DCM and later the promising compounds were immobilised in the PVC membrane. A selective ionophore for Pb^{2+} has been found.

The thesis described the development of optical sensors for the determination of heavy metal ions in aqueous samples. The heavy metal ions include Ni^{2+}, Cu^{2+} and Pb^{2+}. Several indicators have also been studied by solution chemistry; some of them have shown good affinities with heavy metals. They have showed the potential for the fabrication of optical sensors for heavy metal ions.

6.2 Chapter 1

Chapter 1 gives an up-to-date literature survey of optical chemical sensors for the determination of heavy metal ions.

6.2 Chapter 2

Chapter 2 involved a detailed solution study of several commercially available indicators used for the determination of heavy metal ions by UV-Vis spectrophotometric methods.

This investigation yielded information on the properties of the coordination compounds, which was essential for understanding their behavior in sensing materials. Ligand pKa values and their complexing ability with various di- and tri-valent metal ions in buffered solutions were determined. The stoichiometry, linear dynamic ranges, formation constants and molar absorptivities of the ligand/metal complexes were reported. In this chapter, spectrophotometric solution chemistry has been demonstrated as a simple and quick method for the determination of heavy metal ions by using colorimetric indicators. The optical properties of some commercially available indicators and their complexibilities with heavy metal ions have been characterised by using UV-Vis spectrophotometric methods. The binding abilities of these indicators with a variety of heavy metal ions have been investigated. The molar absorptivity, dynamic linear working ranges and the also the formation constants of the indicator-metal complexes have also been studied. Br-PADAP obtained a relatively high molar absorbtivity and formation constant with many environmentally significant heavy metal ions, i.e. nickel, copper and cobalt respectively. CAS, CAL, AVN and Nitroso-PASP are widely used as water soluble indicators. AVN was found to be a selective indicator for Fe^{2+} which obtained absorption maxima at 655nm. Nitroso-PASP showed an interesting potential for the determination of Fe^{2+} and Fe^{3+} simultaneously. CAL showed a promising result for the determination of copper in solution chemistry, although the new absorption maxima observed by CAL-Cu complex is very close to the original CAL absorption maxima, but it also has the potential as indicator for the determination of copper in sensor technology. CAS showed promising results on the complexation reactions with Cu^{2+}, Fe^{3+} and Co^{2+} ions at pH 9 buffer solution. All these results are shown in **Table 2.3.** Nitroso-PASP, CAS, AVN and CAL are the indicators which contain sulfonated groups. This structure makes them very soluble in water solution which is a drawback for them to immobilise into polymetric solid support due to the leaking problem. Therefore, these indicators have not been widely used in the optical sensor area. The purpose of this project is focused on the investigation of suitable solid matrices based on the immobilisation of these indicators for sensing heavy metal ions.

6.3 Chapter 3

Chapter 3 described a novel optical sensor based on Br-PADAP immobilised into hybrid nafion/sol-gel membranes for the determination of Ni^{2+} ion in aqueous samples. The

indicator Br-PADAP was chosen due to the high K_f value determined in chapter 2. A sensing film was generated that was capable of detecting low concentration levels of Ni^{2+}. It also provided a fast response time for the diffusion of metal ions from the aqueous samples into the silicate membrane. Although this indicator is unselective, the interferences of other metal ions can be reduced by using masking agents. And the interferences of negatively charged ions can be reduced due to the $-SO_3$ ions of the nafion structure composited into the silicate membranes. The linear range is from 0.5-15 mg/L, with a limit of detection value of 0.05 mg/mL. The sensor shows a fast response time within 7 min and it can be reused for 5 times after the decomplexation with 1M HCl.

An optical sensor based on the immobilisation of Br-PADAP in hybrid nafion/sol-gel silicate film for the determination of Ni^{2+} was successfully developed. The performance of the sensor based on several sensing materials, i.e. inorganic sol-gel, ORMOSILs thin films, Nafion/Sol-gel hybrid sol-gel thin film and plasticised PVC membranes, were evaluated. It was found that the nafion/sol-gel membrane cannot only overcome the brittleness of the pure sol-gel-derived silicate film but also increase the reusability and reduce the leaching of the indicators from the sol-gel network. In addition, the hybrid Nafion/sol-gel film can be easily prepared in comparison to other composites based on ORMOSILs films. Since nafion has a negative charge, therefore, it could facilitate the diffusion of positively charged metal ions into the membrane to react with Br-PADAP indicators that are entrapped into the hybrid Nafion/sol-gel film network. Moreover, it also reduced the interferences from the negatively charged ions.

Due to the increased hydrophibicity and pore size of the hybrid Nafion/sol-gel thin films, the proposed sensor exhibited a relatively fast response time (7 min). The sensing film generated was sensitive to low concentrations of Ni^{2+} in real environmental samples. Quantitative determination of Ni^{2+} was practical in the range of 0.5-15 mg/L. The behaviour of the indicator in Nafion modified sol gel thin film was compared with unmodified sol gel thin films. It was shown that the co-entrapment of the Nafion with dopant molecules within the xerogel matrix could be modified with the cage properties. Also the analytical performance of the dopant can be modified by the entrapped Nafion in the sol gel films. Consequently, the shrinking and cracking problems of the xerogel thin films have been solved. The optical sensing films can be regenerated by using 1M HCl solution and the membrane can be reused 10 times. The fabrication of the sensing films is

cheap and easy to prepare and portable. The preparation of plasticised PVC membrane is simple and straightforward, and it showed good homogeneity with Br-PADAP. However, the leaching of Br-PADAP occurred after the membrane contacting with Ni^{2+} ions due to the weak interaction of Br-PADAP with PVC membrane. This membrane also showed weaker adhesion with the glass supports compared with sol-gel membranes.

6.4 Chapter 4

Chapter 4 described a novel method for the preparation of sensing membranes from raw cellulose fibres by using a "green" process. This method has greatly reduced the leaching of water soluble dyes from the solid supporting matices. The CAS/QC membrane was used as a test strip for the determination of copper ions in aqueous solution. The working conditions have been optimized. No response at the working wavelength was observed from other potential heavy metal interferences. The membrane responds to copper by changing colour irreversibly from yellow to violet-blue ($\lambda_{max} = 620$ nm). The test strips are sensitive to Cu^{2+} in the 0-50 ppm range for an exposure time of 5 min. The membranes are sensitive to pH as well. The determination of Cu^{2+} must be performed in a buffer solution, ideally at pH 8. The developed CAS/QC membranes are transparent and bendable; thus the membranes are suitable for use with commercially available miniaturized optical devices.

In this work, cationic derivatives of cellulose were heterogeneously synthesised and applied to immobilise a series of water-soluble indicators. To the author's best knowledge, this is the first time that water-soluble ligands have been immobilised onto a cellulose membrane with electrostatic binding. Through this interaction, the water-soluble indicator CAS, Nitroso-PASP, CAL and AVN are embedded onto cationic cellulose and the leaching of these indicators from the membrane has been overcome. This technique has provided a new way to immobilise water soluble chelators onto cellulose, which can be applied to metal ion sensing, separation and pre-concentration processes. Since cellulose is a biodegradable, nontoxic and abundant raw material, therefore, the starting materials are environmentally friendly. The fabrication of the cationic cellulose used a "green" synthesis approach by using NaOH/urea as solvent and the byproducts can be recycled.

The CAS/QC membrane was used as a test strip for the determination of copper ions in aqueous solution. The working conditions have been optimised. No response at the working wavelength was observed from other potential heavy metal interferences. The membrane responds to copper by changing colour irreversibly from yellow to violet-blue (λmax = 620 nm). The test strips are sensitive to Cu^{2+} in the 6.6-50 ppm range for an exposure time of 5 min. The membranes are also sensitive to pH. The determination of Cu^{2+} must be performed in a buffer solution, ideally at pH 8. The developed CAS/QC membranes are transparent and bendable; thus the membranes are suitable for use with commercially available miniaturised optical devices.

Copper is an important heavy metal ions that must be monitored in many aqueous environments. The raw materials used in the preparation of this sensor strip are at low cost, renewable and it is simple to prepare. Therefore this one-shot sensing strip has a large potential market for on-line portable environmental monitoring, e.g. for organic and inorganic pollutants in aqueous environments.

6.5 Chapter 5

In order to increase the selectivity of the optical sensors for a specific heavy metal ion, a novel generation of double-armed spirocyclic calix[4]arene compounds have been designed and investigated in chapter 5. It was found that these ligands can be used as extractants for most of the metal ions, particularly; 2-144 obtained a good selectivity to Pb^{2+} over other alkali metal ions, alkaline and heavy metal ions. 2-144 shows the potential to be used as ionophore for selective determination of Pb^{2+} ions.

In this work, eight double armed spirocyclic calix[4]arene compounds have been designed, synthesised and tested as chelating agents for metal ions. Their binding abilities have been investigated with metal ions by using Pedersen's extraction method. Extraction studies with metal picrates from an aqueous solution into a DCM solution have shown that all of these spirocyclic calix[4]arene compounds obtain strong binding affinity with heavy metal ions over alkali metal ions and alkaline earth metal ions.

Furthermore, compound 2-144 showed a sharp selectivity for Pb^{2+} and Fe^{3+} in the presence of other alkaline earth metal ions, alkali metal ions and other heavy metal ions. This could be due to the fixed cavity size and constrained conformation of compound 2-144 that are suitable for Pb^{2+} and Fe^{3+}. The flexibility of the structure of the calix[4]arene backbone has been reduced by the introduction of the spirocyclic attaching group (a).

The optical sensor based on the immobilisation of 2-144 as selective ionophore and Nile blue as chromophore into plasticised PVC has been investigated for the determination of Pb^{2+}. However, the results reported in this work indicated that the spirocyclic calix[4]arene 2-144 cannot be adequately incorparated into the PVC membranes. Future work should be carried out using different support materials, such as hybrid sol-gel materials and/or cellulose materials. The spirocyclic calixarenes ligands, such as 3-202, 3-204 and 3-203 also displayed promising extraction efficiency towards heavy metal ions, therefore, they have a potential in the use of separation chelating groups in separation technologies.

6.6 Avenues for Future Work

The achievements of this initial research have identified a number of new opportunities for subsequent work. Some avenues for further investigation include:

1. Real samples application. Application of developed optical sensors for real samples from industrial wastewaters.

2. Immobilize the ionophores 2-144 into suitable sensing materials to fabricate an optical sensor for the determination of Pb^{2+} and apply this sensor to real environmental samples. Future work should focus on the researching of calixarene compounds in respect of detailed structural and conformational studies on them and their complexes with metal ions by using NMR studies and, molecular modelling studies.

3. Optimize the cationic cellulose membrane for the immobilization of other sulfonic groups containing water soluble indicators. Furthermore these cationic cellulose membranes should be investigated for their potential to develop portable sensing

membranes that can be incorporated within miniaturized optical devices for *in-situ* monitoring of metal ions.

Appendix I

The pK$_a$ Studies of the Indicators

1. The pKa of CAS

From **Figure 1**, it can be seen that the absorption band due to the chromophore transitions shifted from 494 nm to 422 nm. The latter wavelength was therefore chosen to monitor the deprotonated basic form of CAS. A wavelength of 296 nm was used to monitor the acidic species. The orange cationic species of CAS exists in extremely acidic media (pH ≤ 1). A mixture of red-yellow species exists in the pH range 2-6, and the yellow anionic from of the ligand predominates at pH ≥ 7. The species of CAS were characterised by a blue shift when CAS was present in buffers above its pKa value i.e. 4.2 (**Figure 2**). The pKa was determined as 4.2 as described before. It can be seen from **Figure 2**, the CAS in pH 5 solution obtained absorption at the wavelength of 430 nm
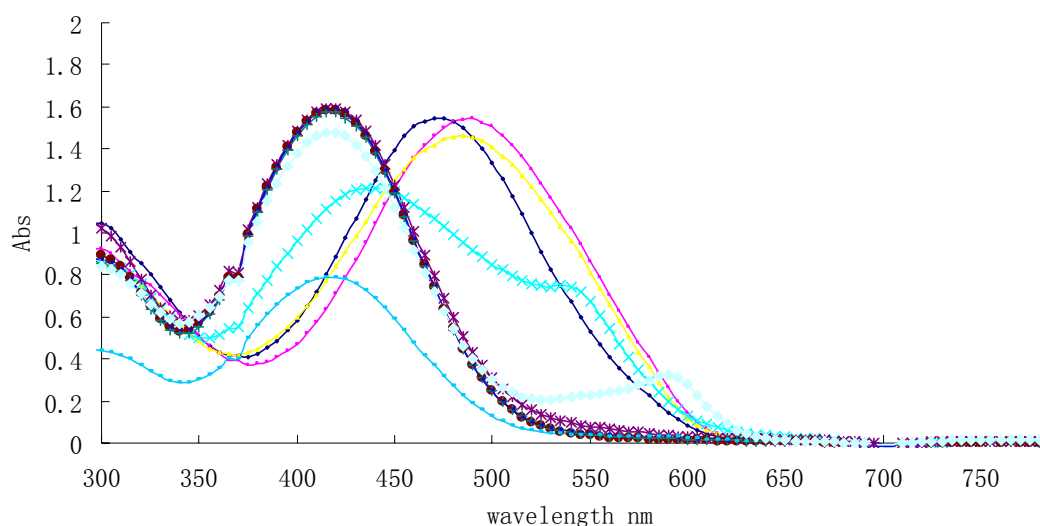
F

igure 1 UV-Vis absorption spectra of 1 x 10^{-3} M CAS in buffer solutions of pH 1-10. ■ pH 1; ■ pH 2; ■ pH 3; ■ pH 4; ■ pH 5; ■ pH 6; ■ pH 7; ■ pH 8, ■ pH 9; pH 10.
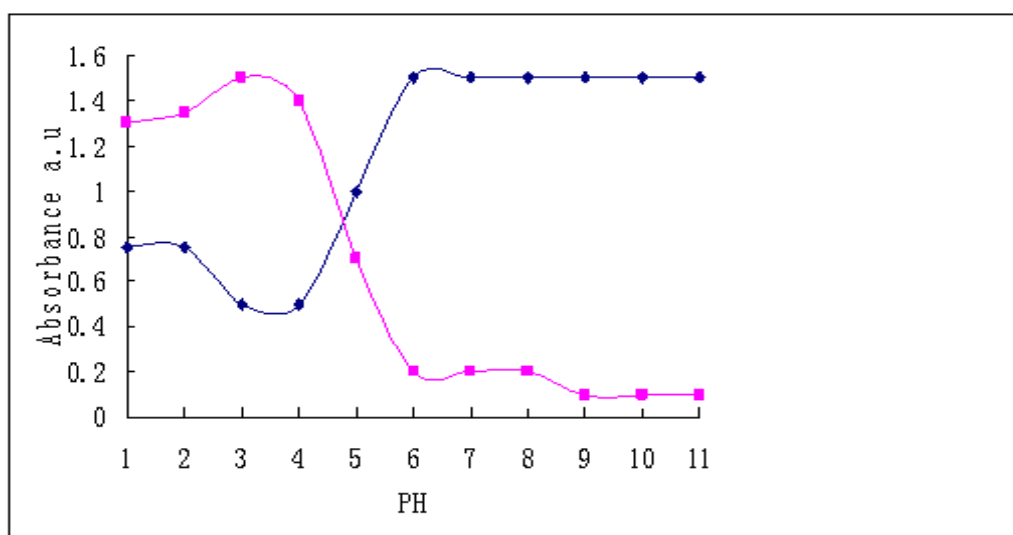
Figure 2 Plot of absorbance as a function of pH of 2×10^{-4} M CAS. Measurements made at ■ a wavelength (λ_1=290 nm) at which HIn sbsorbs radiation; ■ a wavelength (λ_2= 500 nm) at which In⁻ absorbs radiation. pKa = 4.2.

2. The pKa study of CAL

CAL has a similar structure to AVN i.e. it is an azo dye and has hydroxyl groups in the *ortho* position to the azo bridge. The same absorption regions were observed for this ligand. Bands were observed below and above 350 nm. Two principal species were also present for CAL in buffered solutions from pH 1-10. This was again confirmed by the presence of an isosbestic point as shown **Figure 3.**
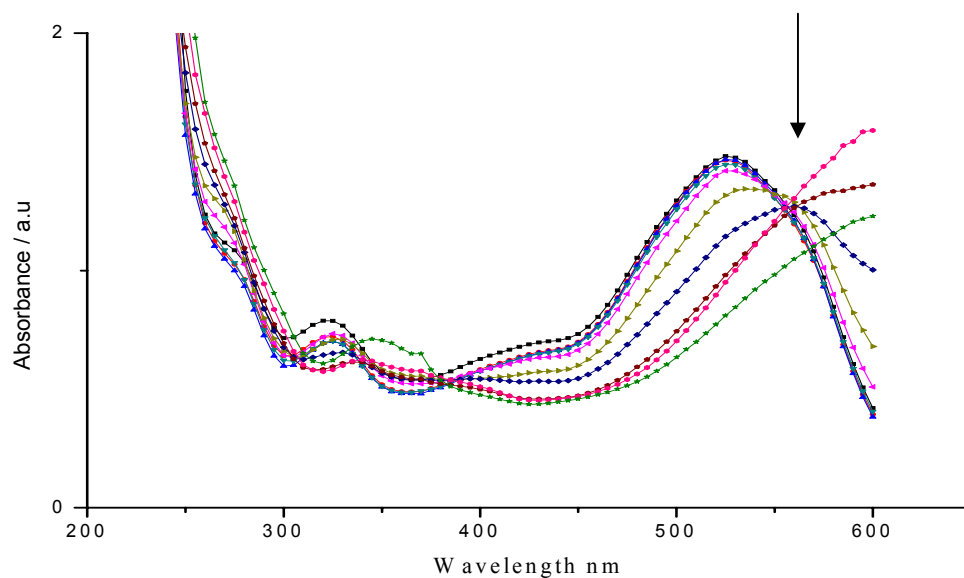
Figure 3 UV/Visable absorption spectra of 2 x 10⁻⁴ M CAL in buffer solutions in the pH range 1-10. ■ pH 1; ■ pH 2; ■ pH 3; ■ pH 4; ■ pH 5; ■ pH 6; ■ pH 7; ■ pH 8; ■ pH 9; ■ pH 10.

The pKa of CAL is 8.2 and shown in **Figure 4**. Similar results has been reported in literature.[3] At this pKa one proton from a hydroxyl group is lost. The second is reported to be lost at pH 12.4; a red shift (530 nm → 602 nm) was observed when CAL was in buffered solutions with pH values above the pKa.

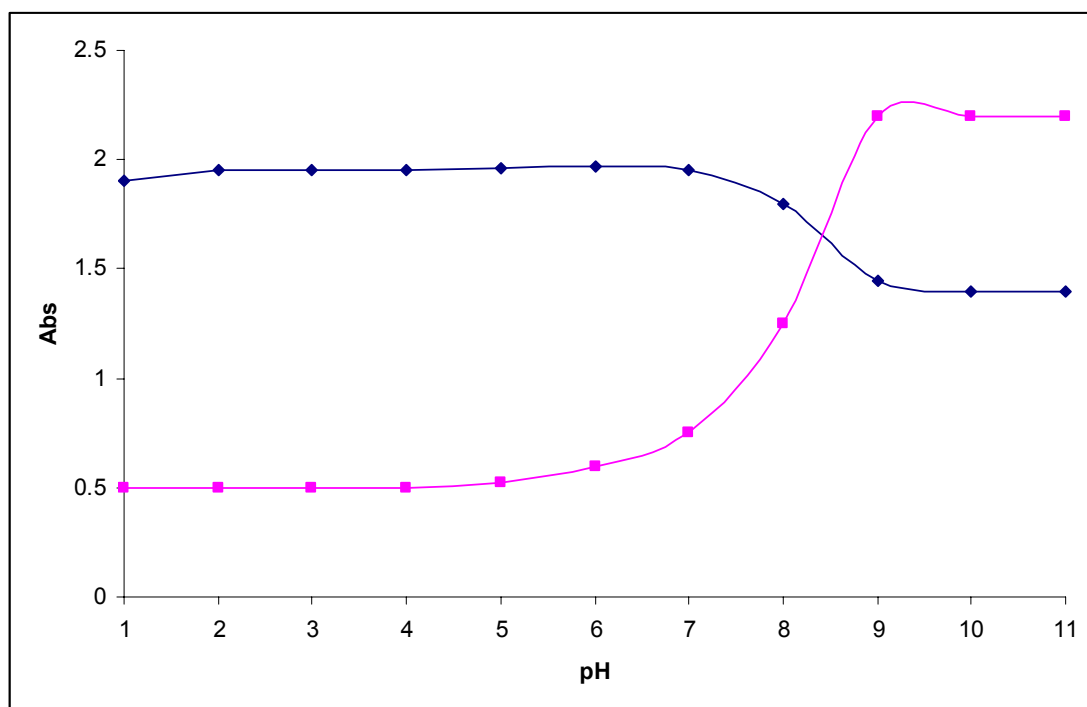**Figure 4** Plot of absorbance as a function of pH of 2×10^{-4} M CAL. Measurements made at ■ a wavelength (λ_1= 520 nm) at which HIn sbsorbs radiation; ■ a wavelength (λ_2= 600 nm) at which In⁻ absorbs radiation. pK_a = 8.2.

3. The pKₐ Study of Br-PADAP

Br-PADAP exists in different forms depending on the pH value of the solution. The UV/Vis absorbance spectra showed the response of the different forms of Br-PADAP over the pH 1-10 in **Figure 5**. The pKa values of Br-PADAP at 25 ^{o}C were determined to be 0.63, 2.77 and 11.2 by Jiang[45] and 1.0, 3.0 and 11.2 by Oxspring et al.[20] The pK_a value of Br-PADAP was found under current experimental condition is 3.0 corresponds to the N, N-diethyl-anilinium ion. The other pK_a values according to literatures, i.e. pK_a 1.0 are due to the 3-bromopyridinium ion and pK_a 11.2 due to the phenolic group. These results are confirmed with the previous studies of Jiang and Oxspring.
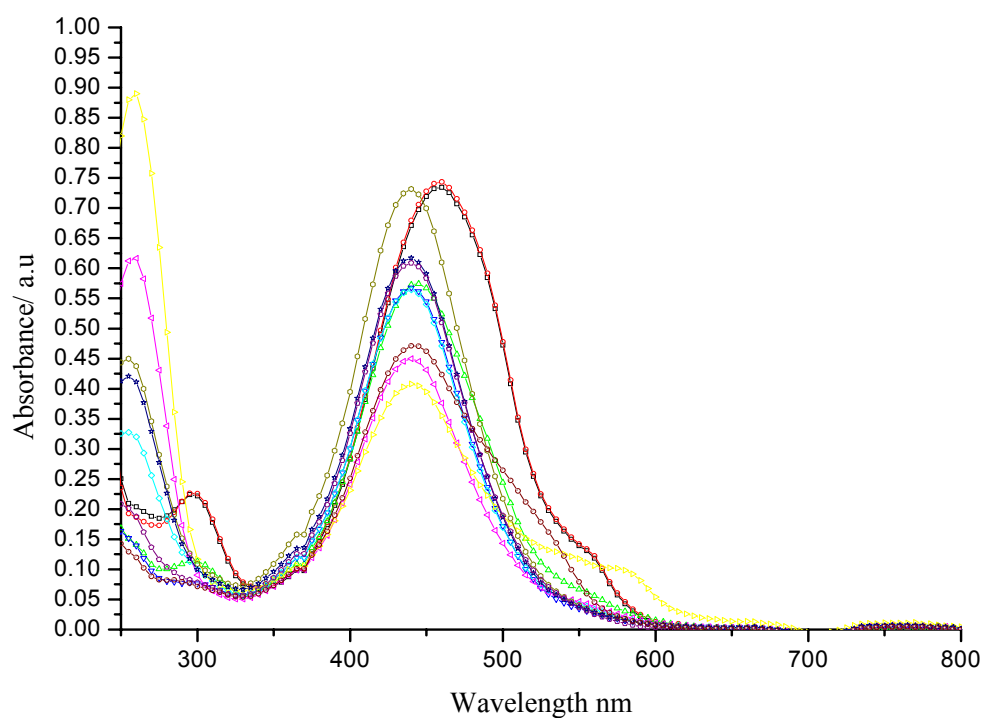
216

Figure 5 UV/Vis absorbance spectrum of 2 x 10^{-5} M Br-PADAP in buffer solution of pH 1-10. ■ pH 1; ■ pH 2; ■ pH 3; ■ pH 4; ■ pH 5; ■ pH 6; ■ pH 7; ■ pH 8; ■ pH 9; ■ pH 10.

The pKa value of 3.0 corresponded o the *N,N*-diethyl-anilinium ion. The other pKa values, i.e. pKa_1 (1.0) due to the 3-bromopyridinium ion, and pK_2 (11.2) due to the phenolic group was not observed on the pKa plot in **Figure 6,** as the entire pH range was not investigated in this study.
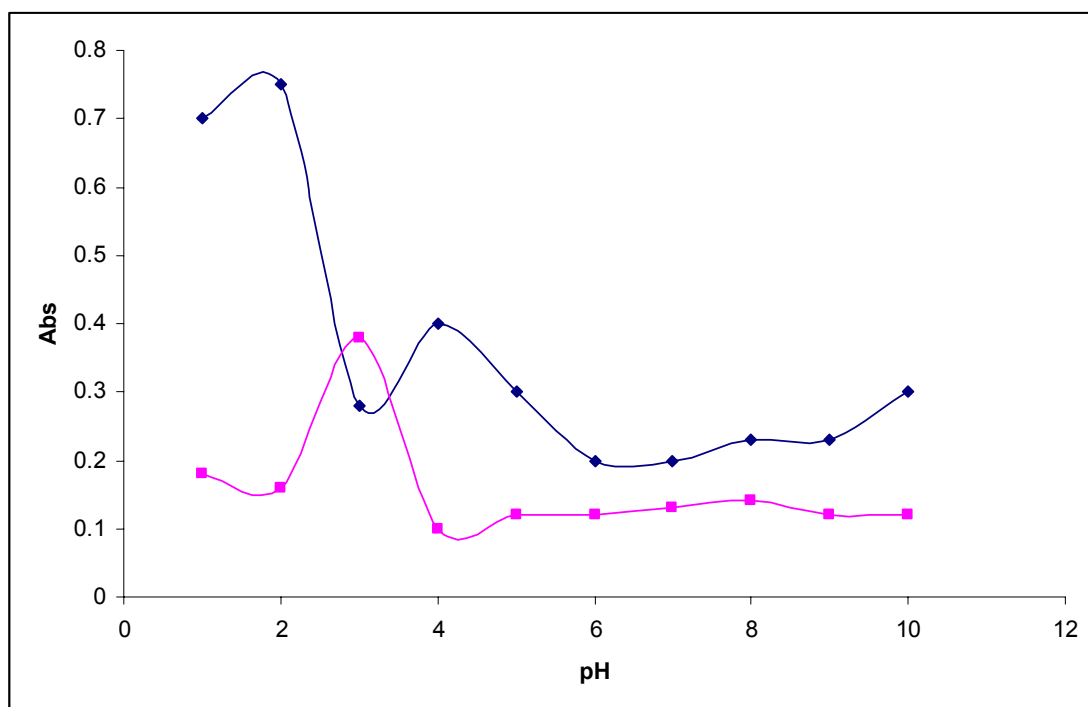
Figure 6 Plot of absorbance as a function of pH of 2 x10^{-5} M Br-PADAP. Measurements made at ■ 446 nm, and ■ 575 nm. pKa = 3.0

Appendix II

The Stoichiometry Study and the Formation Study

1. The Stoichiometry of Indicator-Metal Complexes

1.1 Job's Method

The stoichiometries of all the linear complexes are studied by Job's method and mole-ratio method. The proposed geometries here are ascertained through initial studies and reviews. This was carried out to gain an understanding of the complexation procedures involved. While conformation of the geometries is not the focus of the research, these results could be confirmed with a more detailed study of the ligand: metal interaction. An example of the Job's method is illustrated below in **Figure 1** for the determination of the stiochiometry of Nitroso-PSAP with Fe^{2+} ions in pH 6 solution. The absorbances of the complexes of Nitroso-PSAP-Fe^{2+} vs ligand:metal ratio is plotted. From **Figure 1**, it can be seen that the stoichiometry of 2:1 Nitroso-PSAP: Fe^{2+} was obtained, it means that two nitroso-PSAP molecule complex with each Fe^{2+} ion which suggest that nitroso is a tridentate ligand and the complex is octahedral. Fe^{2+} is known to form octahedral complex with a variety of ligands. From the pKa study, a pKa value of 8.4 was determined, which would suggest that nitroso is fully protonated at pH 6 i.e. the pH at which it was observed to complex with Fe^{2+}.
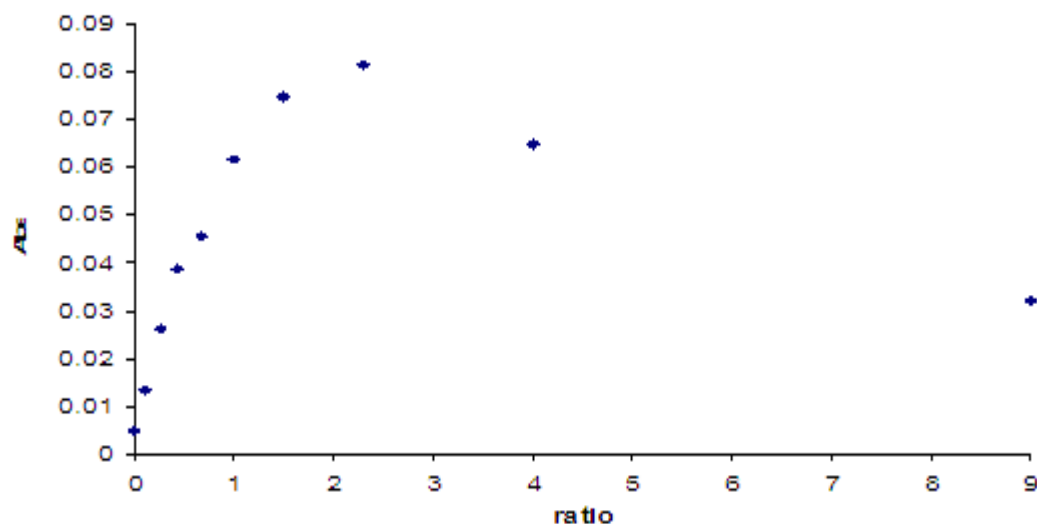

Figure 1. Job's method of the nitroso-Fe^{2+} complex at pH 6.

1.2 Mole-ratio method

From the stoichiometry study (**Figure 2**) by mole ratio method, the stoichiometry of Ni^{2+} with Br-PADAP in ethanol solution is 1:2. This has been confirmed with a previous study. And the possible coordination between Ni and Br-PADAP was illustrated in **Figure 2**. There is a complex array of stereochemistries associated with nickel ion. The chemistry of nickel is complicated but it mainly forms octahedral and square plannar complexes.
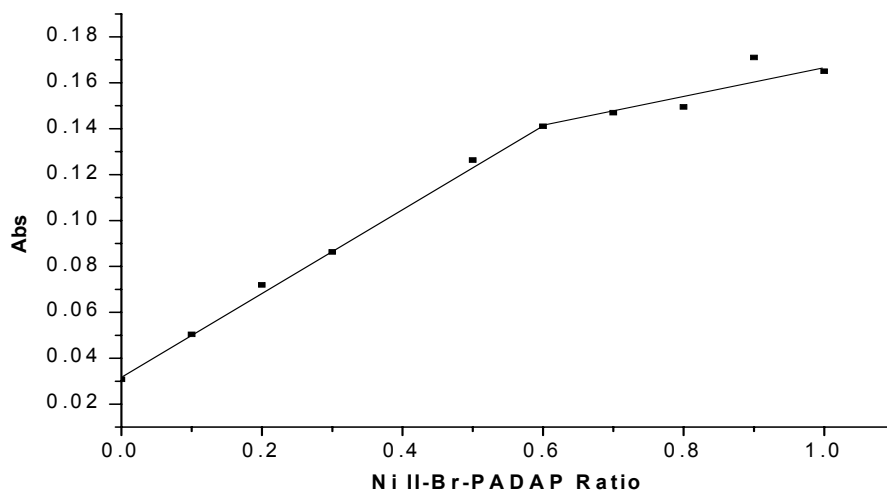

Figure 2 Mole ratio of the Ni-Br-PADAP complex at pH 9 solutions consisted of fixed Br-PADAP concentration of 1×10^{-5} M and Ni^{2+} was varied between 1-10 mgL^{-1}.

2. Formation Constant Calculation

An example is shown for the determination of the stoichiometry and formation constant of the 1, 10-Phenanthroline/Fe (II) complex. All formation constants detailed in Chapter 2, Table 2.5, were calculated by using this method, using the appropriate wavelength, concentrations and volume etc.

A series of solutions was prepared in which the amount of Fe^{2+} was held constant at 2 mL of 7.12 10^{-4} M. Phenanthroline was varied as shown in the Table below. Following dilution to 25 mL, absorbance data for these solutions in cm cuvette at 510 nm was obtained.

1,10-Phenanthroline/mL	Absorbance at 510 nm
2	0.240
3	0.380
4	0.470
5	0.590
6	0.680
8	0.730
10	0.727
12	0.734

A plot of absorbance as a function of the volume of added 1, 10-Phenanthroline was constructed. Two linear branches were observed. The intersection of the linear ligand was presented. The graph shows that at a 6 mL addition of phenanthroline, stoichiometric amounts of the Fe^{2+} and phenanthroline were present.
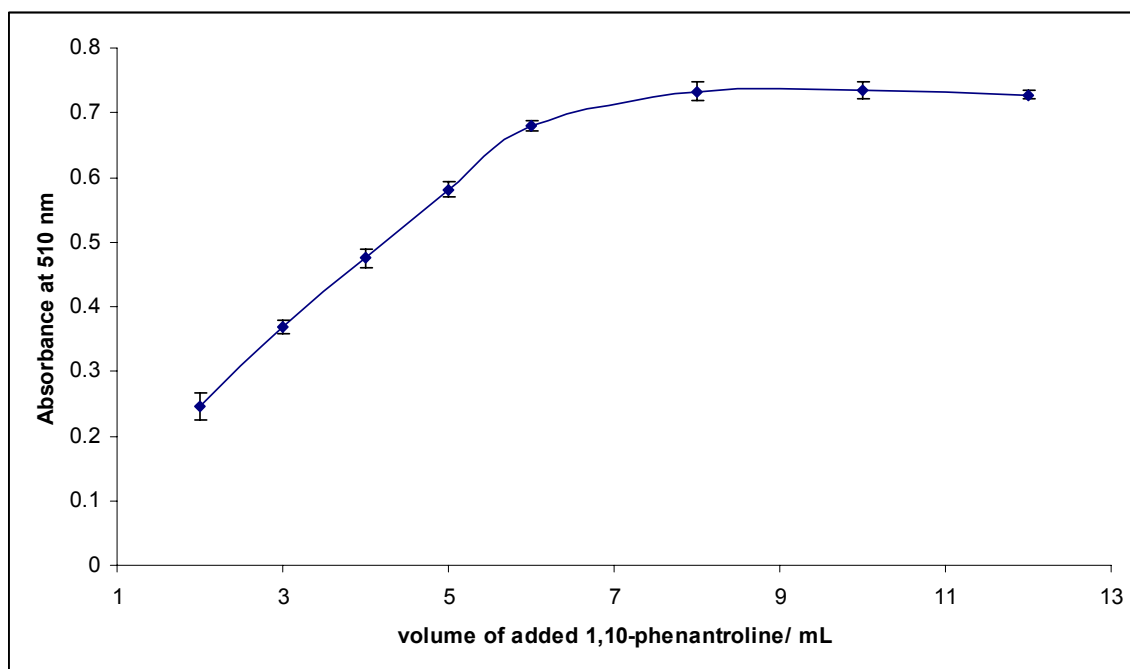
To determine the number of moles of each species present the following formula was use:

Number of Moles = Volume in Liters x Molarity

Number of Moles of:

Phenanthroline = $(0.006) \times (7.12 \times 10^{-4}) = 4.272 \times 10^{-6}$ moles

Fe (II) = $(0.002) \times (7.12 \times 10^{-4}) = 1.424 \times 10^{-6}$ moles

Stoichiometry of ligand : metal = $4.272 \times 10^{-6}/1.424 \times 10^{-6} = 3:1$

Therefore

$Fe^{2+} + 3phenanthroline = [Fe(phen)_3]^{2+}$

$$K_f = \frac{[Fe(phen)_3]^{2+}}{[Fe^{2+}][phen]^{3+}}$$

To determine the Kf, the concentration of the ligand, metal and the complex must be known. The following formula was used:

Molarity = moles/Volume in liters

223

The concentration of the phen. was = 4.272 x 10^{-6}/ 0.025 = 1.709 x 10^{-4} M phen.

1 mole of Fe^{2+} reacted to give 1 mole of the complex.

The concentration of the Fe^{2+} was therefore: 1.424 x10^{-6}/ 0.0025 = 5.696 x 10^{-5} M

To determine the concentration of the complex the ε was first determined using Beer's law (**Figure 2.1**).

A= 0.72 at 12 mL of added 1, 10-phenantroline.

Therefore, ε= 0.720 / (5.696 x 10^{-5}) x (1) = 1.264 x 10^{4} M^{-1} cm^{-1}.

The concentration of the complex was also calculated using Beer's law, i.e   C =A/εb

At a 6 mL addition of 1, 10-phenanthroline, the absorbance was 0.700 and the ε was 1.264 x 10^{4} M^{-1} cm^{-1}. The concentration of the complex was therefore:

0.700/1.264 x 10^{4} = 5.538 x 10^{-5} M.

From the equilibrium Equation

	[Fe^{2+}] M	[phenanthroline]	[Fe (phen)$_3$]$^{2+}$
Intial	5.696 x 10^{-5}	**1.709 x 10^{-4}	0
Equilibrium	* 1.58 x 10^{-6}	4.76 x 10^{-6}	5.538 x 10^{-5}

* value obtained by substracting 5.538 x 10^{-5} from the initial concentration.

** value obtained by substrating 3 x (5.538 x 10^{-5}) from the initial concentration.

Therefore,

$$K_f = \frac{5.538 \times 10^{-5}}{(1.58 \times 10^{-6}) \times (4.76 \times 10^{-6})^3} = 3.25 \times 10^{17}$$

224

Appendix III

Results from the Pederson's Study
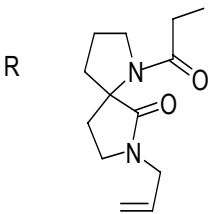
Table 5.2 (1) Extraction results with spirocyclic-a (n=3).

Binding Agent	Cation	Extraction %	R.S.D %	Cation	Extraction %	R.S.D %
	Pb^{2+}	8.7	3.3	Na^+	4.2	0.36
	Cd^{2+}	5.39	0.46	K^+	4.1	1.6
	Zn^{2+}	2.0	1.1	Li^+	3.8	1.4
Spirocyclic-a	Cu^{2+}	18.4	2.9	Fe^{3+}	0.6	0.25
	Ni^{2+}	6.5	2.0	Ca^{2+}	2.0	0.02
	Co^{2+}	4.8	1.0	Mg^{2+}	4.8	4.7

Table 5.2 (2) Extraction results with compound 2-144 (n=3)
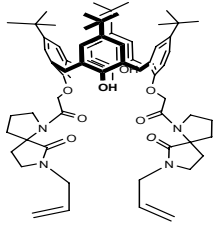
Binding Agent	Cation	Extraction %	R.S.D %	Cation	Extraction %	R.S.D %
	Pb^{2+}	56.7	0.89	Na^+	12.88	4.1
	Cd^{2+}	3.9	0.94	K^+	15.8	1.2
	Zn^{2+}	1.0	1.9	Li^+	5.0	0.6
	Cu^{2+}	4.0	4.89	Fe^{3+}	46.7	2.6
	Ni^{2+}	0	2.0	Ca^{2+}	11.2	4.6
2-144	Co^{2+}	0.5	5.3	Mg^{2+}	3.4	2.0

Table 5.2 (3) Extraction results with 3-201 (n=3).
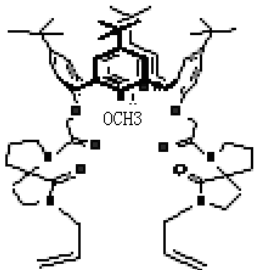
Binding Agent	Cation	Extraction%	Cation	Extraction%
	Pb^{2+}	64.8	Cu^{2+}	47.3
	Cd^{2+}	50.4	Ni^{2+}	64.5
3-201	Zn^{2+}	50.5	Co^{2+}	62.5

Table 5.3 (1) Extraction results with spirocyclic-b (n=3).

Binding Agent	Cation	Extraction %	R.S.D %	Cation	Extraction %	R.S.D %
	Pb^{2+}	11.7	2.0	Na^+	10.6	4.7
	Cd^{2+}	10.09	1.2	K^+	9.8	0.7
	Zn^{2+}	9.6	0.5	Li^+	2.2	1.1
Spirocyclic-b	Cu^{2+}	11.17	4.6	Fe^{3+}	56.16	0.19
	Ni^{2+}	12.11	1.3	Ca^{2+}	8.7	0.14
	Co^2	9.6	0.8	Mg^{2+}	9.16	0.39

Table 5.3 (2) Extraction results with 2-145, (n=3).
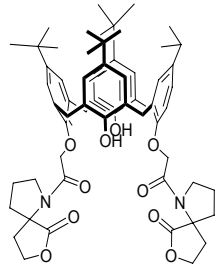
Binding Agent	Cation	Extraction %	R.S.D %	Cation	Extraction %	R.S.D %
	Pb^{2+}	31.5	4.7	Na^+	13.8	0.85
	Cd^{2+}	15.4	1.96	K^+	14.0	2.3
	Zn^{2+}	20.7	5.0	Li^+	9.0	0.2
	Cu^{2+}	18.2	3.5	Fe^{3+}	62.5	0.59
2-145	Ni^{2+}	23.3	3.0	Ca^{2+}	15.9	1.4
	Co^{2+}	21.5	2.4	Mg^{2+}	15.9	1.3

Table 5.3 (3) Extraction results with 3-204, (n=3).
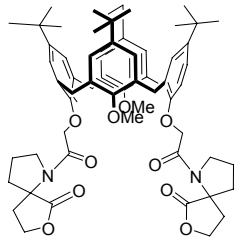
Binding Agent	Cation	Extraction%	Cation	Extraction%
	Pb^{2+}	74.6	Cu^{2+}	63.16
	Cd^{2+}	88.4	Ni^{2+}	53.2
3-204	Zn^{2+}	90.56	Co^{2+}	85.9

227

Table 5.4 (1) Extraction results with spirocyclic–c, (n=3).

Binding Agent	Cation	Extraction %	R.S.D %	Cation	Extraction %	R.S.D %
	Pb^{2+}	13.90	1.5	Na^+	3.0	7.2
	Cd^{2+}	7.0	0.44	K^+	6.4	3.2
	Zn^{2+}	7.6	0.8	Li^+	4.8	3.4
Spirocyclic-c	Cu^{2+}	7.9	10	Fe^{3+}	58.36	0.8
	Ni^{2+}	2.8	0.7	Ca^{2+}	5.9	0.23
	Co^{2+}	8.2	0.12	Mg^{2+}	5.38	0.4

Table 5.4 (2) Extraction results with calyx[4]arene 3-175, (n=3).
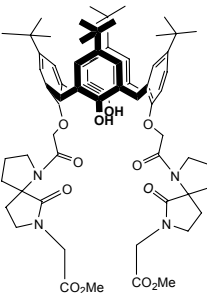
Binding Agent	Cation	Extraction %	R.S.D %	Cation	Extraction %	R.S.D %
	Pb^{2+}	63.5	3.9	Na^+	10	0.5
	Cd^{2+}	29.0	2.9	K^+	19.58	2.2
	Zn^{2+}	23.5	1.6	Li^+	19.68	0.8
	Cu^{2+}	24.8	1.3	Fe^{3+}	47.35	0.5
	Ni^{2+}	36.6	1.0	Ca^{2+}	22.35	1.3
3-175	Co^{2+}	27.9	1.0	Mg^{2+}	22.07	2.7

Table 5.4 (3) Extraction results with 3-202, (n=3).
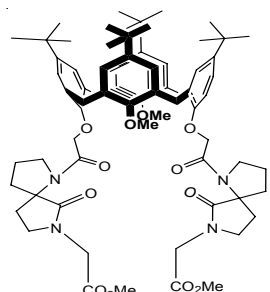
Binding Agent	Cation	Extraction %	Cation	Extraction%
	Pb^{2+}	86.5	Cu^{2+}	56.5
	Cd^{2+}	63.4	Ni^{2+}	57.3
3-202	Zn^{2+}	66.8	Co^{2+}	66.0

Table 5.5 (1) Extraction results with spirocyclic-d, (n=3).
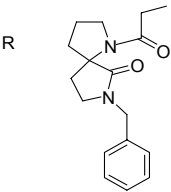
Binding Agent	Cation	Extraction %	R.S.D %	Cation	Extraction %	R.S.D %
Spirocyclic-d	Pb^{2+}	29.25	0.6	Na^+	26.6	0.96
	Cd^{2+}	7.3	0.3	K^+	28.6	0.25
	Zn^{2+}	2.3	0.4	Li^+	11.29	0.66
	Cu^{2+}	34.49	0.4	Fe^{3+}	21.75	0.3
	Ni^{2+}	7.4	0.3	Ca^{2+}	1.4	0.03
	Co^{2+}	4.0	0.6	Mg^{2+}	5.8	0.03

Table 5.5 (2) Extraction results with 3-176, (n=3).
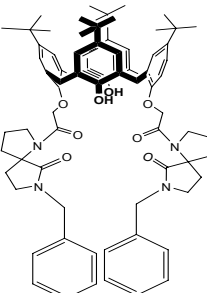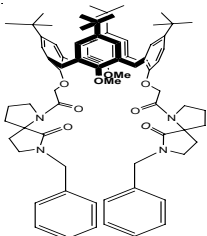
Binding Agent	Cation	Extraction %	R.S.D%	Cation	Extraction %	R.D.S %
3-176	Pb^{2+}	75.3	1.0	Na^+	24.58	0.96
	Cd^{2+}	19.2	2.1	K^+	18.71	0.8
	Zn^{2+}	26.06	2.2	Li^+	25.20	0.8
	Cu^{2+}	74.9	2.6	Fe^{3+}	81.96	0.3
	Ni^{2+}	8.03	2.3	Ca^{2+}	29.41	1.68
	Co^{2+}	20.49	1.5	Mg^{2+}	27.28	0.4

Table 5.5 (3) Extraction results with 3-203, (n=3).

Binding Agent	Cation	Extraction%	Cation	Extraction%
3-203	Pb^{2+}	78.5	Cu^{2+}	30
	Cd^{2+}	46.5	Ni^{2+}	21.6
	Zn^{2+}	42.7	Co^{2+}	42.1

Appendix IV

Publications and Presentations

Publications

1 **"N**ovel Double-Armed Calix[4]arene compounds as Selective Extractants for The Determination of Heavy Metal Ions in Aqueous Environment"

In preparation

2 **"**The Development of a *Sol-gel* Optical Sensor for Analysis of Nickel Ion in Aqueous Environment*"*

In prepararition

3 "Immobilizations of Water Soluble Indicators onto Cationic Cellulose Materials for Metal ions Sensing"

In prepararition

Conferences/Oral Comunications

1. **Li Li**, Fiona Regan, The Development of an Optical Chemical Sensor for the Determination of Heavy Metal Ions for Industrial Waste Water, *QUESTOR Meeting,* University of Queens, **2007** May, Belfast. United Kingdom.

2. **Li Li**, Fiona Regan, Optical Chemical Sensor the Determination of Heavy Metal Ions in Aqueous Environment, *The 18th Irish Environment Colloquium,* **2008** Feb. 14-17, Dundalk, Ireland.

3. **Li Li,** James Ward, Mary Deasy, Fiona Regan, Newly Synthesized Novel Double-Armed Calix[4]arene compounds as Selective Extractants for The Determination of Heavy Metal Ions in Aqueous Environment The Euroanalysis 2009, 6-10 September, Innsbruck, Austria. (Oral presentation Abstract has been accepted)

Conferences/Poster Comunications

1. **Li Li**, Fiona Regan, Novel Materials for Sensing Metal Ions in the Environment, *The 11th Workshop on Progress in Analytical Methodologies for Trace Metal Speciation,* **2007** Sep. 4-7. Munster, Germany.

2. **Li Li**, Fiona Regan, The Development of an Optical Chemical Sensor for the Determination of Heavy Metal Ions in Industrial Waste Water, *The RSC Analytical Research Forum*, University of Strathclyde, **2007** July 16-18, Glasgow, United Kingdom.

3. **Li Li,** Fiona Regan, The Development of a *Sol-gel* Optical Sensor for Analysis of Nickel Ion in Aqueous   Environment, *The RSC Analytical Research Forum*, **2008** July 21-23, Hull, United Kingdom.

4. **Li Li**, Haibo Xie, Fiona Regan, Nick Gathergood, Functionalized Cellulose Membrane from Ionic Liquids as Sensor Support Matrix for Heavy Metal Ions in Aqueous Environments, *30th Society of Environmental Toxicology and Chemistry*, **2009** November, 19- 23, New Orleans, Louisiana, USA,